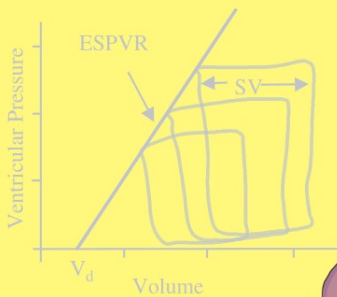


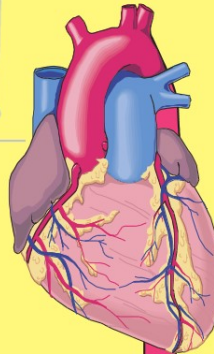
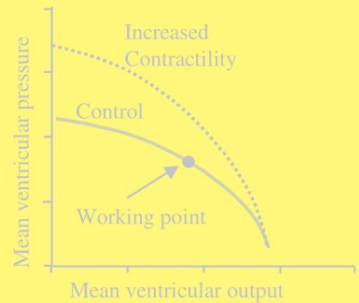
# Snapshots of Hemodynamics

*An Aid for Clinical Research and Graduate Education*

The Pressure-Volume relation

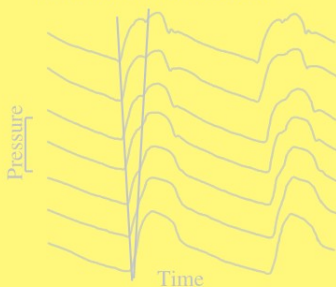


The Pump Function Graph

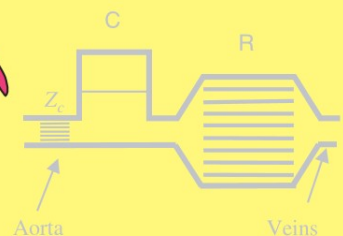


*Nico Westerhof  
Nikos Stergiopoulos  
Mark I.M. Noble*

Wave travel and reflection



The Windkessel model



SNAPSHOTS  
OF  
HEMODYNAMICS

## BASIC SCIENCE FOR THE CARDIOLOGIST

---

1. B. Swynghedauw (ed.): *Molecular Cardiology for the Cardiologist*. Second Edition. 1998 ISBN 0-7923-8323-0
  2. B. Levy, A. Tedgui (eds.): *Biology of the Arterial Wall*. 1999 ISBN 0-7923-8458-X
  3. M.R. Sanders, J.B. Kostis (eds.): *Molecular Cardiology in Clinical Practice*. 1999 ISBN 0-7923-8602-7
  4. B.Ostadal, F. Kolar (eds.): *Cardiac Ischemia: From Injury to Protection*. 1999 ISBN 0-7923-8642-6
  5. H. Schunkert, G.A.J. Riegger (eds.): *Apoptosis in Cardiac Biology*. 1999 ISBN 0-7923-8648-5
  6. A. Malliani, (ed.): *Principles of Cardiovascular Neural Regulation in Health and Disease*. 2000 ISBN 0-7923-7775-3
  7. P. Benlian: *Genetics of Dyslipidemia*. 2001 ISBN 0-7923-7362-6
  8. D. Young: *Role of Potassium in Preventive Cardiovascular Medicine*. 2001 ISBN 0-7923-7376-6
  9. E. Carmeliet, J. Vereecke: *Cardiac Cellular Electrophysiology*. 2002 ISBN 0-7923-7544-0
  10. C. Holubarsch: *Mechanics and Energetics of the Myocardium*. 2002 ISBN 0-7923-7570-X
  11. J.S. Ingwall: *ATP and the Heart*. 2002 ISBN 1-4020-7093-4
  12. W.C. De Mello, M.J. Janse: *Heart Cell Coupling and Impulse Propagation in Health and Disease*. 2002 ISBN 1-4020-7182-5
  13. P.P.-Dimitrow: *Coronary Flow Reserve – Measurement and Application: Focus on transthoracic Doppler echocardiography*. 2002 ISBN 1-4020-7213-9
  14. G.A. Danielli: *Genetics and Genomics for the Cardiologist*. 2002 ISBN 1-4020-7309-7
  15. F.A. Schneider, I.R. Siska, J.A. Avram: *Clinical Physiology of the Venous System*. 2003. ISBN 1-4020-7411-5
  16. Can Ince: *Physiological Genomics of the Critically Ill Mouse*. 2004 ISBN 1-4020-7641-X
  17. Wolfgang Schaper, Jutta Schaper: *Arteriogenesis*. 2004 ISBN 1-4020-8125-1  
eISBN 1-4020-8126-X
  18. Nico Westerhof, Nikos Stergiopoulos, Mark I.M. Noble: *Snapshots of Hemodynamics: An aid for clinical research and graduate education*. 2005 ISBN 0-387-23345-8  
eISBN 0-387-23346-6
-

# Snapshots of Hemodynamics

*An aid for clinical research and  
graduate education*

Nico Westerhof

*Laboratory for Physiology,  
VU University medical center  
Amsterdam, the Netherlands*

Nikos Stergiopoulos

*Laboratory of Hemodynamics and Cardiovascular Technology,  
Swiss Federal Institute of Technology  
Lausanne, Switzerland*

Mark I.M. Noble

*Cardiovascular Medicine,  
Aberdeen University  
Aberdeen, Scotland*

**Springer**

eBook ISBN: 0-387-23346-6  
Print ISBN: 0-387-23345-8

©2005 Springer Science + Business Media, Inc.

Print ©2005 Springer Science + Business Media, Inc.  
Boston

All rights reserved

No part of this eBook may be reproduced or transmitted in any form or by any means, electronic, mechanical, recording, or otherwise, without written consent from the Publisher

Created in the United States of America

Visit Springer's eBookstore at:  
and the Springer Global Website Online at:

<http://ebooks.kluweronline.com>  
<http://www.springeronline.com>

# CONTENTS

PREFACE .....	vii
ACKNOWLEDGEMENT.....	xi
<b>PART A BASICS OF HEMODYNAMICS.....</b>	<b>1</b>
CHAPTER 1 VISCOSITY .....	3
CHAPTER 2 LAW OF POISEUILLE .....	7
CHAPTER 3 BERNOULLI'S EQUATION.....	11
CHAPTER 4 TURBULENCE.....	15
CHAPTER 5 ARTERIAL STENOSIS.....	17
CHAPTER 6 RESISTANCE .....	21
CHAPTER 7 INERTANCE .....	25
CHAPTER 8 OSCILLATORY FLOW THEORY .....	29
CHAPTER 9 LAW OF LAPLACE .....	31
CHAPTER 10 ELASTICITY .....	35
CHAPTER 11 COMPLIANCE.....	41
<b>PART B CARDIAC HEMODYNAMICS .....</b>	<b>49</b>
CHAPTER 12 CARDIAC MUSCLE MECHANICS .....	51
CHAPTER 13 PRESSURE-VOLUME RELATION.....	57
CHAPTER 14 PUMP FUNCTION GRAPH.....	63
CHAPTER 15 WORK, ENERGY AND POWER .....	69
CHAPTER 16 OXYGEN CONSUMPTION & HEMODYNAMICS.....	71
CHAPTER 17 POWER AND EFFICIENCY .....	75
CHAPTER 18 CORONARY CIRCULATION.....	81
CHAPTER 19 ASSESSING VENTRICULAR FUNCTION.....	91
<b>PART C ARTERIAL HEMODYNAMICS.....</b>	<b>97</b>
CHAPTER 20 WAVE TRAVEL AND VELOCITY .....	99
CHAPTER 21 WAVE TRAVEL AND REFLECTION.....	105
CHAPTER 22 WAVEFORM ANALYSIS.....	109
CHAPTER 23 ARTERIAL INPUT IMPEDANCE.....	113
CHAPTER 24 ARTERIAL WINDKESSEL .....	121
CHAPTER 25 DISTRIBUTED MODELS .....	127
CHAPTER 26 TRANSFER OF PRESSURE.....	131
CHAPTER 27 VASCULAR REMODELING .....	137
CHAPTER 28 BLOOD FLOW AND ARTERIAL DISEASE.....	143
<b>PART D INTEGRATION.....</b>	<b>147</b>
CHAPTER 29 DETERMINANTS OF PRESSURE & FLOW .....	149
CHAPTER 30 COMPARATIVE PHYSIOLOGY .....	155
<b>PART E APPENDICES .....</b>	<b>161</b>
APPENDIX 1 TIMES & SINES: FOURIER ANALYSIS .....	163
APPENDIX 2 BASIC HEMODYNAMIC ELEMENTS.....	167
APPENDIX 3 VESSEL SEGMENT.....	169
APPENDIX 4 BASIC ASPECTS .....	173
APPENDIX 5 BOOKS FOR REFERENCE .....	177
APPENDIX 6 SYMBOLS .....	179
APPENDIX 7 UNITS AND CONVERSION FACTORS.....	181
<b>INDEX .....</b>	<b>183</b>

## **PREFACE**

This book is written to help clinical and basic researchers, as well as graduate students, in the understanding of hemodynamics. Recent developments in genetics and molecular biology on the one hand, and new non-invasive measurement techniques on the other hand, make it possible to measure and understand the hemodynamics of heart and vessels better than ever before. Hemodynamics makes it possible to characterize, in a quantitative way, the function of the heart and the arterial system, thereby producing information about what genetic and molecular processes are of importance for cardiovascular function.

We have made the layout of the book such that it gives a short overview of individual topics, in short chapters only giving the essentials, so that it is easy to use it as a quick reference guide. It is not necessary to read the book from cover to cover. Each chapter is written in such a way that one is able to grasp the basic and applied principles of the hemodynamic topic. If more details or broader perspectives are desired one can go to the other, related, chapters to which the text refers, or the textbooks listed in the 'Reference books' section (Appendix 5).

To bring the essentials even more directly across, every chapter starts with a 'box' containing a figure and caption, which give the basic aspects of the subject. It is often sufficient to study the contents of this box alone to obtain this basic information. Chapters end with a section 'Physiological and Clinical relevance' to place the information into perspective. The part in between, called 'Description', can be used to get more detailed information and find some references to more detailed work.

More comprehensive information on the subjects discussed can be found in textbooks on physiology and cardiology, as well as special books on hemodynamics. A number of these books are listed in the section 'Reference books' (Appendix 5). More literature also can easily be found on the internet. In the chapters the number of references therefore is limited to a few only.

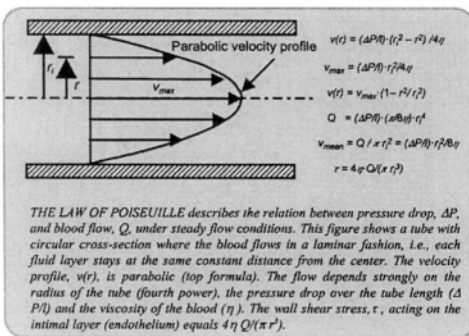
NW, NS, and MIMN

# How to use the

## Snapshots of Hemodynamics

### Chapter 2 Law of Poiseuille

### Chapter and title



#### Description

With laminar flow through a uniform tube of radius  $r$ , the velocity profile over the cross-section is a parabola.

#### Physiological and clinical relevance

The more general form of Poiseuille's law given above, i.e.,  $Q = \Delta P/R$  allows us to derive resistance,  $R$ , from mean pressure and mean flow measurement.

#### References

1. The Murgu JP, Westerhof N, Giolma JP, Altobelli SA. Aortic input impedance in normal man: relationship to pressure wave forms. *Circulation* 1980;62:101-116.
2. Murgu JP, WesterhofN, Giolma JP, Altobelli

The box contains a figure with a short text that illustrates the main message of the chapter.

The 'Description' section gives the essential background and discusses the different aspects of the subject.

The 'Physiological and clinical relevance' section places the subject in a broader physiological context and shows clinical applications.

A limited number of references is given. Major reference books are given in Appendix 5.

## **ACKNOWLEDGEMENT**

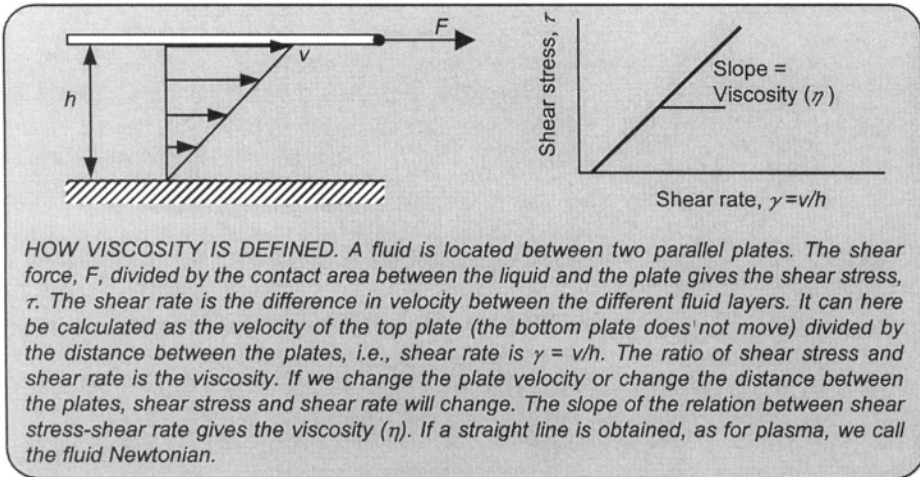
The authors wish to thank

Dr. Ben Delemarre, Prof. Dr. Walter Paulus and Prof. Dr. P Segers for reading the manuscript and giving many excellent suggestions.

We thank Jan Paul Barends for all his help in aspects of layout and presentation.

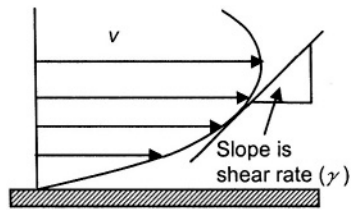
Part A  
Basics of Hemodynamics

# Chapter 1 VISCOSITY



## Description

Consider the experiment shown in the figure in the box. The top plate is moved with constant velocity,  $v$ , by the action of a shear force  $F$ , while the bottom plate is kept in place (velocity is zero). The result is that the different layers of blood move with different velocities. The difference in velocity in the different blood layers causes a shearing action between them.



VELOCITY and shear rate for a general profile.

The rate of shear,  $\gamma$ , is the relative displacement of one fluid layer with respect to the next. In general, the shear rate is the slope of the velocity profile, as shown in the figure on the right. In our particular example the velocity profile is linear, going from zero at the bottom to  $v$  at the top plate. Therefore, the slope of the velocity profile, and thus the rate of shear, is equal to  $v/h$ ,  $h$  being the distance between the plates. The units of shear rate are  $1/s$ . The force needed to obtain a certain velocity, is proportional to the contact area,  $A$ , between fluid and plates. It is therefore convenient, instead of force, to use the term shear stress, defined as the force per area  $\tau = F/A$ , with units  $\text{Pa}$  or  $\text{N/m}^2$ .

We may think of the following experiment: we pull the top plate at different velocities  $v$  and we measure the shear force  $F$ . Then we plot the shear stress,  $\tau$ , against the shear rate,  $\gamma$ . The resulting relation is given in the figure in the box and the slope is the viscosity:

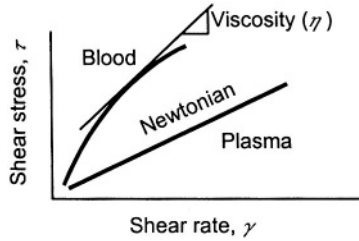
$$\eta = \text{shear stress/shear rate} = \tau / \gamma$$

The units of viscosity are  $\text{Pa}\cdot\text{s} = \text{Ns/m}^2$ , or Poise ( $\text{dynes}\cdot\text{s}/\text{cm}^2$ ), with  $1 \text{ Pa}\cdot\text{s} = 10 \text{ Poise}$ . Fluids with a straight relationship between shear stress and shear rate are called Newtonian fluids, i.e., viscosity does not depend on shear stress or shear rate. Viscosity is sometimes called dynamic viscosity in

contrast to the kinematic viscosity, which is defined as viscosity divided by density  $\rho$ , thus  $\eta/\rho$ .

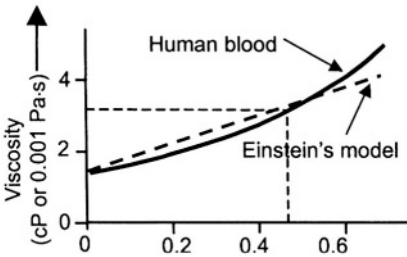
*Viscosity of blood*

Blood consists of plasma and particles, with 99% of the particle volume taken by the red blood cells, RBC's, or erythrocytes. Thus the red blood cells mainly determine the difference between plasma and blood viscosity. The viscosity of blood therefore depends on the viscosity of the plasma, in combination with the hematocrit (volume % of red blood cells, Ht) and red cell deformability. Higher hematocrit and less deformable cells imply higher viscosity. The relation between hematocrit and viscosity is complex and many formulas exist. One of the simplest is the one by Einstein:



VISCOSITY of plasma and blood.

$$\eta = \eta_{plasma} \cdot (1 + 2.5 Ht)$$



VISCOSITY as function of hematocrit.

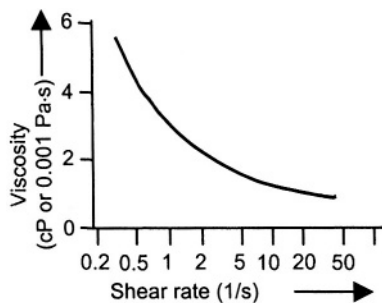
also on the size, shape and flexibility of the red blood cells. For instance, the hematocrit of camel blood is about half of that of human blood, but the camel's red blood cells are more rigid, and the overall effect is a similar blood viscosity.

Einstein's relation for the viscosity of fluids containing particles applies only to very low particle concentrations. Nevertheless, it gives some indication. The viscosity of plasma is about 0.015 Poise (1.5 centipoise, cP) and the viscosity of whole blood at a physiological hematocrit of 40 - 45% is about 3.2 cP, or  $3.2 \cdot 10^{-3}$  Pa.s.

Blood viscosity depends not only on plasma viscosity and hematocrit, but

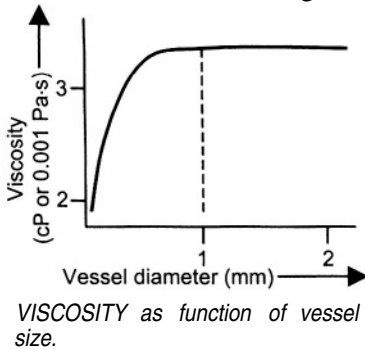
*Anomalous viscosity or non-Newtonian behavior of blood*

The viscosity of blood depends on its velocity. More exactly formulated, when shear rate increases viscosity decreases. At high shear rates the doughnut-shaped RBC's orient themselves in the direction of flow and viscosity is lower. For extremely low shear rates formation of RBC aggregates may occur, thereby increasing viscosity to very high values. It has even been suggested that a certain minimum shear stress is required before the blood will start to flow, the so-called yield stress. In large and medium size arteries shear rates are higher than  $100 \text{ s}^{-1}$ , so viscosity is practically constant.



VISCOSITY as function of shear rate for hematocrit of 48.

The physiological range of wall shear stress is 10 to 20 dynes/cm<sup>2</sup>, or 1 to 2 Pa, with 1 Pa = 0.0075 mmHg. Several equations exist that relate shear stress and shear rate of blood, e.g., Casson fluid, and Herschel-Bulkley fluid [1,2].



Viscosity also depends on the size of blood vessel. In small blood vessels and at high velocities, blood viscosity apparently decreases with decreasing vessel size. This is known as the Fahraeus-Lindqvist effect, and it begins to play a role in vessels smaller than 1 mm in diameter. Red blood cells show axial accumulation, while the concentration of platelets appears highest at the wall. The non-Newtonian character of blood only plays a role in the microcirculation.

Viscosity depends on temperature. A decrease of 1°C in temperature yields a 2% increase in viscosity. Thus in a cold foot blood viscosity is much higher than in the brain.

#### How to measure viscosity

Blood viscosity is measured using viscometers. Viscometers consist essentially of two rotating surfaces, as a model of the two plates shown in the box figure. Blood is usually prevented from air contact and temperature is controlled. When comparing data on viscosity one should always keep in mind the measurement technique, as results are often device dependent.

#### Physiological and clinical relevance

The anomalous character of blood viscosity results from the red blood cells, and the effects are mainly found in the microcirculation at low shear and small diameters. The effects are of little importance for the hemodynamics of large arteries. Thus, in hemodynamics, it may be assumed that viscosity is independent of vessel size and shear rate.

Determination of blood viscosity *in vivo* is almost impossible. In principle, the pressure drop over a blood vessel and the flow through it, together with vessel size, can be used to derive viscosity on the basis of Poiseuille's law. However, the vessel diameter in Poiseuille's law (Chapter 2) appears as the fourth power, so that a small error in the vessel diameter leads to a considerable error in the calculated viscosity. Also, the mean pressure drop over a segment of artery is typically a fraction of 1 mmHg. Moreover, hematocrit is not the same in all vessels due to plasma skimming effects. And finally, Poiseuille's law may only be applied when there are no effects of inlet length (see Chapter 2).

The main purpose of the circulation is to supply tissues with oxygen. Oxygen supply is the product of flow and oxygen content. The hematocrit determines the (maximum) oxygen carrying capacity of blood and its viscosity, and therefore the resistance to blood flow. These counteracting effects on oxygen transport result in an optimal hematocrit of about 45 in the human at sea level, with a small difference between males and females. It appears that in mammals, blood viscosity is similar, but the hematocrit is not

---

because of the different size, shape and flexibility of the red blood cells as mentioned above.

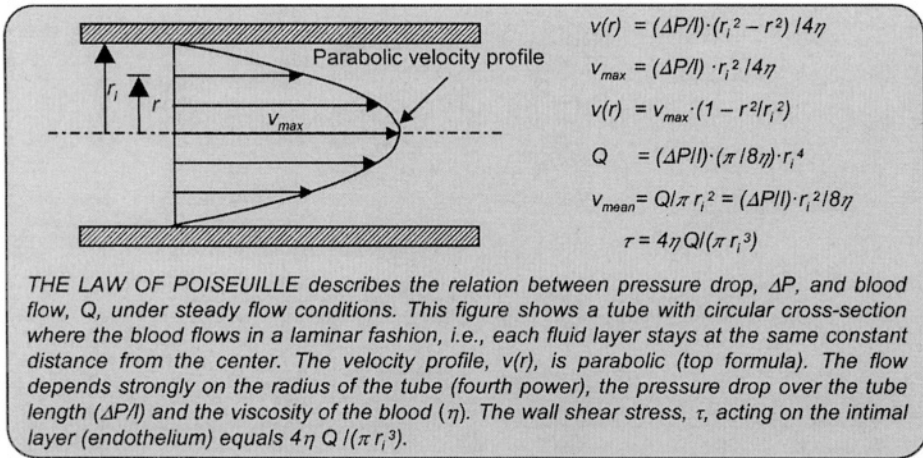
Low hematocrit, as in anemia, decreases oxygen content and viscosity of blood. The former lowers oxygen supply and the latter increases blood flow thus increasing supply. Inversely, polycythemia increases oxygen content but lowers blood flow. At high altitude, where oxygen tension is lower and thus oxygen saturation in the blood is lower, a larger hematocrit is advantageous. In endurance sports higher hematocrit is more efficacious during increased oxygen demand. This is the reason EPO is sometimes used by the athletes.

## References

1. Merrill EW. Rheology of blood. *Physiol Rev* 1969;49:863-888.
2. Scott Blair GW, Spanner DC. *An introduction to biorheology*. 1974, Amsterdam, Elsevier Sc Publ.

## Chapter 2

## LAW OF POISEUILLE



### Description

With laminar and steady flow through a uniform tube of radius  $r_i$  the velocity profile over the cross-section is a parabola. The formula that describes the velocity ( $v$ ) as a function of the radius,  $r$  is:

$$v_r = \frac{\Delta P \cdot (r_i^2 - r^2)}{4 \cdot \eta \cdot l}$$

$\Delta P$  is the pressure drop over the tube of length ( $l$ ), and  $\eta$  is blood viscosity. At the axis ( $r = 0$ ), velocity is maximal,  $v_{max}$ , while at the wall ( $r = r_i$ ) the velocity is zero. Mean velocity is:

$$v_{mean} = \frac{\Delta P \cdot r_i^2}{8 \cdot \eta \cdot l}$$

and is found at  $r \approx 0.7 r_i$ .

Blood flow ( $Q$ ) is mean velocity times the cross-sectional area of the tube,  $\pi r_i^2$ , giving:

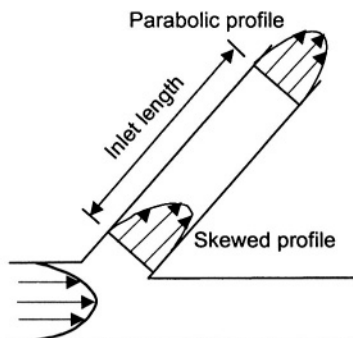
$$Q = \frac{\Delta P \cdot \pi \cdot r_i^4}{8 \cdot \eta \cdot l}$$

This is Poiseuille's law relating the pressure difference,  $\Delta P$ , and the steady flow,  $Q$ , through a uniform (constant radius) and stiff blood vessel. Hagen, in 1860, theoretically derived the law and therefore it is sometimes called the law of Hagen-Poiseuille. The law can be derived from very basic physics (Newton's law) or the general Navier-Stokes equations.

The major assumptions for Poiseuille's law to hold are:

- The tube is stiff, straight, and uniform

- Blood is Newtonian, i.e., viscosity is constant
- The flow is laminar and steady, not pulsatile, and the velocity at the wall is zero (no slip at the wall).



**INLET LENGTH.** Flow entering a side branch results in skewed profile. It takes a certain inlet length before the velocity develops into a parabolic profile again.

Reynolds number is about 500 and diameter 0.6 cm giving an inlet length of ~18 cm. In other, more peripheral arteries the inlet length is much shorter but their length is shorter as well. Clearly, a parabolic flow profile is not even approximated in the arterial system. Nevertheless, the law of Poiseuille can be used as a concept relating pressure drop to flow.

A less detailed and thus more general form of Poiseuille's law is  $Q = \Delta P/R$  with resistance  $R$  being:

$$R = 8\eta \cdot l/\pi r_i^4$$

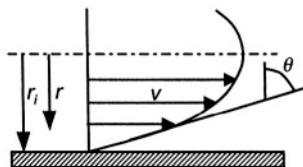
This law is used in analogy to Ohm's law of electricity, where resistance equals voltage drop/current. The analogy is that voltage difference is compared to pressure drop and current to volume flow. In hemodynamics we call also it Ohm's law. Thus:

$$\Delta P/Q = R$$

This means that resistance can be calculated from pressure and flow measurements.

#### Calculation of wall shear stress

The wall shear rate can be calculated from the slope of the velocity profile near the wall (angle  $\theta$  in the figure above), which relates to the velocity gradient,  $\tan \theta = dv/dr$ , near the wall (see Chapter 1). The derivative of the velocity profile gives the shear rate  $\gamma = (\Delta P/l) \cdot r/2\eta$ . Shear stress is shear rate times viscosity  $\tau = (\Delta P/l) \cdot r/2$ . The shear rate at the vessel axis,  $r = 0$ , is zero, and at the wall,  $r = r_i$ , it is  $\tau = (\Delta P/l) \cdot r_i/2$ , so the blood cells encounter a range of shear stresses and shear rates over the vessel's cross-section.



**THE SHEAR RATE** at the wall of a blood vessel can be calculated from the 'rate of change of velocity' at the wall, as indicated by angle  $\theta$ .

In curved vessels and distal to branching points the velocity profile is not parabolic and the blood flow profile needs some length of straight tube to develop, this length is called inlet length. The inlet length depends on the Reynolds number ( $Re$ , see Chapter 4) as:

$$l_{inlet}/D \approx 0.06 Re$$

with  $D$  vessel diameter. For the aorta mean blood flow is about 6 l/min, and the diameter 3 cm, so that the mean velocity is ~ 15 cm/s. The Reynolds number is therefore ~ 1350. This means that  $l_{inlet}/D$  is ~ 80, and the inlet length ~240 cm, which is much longer than the length of the entire aorta. In the common iliac artery the

Reynolds number is about 500 and diameter 0.6 cm giving an inlet length of ~18 cm. In other, more peripheral arteries the inlet length is much shorter but their length is shorter as well. Clearly, a parabolic flow profile is not even approximated in the arterial system. Nevertheless, the law of Poiseuille can be used as a concept relating pressure drop to flow.

A less detailed and thus more general form of Poiseuille's law is  $Q = \Delta P/R$  with resistance  $R$  being:

$$R = 8\eta \cdot l/\pi r_i^4$$

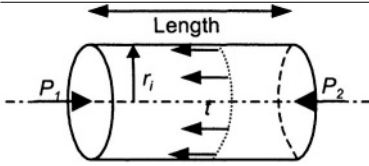
This law is used in analogy to Ohm's law of electricity, where resistance equals voltage drop/current. The analogy is that voltage difference is compared to pressure drop and current to volume flow. In hemodynamics we call also it Ohm's law. Thus:

$$\Delta P/Q = R$$

This means that resistance can be calculated from pressure and flow measurements.

#### Calculation of wall shear stress

The wall shear rate can be calculated from the slope of the velocity profile near the wall (angle  $\theta$  in the figure above), which relates to the velocity gradient,  $\tan \theta = dv/dr$ , near the wall (see Chapter 1). The derivative of the velocity profile gives the shear rate  $\gamma = (\Delta P/l) \cdot r/2\eta$ . Shear stress is shear rate times viscosity  $\tau = (\Delta P/l) \cdot r/2$ . The shear rate at the vessel axis,  $r = 0$ , is zero, and at the wall,  $r = r_i$ , it is  $\tau = (\Delta P/l) \cdot r_i/2$ , so the blood cells encounter a range of shear stresses and shear rates over the vessel's cross-section.



SHEAR STRESS at the wall can also be calculated directly by the balance of pressure and frictional forces.

The shear stress at the wall can also be calculated from basic principles. For an arterial segment of length  $l$ , the force resulting from the pressure difference  $(P_1 - P_2) = \Delta P$ , times the cross-sectional area,  $\pi r_i^2$ , should equal the opposing force generated by friction. This frictional force on the wall equals the shear stress,  $\tau$ , times the lateral surface,  $2\pi r_i \cdot l$ . Equating these

forces gives  $\Delta P \cdot \pi r_i^2 = \tau \cdot 2\pi r_i \cdot l$ , and

$$\tau = (\Delta P / l) \cdot (r_i / 2)$$

This formulation shows that with constant perfusion pressure an increase in viscosity does not affect wall shear stress.

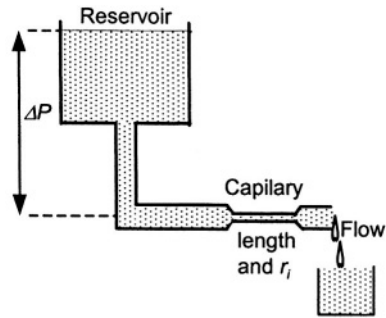
The wall shear stress may also be expressed as a function of volume flow using Poiseuille's law

$$\tau = 4\eta \cdot Q / \pi r_i^3$$

this is a more useful formula for estimating shear stress because flow and radius can be measured noninvasively using ultrasound or MRI, whereas pressure gradient cannot.

*Example of the use of Poiseuille's law to obtain viscosity*

A relatively simple way to obtain viscosity is to use a reservoir that empties through a capillary. Knowing the dimensions of the capillary and using Poiseuille's law viscosity can be calculated. Even simpler is the determination of viscosity relative to that of water. In that case only a beaker and stopwatch are required. The amounts of blood and water obtained for a chosen time are inversely proportional to their viscosities. The practical design based on this principle is the Ostwald viscometer.



A WIDE BORE RESERVOIR maintaining constant pressure, provides the blood flow through a capillary. The application of Poiseuille's law, or comparison with water, gives absolute or relative viscosity, respectively.

*Murray's law*

Murray' law (1926) was originally proposed by Hess in 1913 and assumes that the energy required for blood flow and the energy needed to maintain the vasculature is assumed minimal [1]. The first term equals pressure times flow and, using Poiseuille's law, this is  $P \cdot Q = Q^2 \cdot 8 \cdot \eta \cdot l / \pi r_i^4$ . The second term is proportional to vessel volume and thus equals  $b \cdot \pi r_i^2 \cdot l$ , with  $b$  a proportionality constant. The total energy,  $E_m$ , is:

$$E_m = Q^2 \cdot 8 \eta \cdot l / \pi r_i^4 + b \cdot \pi r_i^2 \cdot l$$

The minimal value is found for  $dE_m/dr = 0$  and this leads to:

$$Q = (\pi/4l) \cdot (b/\eta)^{0.5} \cdot r_i^3 = k \cdot r_i^3$$

For a bifurcation it holds that

$$Q_{mother} = Q_{daughter1} + Q_{daughter2}$$

and thus

$$r^3_{mother} = r^3_{daughter1} + r^3_{daughter2}$$

with two equal daughters it holds that:

$$r^3_{mother} = 2 \cdot r^3_{daughter}$$

and we find that

$$r_{daughter} = (\frac{1}{2})^{1/3} r_{mother} \approx 0.79 r_{mother}$$

The area of both daughters together is  $2 \cdot 0.79^2 \approx 1.25$  the area of the mother vessel. This area ratio is close to the area ratio predicted by Womersley on the basis of the oscillatory flow theory, to obtain minimal reflection of waves at a bifurcation, namely between 1.15 and 1.33 [2]. Thus Murray's law suggests a minimal size of blood vessels and an optimum bifurcation [1].

### Physiological and clinical relevance

The more general form of Poiseuille's law given above, i.e.,  $Q = \Delta P/R$  allows us to derive resistance,  $R$ , from mean pressure and mean flow measurement.

The wall shear stress, i.e., the shear force on the endothelial cells plays an important role in short term, second to minutes, and long term, weeks, months or years, effects. Short-term effects are vasomotor tone and flow mediated dilatation (FMD). Long-term effects are vascular remodeling, endothelial damage, changes in barrier function, and atherosclerosis.

It is still not possible to directly measure wall shear stress or shear rate *in vivo*. Shear rate is therefore derived from the velocity profile. Velocity profiles can be measured with MRI and Ultrasound Doppler. From the velocity profile the velocity gradient is often calculated. However, the calculations to obtain shear rate require extrapolation, because very near the wall velocity measurements are not possible. To calculate wall shear stress the blood viscosity near the wall has to be known as well, but viscosity close to the wall is not known because of plasma skimming. Plasma skimming refers to the relative absence of erythrocytes in the region near the wall. Also the diameter variation over the heartbeat is almost impossible to account for.

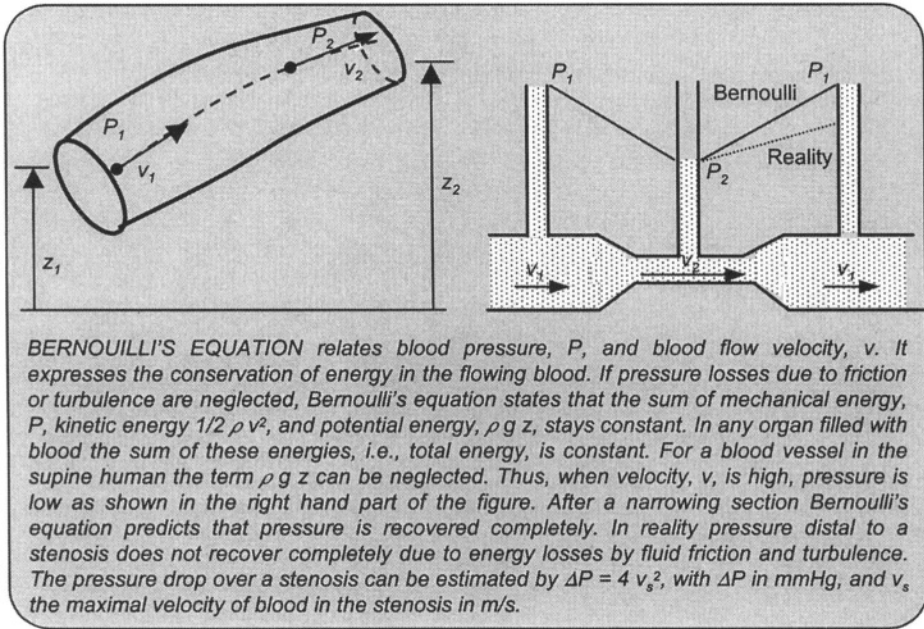
Wall shear stresses are  $\sim 10 - 20 \text{ dynes/cm}^2$ , which is about 10,000 times less than the hoop stress (Chapter 9). Despite this enormous difference in magnitude, both stresses are equally important in the functional wall behavior in physiological and pathological conditions (see Chapters 27 and 28).

### References

1. Weibel E. *Symmorphosis*. 2000, Cambridge MA, Harvard Univ Press.
2. Womersley JR. *The mathematical analysis of the arterial circulation in a state of oscillatory motion*. 1957, Wright Air Dev. Center, Tech Report WADC-TR-56-614.

## Chapter 3

## BERNOULLI'S EQUATION



### Description

The Bernoulli equation can be viewed as an energy law. It relates blood pressure ( $P$ ) to flow velocity ( $v$ ). Bernoulli's law says that if we follow a blood particle along its path (dashed line in left figure in the box) the following quantity remains constant:

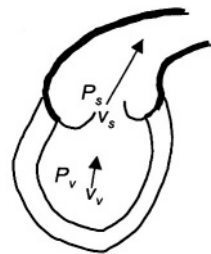
$$P + \frac{1}{2} \rho v^2 + \rho g z = \text{constant}$$

where  $\rho$  is blood density,  $g$  the acceleration of gravity and  $z$  the elevation with respect to a reference horizontal surface (i.e., ground level or heart level). The equation of Bernoulli says that as a fluid particle flows, the sum of the hydrostatic pressure,  $P$ , potential energy,  $\rho g z$ , and the dynamic pressure or kinetic energy,  $\frac{1}{2} \rho v^2$ , remains constant. One can easily derive Bernoulli's equation from Newton's law: Pressure forces + gravitational forces = mass  $\times$  acceleration. Strictly speaking, the Bernoulli equation is applicable only if there are no viscous losses and blood flow is steady.

### Physiological and clinical relevance

Bernoulli's law tells us that when a fluid particle decelerates pressure increases. Conversely, when a fluid particle accelerates, such as when going through a severe stenosis, pressure drops.

Because of the direct relationship between pressure and velocity, the Bernoulli equation has found several interesting clinical applications, such as the Gorlin [2]



**PRESSURES,  $P_v$  and  $P_s$ , and velocities,  $v_v$  and  $v_s$ , in ventricular lumen and valvular stenosis.**

equation for estimating the severity of an aortic or mitral valve stenosis. Let us consider flow through a stenosed valve according to the figure on the previous page.

*Applying Bernoulli's law*

$$P_v + \frac{1}{2} \cdot \rho \cdot v_v^2 = P_s + \frac{1}{2} \cdot \rho \cdot v_s^2$$

and

$$P_v - P_s = \frac{1}{2} \cdot \rho \cdot (v_s^2 - v_v^2)$$

The flow  $Q$  is the same at both locations, thus  $A_v \cdot v_v = A_s \cdot v_s = Q$ , where  $A_v$  and  $A_s$  are the cross-sectional areas of ventricle and valve, respectively. Substituting this into the Bernoulli's equation we obtain:

$$\Delta P = P_v - P_s = \frac{1}{2} \cdot \rho \cdot Q^2 \cdot (1/A_s^2 - 1/A_v^2)$$

Since the cross-sectional area of the stenosed valve  $A_s$  is much smaller than the cross-sectional area of the ventricle ( $A_s \ll A_v$ ), the equation can be simplified to:

$$\Delta P = \frac{1}{2} \cdot \rho \cdot Q^2 / A_s^2 = \frac{1}{2} \cdot \rho \cdot v_s^2$$

When velocity in the stenosis,  $v_s$ , is expressed in m/s the pressure drop ( $P$ , in mmHg) is approximately  $4 \cdot v_s^2$ .

Earlier this approach was used to approximate to estimate effective area [2],  $A_s$ , of the valvular stenosis by measuring flow and pressure gradient (e.g., using a pressure wire).

$$A_s = Q \sqrt{\frac{\rho}{2\Delta P}}$$

When the pressure is in mmHg and flow in ml/s, this gives an effective area:  $A_s$  (in  $\text{cm}^2$ ) =  $0.02 \cdot Q / \sqrt{\Delta P}$ . If pressure recovery downstream of the vena contracta is included then:  $A_s = 0.0225 \cdot Q / \sqrt{\Delta P} = Q / (44 \sqrt{\Delta P})$ , [3].

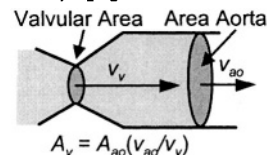
*Calculation of aortic valvular area*

Doppler velocimetry applied to both the valvular annulus and the aorta allows for the direct calculation of valve area. Since volume flow is the same, the product of velocity and area is also the same at both locations. Thus

$$A_{\text{valve}} = A_{\text{aorta}} \cdot v_{\text{aorta}} / v_{\text{valve}}$$

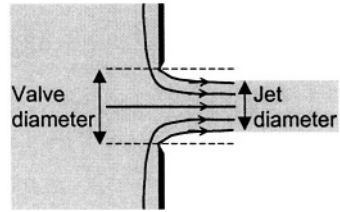
*Jets*

Jets and vena contracta are formed when blood flow emerges from an opening such as a valve, and play a role in valvular stenosis and regurgitation (see figure on the next page). The contraction coefficient, i.e., the area ratio of the jet and the valve depends on the shape of the valve. The coanda effect is the phenomenon that a jet along the, atrial or ventricular, wall appears



AORTIC VALVE AREA can be derived from Doppler velocity measurements, in aorta and valve, and aortic area.

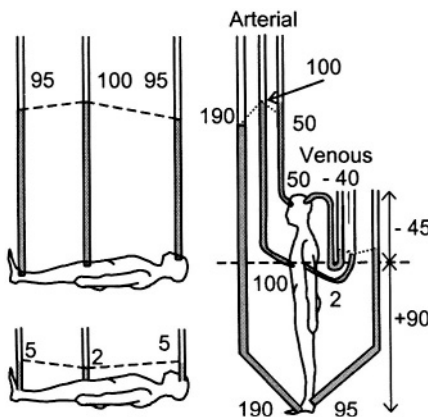
smaller than a free jet. Estimation of valvular area from the jet area is therefore not straightforward. Computational flow dynamics, i.e., the numerical solution of the Navier-Stokes equations, allows the calculation flow velocity in complex geometries and makes it possible to learn more about jets.



*VENA CONTRACTA effect is the result of the inability of the fluid to turn a sharp corner. The contraction coefficient  $A_{jet}/A_{valve}$  depends on the anatomical shape.*

### *Kinetic energy*

Bernoulli's equation pertains to conservation of energy. The term  $\frac{1}{2} \cdot \rho \cdot v^2$  is the kinetic energy. At peak systole ( $P = 130$  mmHg), the blood flowing in the lower abdominal aorta with a velocity  $v = 1$  m/s hits the wall of the apex of the iliac bifurcation. When it would come to a rest, velocity is negligible ( $v = 0$ ). On the basis of the Bernoulli equation this implies a pressure rise of  $\frac{1}{2} \cdot \rho \cdot v^2 = \frac{1}{2} \cdot 1060 \cdot 1^2 = 530 \text{ N/m}^2 \approx 0.5 \text{ kPa}$ . With  $1 \text{ kPa} = 7.5 \text{ mmHg}$ , this pressure due to flow deceleration is thus about 3.5 mmHg.



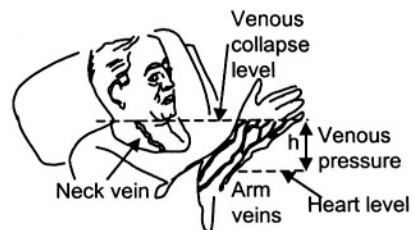
*EFFECT OF POSTURE on arterial and venous pressures (estimates, in mmHg). Effect of level is given by the hydrostatic pressure  $\rho g h$ , with  $\rho$  blood density,  $g$ , acceleration of gravity, and  $h$  height difference  $z_1 - z_2$ . Dashed line indicates the heart level. Adapted from [1], used by permission.*

since the arterial system is rather stiff. The venous pooling of blood reduces cardiac filling and therefore has a, temporary, effect on the pump function of the heart. The capillary transmural pressure increase gives rise to edema formation.

When a person is lying in a reclined position the venous pressure can be estimated in the veins of the neck and

### *The hydrostatic pressure*

Most measurements are performed in the supine position. However, most activity takes place in the standing position. The figure shows the pressures in the arterial and venous systems when a person is in the supine and the (motionless) standing position. It may be seen that the arterio-venous pressure gradients are not much affected. Thus the driving forces for the flow are not much different in the two positions. The transmural pressures are strongly different and this mainly has an effect on the venous and capillary systems

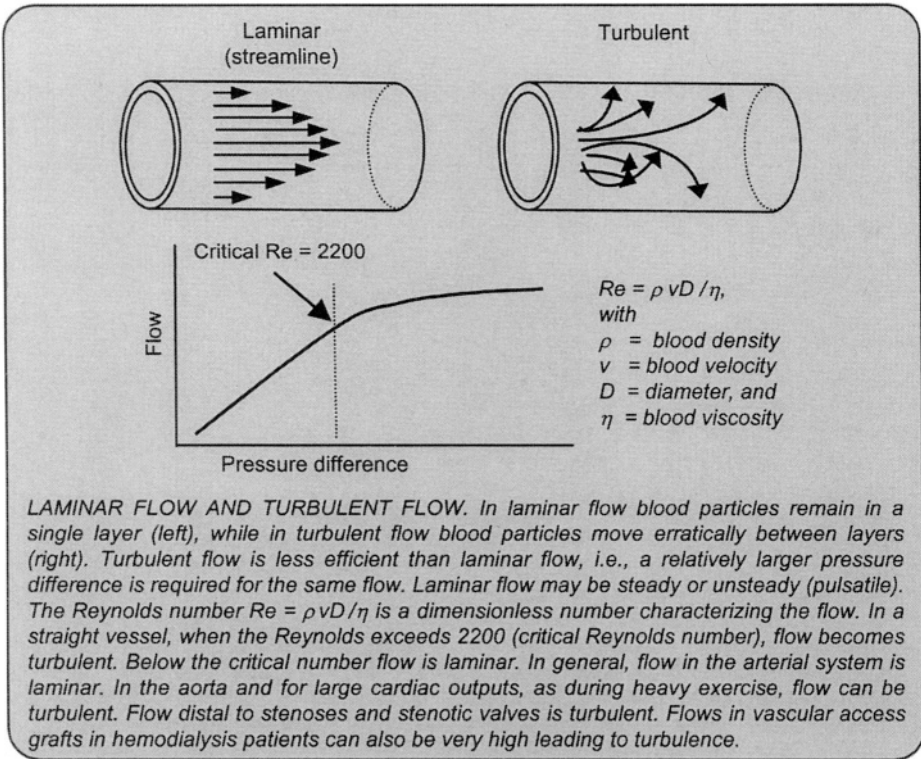


*ESTIMATION OF VENOUS PRESSURE by collapse. The level above the heart where collapse takes place,  $h$ , is measured in cm. The venous pressure is then  $h/1.33$  mmHg. Adapted from [1], used by permission.*

hand. The height difference between the point of collapse of superficial veins and the heart, is the venous pressure. If the height difference is  $z$  in cm, the venous pressure can be calculated as  $\rho \cdot g \cdot z = 1.05 \cdot 980 \cdot z$  dynes/cm<sup>2</sup> or  $1.05 \cdot 980 \cdot z / 1360 = z / 1.33$  mmHg.

### References

1. Burton AC. *Physiology and Biophysics of the Circulation*. 1972, Chicago, Year Book Medical Publ., 2nd edn.
2. Gorlin R, Gorlin SG. Hydraulic formula for calculations of the area of the stenotic mitral valve value, orthocardiac values and central circulating shunts. *Am Heart J* 1951;41:1-29.
3. Wilkinson JL. Haemodynamic calculations in the catheter laboratory. *Heart* 2001; 85:113-120.



**Description**

When flow in a straight cylindrical pipe is relatively low, fluid particles move smoothly in concentric layers. This type of flow is called laminar flow. The relation between the pressure gradient and flow is linear and described by Poiseuille’s law (box figure, left). As flow becomes increasingly larger, the smooth parallel fluid motion becomes wavy, leading to vortices propagated downstream, subsequently the number of vortices increases and finally fluid motion becomes irregular [2]. This irregular and seemingly random fluid particle motion is called turbulence. Turbulent flow is energetically more costly than laminar flow, because part of the mechanical energy used to maintain flow (i.e., pressure gradient) is lost in the erratic motion between the fluid particles. The resistance to flow is thus higher, which is reflected by the change in slope in the relation between pressure drop and flow (box figure).

To judge whether a fluid flow is laminar or turbulent, the Reynolds number,  $Re$ , is often used.  $Re$  is defined as  $Re = \rho \cdot v \cdot D / \eta$ , with  $\rho$  the fluid density,  $v$  the mean fluid velocity,  $D$  the tube inner diameter and  $\eta$  fluid viscosity. The Reynolds number is the ratio of inertia and viscous effects. For low Reynolds numbers the viscous effects are dominant and laminar flow exists. Thus, it is not only the fluid velocity that determines whether or not the flow is laminar, but tube size, viscosity and blood density also play a role.

There exists a transitional zone around critical Reynolds number of 2200 where flow is neither strictly laminar nor strictly turbulent. Also when flow is

slowly increased turbulence may start at Reynolds numbers somewhat higher than 2200 and, inversely, when flow is decreased from a turbulent case it may remain turbulent for Reynolds numbers smaller than 2200. In some hemodynamic texts the radius is used instead of the diameter; the critical Reynolds number is then 1100.

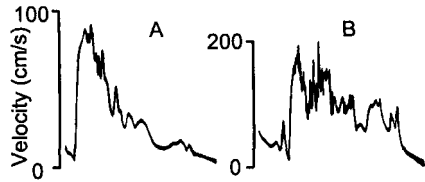
### Physiological and clinical relevance

At normal resting conditions arterial flows are laminar. For instance, in the human aorta at rest with a Cardiac Output,  $CO$ , of 6 l/min the Reynolds number can be calculated as follows. Mean velocity  $v = CO/\pi r_i^2$  and with an  $r_i = 1.5$  cm it equals about  $6000/(60 \cdot \pi \cdot 1.5^2) \approx 15$  cm/s. The Reynolds number is then, assuming blood density to be  $1.06$  g/cm<sup>3</sup> and blood viscosity to be  $3.5$  cP:  $Re = v \cdot D \cdot \rho / \eta = 1.06 \cdot 15 \cdot 2 \cdot 1.5 / 0.035 \approx 1350$ . This Reynolds number is far below the critical number of 2200 and thus flow is laminar. With heavy exercise, where flow can increase by a factor of 5 or so, the Reynolds number increases to values above 2200 and turbulence occurs.

The criterion for transition to turbulence, i.e.,  $Re > 2200$  applies to steady flow in straight tubes. Because arterial flows are highly pulsatile, this criterion does not strictly apply. For pulsatile flow laminar flow persists longer and transition to turbulence takes place at higher Reynolds numbers.

Turbulence is delayed when the fluid is accelerating whereas transition to turbulence occurs faster in decelerating flows. Loss of pressure due to turbulence is an effective means to decelerate flow fast. A classical example is turbulence distal to a stenosis. Fluid particles, which have been accelerated through the converging part of the stenosis need to decelerate fast in the distal expanding part, flow separates and turbulence develops. Turbulence in severe stenoses can be initiated for Reynolds numbers as low as 50.

Turbulence may affect endothelial function and play an important role in certain pathologies. For example, it has been suggested that turbulence distal to stenoses contributes to the phenomenon of post-stenotic dilatation. Aortic dilatation in valvular stenosis is also known to exist. Also, turbulence occurring at the venous anastomoses of vascular access grafts used in hemodialysis patients has been correlated with the local development of intima hyperplasia, which ultimately leads to a stenosis and graft failure.



*TURBULENCE* evidenced as rapid fluctuation in the aortic velocity signal measured in (A) a patient with normal aortic valve and a normal cardiac output of 5.3 l/min, and (B) a patient with normal aortic valve but with an elevated cardiac output of 12.9 l/min. Turbulence is much more present and intense in the case of high aortic flow. Adapted from [1], used by permission.

### References

1. Nichols WW, O'Rourke MF. *McDonald's blood flow in arteries*. 1990, London, Edward Arnold, 3rd edn.
2. Munson BR, Young DF, Okiishi TH. *Fundamentals of Fluid mechanics*. 1994, New York, John Wiley & Sons.

# Chapter 5

# ARTERIAL STENOSIS

$\Delta P$   
 $l_s$   
 $Q$     $A_0$     $A_s$

$$\Delta P = \frac{8\pi \cdot \eta \cdot l_s}{A_s^2} \cdot Q + \frac{K_t \cdot \rho}{2A_0^2} \cdot [A_0/A_s - 1]^2 \cdot Q^2$$

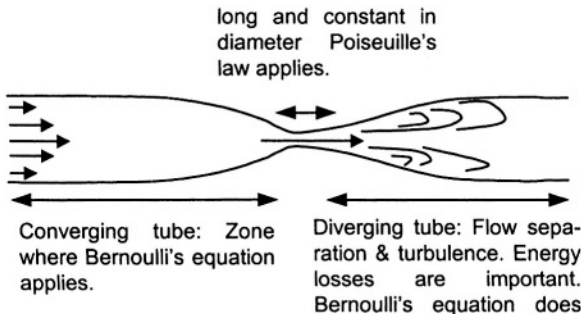
$$\Delta P = a_1 Q + a_2 Q^2$$

*Aortic coarctation and arterial stenosis is a localized narrowing in the arterial lumen, typically a result of atherosclerosis. A stenosis is quantified by the ratio  $A_s/A_0$ , called the area ratio, often expressed as % area occlusion, given as  $(1 - A_s/A_0) \cdot 100$ . The relation between pressure drop across the stenosis,  $\Delta P$ , and flow,  $Q$ , is quadratic, which means that stenotic resistance increases with flow. The linear term in the pressure drop-flow equation accounts for the viscous losses within the stenosis, whereas the quadratic term accounts for losses due to turbulence. In severe stenoses (area occlusion higher than 85%), turbulent losses dominate. Severe stenoses add significant resistance to flow and can be potentially harmful by preventing adequate blood supply to distal beds.*

## Description

Stenosis, from the Greek term for ‘narrowing’, is a medical term used to describe a localized constriction in an artery. Stenoses are usually caused by the development of atheromatous plaques in the subintimal layer of the arterial wall, which subsequently protrude into the lumen of the artery, thus causing a narrowing to the free passage of blood.

A coarctation or arterial stenosis is a combination of a converging section, a narrow section, the stenosis, and a diverging section. In the converging section Bernoulli’s equation holds (see Chapter 3). Within the narrow section Poiseuille’s law is assumed to apply, provided that this narrow section is long enough with approximately constant diameter. In the diverging section flow separates and is often turbulent with significant viscous losses, which means that in this region neither Bernoulli’s nor Poiseuille’s law applies.

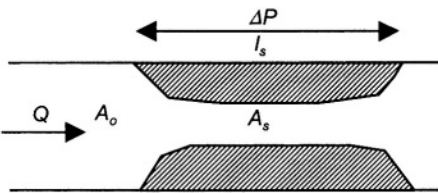


*A COARCTATION consists of a converging section, a narrow section and a diverging section, each with their particular pressure-flow relations.*

Pressure losses over a coarctation can be treated through semi-empirical relations. Such a relationship was developed by Young & Tsai [4] who performed a series of experiments of steady and pulsatile flows in models of concentric and eccentric stenosis. Young and Tsai found that the pressure

drop,  $\Delta P$ , across an arterial stenosis can be related to flow,  $Q$ , through the following relation:

$$\Delta P = \frac{8\pi \cdot \eta \cdot l_s}{A_s^2} \cdot Q + \frac{K_t \cdot \rho}{2A_0^2} \cdot [A_0 / A_s - 1]^2 \cdot Q^2 = a_1 Q + a_2 Q^2$$



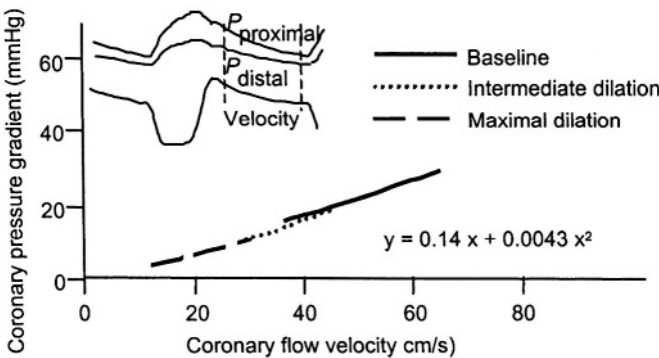
A STENOSIS or COARCTATION is quantified by the ratio  $A_s/A_0$ , called the area ratio, and the stenosis length,  $l_s$ . In practice, the severity of a stenosis is expressed as % area occlusion, given as  $(1 - A_s/A_0) \cdot 100$ . Sometimes diameter is used instead of area.  $K_t$  is an empirical coefficient approximately equal to 1.5. The equation is derived for steady flow, but for oscillatory pressure-flow relations a similar equation holds [2].

where  $A_0$  is the unobstructed cross-sectional lumen area and  $A_s$  the minimal free cross-sectional lumen area within the coarctation. The first term of the stenosis equation accounts for the viscous losses as blood flows through the narrow coarctation lumen. It is essentially Poiseuille's law for the flow through the stenosed part. The second term accounts for the pressure losses distal to the stenosis and it is derived from the mechanics of flow in a tube with an abrupt expansion. The

**Physiological and clinical relevance**

The empirical formula for the pressure drop across a stenosis shows that both flow and area appear as quadratic terms. This is an important aspect of the hemodynamics of a coarctation. This can best be discussed assuming the stenosis length,  $l_s$ , to be small so that the first term in the equation above,  $a_1 \cdot Q$ , is negligible.

The pressure drop is proportional to the flow squared while in laminar



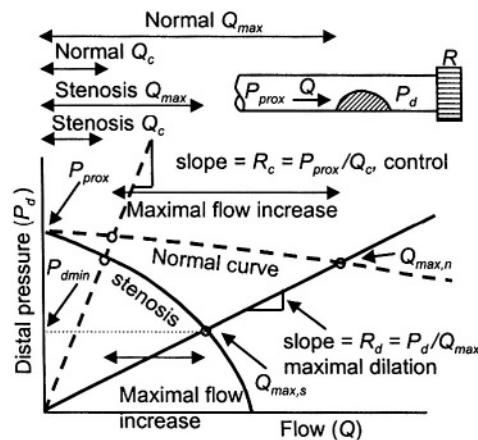
*PRESSURE DROP OVER A CORONARY STENOSIS, as a function of blood velocity. The relations pertain to diastole and the range of velocities is obtained by vasodilation of the distal vasculature. The quadratic expression can be applied. Adapted from [1], used by permission.*

flow the pressure drop is proportional to the flow. Suppose that a patient with a mild coarctation in the femoral artery has, at rest, a pressure drop over the narrowed section of 10 mmHg. When the patient starts walking and the peripheral bed dilates to allow for more perfusion flow the pressure drop increases.

When flow needs to increase by a factor three the pressure gradient would become  $10 \cdot 3^2 = 90$  mmHg. This is clearly impossible and the decrease in peripheral resistance of the leg does not help to increase flow sufficiently.

The pressure drop is inversely related to the square of the cross-sectional area in the stenosis. For a 80% area stenosis, the term  $[A_0/A_s - 1]^2$  equals  $[1/0.2 - 1]^2 = 16$ , whereas for a 90% stenosis this term increases to 81. Thus a 90% stenosis is 81/16 or about 5 times more severe than an 80% stenosis in terms pressure drop for a similar flow. This strongly nonlinear effect means that complaints from ischemia (e.g., exercise induced stable angina pectoris) will arise 'suddenly' when the narrowing becomes more severe, typically for a stenosis of 60-70%.

From Bernoulli's equation it follows that at high velocity pressure is low (Chapter 3). This implies that when flow and thus velocity is high, as is the case during vasodilation, the pressure in the narrow section may decrease to low values. For stenoses with compliant walls the decrease transmural pressure may lead to extra narrowing, thereby worsening the situation.



*Flow reserve*

Angiographic data often do not give accurate information about the functional aspects of a stenosis or coarctation. This has led several investigators to propose methods to obtain a quantitative description in functional terms. One approach is the determination of flow reserve. The absolute, flow reserve is defined as the ratio of flow during maximal dilatation and control flow ( $Q_{max} / Q_c$ ). In the figure, pressure distal to a stenosis,  $P_d$ , is plotted as a function of flow. Proximal pressure is assumed to be constant. It is apparent that when the periphery dilates, i.e., the peripheral resistance decreases from  $R_c$  to  $R_d$ , the flow increases. However, in the presence of a severe stenosis, distal pressure is decreased, and this decrease is accentuated when flow is high (lower curve in the figure). This means that while in control conditions flow is hardly affected by the presence of stenosis, at maximal vasodilation a severe stenosis limits maximal flow  $Q_{max}$

*FLOW RESERVE* is defined as the ratio of flow during maximal vasodilation to flow during control,  $Q_{max} / Q_c$ , and this ratio is much lower with a stenosis present than in the normal bed. In this figure distal pressure is plotted as a function of flow. When the periphery bed undergoes a maximal vasodilation, peripheral resistance decreases from  $R_c$  to  $R_d$  and flow increases, but distal pressure decreases. The decrease in distal pressure limits the maximal flow under vasodilation, thereby reducing the flow reserve. Thus, the flow reserve depends on the stenosis severity and both the peripheral resistance in control and after maximal dilation. The Fractional Flow Reserve, FFR, is the ratio of the maximal flow with the stenosis present and maximal flow in the unaffected bed,  $Q_{max,s} / Q_{max,n}$ . The FFR depends on the stenosis severity and how much the distal bed can dilate. The FFR is close to the ratio of the distal pressure and proximal pressure,  $P_{dmin} / P_{prox}$ . The, nonlinear, relation between pressure drop over the stenosis and flow through it,  $(P_{prox} - P_d) / Q$ , depends on the stenosis severity only.

considerably. In other words, in presence of stenosis, maximal flow is not determined by the vasodilation of the periphery alone, but by both the stenosis and the microvasculature.

### *Fractional Flow reserve*

Another estimate of stenosis severity is the Fractional Flow Reserve, FFR, which is the ratio of the maximal flow,  $Q_{max,s}$  in the bed perfused by the stenosed artery and the maximal flow in a normal, unstenosed area,  $Q_{max,n}$ . The FFR is thus

$$FFR = [(P_d - P_v)/R_{st}]/[(P_{prox} - P_v)/R_n] \cong P_d/P_{prox}$$

with  $P_d$  being the distal pressure during maximal dilation, and  $P_{prox}$  the proximal pressure. For coronary stenoses the proximal pressure equals aortic pressure. Under the assumption that the microvascular bed of the stenosed area has the same resistance as the bed of the normal area and assuming that venous or intercept pressure is small with respect to  $P_d$  it holds that the FFR is close to the ratio  $P_d/P_{prox}$ . [3].

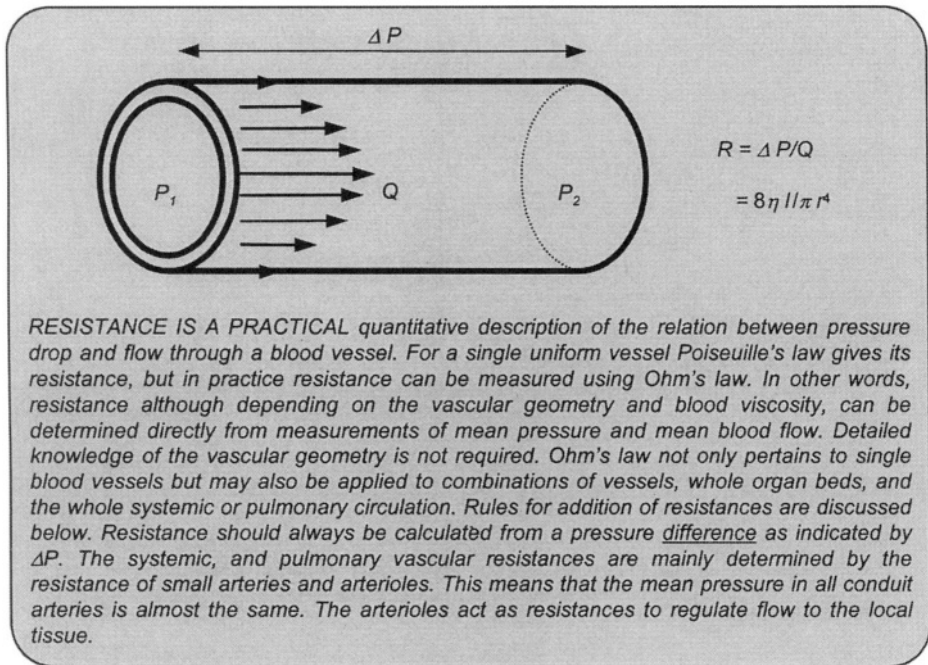
The cut-off value of the FFR is 0.74, i.e. for values higher than 0.74 the stenosis is not pathological. For segmented stenoses the approach is more complicated.

## **References**

1. Marques KM, Spruijt HJ, Boer C, Westerhof N, Visser CA, Visser FC. The diastolic flow-pressure gradient relation in coronary stenoses in humans. *J Am Coll Cardiol* 2002; 39:1630-1636.
2. Newman DL, Westerhof N, Sipkema P. Modelling of aortic stenosis. *J Biomech* 1979;12:229-235.
3. Pijls NHJ, De Bruyne B. *Coronary pressure*. 1997, Dordrecht & Boston, Kluwer Academic Publishers.
4. Young DF, Tsai FY. Flow characteristics in models of arterial stenoses: I Steady flow. *J Biomech* 1973;6:395-410.

## Chapter 6

## RESISTANCE



### Description

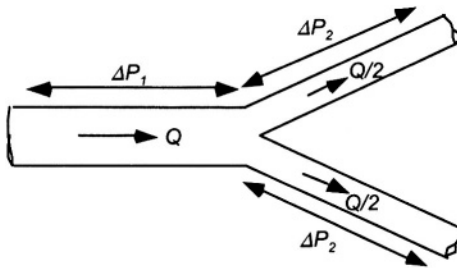
Poiseuille's law (Chapter 2) showed that resistance depends on the length and diameter of the vessel and the viscosity of blood. However, even for a single blood vessel, it is difficult to derive the relation between pressure and flow on the basis of Poiseuille's law. The diameter of the vessel needs to be accurately known because of the fourth power law. Furthermore, the vessel should be uniform, and, especially for small vessels, the anomalous properties of blood make it impossible to use a single number for viscosity. Accurate calculation of resistance on the basis of Poiseuille's law is therefore virtually impossible. However, resistance can be calculated from the ratio of the pressure gradient and flow constituting a practical experimental approach. Thus although Poiseuille's law makes it possible to arrive at several important conclusions regarding vascular function, in practice we use resistance, calculated using Ohm's law.

To understand where resistance is mainly located in the arterial tree we need to know some rules about resistances.

### Addition of resistances

Two resistances in parallel add up in a so-called 'inverse' fashion. When in parallel the pressure drop is the same over both vessels,  $\Delta P$ , and the two flows add up to total flow,  $Q_{total}$ . Thus  $Q_{total} = Q_1 + Q_2 = \Delta P / R_1 + \Delta P / R_2 = \Delta P(1/R_1 + 1/R_2) = \Delta P / R_{total}$ .

Thus we find



A BLOOD VESSEL, MOTHER, DIVIDES into two smaller, daughter vessels. We determine the resistance of this network by proper addition of the two distal vessels in parallel and then add the resistance of the mother vessel. Note that we work from the distal end.

pressure drop over two resistances in series is the sum of the individual pressure drops, i.e.,  $\Delta P_{total} = \Delta P_I + \Delta P_{II}$  and flow is the same through both. Thus  $\Delta P_{total} = Q \cdot R_I + Q \cdot R_{II} = Q \cdot (R_I + R_{II}) = Q \cdot R_{total}$ . Thus, in general,  $R_{total} = R_I + R_{II}$ , and the total resistance is the sum and thus larger than each individual resistance.

#### *Physical reason why the resistance is located in the arterioles*

We first compare the resistance of the aorta with the resistance of an arteriole using Poiseuille's law. Assuming an aortic radius of 15 mm and an (arbitrary) length of 50 cm and an arteriole with a radius of 7.5 micrometer and a length of 1 mm we can estimate the resistance ratio of these two. The radius ratio is 2000 and the length ratio 500, thus the resistance ratio is  $(2000)^4/500$ , i.e.,  $3.2 \cdot 10^{10}$ . Thus the resistance of a single arteriole is  $3.2 \cdot 10^{10}$  as large as that of a 50 cm long aorta.

However, there is only one aorta and about  $3 \cdot 10^8$  arterioles, and since these arterioles all sprout (indirectly) from the single aorta we can consider them as in parallel. Thus the total arteriolar resistance is about  $3.2 \cdot 10^{10}/3 \cdot 10^8 \approx 100$  times as large as the resistance of the aorta.

#### *Resistance of capillaries and veins*

Capillaries have diameters that are of the same order as arterioles but their number is larger (4 - 5 capillaries per arteriole) and therefore their resistance is about 4-5 times smaller. Recently it became clear that the glycocalyx, the carbohydrate structures on the luminal surface of the microvascular endothelial cells, not only protects against edema, but also reduces the effective capillary diameter and thus increases capillary resistance [2]. Still capillaries contribute little to total resistance.

Venules and veins have larger diameters than their accompanying arteries and often appear as two veins to one artery. Therefore, total venous resistance is about 1/20 of arteriolar resistance.

Thus, the total vascular resistance is mainly located in the small arteries and arterioles and is often called peripheral resistance.

$$R_{total} = 1/(1/R_I + 1/R_2)$$

An easier calculation is through conductance ( $G$ ), which is the inverse of resistance,  $G = 1/R$ . Ohm's law written in terms of conductance is  $Q = \Delta P \cdot G$ . Parallel conductances can be added directly:  $G_{total} = G_I + G_2$ . Thus 2 equal resistances in parallel add to a total resistance of half the resistance of each. Ten equal arterioles in parallel result in an overall resistance equal to 1/10 of that of a single arteriole.

Two resistances in series result in a total resistance equal to the sum of the resistances. This rule can be derived as follows. The total

### Calculation of vascular resistance

The total resistance of the systemic circulation can be calculated as follows. When mean aortic pressure is taken to be about 105 mmHg and central venous pressure is about 5 mmHg the pressure difference is 100 mmHg. With a Cardiac Output of 6 l/min, thus 100 ml/s, the total resistance is  $100/100 = 1$  mmHg/ml/s. The units mmHg/ml/s or mmHg·s/ml are called peripheral resistance units, PRU. Often physical units are used in the clinic and impedance is then expressed in  $\text{dyn}\cdot\text{s}\cdot\text{cm}^{-5}$ . As can be seen from Appendix 7 the following holds:  $7.5\cdot 10^{-9}$  mmHg·s/ml =  $10^{-5}$  dyn·s/cm<sup>5</sup> = 1 Pa·s/m<sup>3</sup>.

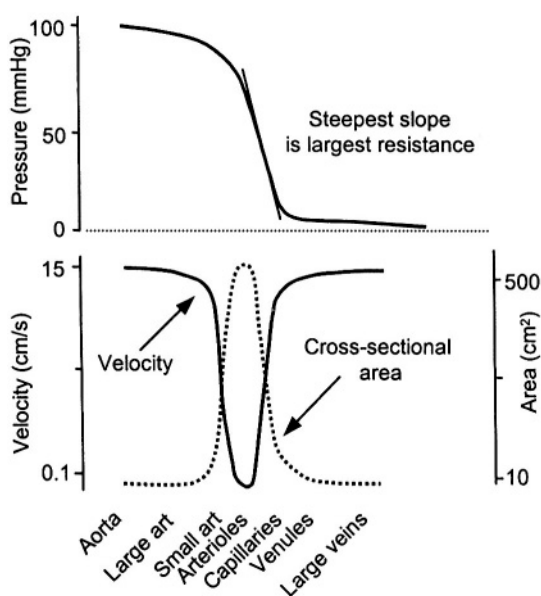
For the systemic circulation subtraction of venous pressure is often omitted without introducing large errors. However, in the pulmonary circulation with mean pulmonary artery pressure of about 20 mmHg and pulmonary venous pressure of 5 mmHg, calculation of the pressure difference is mandatory. Pulmonary resistance thus is  $(20 - 5)/100 = 0.15$  PRU, which is about 15% of the resistance of the systemic circulation.

### Physiological and clinical relevance

The small arteries and arterioles mainly determine peripheral resistance. Resistance can be regulated by the arterioles, because they are muscular arteries and it follows from Poiseuille's law that rather small changes in diameter result in large resistance changes. A 10% change in diameter corresponds to a change in resistance of about 50%.

The resistance of the aorta and conduit arteries is so low that the mean pressure hardly decreases from heart to the small peripheral arteries, the pressure drop being only a few mmHg. This means that in the supine human, mean blood pressure is practically the same in all conduit arteries, and therefore mean blood pressure may be determined in any conduit artery. This also implies that conduit arteries can be seen as a supply reservoir with peripheral resistances adjusting themselves such that demand of flow to the tissue is met.

When perfusion flow is high, e.g., during exercise, the large arteries could cause a sizable pressure drop. However, with increased flow conduit arteries dilate through 'Flow Mediated Dilation', FMD, to decrease their resistance. An FMD of 7% gives a resistance decrease of more than 30%.



PRESSURE, VELOCITY AND AREA distribution in the systemic circulation. Adapted from [1], used by permission.

Arterioles protect the capillaries from changes in pressure. Increased systemic pressure increases arteriolar resistance (autoregulation) and capillary pressure is maintained constant. Vascular smooth muscle tone is regulated by the nervous and hormonal systems and through autoregulation. Autoregulation is based on metabolic, myogenic, and endothelial effects. It is important to keep capillary pressure constant for the tissue fluid equilibrium, the Starling equilibrium.

The total cross-sectional area is the largest in capillaries. It is not correct to apply Poiseuille's law using total cross-sectional area. The area (radius) of individual vessels should be used to calculate resistance and then resistances must be added in series and in parallel according to the anatomy. The velocity of blood is lowest in the capillaries allowing ample time for exchange with the tissues.

#### *Low resistance of an arterio-venous fistula*

Several arterio-venous fistulas may exist, such as an open ductus arteriosus, and the fistula between the radial artery and vein made for dialysis. As an example, the latter shunt causes a low resistance in parallel with the resistance of the lower arm. However, the shunt does not always cause ischemia in the hand for the following reason (steal syndrome). The mean blood pressure in the aorta is 100 mmHg, and is in the radial artery normally about 3 mmHg lower, and thus 97 mmHg. The venous pressure is about 5 mmHg and in the vena cava pressure is 2 mmHg. The low resistance of the conduit arteries and veins will, with the much larger shunt flow, decrease arterial pressure by, say only 10 mmHg and increase the venous pressure by the same amount. The driving pressure for the hand is then  $87 - 15 = 72$  mmHg, which is high enough to avoid ischemia. The fistula will, however, lower the total systemic peripheral resistance and increase Cardiac Output thereby affecting cardiac function.

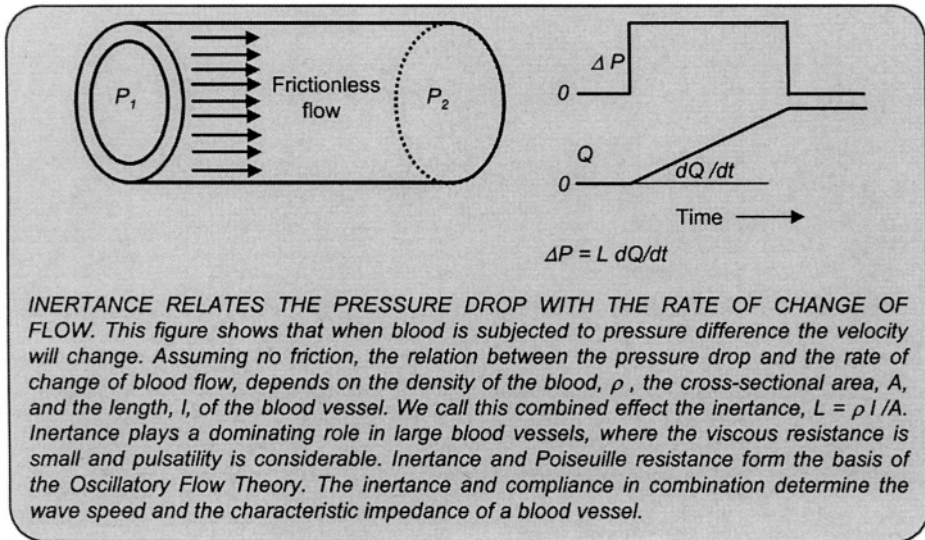
Qualitatively stated: the conduit arterial and venous systems can be viewed as pressure reservoirs, i.e. pressure is virtually independent of flow. Another way of stating this is that these systems are pressure sources, pressure is hardly affected by flow.

#### **References**

1. Berne RM, Levy MN, Koeppen BM, Stanton BA. *Physiology*. 2003, St Louis & Baltimore, Mosby-Elsevier, 5th edn.
2. Van den Berg BM, Vink H, Spaan JAE. The endothelial glycocalyx protects against myocardial edema. *Circ Res* 2003;92:592-594.

## Chapter 7

## INERTANCE



### Description

Blood is accelerated and decelerated with every heartbeat, and therefore the mass of the blood plays a role. The mass is density times volume, and the volume depends on the geometry of the blood vessel or heart. Blood density is a material property and is about  $1.06 \text{ g/cm}^3$ . In hemodynamics, we calculate the effective mass and call it inertance. Inertance connects the oscillatory pressure drop with the rate of change of blood flow.

We can derive inertance by using Newton's law relating force,  $F$ , mass,  $m$ , and the rate of change of velocity,  $dv/dt$ , which is the acceleration,  $a$ :

$$F = m \cdot a = m \cdot dv/dt$$

For a vessel, with length  $l$ , the net force  $F = \Delta P \cdot A$ ,  $A$  being the luminal cross-sectional area. The mass in the segment equals blood density,  $\rho$ , times the volume (length times area):  $\rho \cdot (l \cdot A)$ . The acceleration is the rate of change of velocity with time, i.e.,  $dv/dt$ . In terms of volume flow this is  $(1/A) \cdot dQ/dt$ . With Newton's equation this gives:

$$\Delta P \cdot A = \rho \cdot l \cdot A \cdot (1/A) \cdot dQ/dt = \rho \cdot l \cdot dQ/dt$$

so

$$\Delta P = \rho \cdot l / A \cdot (dQ/dt) = L \cdot dQ/dt$$

Where  $L = \rho \cdot l / A$  is called inertance. We recall that resistance is inversely proportional to  $r^4$  (Chapter 2) while inertance is inversely related to  $r^2$ . Thus, in large vessels the inertance plays a larger role than resistance while in very small arteries and arterioles it is the resistance that plays a larger role.

The inertance in combination with the compliance of a vessel segment determines the characteristic impedance and the wave speed (see Chapter 20 and Appendix 3).

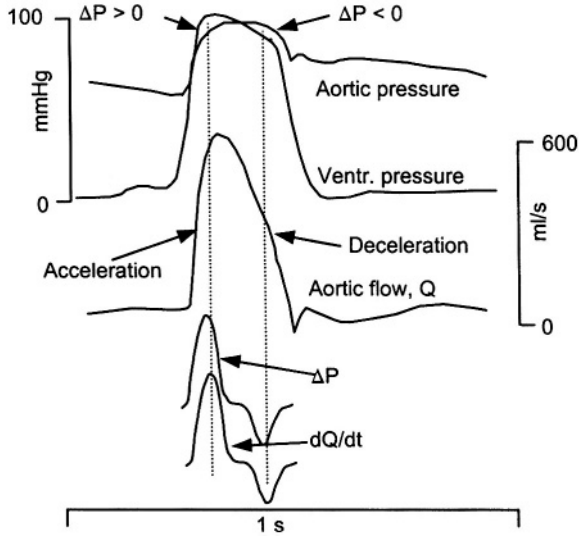
*Addition of series and parallel inertances*

The principal rules for addition of inertance of vessels in parallel and in series are as for resistances (see Chapter 6).

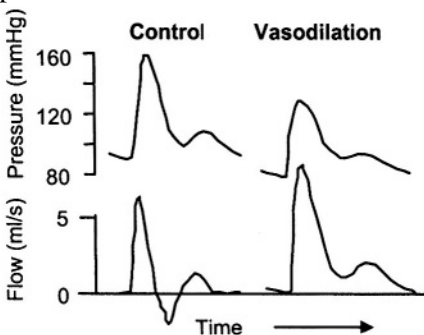
**Physiological and clinical relevance**

The inertance is determined by the cross-sectional area and length of the blood vessel, and by blood density. Blood density varies little, even in pathologic conditions. Inertance is therefore primarily a geometrical parameter.

An example where the effect of the inertance can be seen is when left ventricular and aortic pressures are measured simultaneously. This is shown in the figure on the right. During the ejection phase aortic flow is first accelerating (early ejection) and then decelerating. When the blood is accelerated the left ventricular pressure is higher than aortic pressure. When the



*INERTANCE PLAYS A ROLE IN ACCELERATING AND DECELERATING the blood. In early systole, when left ventricular pressure is higher than aortic pressure the blood accelerates, i.e., flow increases. In late systole, aortic pressure is higher than ventricular pressure the blood still flows forward but the velocity decreases (deceleration). Adapted from [1], used by permission.*



*BLOOD FLOW MAY BE REVERSED, or negative, during part of the cardiac cycle. This results from inertia and reflections. With vasodilation the reflections decrease and flow reversal disappears (example from femoral artery). Adapted from [2], used by permission.*

blood is decelerated the pressure difference reverses, as in the later phase of ejection. It may be seen that the pressure difference and the time derivative of flow are almost proportional in systole, suggesting inertance effects.

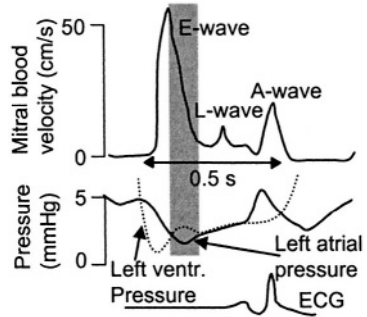
Inertance in combination with reflections (see Chapter 21) can result in flow reversal, i.e., negative flow during part of the cardiac cycle. This negative flow is therefore physiologic. The mean flow is, of course, always in the direction of the periphery.

Another example (see figure on the next page) is the diastolic filling of the ventricle through the mitral valve. As a

result of the inertance, flow persists when left ventricular pressure is higher than left atrial pressure.

## References

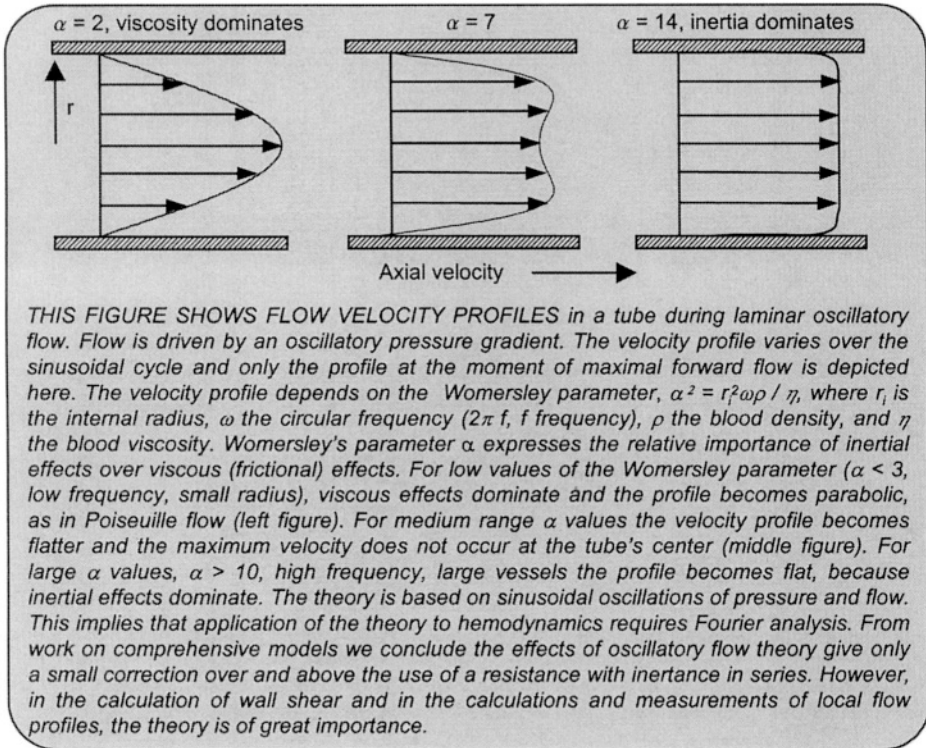
1. Noble MIM. The contribution of blood momentum to left ventricular ejection in the dog. *Circ Res* 1968;23:663-670.
2. O'Rourke MF, Taylor MG. Vascular impedance of the femoral bed. *Circ Res* 1966;18:126-139.
3. Solomon SB, Nikolic SD, Glantz SA, Yellin EL. Left ventricular diastolic function of remodeled myocardium in dogs with pacing induced heart failure. *Am J Physiol* 1998;274: H945-954.



*IN LEFT VENTRICULAR DIASTOLIC FILLING inertia plays a role. Flow is still forward, but decelerates, while the pressure difference between atrium and ventricle reverses. Adapted from [3], used by permission.*

## Chapter 8

## OSCILLATORY FLOW THEORY



### Description

The pressure-flow relation for steady flow, where only frictional losses are considered (resistance, law of Poiseuille), and the relation between oscillatory or pulsatile pressure and flow when only blood mass (inertance) is taken into consideration, are simplifications of reality.

The relation between oscillatory, sinusoidal, pressure drop and flow through a blood vessel can be derived from the Navier-Stokes equations. The assumptions are to a large extent similar to the derivation of Poiseuille's law: uniform and straight blood vessel, rigid wall, Newtonian viscosity, etc. The result is that flow is still laminar but pulsatile, i.e., not constant in time, and the flow profile is no longer parabolic. The theory is based on sinusoidal pressure-flow relations, and therefore called oscillatory flow theory.

The flow profile depends on the, circular, frequency of oscillation,  $\omega$ , with  $\omega = 2\pi f$ , with  $f$  the frequency, the radius,  $r_i$ , the viscosity,  $\eta$ , and density,  $\rho$ , of the blood. These variables were taken together in a single dimensionless (no units) parameter called Womersley's alpha parameter [1]:

$$\alpha^2 = r_i^2 \omega \rho / \eta$$

If the local pressure gradient,  $\Delta P/l$ , is a sinusoidal wave with amplitude  $A^*$  and circular frequency  $\omega$ , then the corresponding velocity profile is given by the formula [1]:

$$v(r,t) = \text{Real} [(A^*/i\omega\rho) \cdot \{1 - J_0(\alpha y i^{3/2})/J_0(\alpha i^{3/2})\} e^{i\omega t}]$$

where  $y$  is the relative radial position,  $y = r/r_i$ , and  $i = \sqrt{-1}$ . Flow is given as:

$$Q(t) = \text{Real} [(\pi r_i^2 A^*/i\omega\rho) \cdot \{1 - 2J_1(\alpha i^{3/2})/\alpha i^{3/2} J_0(\alpha i^{3/2})\} e^{i\omega t}]$$

$J_0$  and  $J_1$  are Bessel functions of order 0 and 1, respectively. The Real means that only the real part of the mathematically complex formula is taken.

Since the heart does not generate a single sine wave but a series of sine waves (see Appendix 1) the flow profile *in vivo* is found by addition of the various harmonics, and is very complex. The relation between pressure drop and flow as given above is the so-called longitudinal impedance of a vessel segment (see Appendix 3). Experiments have shown that the theory is accurate.

On the basis of the oscillatory flow theory Womersley predicted that for  $\alpha > 0.5$ , the area ratio of two equal daughters and a mother vessel should be between 1.33 and 1.15 to minimize local wave reflection. For large  $\alpha$ , i.e.,  $\alpha > 10$ , where inertia dominates the viscous effects, the area ratio is 1.15. Murray's law predicts 1.25 for the area ratio.

### Physiological and clinical relevance

Womersley's oscillatory flow theory [1] reduces to Poiseuille's law for very low  $\alpha$ . This means that in the periphery with small blood vessels (small  $r$ ) and little oscillation, there is no need for the oscillatory flow theory and we can describe the pressure-flow relation with Poiseuille's law. For the very large conduit arteries, where  $\alpha > 10$ , friction does not play a significant role and the pressure-flow relation can be described with inertance alone. For  $\alpha$  values in between, the combination of the resistance plus the inductance approximates the oscillatory pressure-flow relations (see Appendix 3).

Models of the entire arterial system have indicated that, even in intermediate size arteries, the oscillatory flow effects on velocity profiles are not large. The main contributions of the arterial tree to pressure and flow wave shapes are due to branching, non-uniformity and bending of the blood vessels etc. Thus for global hemodynamics, i.e., wave travel, input impedance, Windkessel models etc., a segment of artery can be described, in a sufficiently accurate way, by an inertance in conduit vessels, and a resistance in peripheral arteries.

The oscillatory flow theory is, however, of importance when local phenomena are studied. For instance, detailed flow profiles and calculation of shear stress at the vascular wall require the use of the oscillatory flow theory.

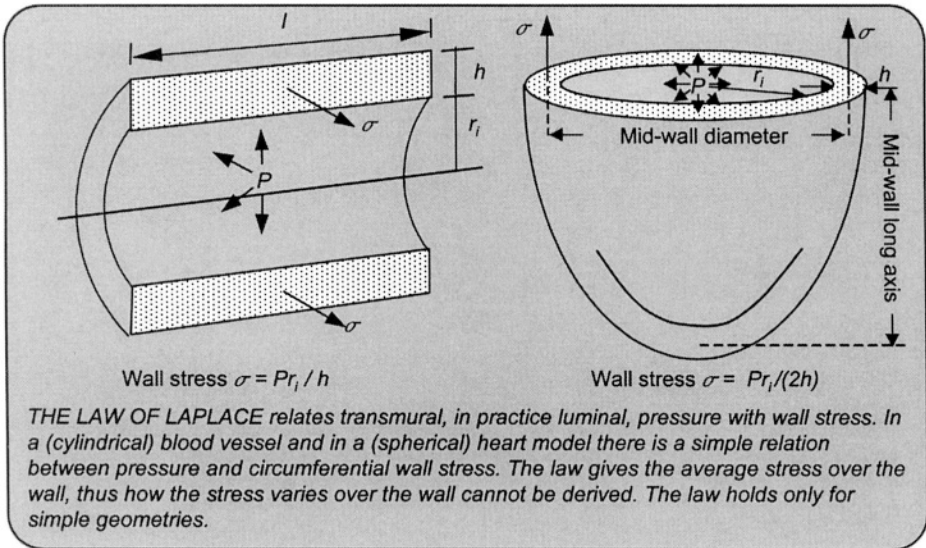
Before Ultrasound Doppler velocity and other flow measurement techniques became available, attempts were made to derive blood flow wave shapes and Cardiac Output from the measurement of two pressures in the aorta a few centimeters apart. The pressure drop and aortic size allowed for the calculation of flow using the oscillatory flow theory.

### Reference

1. Womersley JR. The mathematical analysis of the arterial circulation in a state of oscillatory motion. 1957, Wright Air Dev. Center, Tech Report WADC-TR-56-614.

## Chapter 9

## LAW OF LAPLACE



### Description

The original law of LaPlace pertains to soap bubbles, with radius  $r$ , and gives the relation between transmural pressure,  $P$ , and wall tension,  $T_{su}$ , in a thin-walled sphere as  $T_{su} = P \cdot r$ . It can be used to calculate tension in alveoli. This tension is directly related to surface tension and has the dimension N/m. The form of the law of LaPlace as most often used in hemodynamics gives the relation between pressure within the lumen of a hollow organ and the stress in the wall. Stress has the dimension  $N/m^2$ . For a circular cylinder, as model of a blood vessel, the pressure acts to push the two halves apart with a force equal to pressure times the area (left figure in the box). Thus force is  $2P \cdot l \cdot r_i$ . The two halves are kept together by wall stress,  $\sigma$ , acting in the wall only. This force is thus  $2 \cdot \sigma \cdot h \cdot l$ . These forces are in equilibrium and thus:  $2P \cdot l \cdot r_i = 2\sigma \cdot h \cdot l$ , which gives  $\sigma = P \cdot r_i / h$ . This form of the law of LaPlace is more correctly called Lamé's equation. For a sphere, a similar derivation holds and the result is  $\sigma = P \cdot r_i / 2h$ .

We see that pressure and wall stress are related by the ratio of radius over wall thickness.

### Applicability of the Law of LaPlace

The law of LaPlace applies to cylindrical or spherical geometries, irrespective of whether the material is linear or nonlinear or if the wall is thin or thick. The only limitation of LaPlace's law is that it yields the average wall stress and thus it cannot give any information on the stress distribution across the wall. For cylindrical geometries, and assuming linearly elastic (Hookean) material the distribution of circumferential stress or hoop stress across the wall thickness can be approximated by:

$$\sigma(r) = P \cdot r_i^2 \cdot (1 + r_o^2/r^2) / [r_o^2 - r_i^2]$$

where  $r_i$  and  $r_o$  is the internal and external radius, respectively, and  $r$  is the position within the wall for which local stress is calculated.

There is a large body of literature, especially for the thick walled heart, where (local) wall stress or muscle fiber stress is related with pressure for different complex geometries (for information see [3]).

Hefner [2] extended the Law of LaPlace for the left ventricle by showing that the equatorial wall force ( $F$ ) is  $P \cdot A_e$ , where  $A_e =$  **equatorial** cavity cross-sectional area and  $P$  luminal pressure. The wall stress,  $\sigma$ , is given by  $F/A_w$  with  $A_w$  the equatorial cross-sectional area of the muscle ring. Thus  $\sigma = P \cdot A_e / A_w$ .

Mirsky and Rankin [5] suggested an often used estimation of mid-wall stress. For an ellipsoidal heart shape the mid-wall stress is:

$$\sigma/P = (D/2h) \cdot (1-h/D - D^2/2l^2)$$

with  $D$  and  $l$  the mid-wall diameter and mid-wall length of the ventricle (see figure in box).

Arts et al. [1] derived a simple and practical relation between fiber stress,  $\sigma_f$ , and ventricular pressure,  $P_{lv}$ , that reads:

$$P_{lv}/\sigma_f = 1/3 \ln(1 + V_w/V_{lv})$$

where  $V_{lv}$  and  $V_w$  are ventricular lumen and ventricular wall volume, respectively. This equation can be used in all moments of the cardiac cycle and thus allows the calculation of fiber stress in both diastole and systole, including the ejection phase.

Many other relations between wall force or stress and ventricular pressure have been reported, but since measurement of wall force is still not possible [3], it is difficult to decide which relation is best.

The law of LaPlace pertains to geometrically simple bodies but may be applied to non-linear material. Assuming a simple shape such as a sphere, or circular cylinder, the law may be applied to the ventricular wall in diastole and systole, as well as to the vessel wall. The Law of LaPlace can also be used in the contracting heart, where the force is generated in the wall and the rise in pressure is the result of the contracting muscle.

#### *Relation to the Young modulus*

Assuming that the arterial wall is relatively thin ( $h \ll r_i$ ) and incompressible, one can use LaPlace's Law to derive the following expression for the incremental elastic modulus (Chapters 10 and 11):

$$E_{inc} = (r_i^2/h) \cdot \Delta P / \Delta r_i$$

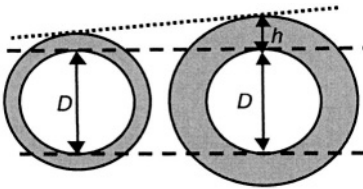
where the  $\Delta r_i$  and the  $\Delta P$ , are the change in internal radius and transmural pressure.

If the wall cannot be considered thin, as is often the case in arteries, the Young modulus is best derived from the measurement of pressure and radius using the following expression [4].

$$E_{inc} = 3 r_i^2 \cdot r_o \cdot (\Delta P / 2 \Delta r_o) / [r_o^2 - r_i^2]$$

**Physiological and clinical relevance**

The Law of LaPlace, although basic and pertaining to simple geometries, helps in understanding cardiac and vascular function. The law is therefore of great conceptual importance. For instance, the ratio  $r/h$  is a main determinant of the wall stress. The radius of curvature of the left ventricle is smaller at the apex than at the base, and so is the wall thickness  $h$ . The ratio  $r/h$  at the apex and base is, however, the same, resulting in similar wall stress at these locations in the wall. In hypertension the cardiac muscle cells increase in thickness by building more contractile proteins in parallel, leading to



*IN CONCENTRIC HYPERTROPHY, when compensated, ventricular pressure and wall thickness both are increased in approximately the same proportion and wall stress is similar.*

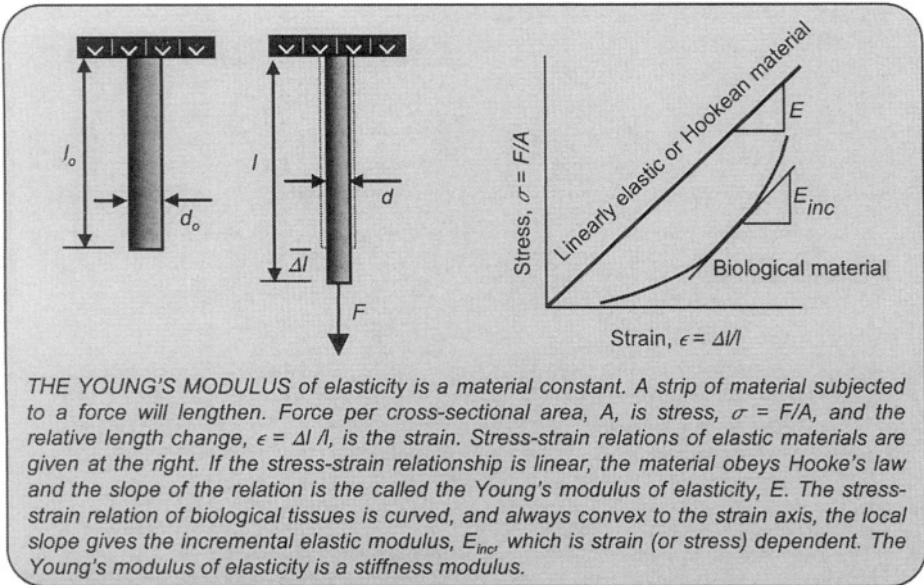
concentric hypertrophy. The thicker wall, but similar lumen, i.e., decreased  $r/h$ , causes the systolic wall stress to return to presumably normal levels despite the higher pressure in systole. In hypertension the large arteries hypertrophy and the thicker wall decreases wall stress. How stresses in the cells are sensed is still largely unknown. In dilated cardiomyopathy where lumen size is greatly increased while wall thickness is not, wall stresses are large. This leads to high oxygen demand, often too large for oxygen supply.

**References**

1. Arts T, Bovendeerd HHM, Prinzen FW, Reneman RS. Relation between left ventricular cavity pressure and volume and systolic fiber stress and strain in the wall. *Biophys J* 1991;59:93-102.
2. Hefner LL, Sheffield LT, Cobbs GC, Klip W. Relation between mural force and pressure in the left ventricle of the dog. *Circ Res* 1962;11:654-663.
3. Huisman RM, Sipkema P, Westerhof N, Elzinga G. Comparison of models used to calculate left ventricular wall force. *Med & Biol Eng & Comput* 1980; 18:133-144.
4. Love AEH. *A treatise on mathematical elasticity*. 1952, London & New York, Cambridge Univ Press, third Edn.
5. Mirsky I, Rankin JS. The effects of geometry, elasticity, and external pressures on the diastolic pressure-volume and stiffness-stress relations. How important is the pericardium? *Circ Res*. 1979; 44:601-11. Review.

# Chapter 10

# ELASTICITY



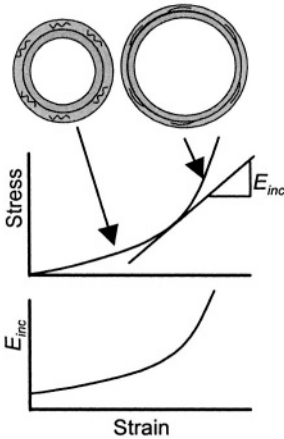
## Description

When a force,  $F$ , is applied to a specimen with cross-sectional area  $A$ , and length  $l$ , the length will be increased by  $\Delta l$ . With a specimen of larger cross-sectional area the same force will result in a smaller length change. Also, when the starting length of the specimen is longer the same force will result in a larger length change. To be able to give a unique characterization of the material, independent of the sample size, we normalize force by the area and the Lagrangian stress is obtained,  $\sigma = F/A$ . Similarly we normalize the length change to the starting length,  $l_0$ , and obtain strain,  $\epsilon = \Delta l/l_0$ .

The relation between stress and strain is given in the right part of the figure in the box. When the relation is straight we say that the law of Hooke applies, and the material is called Hookean or linearly elastic. The slope of the graph is called the Young modulus of elasticity  $E = \sigma/\epsilon$ . The Young modulus is a material property and is a measure of the stiffness, not elasticity, of the material. The units of the Young modulus are force per area, thus the same units as for stress and pressure, i.e.,  $\text{N/m}^2 = \text{Pa}$ , or mmHg.

When lengthened the specimen also gets thinner. The strain in the transverse direction,  $\epsilon_t$ , is  $\epsilon_t = \Delta d/d_0 = (d - d_0)/d_0$ . The ratio of the transverse strain and the longitudinal strain,  $\epsilon_t/\epsilon$ , is called the Poisson ratio. When with stretch the specimen's volume is constant, as appears to be the case for most biological tissue, the Poisson ratio is 0.5.

Biological materials almost always exhibit a curved stress-strain relationship with convexity towards the strain axis. The curved relation implies that the material cannot be characterized by a single Young modulus. The solution is to introduce an incremental modulus,  $E_{inc}$ , defined as the local slope of the stress-strain relation. For biological tissue the incremental elastic



BIOLOGICAL TISSUES show a stress-strain relation that is convex to the strain axis. The local slope gives the incremental Young modulus,  $E_{inc}$ , which increases with strain (or stress) mainly as a result of unfolding of collagen molecules.

deformations they can be characterized by an almost constant Young modulus. Collagen fibers, on the other hand, are very stiff:  $E_{collagen} \approx 1000 E_{elastin}$ . At lower strains, collagen fibers are wavy bearing no load, and the elastin and smooth muscle mainly determine the wall elasticity. At larger strains collagen starts bearing load leading to an increasingly stiff wall, i.e., a larger  $E_{inc}$ . The same holds for cardiac tissue.

The curved relation between stress and strain can be described in several ways. One simple relation, with only two parameters, is the equation originally suggested by Fung [1].

$$\sigma = a \cdot [e^{b \cdot (\epsilon - 1)} - 1]$$

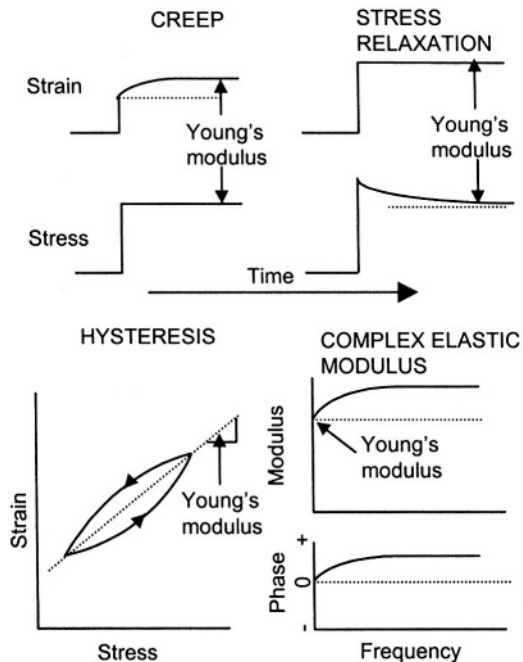
This model gives fairly accurate fits of the stress-strain relations.

modulus increases with strain, i.e., the biological material becomes stiffer with increasing stress and strain.

There are no clear conventions about the choice of the horizontal and vertical axes for stress and strain. This often leads to confusion when the slope of the relation is determined. It should be remembered that biological relations are convex towards the strain axis, i.e., the strain is limited. This limitation protects against overstretch and damage.

*The elasticity of cardiovascular tissue*

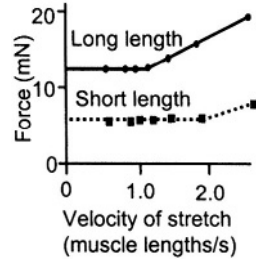
Vascular tissue is mainly composed of elastin, vascular smooth muscle and collagen. Elastin fibers are highly extensible and even at large



THE VISCOELASTIC PROPERTIES of biological material appear in four forms depending on the intervention and measurements. Step increases in stress and strain lead to creep and stress-relaxation, respectively. Repeated increases and decreases in stress and strain result in a hysteresis loop. Application of sinusoidal forces and measuring strains permits the determination of the complex Young modulus. The dashed lines pertain to purely elastic material. Viscoelasticity also appears in a similar fashion in pressure-diameter and pressure-volume relations.

*Viscoelasticity*

Viscoelasticity (see figures on previous page and at right) means that a material is not only elastic but also has viscous ('fluid-like') properties [3]. If one wants to stretch (strain) a viscoelastic material rapidly to a new length, initially a larger force is needed for the same amount of stretch as for a purely elastic material. With time the viscous contribution to the stress decreases. This is called stress relaxation. Inversely, with a sudden increase in stress the strain (stretch) is delayed. The delayed stretch is called creep. When, stress and strain are pulsatile, as *in vivo*, strain always lags stress. Plotting strain versus stress yields a hysteresis loop. The area of the loop is the energy lost due to the viscosity of the material. When sinusoidal force or pressure is applied, the amplitude ratio and phase difference between stress and strain describe the complex elastic modulus. The complex elastic modulus depends on the frequency of oscillation. When the stress or strain is applied very slowly the viscous aspects do not become apparent and the material behaves as purely elastic.



*VISCOELASTICITY OF HEART muscle requires extra pressure during filling. At velocities of stretch above one muscle length per second an additional force appears in excess of the elastic force/length curve; this effect is more obvious at high length. Adapted from [2], used by permission.*

*Viscoelastic models*

Several models have been proposed to describe the viscoelastic properties of biological tissue. Some of these models fall short in the sense that they do not describe all aspects of Viscoelasticity. One of the examples is the Maxwell model where a spring and dash-pot or damper, are placed in series. With a constant stress this model predicts a continuous, never ending, increase in length, which is clearly not true in biological tissue. Adding another spring in parallel to the Maxwell model yields Kelvin's viscoelastic model, which is the simplest, yet realistic viscoelastic model of the vascular wall.

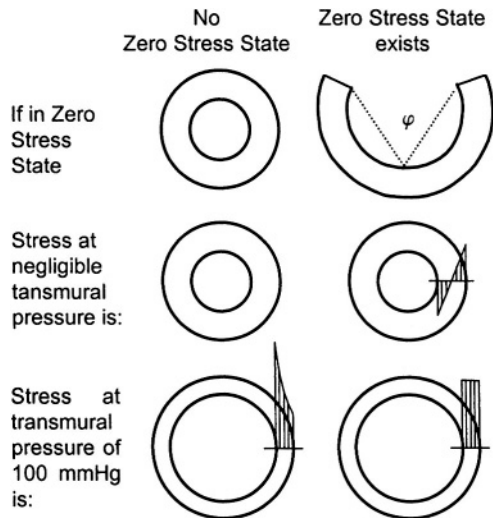
	Purely elastic	Maxwell	Voigt	Kelvin	Levin-Weyman	Generalized (See [3])
Stress relaxation	n.a.	no	no	yes	yes	yes
Creep	n.a.	no	yes	yes	yes	yes

*MODELS OF VISCOELASTIC MATERIAL in the form of springs and dashpots (dampers). The simplest two-element models represent biological material poorly, they either show no stress relaxation and strain that is unlimited or show an infinite stress response to a step change in length. The three-element models (Kelvin and Levin-Weyman) are equivalent and qualitatively sufficient. To quantitatively describe Viscoelasticity more elements are usually required.*

*Residual stresses and stress distribution at physiological loads*

The vascular tissue is not at a zero stress state when all loads, i.e., pressure and longitudinal tension, are removed. The same holds true for cardiac tissue. Stresses that still exist in the tissue when no external loads are applied are called residual stresses. The classical experiment to illustrate the existence of residual stress in arteries after removal of all loads is to excise a ring of artery and cut it longitudinally. The ring springs open and takes the shape of a circular arc, as shown in the figure on the right. The change in configuration means that stresses existed within the wall before the cut. Further cuts do not seem to release more stresses, therefore we assume that the opened-up configuration after the first cut is a stress free configuration. This stress free state or zero stress state, ZSS, can be characterized by the 'opening angle'  $\varphi$ , which is the angle formed by the two ends and the mid point of the inner arc length.

Knowledge of the ZSS is of primary importance when one wants to calculate the detailed stress field within the arterial wall. This is because strains can be calculated only in reference to the ZSS. Knowledge of the ZSS is not required when one calculates the average circumferential stress in the wall using Laplace's law. Residual stresses play an important role in maintaining a fairly uniform stress distribution across the arterial wall at physiological loads. This can be visualized with the help of the schematic drawings shown in the figure on the right. The left column shows an arterial cross-section where the ZSS is a circular ring (top). This means that at  $P = 0$  mmHg there are no residual stresses (middle). At a physiological transmural pressure level ( $P = 100$  mmHg) however, significant stresses develop with a pronounced stress peak at the inner most layer of the wall (bottom). The higher stress concentration in the inner wall is a direct consequence of the fact that these layers are stretched much more during the pressure-induced inflation. The right column shows an artery where the ZSS is characterized by an opened-up configuration (top). The ZSS means that at zero load, and in a closed ring configuration (middle figure) residual stresses exist. Residual stresses are compressive in the inner wall and tensile in the outer wall. During inflation, the inner layers will be stretched more than the outer layers of the wall. However, because at the beginning of the inflation,  $P = 0$  mmHg, the inner



*INFLUENCE OF ZERO STRESS STATE on wall stress distribution at operating pressures. Left column: stress distribution if no prestresses exist. Right column: arterial ring after being cut open (top). The ring is now in its stress-free or zero stress state (ZSS). This characterized by the opening angle  $\varphi$ . Prestresses in the wall at zero load ( $P = 0$ ) shown in the middle figure. Stress distribution at operating pressure (bottom).*

wall was under compression whereas the outer wall already was under some extension, at the physiological pressure level the degree of extension is the same in both inner and outer wall layers. The stress distribution is therefore uniform across the wall (bottom).

### Physiological and clinical relevance

Elasticity plays an important role in the circulation. All blood vessels are elastic and their elastic moduli do not differ greatly. A typical value of the incremental elastic modulus of arteries in the normal human at a pressure of 100 mmHg, is about  $5 \cdot 10^6 \text{ dyn/cm}^2$  or 500 kPa. With  $1 \text{ kPa} = 7.5 \text{ mmHg}$  the elastic modulus is 3750 mmHg. For diastolic heart tissue the incremental elastic modulus at a filling pressure of 5 mmHg is about  $4 \cdot 10^5 \text{ dyn/cm}^2$  or 40 kPa. In systole these values are about 20 or more times larger. Thus cardiac muscle is much stiffer in systole than in diastole.

Elasticity of the conduit arteries stands at the basis of their Windkessel function (see Chapter 24).

The nonlinear relation between stress and strain has led to much confusion. An example is in hypertension. When elastic properties are derived at the working point, i.e., the operating mean pressure of the individual patient, the vessels of hypertensive patients are found to have a higher incremental elastic modulus as compared with normal human subjects. However, this apparently increased stiffness in hypertensive patients is mainly the result of their higher blood pressure (see Chapter 27). Thus either a stress-strain graph should be made or the incremental elastic modulus should be compared at similar strains or stresses to be able to conclude if mechanical properties have changed or not.

#### *Determination of the Young modulus*

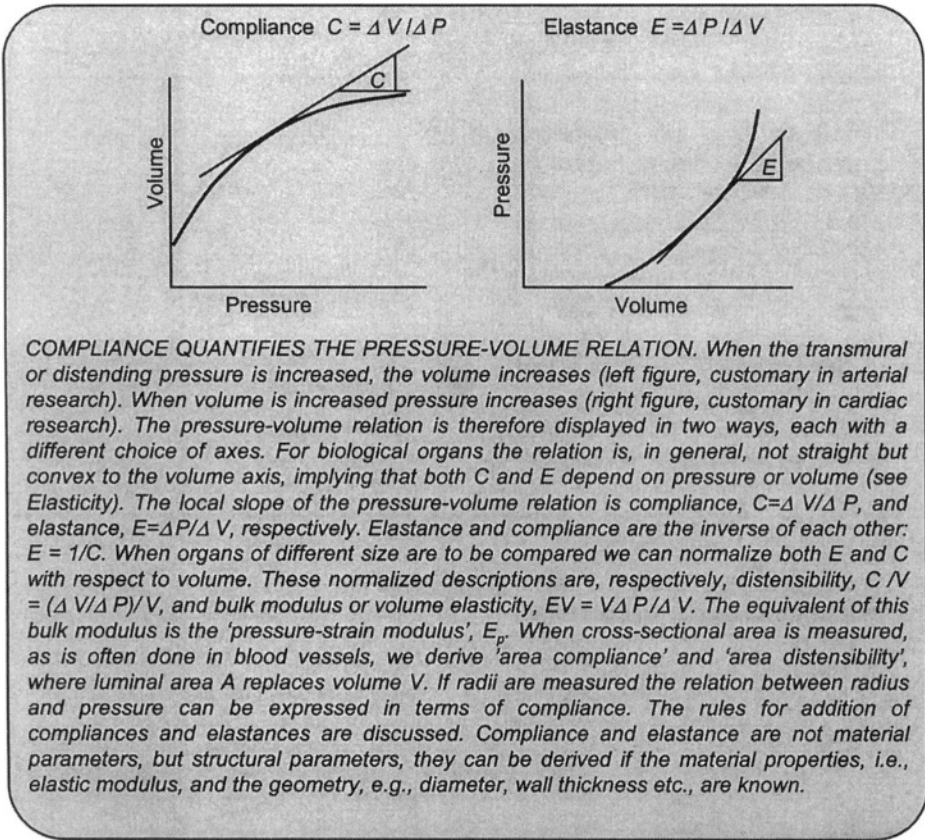
In practice the Young modulus is often not measured directly, because isolated tissue samples without perfusion are not viable. Therefore, for hollow organs like heart and vessels, pressure-volume or, for vessels, pressure-diameter relations are determined. However, through the law of LaPlace, and accounting for geometry, the calculation of the Young modulus is feasible (Chapters 9 and 11).

### References

1. Fung Y.C. Elasticity of soft tissues in simple elongation. *Am J Physiol* 1967;28:1532-1544.
2. Noble MIM. The diastolic viscous properties of cat papillary muscle *Circ Res* 1977;40:287-292.
3. Westerhof N, Noordergraaf A. Arterial elasticity: A generalized model. Effect on input impedance and wave travel in the systemic arterial tree. *J Biomech* 1970;3:357-379.

# Chapter 11

# COMPLIANCE

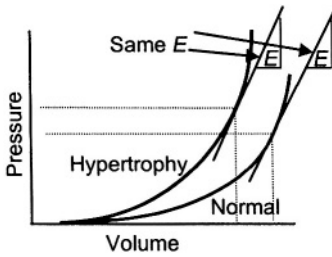


COMPLIANCE QUANTIFIES THE PRESSURE-VOLUME RELATION. When the transmural or distending pressure is increased, the volume increases (left figure, customary in arterial research). When volume is increased pressure increases (right figure, customary in cardiac research). The pressure-volume relation is therefore displayed in two ways, each with a different choice of axes. For biological organs the relation is, in general, not straight but convex to the volume axis, implying that both  $C$  and  $E$  depend on pressure or volume (see Elasticity). The local slope of the pressure-volume relation is compliance,  $C = \Delta V / \Delta P$ , and elastance,  $E = \Delta P / \Delta V$ , respectively. Elastance and compliance are the inverse of each other:  $E = 1/C$ . When organs of different size are to be compared we can normalize both  $E$  and  $C$  with respect to volume. These normalized descriptions are, respectively, distensibility,  $C/V = (\Delta V / \Delta P) / V$ , and bulk modulus or volume elasticity,  $EV = V \Delta P / \Delta V$ . The equivalent of this bulk modulus is the 'pressure-strain modulus',  $E_p$ . When cross-sectional area is measured, as is often done in blood vessels, we derive 'area compliance' and 'area distensibility', where luminal area  $A$  replaces volume  $V$ . If radii are measured the relation between radius and pressure can be expressed in terms of compliance. The rules for addition of compliances and elastances are discussed. Compliance and elastance are not material parameters, but structural parameters, they can be derived if the material properties, i.e., elastic modulus, and the geometry, e.g., diameter, wall thickness etc., are known.

## Description

The advantage of the pressure-volume relation is that it can be measured *in vivo*. It is important to note that the pressure-volume relation does not characterize the material but the structure of the organ as a whole. Thus, the relation between pressure and volume of a hollow organ, in principle of any shape, characterizes its overall structural behavior.

If the pressure-volume relations were straight and going through the origin, the slope, compliance or elastance would give the full characterization of the organ by a single quantity. However, the pressure-volume relations are never straight. For a small change around a chosen working point, the curve is approximately straight, and the tangent of the pressure-volume curve is used. We can determine compliance in the 'working point' as  $C = \Delta V / \Delta P$ . The elastance, the inverse of compliance is  $E = \Delta P / \Delta V$ . Of course, these local slopes depend on the pressure or volume chosen. Thus, when comparing compliance or elastance data one should report the chosen working point, i.e., the pressure at which compliance or elastance was determined. For instance, when the elastance of a heart in diastole is studied and appears increased, the increase can result from either a higher filling



*DIASTOLIC PRESSURE VOLUME RELATIONS of a normal and hypertrophied heart are shown. If only the similar elastance values are reported without further information it cannot be decided if the heart is normal but overfilled, or hypertrophied, since both have the same  $E$ . The full graph is required to give the complete information.*

the cardiac muscle. Diameter as estimate of volume is inaccurate.

Vessel diameters are a good measure of local vascular volume. Diameter changes can be measured by wall-tracking and for large vessels like the aorta by MRI. From the local diameter the cross-sectional area is calculated assuming a circular cross-section. When area and pressure are related the term area compliance,  $C_A = \Delta A / \Delta P$ , is used to distinguish it from (volume) compliance. For instance, the systolic-diastolic differences in area,  $\Delta A$ , and pressure,  $\Delta P$ , when measured *in vivo*, can be used to obtain the area compliance. With modern echo-tracking techniques it is possible to determine vessel diameter noninvasively. In that case it is customary to report diameter compliance,  $\Delta D / \Delta P$ . The area compliance,  $C_A$ , and diameter compliance,  $C_D$ , are related by:  $C_A = \pi \cdot D \cdot C_D / 2$ .

#### *Distensibility and bulk modulus*

Compliance depends on the size of the organ under study. To compare properties of blood vessels, or hearts from different animal species we can normalize compliance and elastance with respect to the volume of the organ. We use  $C/V = (\Delta V/V) / \Delta P$ , called distensibility, and the inverse,  $E \cdot \bar{V} = \Delta P / (\Delta V/V)$ , called bulk modulus or volume elasticity. Area and diameter distensibilities are also used, area distensibility is  $(\Delta A/A) / \Delta P$  and diameter distensibility is  $2 \cdot (\Delta D/D) / \Delta P$ .

#### *The pressure-strain elastic modulus*

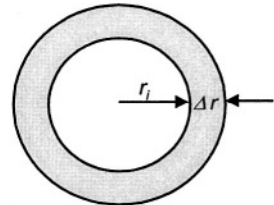
Peterson [8] introduced the pressure-strain elastic modulus in blood vessel research. This measure of blood vessel elasticity requires the measurement of

pressure but otherwise normal heart, or a normal filling pressure but a hypertrophied heart.

The curvature of the pressure-volume relation is mainly the result of the fact that the Young modulus increases with stretch, therefore  $C$  decreases and  $E$  increases with volume.

#### *Measurement of compliance*

Compliance is best determined by the measurement of pressure and volume. A number of techniques are now available to determine volumes, such as Computed Tomography, Magnetic Resonance Imaging, Ultrasound Echo, etc. Cardiac compliance or elastance determination requires volume and pressure measurements in systole and diastole, because of the varying properties of



*FOR GEOMETRICALLY SIMPLE SHAPES, like blood vessels, measurement of changes in internal radius or diameter is sufficient to obtain compliance. In complex geometries as that of the heart this cannot be done.*

diameter and pressure only, and can be used to compare vessels of different size. The pressure-strain elastic modulus, or Peterson modulus [8], is defined as  $E_p = \Delta P / (\Delta r_o / r_o)$ , where usually external radius,  $r_o$ , instead of the internal radius  $r_i$  is used. The  $E_p$  compares to the bulk modulus.

*SUMMARY of STRUCTURAL\* PARAMETERS of elasticity for blood vessels.*

	Volume	Area**	Diameter	Radius
Compliance	$\Delta V / \Delta P$	$\Delta A / \Delta P$	$\pi / 2 \cdot D (\Delta D / \Delta P)$	$2\pi r \cdot (\Delta r / \Delta P)$
Elastance	$\Delta P / \Delta V$	$\Delta P / \Delta A$	$2\Delta P / (\pi D \Delta D)$	$\Delta P / (2\pi r \Delta r)$
Distensibility	$(\Delta V / V) \Delta P$	$(\Delta A / A) \Delta P$	$2(\Delta D / D) / \Delta P$	$2(\Delta r / r) / \Delta P$
Bulk Modulus***	$\Delta P / (\Delta V / V)$	$\Delta P / (\Delta A / A)$	$\Delta P / (2\Delta D / D)$	$r / 2 \cdot (\Delta P / \Delta r)$ ****

$P, V, A, D, r$  are pressure, volume, area, diameter and radius, respectively.

\*Structural: parameters depend on organ geometry and material properties.

\*\* It is generally assumed that vessel length does not change with pressure.

\*\*\* Bulk modulus or Volume elasticity

\*\*\*\*The Pressure-Strain modulus or Peterson Elasticity,  $E_p = r \cdot \Delta P / \Delta r$ ; where outer radius is used. In all other relations internal diameter or radius is used.

*Describing the pressure-area or pressure-diameter relation of blood vessels.*

The pressure-area and pressure-diameter relations of blood vessels have been described in a number of ways. At a working pressure the slope of the relation gives compliance. However, description of the relation over a range of pressures and volumes gives more insight. Although these descriptions are phenomenological, we mention them here because of their general utility in arterial mechanics.

From [2]

(in pressure and diameter)

$$P = (P_0 + b)e^{a(D - D_0)} - b$$

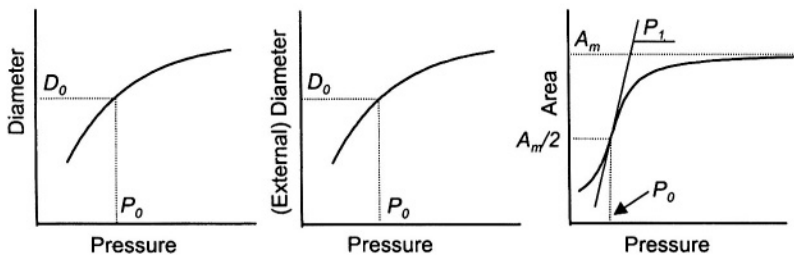
From [3]

$$\ln(P/P_0) = \beta (D/D_0 - 1)$$

$$P = P_0 e^{\beta (D/D_0 - 1)}$$

From [6]

$$A = A_m [1/2 + \tan^{-1}(P - P_0) / P_1]$$

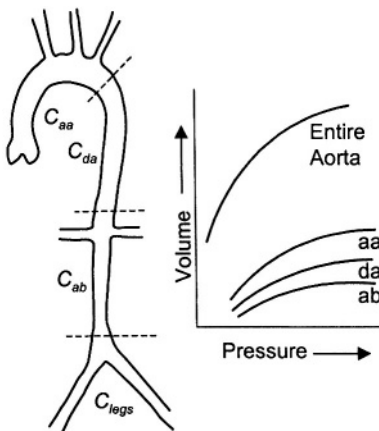


The relation proposed by Langewouters et al. [6], describes the pressure-area relation over the widest range of pressures, i.e., from 0 to 200 mmHg. The relations of Fung [2] and Hayashi [3] can be applied to the physiological range of pressures. The  $D_0$  and  $P_0$  are reference values for the relations of Fung [2] and Hayashi [3]. In the relation by Langewouters  $A_m/2$  and  $P_0$  designate the inflection point and  $P_1$  relates to the slope at the inflection point;  $A_m$  is the maximal, asymptotic, vessel area. The relations can also be presented in terms of volumes.

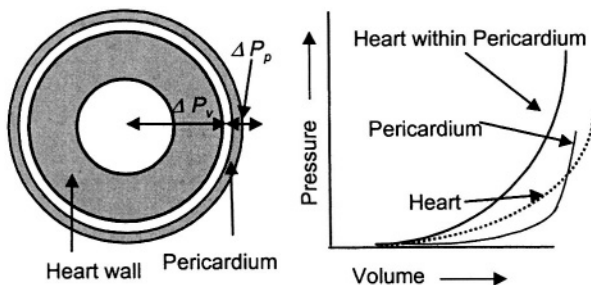
*Addition of compliances and elastances*

Let us consider the compliance of the entire aorta. The individual compliances of 3 sections of the aorta are shown in the figure. In all sections the pressure is virtually equal (see also Chapter 6). This implies that  $C_1 + C_2 + C_3 = \Delta V_1/\Delta P + \Delta V_2/\Delta P + \Delta V_3/\Delta P = (\Delta V_1 + \Delta V_2 + \Delta V_3)/\Delta P = \Delta V_{total}/\Delta P = C_{total}$ . Thus, simple addition of compliances is allowed and the total compliance is the sum and is therefore larger than the individual compliances.

If an organ with compliance  $C_1$  is enveloped with an organ with compliance  $C_2$ , the total volume change equals the individual volume changes. In that case the pressures need to be added. The distending pressure of the inner organ is the luminal pressure minus the pressure in between the organs. The distending pressure of the outer organ is the pressure between the



**THE AORTA AS AN ELASTIC RESERVOIR.** The compliances of different sections can be added to obtain total aortic compliance. The whole graphs may also be added. The aa, da, and ab are ascending, descending, and abdominal aorta.



**THE HEART WITHIN THE PERICARDIUM.** Heart and pericardium have their individual elastances and the total elastance of the heart in the pericardial sac can be obtained directly from addition of their individual elastances. Addition of the whole graphs is also allowed. Thus, for structures within each other elastances should be added directly. Transmural pressure over the ventricular wall is  $\Delta P_v = P_{ventr} - P_{pericard}$  and transmural pressure  $\Delta P_p = P_{pericard} - P_{external}$ .

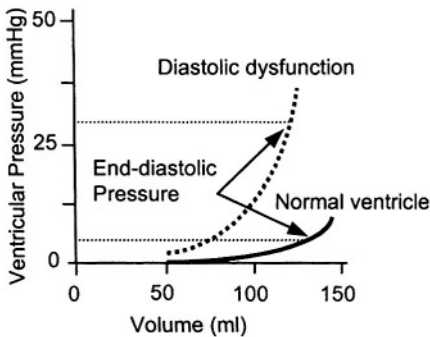
inside the pericardium the transmural pressure equals  $\Delta P_{total} = \Delta P_v + \Delta P_{pe}$ . Therefore  $E_{total} = \Delta P_{total} / \Delta V = (\Delta P_v + \Delta P_{pe}) / \Delta V = \Delta P_v / \Delta V + \Delta P_{pe} / \Delta V = E_v + E_{pe}$ , with  $E_v$ , and  $E_{pe}$  the ventricular elastance and pericardial elastance, respectively. When using compliances this would give:  $1/C_{total} = 1/C_v + 1/C_{pe}$ . The implicit assumption is that the intrapericardial pressure,  $\Delta P_{pe}$ , is the same at all locations. There are indications that the situation is more complex.

organs minus the pressure of the environment. Thus, the distending pressure acting on the two organs combined, i.e., the luminal pressure minus the external pressure is the sum of the distending pressures of each organ. In this situation addition of the elastances is easier. As an example we use the heart with pericardium. When the transmural pressure over the ventricular wall is  $\Delta P_v$  and over the pericardium is  $\Delta P_{pe}$ , for the heart

**Physiological and clinical relevance**

Compliance or elastance gives a quantitative measure of the mechanical and structural properties of an organ. Changes with disease and aging can be quantitatively investigated.

In general arterial compliance decreases with age and this is the main reason why arterial pulse pressure, Systolic minus diastolic pressure, increases with age. The concomitant increase in systolic pressure is an extra load on the heart possibly leading to (concentric) hypertrophy. Concentric hypertrophy increases the elastance of the left ventricle in both diastole and systole. The increase in diastolic elastance results in decreased filling for the same filling pressure and filling can only return to near normal values with an increase in diastolic filling pressure (see Chapter 13), which in turn may lead to pulmonary edema.



*LOSS OF VENTRICULAR COMPLIANCE in the hypertrophied heart means that distension of the left ventricle in diastole becomes more difficult. A higher pressure is required to reach the same end-diastolic volume. An increase in diastolic filling pressure implies an increase in the pulmonary venous pressure, leading to pulmonary edema.*

With the now available wall-track technique arterial diameters can be measured noninvasively in superficial arteries and if pressure is simultaneously determined as well (see Chapter 26), diameter compliance can be derived in large groups of patients. However, we should realize that local area compliance of a single peripheral artery, such as the carotid or radial artery, may not be a good measure of total arterial compliance.

Compliance and elastance depend on volume and pressure. Comparison should thus be carried out at similar pressure. However, compliance and elastance, in contrast to the Young modulus, also depend on the size of the organ. Distensibility and volume elasticity account for vessel size and are often used for comparisons of groups.

*Relating compliance to elasticity*

The measurement of pressure-volume or pressure-radius relationships in arteries allows for derivation of compliance but not of the Young modulus or incremental elastic modulus. As discussed in the chapter on LaPlace's law, estimation of Young modulus or incremental elastic modulus requires, in addition to radius and pressure, the measurement of wall thickness. A simple formula relating the area compliance with the incremental elastic modulus is:

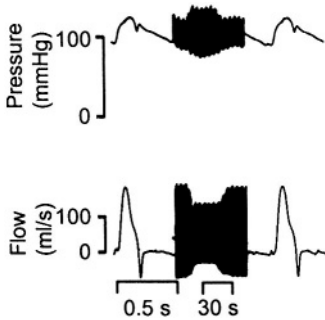
$$C_A = (2\pi r^3)/(E_{inc} h)$$

Compliance, being a structural property, should be plotted against distending pressure. The incremental elastic modulus, being a material property, should be plotted against stress or strain. Plotting  $E_{inc}$  against pressure, as is often done, leads to misinterpretation of vessel properties.

An example where the structural aspect of compliance can be seen, is the comparison of the elastic properties of veins and arteries. The main reason why pressure-volume relations of veins differ from those of arteries is not the difference in wall material but their difference in wall thickness. More accurately stated, the ratio of wall thickness to radius is much smaller in veins than in arteries.

### *Buffering function of compliance*

Compliance is the buffering element for pressure so that the oscillations in pressure during the cardiac cycle are limited. The pulse pressure in the aorta, the difference between systolic and diastolic aortic pressure, is about 40 mmHg in the young healthy adult. It was shown by Randall et al. [9], *in vivo*, that an acute reduction of arterial compliance results in a considerable increase in pulse pressure. It was recently reported that an artificial decrease in aortic compliance also has a longer term effect on pulse pressure which leads to left ventricular hypertrophy [4]. It is now accepted knowledge that increased pulse pressure is the strongest pressure-based indicator of cardiac mortality and morbidity [1,7]. It has been reported recently that diastolic cardiac function is affected when arterial compliance is decreased [5]. The scientific community is becoming more and more convinced that decreased compliance plays a major role in hypertension. In Chapter 29 it is shown that the change in compliance, with age, is considerable and contributes importantly to pulse pressure.



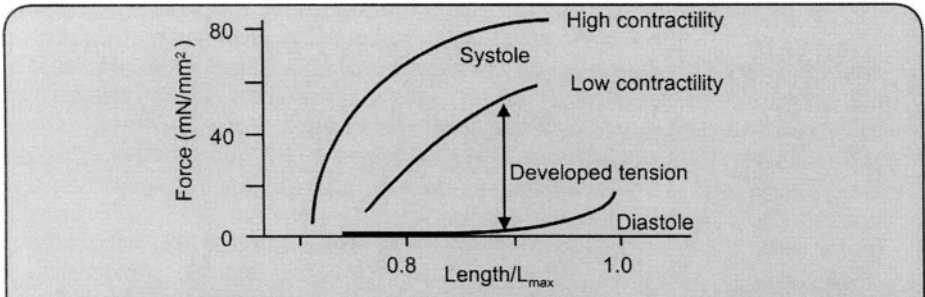
**AORTIC PRESSURE AND FLOW** in the intact dog during an acute decrease in aortic compliance. Cardiac filling increases along with the decrease in compliance. Adapted from [9], used by permission.

## References

1. Benetos A, Safar M, Rudnichi A, Smulyan H, Richard JL, Ducimetiere P, Guize L. Pulse pressure: a predictor of long-term cardiovascular mortality in a French male population. *Hypertension* 1997;30:1410-1415.
2. Fung, Y. C. Biomechanics. *Mechanical Properties of Living Tissues*. 1981, New York & Heidelberg, Springer-Verlag.
3. Hayashi, K, Handa H, Nagasawa S, Okumura A, Moritake K. Stiffness and elastic behavior of human intracranial and extracranial arteries. *J Biomech* 1980; 13:175-184.
4. Ioannou CV, Stergiopoulos N, Katsamouris AN, Startchik I, Kalangos A, Licker MJ, Westerhof N, Morel DR. Hemodynamics induced after acute reduction of proximal thoracic aorta compliance. *Eur J Endovasc Surg* 2003;26:195-204.
5. Kawaguchi M, Hay I, Fetis B, Kass DA. Combined ventricular systolic and arterial stiffening in patients with heart failure and preserved ejection fraction: implications for systolic and diastolic reserve limitations. *Circulation* 2003; 107:714-720.

6. Langewouters GJ, Wesseling KH, Goedhard WJ. The static elastic properties of 45 human thoracic and 20 abdominal aortas in vitro and the parameters of a new model. *J Biomech* 1984; 17:425-435.
7. Mitchell GF, Moya LA, Braunwald E, Rouleau JL, Bernstein V, Geltman EM, Flaker GC, Pfeffer MA. Sphygmomanometrically determined pulse pressure is a powerful independent predictor of recurrent events after myocardial infarction in patients with impaired left ventricular function. *Circulation* 1997;96:4254-4260.
8. Peterson LH, Jensen RE, Parnell J. Mechanical properties of arteries in vivo. *Circ Res* 1960;8:622-639.
9. Randall OS, van den Bos GC, Westerhof N. Systemic compliance: does it play a role in the genesis of essential hypertension? *Cardiovasc Res* 1984; 18:455-462.

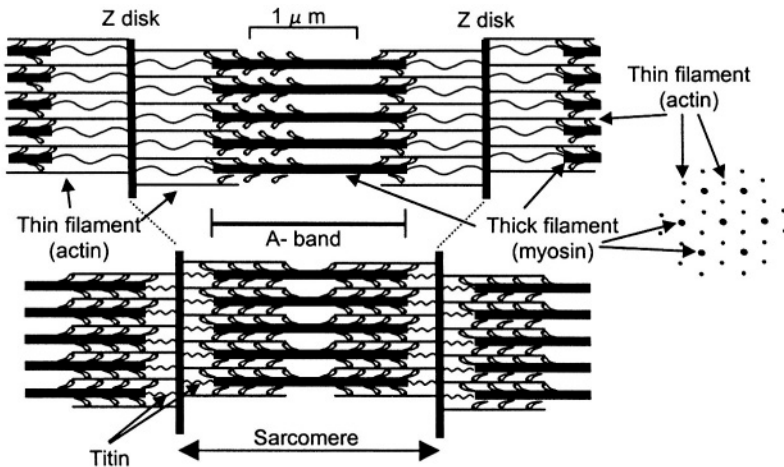
Part B  
Cardiac Hemodynamics



THE RELATION BETWEEN FORCE AND LENGTH in the relaxed state, diastole, and in the active state, systole, of an isolated cardiac muscle are shown. A low and high contractile state can be obtained by, for instance, changing the Calcium concentration in the extracellular fluid. During contraction a family of force-length relations is transversed, but here only the diastolic and the systolic relations are shown. The difference between the systolic and diastolic force is developed force. Force is expressed relative to cross-sectional area of the muscle and called tension (or stress). The length is normalized with respect to  $L_{max}$ , the length where developed force is maximal. The force-length relation forms the basis of the pressure-volume relation. Other important relations are:

- . The force-velocity relation, showing that velocity of contraction decreases when force increases.
- . The relation between intracellular calcium and force, showing that an increase in Calcium results in increased force.

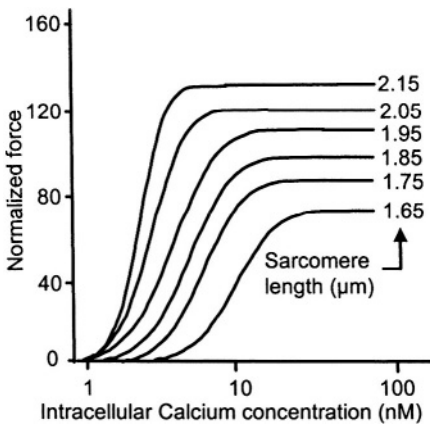
**Description**



THE CONTRACTILE UNIT IS THE SARCOMERE. The basic mechanical elements are presented here at two muscle lengths in the longitudinal direction. On the right hand side the cross section at overlap of thin and thick filaments is shown.

The cardiac muscle cells, or fibers, branch and interdigitate. They are typically 40 μm long and about 10μm in diameter; the fibers contain fibrils that are built up by the basic contractile unit the sarcomere. Each sarcomere, see schematic, is bounded at the ends by Z-disks about 2μm apart. The thin

actin filaments are about  $1\mu\text{m}$  long, are attached to the Z-discs, and extend towards the center of the sarcomere. They can either meet in the center, when sarcomere length is short, i.e., about  $2.0\mu\text{m}$ , overlap each other when sarcomere length is  $<2.0\mu\text{m}$ , or not quite reach each other when sarcomere length  $>2.0\mu\text{m}$ . Spanning the center of the sarcomere length are the thick myosin filaments,  $1.6\mu\text{m}$  long, which interdigitate with the thin filaments. They are connected to the Z-discs with a titin molecule. Changes in sarcomere length are achieved by sliding of thin between thick filaments. This sliding is caused by the action of the active, heavy meromyosin ATPase, i.e., ATP consuming unit, the 'cross-bridges'. The cross bridges project sideways from the thick filaments, apart from a 'bare area' in the central zone of approximately  $0.2\mu\text{m}$  length. The physiological range of sarcomere lengths (SL) is  $1.6 - 2.3\mu\text{m}$ , so that the number of cross-bridges in apposition to thin filaments is constant.



RELATION BETWEEN INTRACELLULAR CALCIUM ion concentration and isometric force. Normalization is with respect to isometric force at a sarcomere length of  $1.85\mu\text{m}$ . Adapted from [3], used by permission.

sigmoid. On the unsloping part of this curve, an increase in  $[\text{Ca}]_i$  resulting from increased  $\text{Ca}^{2+}$  release, causes an increase in  $F_0$ , called an increase in contractility, or positive inotropic effect. This must be distinguished from an increase of  $F_0$  due to increase in sarcomere length, which is due to increased sensitivity of the contractile filaments to  $\text{Ca}^{2+}$ . Increased sensitivity implies an upward and leftward shift of the  $F_0 - [\text{Ca}]_i$  curve. This effect forms the basis of the Frank-Starling Law that states that 'the energy of contraction is a function of initial fiber length'. This effect is brought about by the presence of regulatory proteins on the thin filaments, namely the tropomyosin and the troponin complex. Other proteins and factors also play a role, e.g., Titin and lattice spacing.

The curvilinear shapes of the  $F_0$  versus SL curves for one  $[\text{Ca}]_i$  vary with the given level of  $[\text{Ca}]_i$ , as shown in the figure in the box.

### Calcium

Depolarization of the heart muscle cell membrane causes influx of calcium ions,  $\text{Ca}^{2+}$ , over the cell membrane. This increase in Ca causes a further and larger release of calcium ions from the Sarcoplasmic Reticulum, SR, the so-called calcium induced calcium release. Calcium reacts with myosin ATPase to produce a contraction. The magnitude of the force of contraction produced when the sarcomere is prevented from shortening, i.e., isometric sarcomeres, is a function of sarcomere length and of intracellular calcium ion concentration,  $[\text{Ca}]_i$ . The interrelationships between this isometric force,  $F_0$ , with sarcomere length, SL, and the  $[\text{Ca}]_i$  are shown in the figure on the left.

The relationship between  $F_0$  and  $[\text{Ca}]_i$  at any one sarcomere length is

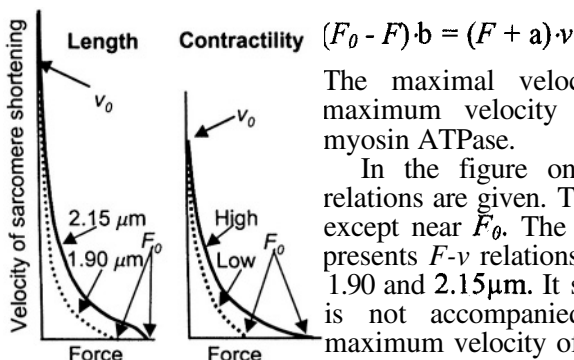
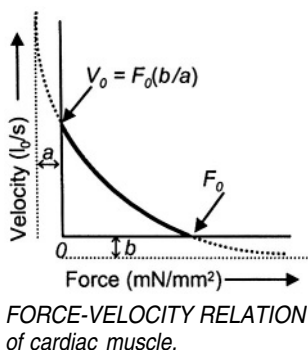
*The force-length relation*

The force-length relation of cardiac muscle (see figure in box) forms the basis of the ventricular pressure-volume relation. The relation between pressure and (local) tension can in principle be obtained by LaPlace's law, but more sophisticated approaches are advised. Many models have been proposed with varying success. The main problems are:

- (local) wall stress can not be measured in the intact heart, so that verification of models is not yet possible [2]. Subendocardial shortening is larger than subepicardial shortening, but forces may or may not be different.
- cardiac geometry is complex. Cylindrical or ellipsoidal models are only approximations.
- relations between ventricular volume and (local) fiber length, as well as between volume changes and changes in fiber length also suffer from heterogeneity and geometric complexity. The simplest approach is to assume that the heart is a cylinder, with the volume proportional to fiber length squared, or a sphere, with volume proportional to fiber length to the third power. So, qualitatively, the force-length relation of the muscle relates to the pressure-volume relation of the heart.

*The force-velocity relation*

Another basic property of cardiac muscle is that for larger force the velocity of shortening is smaller (figure on the right). This inverse relation between force and velocity is called the force-velocity relation ( $F-v$ ). In reality, heart muscle shortens against a force  $F$  that is less than the isometric force,  $F_0$ ; these forces are also called 'loads'. The  $F-v$  relation can be described by a hyperbola with the Hill equation:



*FORCE-SARCOMERE shortening velocity relations are influenced by muscle length and contractility. Adapted from [1], used by permission.*

The maximal velocity,  $v_0$ , depends on the maximum velocity of ATP splitting by the myosin ATPase.

In the figure on the left two sets of  $F-v$  relations are given. The  $F-v$  curves are hyperbolic except near  $F_0$ . The left hand side of the figure presents  $F-v$  relations for two sarcomere lengths, 1.90 and 2.15  $\mu\text{m}$ . It shows that the increase in  $F_0$  is not accompanied by an increase in the maximum velocity of sarcomere shortening,  $v_0$ , at zero force. This phenomenon depends on muscle length and disappears at short lengths. The right hand part of the figure shows the  $F-v$  relation for two contractility levels, or two levels of intracellular Calcium,  $[\text{Ca}]_i$ . With an increasing

level of  $[Ca]_i$ ; the  $v_0$  increases until a saturation level is reached. In the rat this level is below the physiological  $[Ca]_i$  so that  $v_0$  will then not increase with increased contractility of increased intracellular Calcium. In the human there exists a range of Calcium concentrations where  $v_0$  will increase.

#### *The F-v relation and pump function*

$F$  and  $v$  relate, through geometric transformations with pressure, e.g., pressure in the left ventricle, and Cardiac Output,  $CO$ , but the  $F$ - $v$  curves above refer to an instant in time within a contraction, whereas  $CO$  is an time-integrated quantity. During the cardiac cycle the  $F$ - $v$  relation is not constant but rises from one at the end of diastole, to one in systole and subsequently wanes down to the diastolic one again. This waxing and waning is not simply a 'parallel' shift because the time course of  $v_0$  is more rapid than that of  $F_0$ . A greater duration of contraction results in a higher Stroke Volume,  $SV$ , related to the average velocity. It is considered by some that the relevant  $F$ - $v$  curve for the intact heart is the relationship between average  $F$  and average  $v$ , which is equivalent to the pump function graph relating average LVP to  $CO$  (see Chapter 14).

#### *Experimental problems*

Studies on cardiac muscle are usually performed on isolated muscle strips, papillary muscle or trabeculae. These preparations are generally not perfused and therefore conditions have to be chosen such that a so-called anoxic core is avoided. These conditions are low temperature, low frequency, high  $P_{O_2}$  of the superfusion fluid etc. If *in vivo* conditions are desired, such as 37 °C and physiological rate of contraction, a perfused preparation is required. Single skinned (permeable outer membrane) myocytes have been studied in terms of length and tension and calcium sensitivity, and very recently data on intact single myocytes have been reported.

Isolated cardiac muscle allows for studies of basic phenomena, such as tension development, calcium handling, effects of drugs, disease, etc. The advantage is that the muscle can be studied without the confounding effects of changes in cardiac loading. The disadvantage is that conditions are not physiological.

Determination of maximal isometric force requires that one stretches the preparation during contraction to prevent the sarcomeres from shortening because of compliant attachments of the preparation to the apparatus. This requires feedback control of the stretching apparatus keeping sarcomere length constant. The, average, sarcomere length can be derived from light diffraction provided the preparation is sufficiently thin. The method is used successfully in trabeculae, which are fine muscle bundles from the inside of the heart cavity, usually taken from the right ventricle. This has not yet been successfully performed in isolated myocytes.

In most cell cultures cell shortening is used as a measure of function. Unfortunately the shortening depends on the adherence of the cells to the substrate, and this adherence is not known. Also the amount of shortening cannot be related to the force.

*Nomenclature problems*

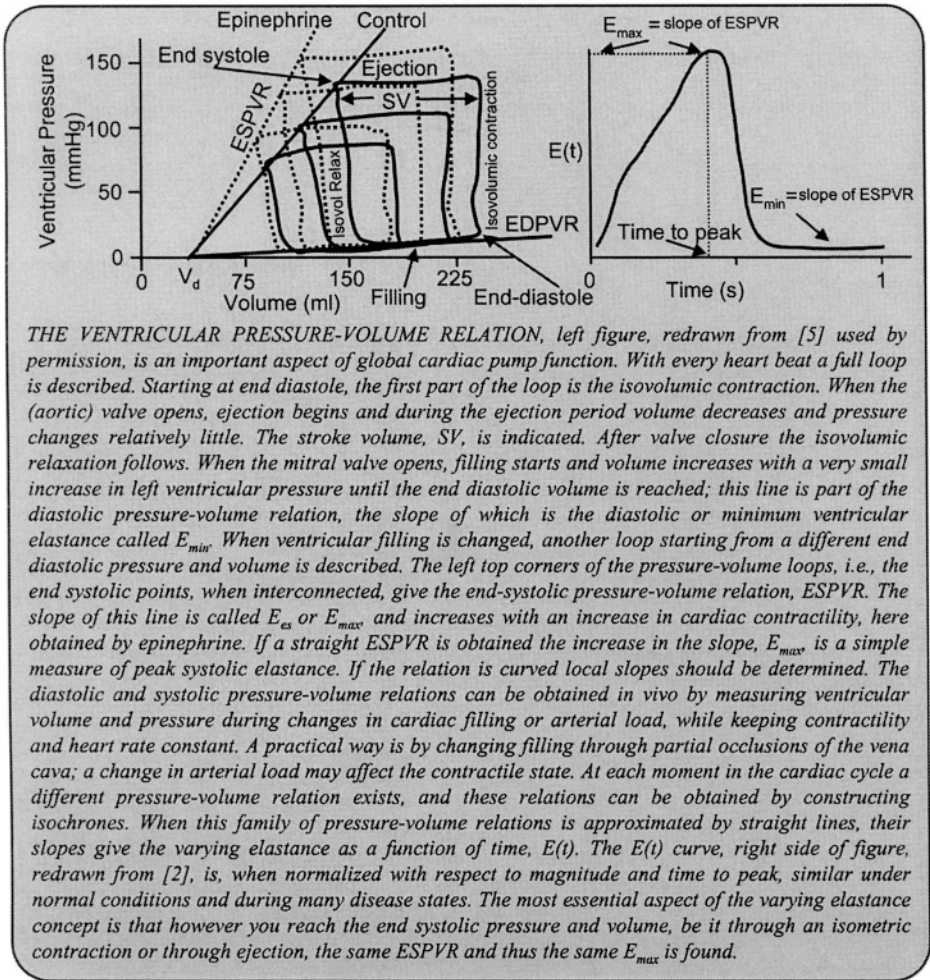
Another term for  $v_0$ , used in the past was  $v_{max}$ , but this is now avoided because of erroneous attempts to calculate it in intact hearts. Traditionally, isolated muscle experiments were arranged so that the force was constant during systole and early relaxation, whereas in life, force decreases during systole and falls to about zero in early relaxation (before diastolic lengthening). This constant force during systole and early relaxation was called 'afterload', a term which is clearly inappropriate to use in the intact heart. Before it was possible to measure sarcomere length throughout an experiment, the muscle was hung vertically and its initial length was set with variable weights; these weights were called 'preloads'. This term is no longer appropriate because the fundamental independent variable, sarcomere length, can now be measured. It is unwise to apply terms derived from cardiac muscle mechanical studies, which are one-dimensional, to the intact heart, which is three-dimensional.

**Physiological and clinical relevance**

The maintenance of the circulation requires that the heart muscles have a sufficiently high  $F-v$  relation and duration of active state. Failure of these, as for example due to reduced contractility, will lead to clinical heart failure. Clinical heart failure can also occur due to damage of part of the heart, e.g. myocardial infarction. Stimulation of contractility may be necessary in the treatment of acute heart failure, using positively inotropic drugs. Unfortunately, this seemingly logical treatment is contra-indicated in chronic heart failure because it causes earlier death, presumably because increased energy supply is required by the cardiac muscle sometimes in excess of possible supply rate; positively inotropic drugs mostly work by increasing  $[Ca]_i$  which can also cause (possibly fatal) arrhythmia.

**References**

1. Daniels M, Noble MIM, ter Keurs HEDJ, Wohlfart B. Force and velocity of sarcomere shortening in rat cardiac muscle: relationship of force, sarcomere length,  $Ca^{++}$  and time. *J Physiol* 1984;355:367-81.
2. Huisman RM, Elzinga G, Westerhof N, Sipkema P. Comparison of models used to calculate left ventricular wall force. *Cardiovasc Res* 1980; 14:142-153.
3. Kentish JC, ter Keurs HEDJ, Ricciardi L, Bucx JJJ, Noble MIM. Cardiac muscle mechanics: Comparison between the sarcomere length-force relations of intact and skinned trabeculae from rat right ventricle. *Circ Res* 1986;58:755-768.



THE VENTRICULAR PRESSURE-VOLUME RELATION, left figure, redrawn from [5] used by permission, is an important aspect of global cardiac pump function. With every heart beat a full loop is described. Starting at end diastole, the first part of the loop is the isovolumic contraction. When the (aortic) valve opens, ejection begins and during the ejection period volume decreases and pressure changes relatively little. The stroke volume, SV, is indicated. After valve closure the isovolumic relaxation follows. When the mitral valve opens, filling starts and volume increases with a very small increase in left ventricular pressure until the end diastolic volume is reached; this line is part of the diastolic pressure-volume relation, the slope of which is the diastolic or minimum ventricular elastance called  $E_{min}$ . When ventricular filling is changed, another loop starting from a different end diastolic pressure and volume is described. The left top corners of the pressure-volume loops, i.e., the end systolic points, when interconnected, give the end-systolic pressure-volume relation, ESPVR. The slope of this line is called  $E_{es}$  or  $E_{max}$  and increases with an increase in cardiac contractility, here obtained by epinephrine. If a straight ESPVR is obtained the increase in the slope,  $E_{max}$ , is a simple measure of peak systolic elastance. If the relation is curved local slopes should be determined. The diastolic and systolic pressure-volume relations can be obtained in vivo by measuring ventricular volume and pressure during changes in cardiac filling or arterial load, while keeping contractility and heart rate constant. A practical way is by changing filling through partial occlusions of the vena cava; a change in arterial load may affect the contractile state. At each moment in the cardiac cycle a different pressure-volume relation exists, and these relations can be obtained by constructing isochrones. When this family of pressure-volume relations is approximated by straight lines, their slopes give the varying elastance as a function of time,  $E(t)$ . The  $E(t)$  curve, right side of figure, redrawn from [2], is, when normalized with respect to magnitude and time to peak, similar under normal conditions and during many disease states. The most essential aspect of the varying elastance concept is that however you reach the end systolic pressure and volume, be it through an isometric contraction or through ejection, the same ESPVR and thus the same  $E_{max}$  is found.

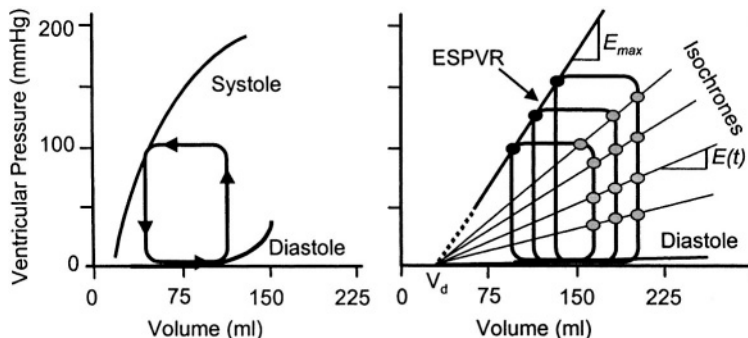
**Description**

Otto Frank studied pressure-volume relations in the isolated frog heart. He found different End-Systolic Pressure-Volume Relations, ESPVR's, for the ejecting heart and the isovolumically contracting heart. In other words, a single unique End-Systolic Pressure-Volume Relation did not appear to exist.

The same measurements in the isolated blood perfused dog heart, where volume was accurately measured with a water-filled balloon, showed that the End-Systolic Pressure-Volume Relation was the same for ejecting beats and isovolumic beats. The original results suggested a linear ESPVR with an intercept with the volume axis,  $V_d$ . The linear relation implies that the slope of the ESPVR, the  $E_{max}$ , with the dimension of pressure over volume (mmHg/ml), can be determined. Increased contractility, as obtained with epinephrine, increased the slope of the ESPVR but left the intercept volume,  $V_d$ , unchanged [5]. Therefore, the  $E_{max}$  could quantify contractility. Later it

turned out that both the diastolic pressure-volume relation and the ESPVR are not linear. The slope depends on the pressure and volume chosen and when approximating this locally with a straight line a virtual intercept volume is obtained, which may be positive or negative. However, the load-independence of the ESPVR is generally shown to be true and this is of great significance in the understanding and characterization of cardiac pump function. The load-dependence of the  $E(t)$  curve is small but does exist [2,5]. An extensive treatment is given in [2].

### *The varying elastance model*

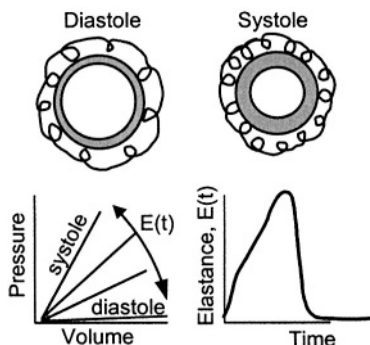


*THE PRESSURE-VOLUME RELATION is almost always presented as linear. This approximation may not always be correct and it may lead to, for instance, negative volume intercepts.*

Pressure-volume loops can be analyzed by marking time points on the loop. When different loops are obtained and the times indicated, we can connect points with the same times, and construct isochrones. The slopes of the isochrones can be determined, and the slope of an isochrone is the elastance at that moment in time. The fact that the elastance varies with time, leads to the concept of time-varying elastance,  $E(t)$ . This means that during each cardiac cycle the elastance increases from its diastolic value to its systolic value  $E_{max}$  and then returns to its diastolic value again.

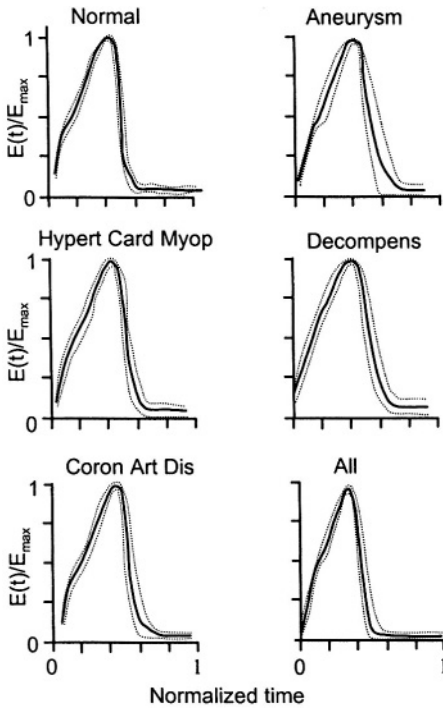
It has been shown that the  $E(t)$  curve, when normalized with respect to its peak value and to the time of its peak (see figure on the next page), is similar for normal and diseased human hearts [4]. Similar  $E(t)$  curves are found in the mouse, the dog and the human. It thus seems that there exists a

universal  $E(t)$  curve in mammals including man, which is unaltered in shape in health and disease. The only differences between hearts and state of health are in the magnitude and time of peak of the  $E(t)$ . This similarity of the varying  $E(t)$ -curve is very useful to construct lumped models of the heart [3].



*THE VARYING ELASTANCE concept assumes that the muscle stiffness increases from diastole to systole and back. This change in stiffness, expressed in the elastance curve is assumed to be unaffected by changes in load.*

However, some doubt has been cast on the invariance of the normalized  $E(t)$  curve [1].



THE DISEASE-INDEPENDENT  $E(t)$  curve. The  $E(t)$  curve, when normalized in amplitude and to time to peak, is similar in many disease states. Adapted from [4], used by permission.

*Determination of  $E_{max}$*

The maximal slope of the pressure-volume relation is called maximal elastance,  $E_{max}$ . It is also called End-Systolic elastance,  $E_{es}$ . To determine  $E_{max}$  one needs to measure several pressure-volume loops to obtain a range of end-systolic pressure-volume points (see figure in the introductory box). The determination should be done sufficiently rapidly to avoid changes in contractility due to hormonal or nervous control systems. Both changes in arterial load and diastolic filling may in principle be used, but the former may illicit contractility changes. Changes in filling are therefore preferred and are also easier to accomplish in practice. For instance, blowing up a balloon in the vena cava may decrease filling over a sufficiently wide range and can be carried out sufficiently rapidly to obtain an accurate ESPVR.

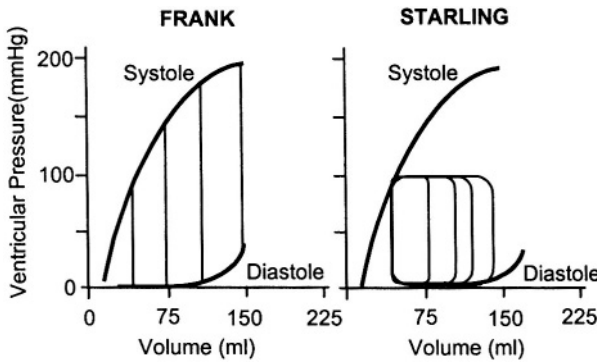
Both ventricular pressure and volume should be measured on a beat-to-beat basis. Volume can be measured in a number of ways, including non-invasive techniques

(US-Echo, X-ray, MRI). Pressure can be measured invasively only. Aortic pressure during the cardiac ejection phase can be used as an acceptable approximation of left ventricular pressure to determine the systolic part of the pressure-volume loop. Methods allowing for the calculation of ascending aortic pressure from peripheral pressure (Chapter 26) could, if proven sufficiently accurate, allow for a completely non-invasive determination of  $E_{max}$ .

**Physiological and clinical relevance**

The ESPVR and  $E_{max}$  together with the diastolic pressure-volume relation, are important measures of cardiac pump function and they are often used in animal research. Clinical use is still limited but increasing. The  $E(t)$  curve depends on heart size and thus on body size. Pressures are similar in different animals but volumes are not. Volumes are proportional to body mass (Chapter 30). Thus  $E_{max}$  can be normalized with respect ventricular lumen volume (see Chapter 11) or to heart mass or body mass to compare mammals. In diseased states the ratio of  $E_{max}/E_{min}$  may be a better measure of contractility than  $E_{max}$  alone (Chapter 30).

*The Frank-Starling law*



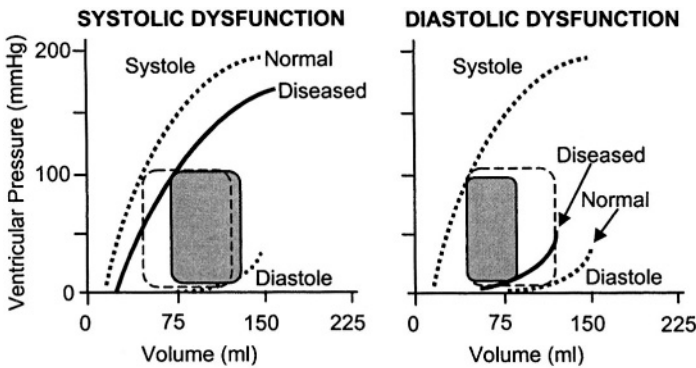
*FRANK (left, isovolumic contractions) and STARLING (right, ejections against constant systolic pressure) experiments to show the effect of ventricular filling in terms of pressure-volume relations.*

The varying elastance concept contains both Frank's and Starling's original experimental results, as shown in this figure. Frank studied the frog heart in isovolumic and ejecting beats, but we show here how isovolumic contractions behave in the pressure-volume plane when diastolic volume is increased. Starling also changed diastolic filling but studied an ejecting heart, which was loaded with a Starling resistor.

This meant that in his experiments the aortic pressure was kept constant. This in turn implies that ventricular pressure during ejection was also constant. The increase in filling resulted in an increase in Stroke Volume and thus in Cardiac Output.

*Systolic and diastolic dysfunction.*

It is important to realize that both diastole and systole play an important role



*SYSTOLIC AND DIASTOLIC DYSFUNCTION are shown here by fully drawn lines. In systolic dysfunction the ESPVR is decreased and Stroke Volume is as well. In diastolic dysfunction filling is decreased and, although filling pressure may be higher, Stroke volume is decreased.*

in cardiac function. This can be illustrated with the following example. Systolic dysfunction results in a decreased Stroke Volume, when not compensated by heart rate or diastolic filling. Diastolic dysfunction, with a stiffer ventricle in diastole causes decreased filling and higher filling

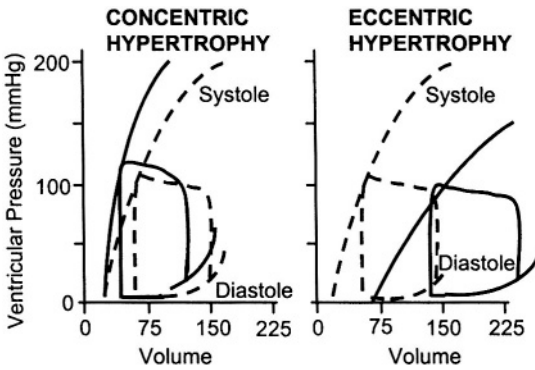
pressure. This results in a decreased Cardiac Output, and an increased pulmonary venous pressure, the latter leading to shortness of breath.

*Concentric and eccentric hypertrophy*

Concentric and eccentric hypertrophy are interesting examples in the context of the varying elastance concept and the pressure-volume relation.

Concentric hypertrophy implies an increased wall thickness with similar lumen volume. This means a stiffer ventricle in diastole and in systole, i.e., both  $E_{max}$  and  $E_{min}$  are increased. The increase in  $E_{max}$  does not necessarily imply increased contractility of the contractile apparatus of the muscle but is mainly a result of more sarcomeres in parallel, a thicker fiber and increased wall thickness. Concentric hypertrophy leads to increased diastolic filling pressure and higher systolic pressure but similar Stroke Volume.

In eccentric hypertrophy the ventricular lumen volume is greatly increased, more sarcomeres in series, and longer cells, while the wall thickness may be unchanged or somewhat increased. The shift of the pressure-volume relation to larger volumes in eccentric hypertrophy implies, by virtue of the law of LaPlace, that wall forces are increased. The increased  $V_d$  in eccentric hypertrophy emphasizes that the slope of the ESPVR cannot be determined from a single pressure and volume measurement because this is allowed only under the assumption that the intercept volume is negligible or known. Thus at least two points on the relation are required, necessitating a change in filling or systolic pressure. The shift of the pressure-volume relation to larger volumes in eccentric hypertrophy implies that wall forces are increased (LaPlace, Chapter 9).



*SCHEMATIC DRAWINGS OF PRESSURE-VOLUME relations in control (dashed lines) and severe concentric hypertrophy (left) and severe dilatation (right), fully drawn lines.*

The shift of the pressure-volume relation to larger volumes in eccentric hypertrophy implies, by virtue of the law of LaPlace, that wall forces are increased. The increased  $V_d$  in eccentric hypertrophy emphasizes that the slope of the ESPVR cannot be determined from a single pressure and volume measurement because this is allowed only under the assumption that the intercept volume is negligible or known. Thus at least two points on the relation are

required, necessitating a change in filling or systolic pressure. The shift of the pressure-volume relation to larger volumes in eccentric hypertrophy implies that wall forces are increased (LaPlace, Chapter 9).

*Modeling on the basis of the varying elastance concept*

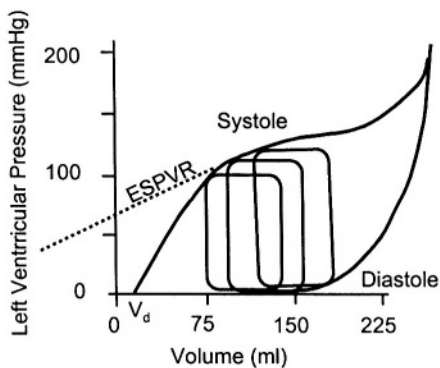
The finding that the normalized  $E(t)$  curve appears to be quite independent of the cardiac condition, and that it is similar in mammals (Chapter 30) allows quantitative modeling of the circulation [3,6].

*Limitations*

It should be emphasized that the time varying elastance concept pertains to the ventricle as a whole. It allows no distinction between underlying cardiac pathologies. For instance, asynchronous contraction, local ischemia or infarction etc., all decrease the slope of the End-Systolic Pressure-Volume Relation.

The pressure-volume relations are not straight. The diastolic relation is, as in most biological tissues, convex to the volume axis. The systolic pressure-

volume relations may be reasonably straight when muscle contractility is



THE END SYSTOLIC PRESSURE-VOLUME relation extends to a negative volume intercept, and a virtual  $V_d$ , which is different from the actual  $V_d$ . When only a single pressure-volume loop is studied assuming that  $V_d = 0$  the wrong  $E_{max}$  is found.

low. They become more and more convex to the pressure axis with increasing contractility. A curved relation implies that the  $E_{max}$  depends on volume and pressure. It is customary to approximate the ESPVR's in the working range by a straight line. Although this sometimes gives an acceptable approximation of reality, often a negative, and thus a virtual,  $V_d$  is found by linear extrapolation of the ESPVR to the volume axis.

In the normal heart the intercept volume may be small, and when this is the case the  $E_{max}$  can be estimated from a single pressure-volume loop. However, when  $V_d$  is not small, large errors will result by using a single point estimation of the End-Systolic Pressure-Volume Relation to derive  $E_{max}$ , (see figure on eccentric hypertrophy).

phy).

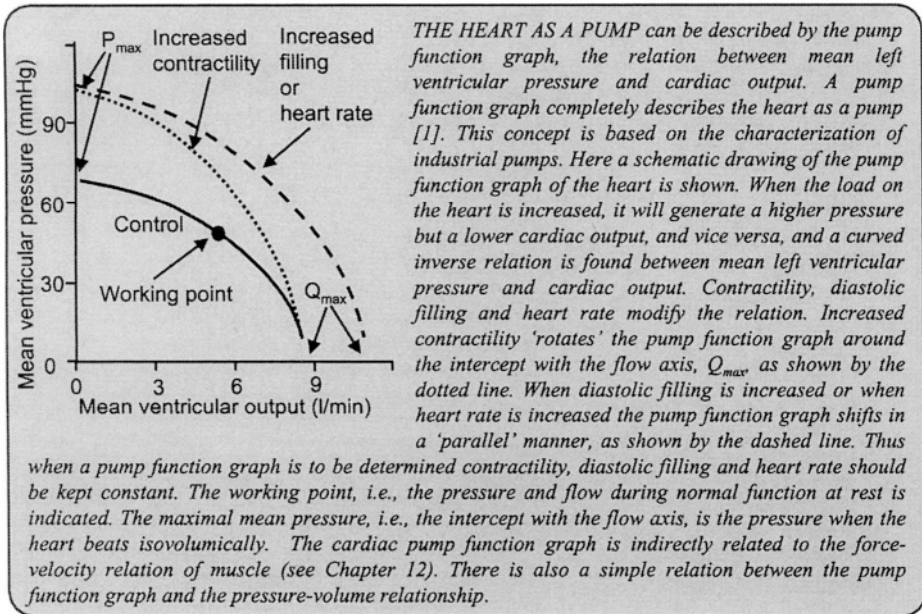
It has been shown by a number of investigators that load changes affect the End-Systolic Pressure-Volume Relation. However, the effect is rather small and may be due to the fact that, at high loads, the duration of ejection is curtailed and may not be long enough for  $E_{max}$  to be attained [2].

## References

1. Palmer BM, Noguchi T, Wang Y, Heim JR, Alpert NR, Burgon PG, Seidman CE, Seidman JG, Maughan DW, LeWinter MM. Effect of cardiac myosin binding protein-C on mechanoenergetics in mouse myocardium. *Circ Res* 2004; 94:1615-1622.
2. Sagawa K, Maughan, WL, Suga H, Sunagawa K. *Cardiac contraction and the pressure-volume relationship*. 1988, New York & Oxford, Oxford Univ Press.
3. Segers P, Stergiopoulos N, Westerhof N. Quantification of the contribution of cardiac and arterial remodeling to hypertension. *Hypertension* 2000;36:760-765.
4. Senzaki H, Chen C-H, Kass DA. Single beat estimation of end-systolic pressure-volume relation in humans: a new method with the potential for noninvasive application. *Circulation* 1996;94:2497-2506.
5. Suga H, Sagawa K, Shoukas A. A. Load independence of the instantaneous pressure-volume ratio of the canine left ventricle and the effect of epinephrine and heart rate on the ratio. *Circ Res* 1973;32:314-322.
6. Westerhof N. Cardio-vascular interaction determines pressure and flow. In: *Biological Flows*. MY Jaffrin, CG Caro Eds., 1995, New York, Plenum Press.

## Chapter 14

## PUMP FUNCTION GRAPH

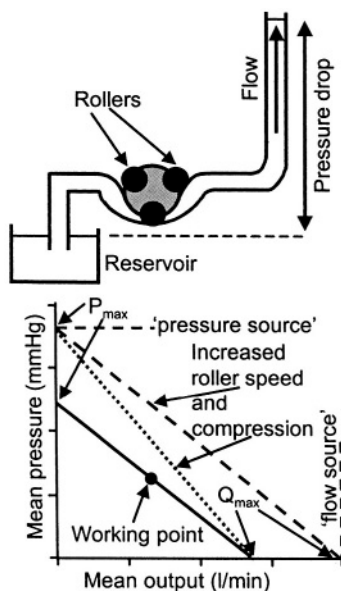


### Description

The heart is a pump that generates pressure and flow. It can be compared with other hydraulic pumps that are usually characterized by their head (pressure) - capacity (flow) curve. As an example consider a roller pump and make a pressure-flow relation by changing the load on the pump.

In the figure on the next page we show the pump function graph of a roller pump used in the laboratory and in heart-lung machines. The pump function graph depends on the roller speed and on how much the rollers compress the tube. A higher speed gives larger pressures and flows, pressure and flow intercept,  $P_{max}$  and  $Q_{max}$ , increase. Better compression of the rollers, increases the pressure generating capability because less leakage is present, the  $P_{max}$  increases. Since at low pressures the leakage is negligible, the maximal flow,  $Q_{max}$ , is hardly affected by changes in compression of the tube. Thus the result of the increased roller compression is a clockwise 'rotation' of the pump function graph around the intercept with the flow axis.

We use the term pump function graph for the pressure-flow relation. The pump function graph of a roller pump can be determined by changing the resistance in the outflow tube, while keeping the pump characteristics the same. Thus roller speed and the inflow pressure level are kept constant. For very high resistance values the pressure is maximal,  $P_{max}$ , but the flow is negligible. When the resistance is negligible flow is maximal,  $Q_{max}$ , but the generated pressure is zero. Thus, an inverse relation between pressure and flow generated is obtained. The relation happens to be straight for this type of pump, and gives information about what pressures and flows the pump can generate. The pump function graph also shows that this particular pump is



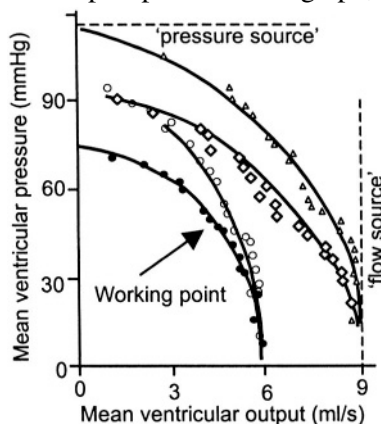
THE PUMP FUNCTION GRAPH of a roller pump. A laboratory pump is shown on the left. When roller speed and compression of the tube by the rollers is kept constant a pump function graph can be determined by changing the load of the pump, here obtained by changes in height of the outflow tube. When roller speed is increased or tube compression is increased the dashed and stippled relations are found, respectively. Adapted from [1], used by permission.

analogy with the derivation of arterial input impedance.

From the pump function graph we can see that the heart decreases its output when a higher pressure is generated. In other words the heart does neither generate the same flow, nor the same pressure under different loading conditions. This means that the heart is neither a pressure source, i.e., the same pressure is generated independently of the load, nor a flow source i.e., the same flow for all loads. At low flows the heart behaves approximately as a

neither a pressure source, i.e., always generating the same pressure, nor a flow source, i.e., always keeping flow constant.

We can perform a similar experiment on the heart. To avoid changes in pump function by humoral and nervous control mechanisms, these studies were originally carried out in the isolated perfused and ejecting heart. When ventricular filling pressure, cardiac contractility and heart rate are kept constant, variation in the load on the heart by either changing peripheral resistance or arterial compliance, or both, results in changes of mean left ventricular pressure and mean flow [1]. Ventricular pressure and flow are related because both quantities pertain to the cardiac side of the very nonlinear aortic valves. Mean ventricular pressure and mean flow used as a first order approximation, comparable with the mean aortic pressure and mean flow to determine peripheral resistance. In principle Fourier analysis (Appendix 1) of ventricular pressure and flow can be used to derive the oscillatory aspects of the pump function graph, in



PUMP FUNCTION GRAPHS as originally measured in an isolated pumping cat heart preparation. The filled circles give the control situation. An increase in contractility 'rotates' the graph around the intercept with the flow axis (open circles). The two other graphs are found during increased diastolic filling (open diamonds) with a subsequent increase in contractility (triangles). Adapted from [4], used by permission.

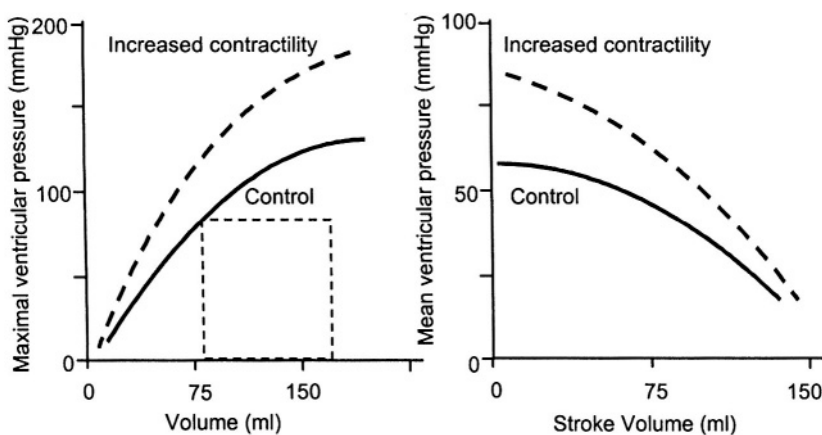
pressure source and at high flows a flow source is approached. The intercept of the pump function graph with the pressure axis is the mean isovolumic ventricular pressure, it is the mean ventricular pressure for a non-ejecting or isovolumic beat. The intercept with the flow axis is the Cardiac Output for the ‘unloaded’ or ‘isobarically contracting’ heart, i.e., contractions without build up of pressure.

The changes in contractility and filling are shown in the figure. Increased heart rate in the physiological range results in a parallel shift of the pump function graph, which is approximately proportional to the heart rate increase. An increase in cardiac contractility rotates the pump function graph around the flow intercept,  $Q_{max}$ .

At the intercept of the pump function graph with the pressure and flow axes,  $P_{max}$  and  $Q_{max}$ , respectively, the product of pressure and flow is zero and the external power is therefore negligible as well [3]. Thus external power generation exhibits a maximum for intermediate values (Chapter 15).

The pump function graph relates directly to basic properties of the cardiac muscle [2].

*Relation between the pump function graph and the pressure-volume relation*

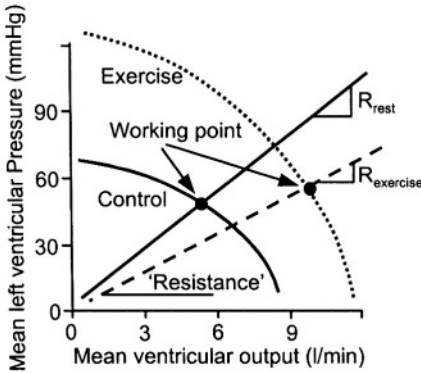


*THE PUMP FUNCTION GRAPH (right) AND THE END-SYSTOLIC PRESSURE-VOLUME RELATION (left) show a ‘mirrored’ relationship. Increased contractility rotates the lines. The pump function graph is here plotted in terms of stroke volume instead of mean flow. Note the scale difference in the pressure axes.*

This figure shows the qualitative relation between the pressure-volume relation and the pump function graph [7]. The pump function graph is here given in terms of Stroke Volume to make it more comparable with the pressure-volume relation, where heart rate is not represented. We see a ‘mirrored’ relation between the two characterizations of the heart. This follows from the fact that Stroke Volume is the decrease in ventricular volume during ejection. The main difference between the relations is that in the pressure-volume relation the end-systolic pressures, is used while in the pump function graph the mean ventricular pressure is used.

**Physiological and clinical relevance**

The pump function graph describes the pump function of the heart for constant filling, heart rate and contractility. The pump function graph teaches us that the heart is neither a flow source nor a pressure source. The flow source or in German the 'Harte Brunne' was the assumed heart model used up until the 1960's. We see that contractility at constant loading pressure has only a small effect on Cardiac Output. Heart rate and diastolic filling contribute importantly to CO.



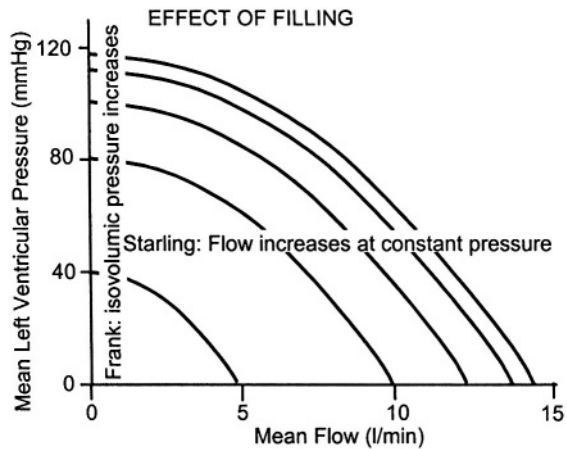
*DURING EXERCISE* vascular resistance decreases and the slope of the pump function graph increases. The cardiac output increases strongly with a limited increase in pressure.

*Exercise*

The graph on the left shows what happens in moderate exercise. Due to the increase in heart rate, and the (small) increase in filling and the increase in contractility, the pump function graphs shifts outward, with a small rotation as well. The increase in heart rate forms the major contribution to the outward shift of the pump function graph. The systemic vascular resistance is decreased. The overall result is an increase in Cardiac Output with only a small increase in pressure.

*The Frank-Starling Law*

This figure shows the effect of filling on the pump function graph and its meaning with respect to the Frank-Starling mechanism. Frank studied the effect of filling on isovolumic contractions. The effect of an increase in ventricular filling on non-ejecting, i.e., isovolumic, contractions is given by the intercepts of the pump function graphs with the pressure axis. Starling studied in the heart-lung preparation the effect of filling on Cardiac Output when aortic pressure was kept constant. The horizontal line represents this: Cardiac Output increases with cardiac filing.



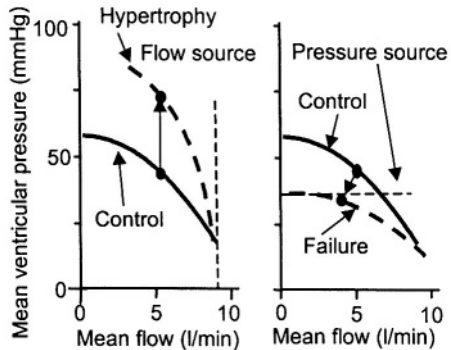
*THE CARDIAC PUMP FUNCTION GRAPH* is a generalized description of the Frank-Starling mechanism. With increased filling the graph moves outward. One of Frank's experiments pertains to isovolumic conditions where pressure increases with filling. Starling's experiment is one that keeps aortic pressure constant so that cardiac output increases with filling.

*Concentric hypertrophy and heart failure*

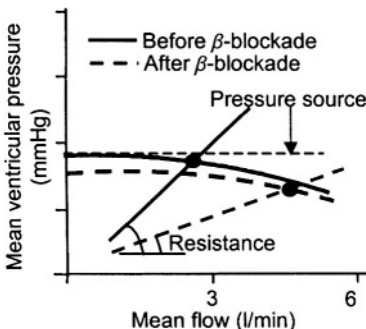
The figure shows the pump function graph in hypertension and failure. In hypertrophy a flow source is approached while in failure the heart acts more like a pressure source [5].

These changes in pump function have an effect on reflected waves returning from the periphery. A flow source means two things: the flow is not affected by reflected waves but pressure is completely reflected and thus augmented, 'closed end reflection'. Inversely, a pressure source implies that pressure is not affected by the reflected wave but the flow fully reflected and thus is decreased by the reflection.

Therefore in hypertrophy the backward pressure wave, is reflected at the heart (flow source) and is added to the forward pressure resulting in augmentation of the wave. The reflection and extra augmentation of pressure in hypertrophy shows the contribution of the hypertrophied heart to hypertension. In failure, when the heart approaches a pressure source the reflected flow wave affects the forward flow wave negatively resulting in a decrease in Cardiac Output (Chapters 21 and 22). Understanding of the contribution of the heart to reflected pressure and flow waves may assist in giving suggestions for possible therapy in heart failure [8].



*THE PUMP FUNCTION GRAPH in hypertrophy and failure. The graph in hypertrophy has a larger slope in the working point, indicating that the heart approaches a flow source. In failure a pressure source is approached. The dots give the working points. Reflections against a flow source augment the pressure without affecting the flow. Reflection against a pressure source, as in failure, decreases flow but does not affect the pressure. Thus in failure cardiac output is diminished by reflections.*



*THE PUMP FUNCTION GRAPH shows that in failure a pressure source is approached. A decrease in contractility in combination with vasodilation affects pressure little but increases cardiac output*

From the figure on the left it also becomes clear why, in chronic failure beta-blockers may be beneficial even though blood pressure may be low. A decrease in contractility combined with vasodilation does, because of the 'pressure source' behavior of the heart, affect pressure little but increases cardiac output. Improved survival by beta-blockade was indeed shown in patients with severe chronic heart failure [6].

*Limitations*

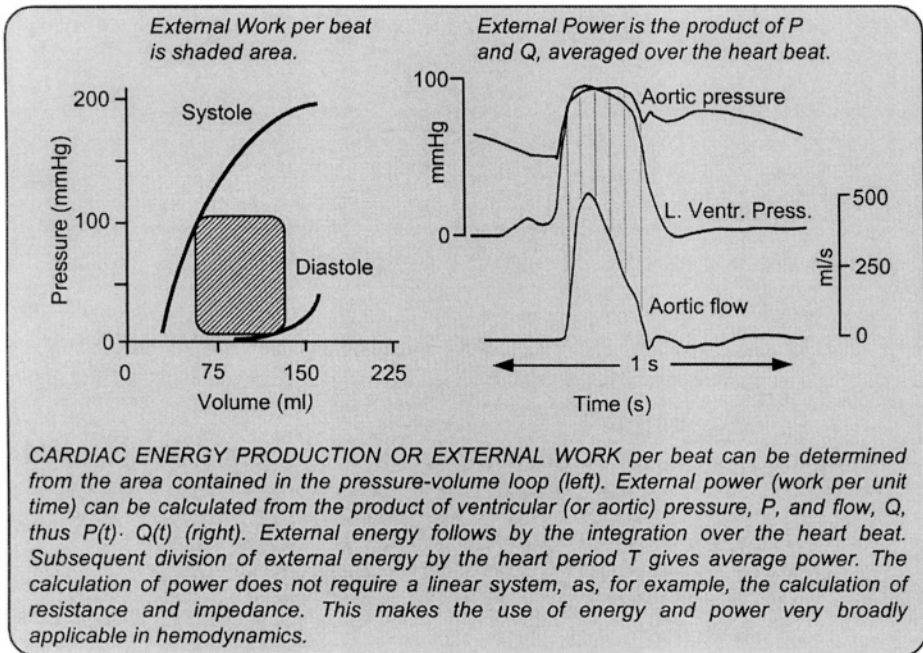
The pump function graph is a global description of the heart as a pump. Changes in muscle contractility, in synchronicity or effects of local ischemia or infarction, all affect this global description.

Since the heart is under the influence of

nervous and humoral control, and the fact that diastolic filling shifts the pump function graph, the determination of the pump function graph *in situ* is difficult. During arterial load changes filling, heart rate and contractility may change due to control mechanisms so that the operating points move over a family of pump function graphs.

## References

1. Elzinga G, Westerhof N. How to quantify pump function of the heart. *Circ Res* 1979;44:303-308.
2. Elzinga G, Westerhof N. Isolated cat trabeculae in a simulated feline heart and arterial system. *Circ Res* 1982;51:430-438.
3. Elzinga G, Westerhof N. Pump function of the feline left heart: changes with heart rate and its bearing on the energy balance. *Cardiovasc Res* 1980;14:81-92.
4. Elzinga G, Westerhof N. The effect of an increase in inotropic state and end-diastolic volume on the pumping ability of the feline left heart. *Circ Res* 1978; 42:620-628.
5. Elzinga G, Westerhof N. Workload as a determinant of ventricular hypertrophy. *Cardiovasc Res* 1985;19:524.
6. Rouleau JL, Roecker EB, Tendera M, Mohacsi P, Krum H, Katus HA, Fowler MB, Coats AJS, Castaigne A, Scherhag A, Holcslaw TL, Packer M. Influence of pretreatment systolic blood pressure on the effect of Carvedilol in patients with severe chronic heart failure (Copernicus study). *J Am Coll Cardiol* 2004;43:1423-1429.
7. Westerhof N. Cardio-vascular interaction determines pressure and flow. In: *Biological Flows*. MY Jaffrin, CG Caro Eds., 1995, New York, Plenum Press.
8. Westerhof N, O'Rourke MG. Haemodynamic basis for the development of left ventricular failure in systolic hypertension and for its logical therapy. *J Hypertension* 1995;13:943-952.



**Description**

Work and the potential to do work, energy, are based on the product of force times displacement, the units being Newton times meter (Nm or Joule). When work is expressed per unit time it is power (Nm/s or Watt). Linearity of the relations between force and displacement (velocity) or, equivalently between pressure and volume is not required in the calculation of work and power, while it is required in the calculation of resistance and impedance.

In the heart, external work can best be derived from pressure and volume through the pressure-volume loop, it is the area contained within that loop. The so calculated work is, of course, the external work produced by the heart during that heartbeat and called stroke work.

Power delivered by the heart to the arterial load equals pressure times flow. Both pressure,  $P$ , and flow,  $Q$ , vary with time, and the instantaneous power, calculated as  $P(t) \cdot Q(t)$  also varies with time. This means that instantaneous power varies over the heartbeat and is zero in diastole because aortic flow is zero. Thus, external work and power are only generated during ejection. Total energy is the integral of power or  $\int P(t) \cdot Q(t) dt$ , the integral sign,  $\int$ , together with  $dt$  implies that at any moment of time pressure and flow values are multiplied and the products added. The average power over the heart beat is  $(1/T) \cdot \int P(t) \cdot Q(t) dt$ , where  $T$  is the heart period. Since aortic pressure and left ventricular pressure are practically equal during ejection, both ventricular pressure and aortic pressure may be used in the calculation.

Sometimes mean power is calculated as the product of mean pressure and mean flow (Cardiac Output). Here aortic pressure is to be used because it is the mean power delivered to the arterial system that we want to calculate.

Since mean aortic pressure is about 2-3 times higher than mean left ventricular pressure, using ventricular pressure would lead to considerable errors. The difference between total power and mean power is pulsatile power (also called oscillatory power). Pulsatile power is about 20% of total power in the systemic circulation and about 35% of total power in the pulmonary circulation.

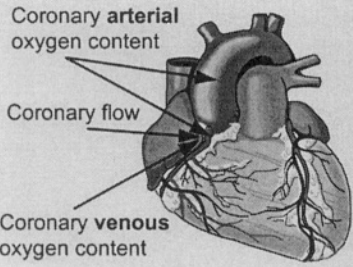
### **Physiological and clinical relevance**

It has sometimes been reasoned that it is the mean power that is related to useful power while pulsatile power is related to moving blood forward and backward only. In other words it was thought that only mean power and work were useful quantities. The logical consequence was then to assume that pulsatile power would be minimal in physiological conditions. This in turn, was used to argue that if the heart rate is related to the frequency of the minimum in the input impedance modulus (Chapter 23), pulsatile power would be minimal. However, this is not correct since it is the real part of the impedance that is related to power, not the impedance modulus. Thus, the separation of mean and pulsatile power is not very useful as a measure of ventriculo-arterial coupling. Under physiological conditions the heart pumps at optimal external power [1]. See also Chapter 17.

Work and energy find their main importance in relation to cardiac oxygen consumption, metabolism, and optimal ventriculo-arterial coupling.

1. Toorop GP, Van den Horn GJ, Elzinga G, Westerhof N. Matching between feline left ventricle and arterial load: optimal external power or efficiency. *Am J Physiol* 1988;254:H279-285.

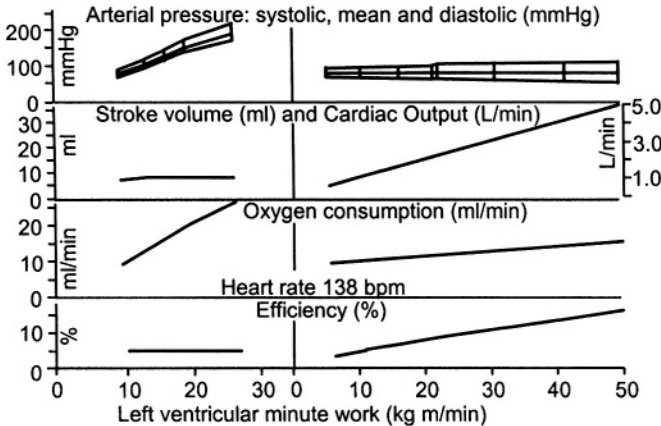
# Chapter 16 OXYGEN CONSUMPTION & HEMODYNAMICS



**CARDIAC OXYGEN CONSUMPTION** can be directly determined from the product of coronary flow,  $Q_{coron}$ , and arterio-venous oxygen content difference,  $\Delta AVO_2$ . Coronary artery oxygen content can be obtained from any arterial blood sample. Coronary venous or great cardiac vein oxygen content requires blood sampling at that location. Total arterial inflow can be determined using Doppler or electromagnetic flow meters. Peripheral, local, flows can be obtained with labelled microspheres. At the venous outflow side total flow can be derived with thermodilution. The, preferentially, simultaneous measurement of flow and oxygen contents is difficult. To circumvent these difficulties many indices for estimating oxygen consumption from mechanical variables have been proposed. It has been shown that tension generation of cardiac muscle costs more oxygen than muscle shortening. This means that pressure generation rather than flow determines oxygen consumption of the heart and therefore almost all methods to derive oxygen consumption from hemodynamics are based on pressure. The most used methods are the Rate Pressure Product (RPP), often used in biochemical studies of the heart, the Tension Time Index (TTI), and the Pressure Volume Area (PVA).

## Description

It was shown by Sarnoff [2] that the production of pressure costs much more oxygen than the production of flow or Cardiac Output. Also, it has been

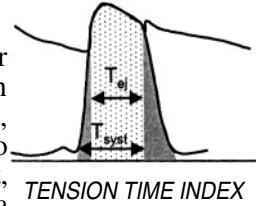


**OXYGEN CONSUMPTION IS PRIMARILY DETERMINED BY PRESSURE**, not by flow or external work. At the left arterial pressure is increased while stroke volume and Cardiac Output are kept the same. The increase in pressure results in an increase in oxygen consumption. At the right Cardiac Output is increased while pressure is kept the same. Oxygen consumption changes only little. Adapted from [2], used by permission.

shown that oxygen consumption,  $\dot{V}O_2$ , is almost proportional to heart rate. These findings imply that the main mechanical variables to estimate cardiac oxygen consumption are pressure and heart rate. If oxygen consumption is expressed per beat, pressure remains its major determinant.

### Rate Pressure product and Tension Time Index

In approximation, the product of the systolic ventricular pressure and heart rate can be used to estimate oxygen consumption. This so-called Rate Pressure Product, RPP, is simple to use, especially when limited to changes in oxygen consumption. The triple product, defined as  $HR \cdot P_{syst} \cdot dP_{LV}/dt$ , has also been suggested as a measure of cardiac oxygen consumption.



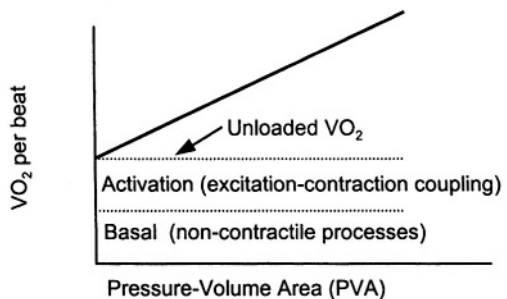
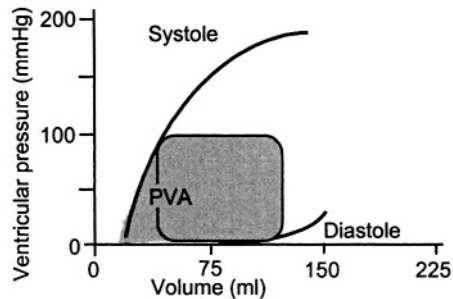
Sarnoff introduced the Tension Time Index, TTI [2]. The oxygen consumption per beat is assumed to be proportional to the area under the systolic part of the *aortic* pressure curve, with the systolic part defined as the period of aortic valve opening, thus actually ejection period (speckled area in figure). Implicitly the authors assumed this area to be proportional to the mean systolic left ventricular pressure times the duration of systole. However, it is better to use the total area under the *ventricular* pressure curve, and when we can neglect the contribution in diastole it follows that this equals mean ventricular pressure,  $P_{lv,mean}$ , times heart period,  $T$ , i.e.,  $TTI \approx P_{lv,mean} \cdot T$ . In isolated heart studies where isovolumic contractions are studied, and the ejection period is negligible, the area under the *ventricular* pressure curve should be used as a measure of cardiac oxygen consumption. The TTI is a global measure of cardiac oxygen consumption, and the term tension is not meant to be local stress, but is pressure. The TTI is also more difficult to measure than the RPP.

### The Pressure Volume Area

The newest way to estimate oxygen consumption per beat is the Pressure Volume Area (PVA, the gray area in top part of the figure). This method requires measurement of ventricular pressure and volume for at least two, and preferably more cardiac loading conditions (Chapters 13 and 15). The relation between oxygen consumption and PVA is shown in the bottom part of the figure and can be written as:

$$VO_2 = a_1 \cdot PVA + a_2 \cdot E_{es} + a_3$$

where  $E_{es}$  or  $E_{max}$ , is the slope of the End-Systolic Pressure-Volume Relation (ESPVR) giving a measure of contractile state. The first term is the



THE PVA RELATES TO CARDIAC OXYGEN CONSUMPTION. Oxygen consumption is also determined by basal processes such as integrity and ion pumps, and by excitation-contraction coupling (activation energy). Increased contractility increases activation energy. The PVA determines the third part of the energy. The inverse slope of the relation is the so-called contractile efficiency. Adapted from [3], used by permission.

relation between mechanics and oxygen consumption. The two other terms give the oxygen consumption for the unloaded contraction or isobaric contraction, i.e., a contraction without build up of pressure. The second term is the energy cost of excitation-contraction coupling and depends on the contractile state of the cardiac muscle, expressed as  $E_{es}$ . The last term is the basal oxygen consumption, used for the maintenance of cell structure, etc. For details see Suga [3].

The following local measures of oxygen consumption have been suggested. Stress time index, i.e., mean wall stress, derived from left ventricular pressure, times heart period. In analogy with the PVA the Tension (or Stress) Area Area and Force Length Area have been suggested as well (figure on the previous page with local area and stress or local length and stress on the axes).

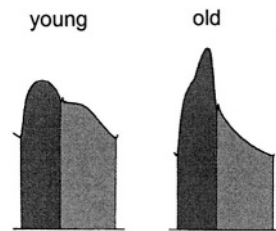
Since the TTI and the PVA predict oxygen consumption per beat, oxygen consumption per minute is found by multiplication with heart rate. If we assume the TTI to be equal to the mean ventricular pressure times heart period, multiplying with heart rate results in mean pressure as a measure of oxygen consumption.

An overview of other, more complex hemodynamic indicators of cardiac oxygen consumption can be found in Rooke and Feigl's report [1].

### Physiological and clinical relevance

Cardiac oxygen consumption, or oxygen demand, and cardiac oxygen supply, are in equilibrium in the normal healthy heart. The TTI gives a measure of oxygen demand. Oxygen supply depends on coronary perfusion. Perfusion, especially to the subendocardial layers, mainly takes place in diastole when the cardiac muscle is relaxed. Thus aortic pressure in diastole and the duration of diastole, together quantified by the area under the diastolic aortic pressure curve, and called the diastolic pressure-time index, gives a measure of oxygen supply. The systolic pressure-time index, or Tension Time Index is a measure of oxygen demand. It has therefore been proposed that the ratio of areas under the diastolic aortic pressure and the area under the systolic pressure curve, gives an estimate of the supply-demand ratio of the subendocardial layers of the heart.

With increasing age wave reflections become more prominent in systole (Chapters 21 and 22), resulting in an increase in mean systolic pressure and a decrease in mean diastolic pressure. This means that with age the supply-demand ratio decreases, which may result in ischemia in subendocardial layers. A similar reasoning can be applied to aortic valvular disease and tachycardia.



*THE OXYGEN DEMAND AND SUPPLY, areas under the systolic and diastolic pressure curve, respectively. The ratio may be unfavorably influenced with increasing age.*

### Limitations

The mechanical determinants of oxygen consumption, discussed above, can be used in individual hearts where pharmacological or other interventions are performed. The use of these determinants in different hearts should be done

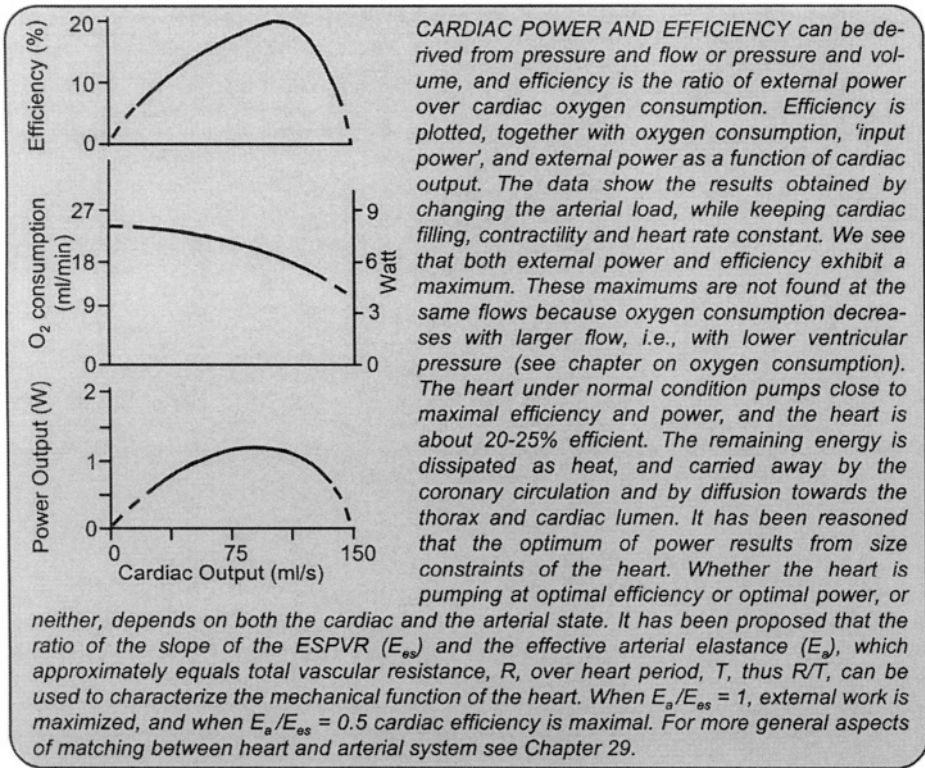
with care. For instance when in an isolated heart study normal and hypertrophied hearts are compared, a similar Tension Time Index or similar Rate Pressure Product does not necessarily imply similar oxygen consumption. Also by applying the Rate Pressure Product to mouse and man, where systolic ventricular pressure is similar but heart rate may differ by a factor of ten, it can not be concluded that cardiac metabolism in the mouse heart is ten times that of the human heart. Even after normalizing for heart mass a difference remains because cardiac metabolism per gram of heart tissue is higher in the mouse than in the human (Chapter 30).

The Pressure Volume Area, PVA, method also falls short when comparing different animals. Since the PVA predicts oxygen consumption per beat heart rate drops out of the equation. When normalized with respect to heart mass or body mass mouse and man would be more comparable but metabolism is not proportional to body mass as will be discussed in Chapter 30.

In compensated concentric hypertrophy pressure is increased and wall thickness is increased in similar proportion while lumen radius is hardly changed, thereby keeping wall stress the same (Chapter 9). This means that the Pressure Volume Area is similar in normal and hypertrophied hearts, while wall mass is increased and thus metabolism is increased. Therefore, correction for wall mass is required. Assuming wall stress to be the major determinant of oxygen consumption, total oxygen consumption would be proportional to wall mass.

## References

1. Rooke GA, Feigl EO. Work as a correlate of canine left ventricular oxygen consumption, and the problem of catecholamine oxygen wasting. *Circ Res* 1982; 50:273-286.
2. Sarnoff Sj, Braunwald E, Welch GH, Case RB, Stainsby WN, Macruz R. Hemodynamic determinants of oxygen consumption of the heart with special relevance to the tension-time index. *Am J Physiol* 1958;192:148-156.
3. Suga H, Ventricular energetics. *Physiological Reviews* 1990;70:247-277.



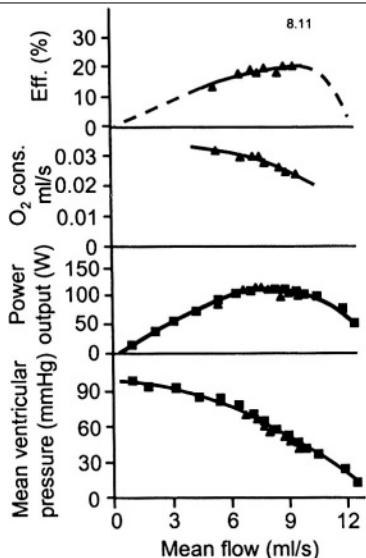
**Description**

*Power and efficiency*

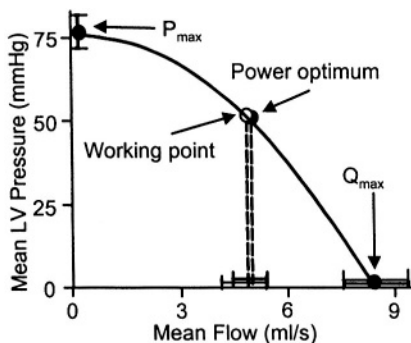
Cardiac efficiency is defined in analogy to that of a hydraulic pump. The external power is calculated from pressure times flow and the 'input power' is calculated from cardiac oxygen consumption. The ratio of external, or produced power, and input power is defined as efficiency. Both need therefore to be expressed in the same units. When glucose or free fatty acids are consumed oxygen consumption can be expressed in Joules and oxygen consumption per time in Watt, through the so-called caloric equivalent. For carbohydrate and fat metabolism it holds that  $1 \text{ ml O}_2 \approx 20 \text{ J}$  and  $1 \text{ ml O}_2/\text{min} \approx 0.33 \text{ Watt}$ .

*Maximum efficiency and maximum power in the intact animal*

The pressure and flow generated by the heart and the arterial load can be studied while keeping the heart rate, diastolic filling and contractility unaltered [3]. Power can be calculated from the pressure and flow. The figure below, on the left, shows that, when power is plotted as a function of Cardiac Output it exhibits an optimal value. This can be understood with the cardiac pump function graph in mind (Chapter 14). For a high load (isovolumic contraction) pressure generated is high but flow is zero. Power, the product



**POWER AND EFFICIENCY** measured in the isolated cat heart. Cardiac filling, contractility, and heart rate were kept constant, while the arterial load was changed. The results show that power and efficiency exhibit maxima, and that oxygen consumption increases when pressure increases. The bottom panel shows the pump function graph. Adapted from [3], used by permission.

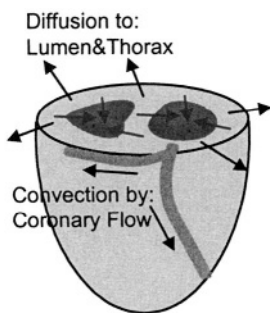


**THE HEART PUMPS AT OPTIMAL POWER** output. Power output of the heart studied in the intact animal for different arterial loads. Other determinants of pressure and flow (heart rate, diastolic filling and contractility), are kept constant. When the physiological arterial load is present, power transfer is maximal. Adapted from [10], used by permission.

working point, i.e., when a physiologic arterial load is present [10]. It has also been reported that the left ventricle works at maximal efficiency [1].

**Heat production and transport**

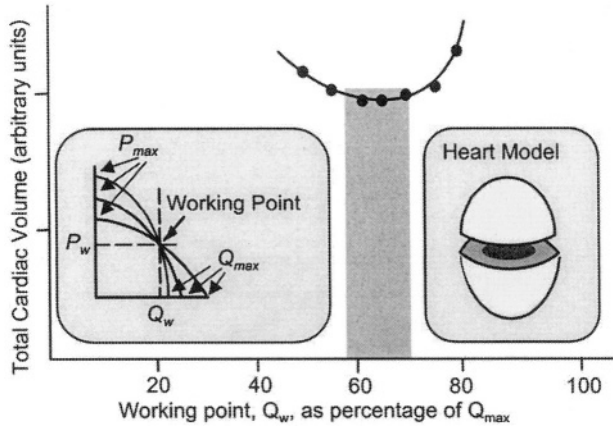
The heart is about 20-25% efficient. This implies that about 75% of the oxygen consumed is converted into heat. The heat is removed by diffusion to lumen and thorax, and convection by coronary flow, in about equal amounts. In the mid-wall of the myocardium the temperature is a few tenths of a degree Celsius higher than in subepicardial and subendocardial layers allowing for diffusion of heat [9].



**OXYGEN CONSUMPTION** produces not only mechanical power but also heat. Convection by coronary flow, and diffusion to thorax and cardiac lumen, account each for about 50% of the heat loss, depending on the magnitude of the coronary flow.

Theory of optimal heart size

Why does the left ventricle pump at maximum power, while a feedback control for power is not known to exist? A simple answer to this question can be given based on the following reasoning [2]. Consider the pump function graph (figure). The working point, i.e., the point where maximum power is found, is for a flow which is about 58% maximal flow,  $Q_{max}$ . Mean systemic pressure and Cardiac Output together determine the working point. Pressure is similar in mammals



*TOTAL VENTRICULAR VOLUME, i.e., wall plus lumen volume, can be calculated assuming a spherical shape, right, and a fixed wall stress for isovolumic contractions,  $\sigma_w/P_m$ . Many pump function graphs through the working point are possible, left, but the pump function graph where the working point is about 60% of  $Q_{max}$ , i.e., where maximal power and efficiency are found, corresponds with the smallest total ventricular volume. Adapted from [2], used by permission.*

and Cardiac Output is determined by body size (Chapter 30). Several pump function graphs can be drawn through this working point. We begin by assuming that muscle stress is a given quantity, and that the ventricle is a sphere. On the one hand, a larger intercept of the pump function graph with the flow axis, i.e., a larger  $Q_{max}$ , implies a larger ventricular lumen requiring a thicker wall (Law of LaPlace), to maintain muscle, or wall stress. On the other hand, with a larger  $Q_{max}$  a smaller  $P_{max}$  results so that the wall may be less thick. In this way it is possible to calculate ventricular volume for the different pump function graphs through the working point, each with its own  $Q_{max}$ . Plotting ventricular volume as a function of  $Q_{max}$  results in the graph given above. The minimum volume is found when the working point is at about 60% of  $Q_{max}$ , and this is the same value as where maximum power and efficiency are found. The minimum in heart volume thus corresponds to a value of the flow at the working point where power and efficiency are about maximal. This calculation shows that the size of the heart is minimized, and, for this heart volume the heart pumps at maximal power.

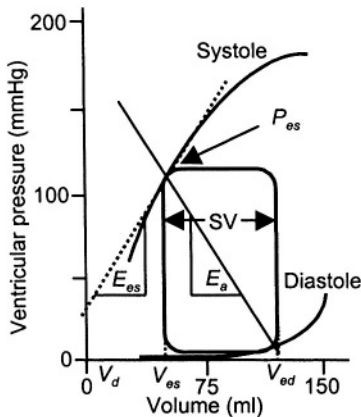
**Physiological and clinical relevance**

‘Input power’, i.e., cardiac oxygen consumption can be studied in human hearts *in vivo* by measurements of arterial and coronary venous oxygen content and coronary flow. Cardiac oxygen consumption and efficiency are still difficult to obtain in the patient. Modern techniques, such as Positron Emission Tomography (PET) and Magnetic Resonance Spectroscopy (MRS) may change this. Assessment of glucose metabolism with  $^{18}\text{F}$ -fluorodeoxyglucose is regarded as the gold standard, and for myocardial

oxidative metabolism by  $^{11}\text{C}$ -labeled acetate PET and  $^{18}\text{F}$ -fluorodeoxyglucose PET give complementary information. Examples are  $^{123}\text{I}$ -beta-methyl-p-iodophenyl pentadecanoic acid and  $^{15}\text{-(O-}^{123}\text{I-phenyl)-pentadecanoic acid}$ . These tracers can be detected by planar scintigraphy and single-photon emission computed tomography (SPECT), which are more economical and more widely available than PET. With current MRS techniques,  $^{31}\text{P}$ -labeled magnetic resonance spectroscopy, Phosphate/Creatine and/or pH can be obtained in humans but this is not common yet. The hemodynamic parameters for oxygen consumption, as discussed in Chapters 16 and 17, are only valid in single hearts during acute interventions and cannot be used in comparing different patients.

'Output power' requires the measurement of aortic or ventricular pressure and flow. Thus for the calculation efficiency, which is the ratio of 'Output power' and 'Input power', many measurements are required and therefore efficiency is not calculated routinely. In Chapter 30 it is shown that cardiac metabolism per gram of heart tissue depends on animal size and is proportional to body mass to the power  $-1/4$ .

#### Assessment of ventriculo-arterial coupling and cardiac efficiency



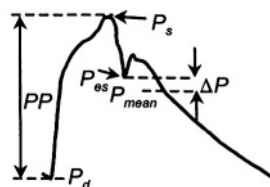
THE CONCEPT OF  $E_{es}$  OR  $E_{max}$  and  $E_a$ . The  $E_{max}$  is the slope of the End-Systolic Pressure-Volume Relation (ESPVR), and  $E_a$  is the slope of the theoretical line through the end-systolic and end-diastolic points of the loop.  $E_a$  therefore equals end-systolic pressure,  $P_{es}$ , over Stroke Volume,  $SV$ . In approximation it is equal to the ratio of peripheral resistance,  $R$ , and heart period,  $T$ , i.e.,  $R/T$ . The  $E_a$  depends therefore on both the heart and the arterial load. Adapted from [7], used by permission.

In this section a method is presented to assess whether the heart functions on optimum power or efficiency, using hemodynamic principles. Optimum power or efficiency are assumed measures of ventriculo-arterial coupling. The two parameters assumed to be the determining ones are effective arterial elastance,  $E_a$ , and the slope of the left ventricular End-Systolic Pressure-Volume Relation,  $E_{es}$ . The effective arterial elastance is defined as  $E_a = P_{es}/SV$ , i.e., end-systolic pressure over Stroke Volume, (see figure on the left). The ratio of these two parameters determines ventriculo-arterial coupling. It has been suggested that the ratio  $E_a/E_{es}$  is a ventriculo-arterial coupling parameter and that when  $E_a/E_{es} = 1$ , external work is maximized, while for  $E_a/E_{es} = 0.5$  cardiac efficiency is maximal [7].

To determine these two parameters, several simplifications have been used. The  $E_a$  can be approximated as follows. End-systolic pressure is close to mean arterial pressure (figure on next page). With Cardiac Output,  $CO$ , being  $SV \cdot HR$ , and Heart Period  $T$ , in seconds, the inverse of  $HR$ ,  $CO = SV/T$ , we find that  $P_{es}/SV \approx P_{mean}/CO \cdot T = R/T$ . Thus the effective arterial elastance,  $E_a$ , is primarily a measure of vascular or peripheral

resistance,  $R$ , and hardly reflects the compliant properties of the large conduit arteries. Therefore the term 'elastance' is misleading. Also  $E_a$  depends on vascular resistance, which is a purely arterial variable, and on heart period,  $T$ ,

which is a purely cardiac variable. Therefore,  $E_a$  is a coupling parameter by itself. However,  $E_a$  can be derived from noninvasive measurements: mean pressure (by sphygmomanometer) and Cardiac Output (US or MRI), and heart rate. The maximum or End-Systolic elastance,  $E_{es}$  is calculated from  $E_{es} = P_{es} / (V_{es} - V_d)$ . End-Systolic volume can be measured noninvasively, but  $V_d$  is hard to estimate. To derive this intercept volume, at least one other point on the ESPVR should be obtained. This would require changes in diastolic filling that are often not feasible in very sick patients and in epidemiological studies. One method to determine the End-Systolic Pressure-Volume Relation is the one suggested by Sunagawa [7], where an isovolumic left ventricular pressure is predicted from the pressure of an ejecting beat. However, none of the so-called single beat methods to determine the ESPVR has been shown to give accurate estimates [5], We therefore advise against their use.



END-SYSTOLIC PRESSURE is close to mean aortic pressure, allowing for non-invasive determination of  $P_{es}$ .

In a number of studies it has simply been assumed that  $V_d = 0$  [6]. This assumption leads to a very interesting simplification of the analysis. With the  $V_d = 0$ ,  $E_{es} = P_{es} / V_{es} = P_{es} / (V_{ed} - SV)$ . The ratio  $E_a / E_{es}$  then becomes equal to:

$$E_a / E_{es} = (P_{es} / SV) / [P_{es} / (V_{ed} - SV)] = (V_{ed} - SV) / SV = 1/EF - 1$$

with EF, the Ejection Fraction. We see that the  $P_{es}$  disappears altogether only leaving the determination of Ejection Fraction. This implies that work is maximal when  $E_a / E_{es} = 1$ , when  $EF = 0.5$ . Similarly, cardiac efficiency is maximal when  $E_a / E_{es} = 0.5$  or when  $EF = 0.67$ .

Thus the assumption of a negligible  $V_d$  simplifies matters. However, negligible  $V_d$  values are difficult to verify, mostly not correct, and are certainly leading to large errors in the dilated heart (Chapters 13 and 15).

### Related issues

*Contractile efficiency.* On the basis of the Pressure Volume Area concept (Chapter 16) the contractile efficiency has been defined as the inverse of the slope of the Pressure Volume Area -  $VO_2$  relation [8]. This definition of efficiency only accounts for the mechanical aspects of oxygen consumption and does not take into account the oxygen expenditure related to activation and basic metabolism. Therefore this contractile efficiency is about twice the actual cardiac efficiency.

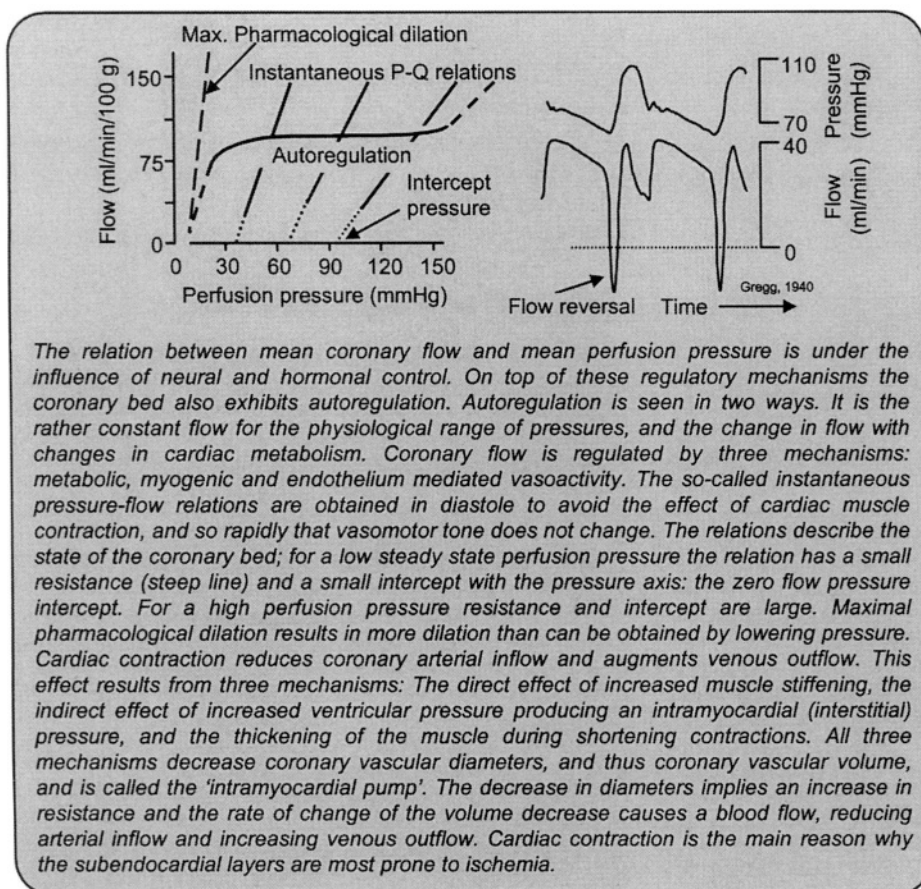
*Power in cardiogenic shock.* Although power, is a rather abstract measure, it has been shown that it is the strongest hemodynamic correlate of mortality in cardiogenic shock [4].

*Economy.* At the extremes of the pump function graph, the heart generates neither pressure nor flow. External power and thus efficiency is zero. In isolated heart studies (Langendorff preparations) where the heart is contracting isovolumically or in isolated cardiac muscle studies, economy can be used instead. Economy of contraction is defined as oxygen consumption used for isovolumic contractions.

---

**References**

1. Burkhoff D, Sagawa K. Ventricular efficiency predicted by an analytical model. *Am J Physiol* 1986;250:R1021-1027.
2. Elzinga G, Westerhof N. Matching between ventricle and arterial load. An evolutionary process. *Circ Res* 1991;68:1495-1500.
3. Elzinga G, Westerhof N. Pump function of the feline left heart: changes with heart rate and its bearing on the energy balance. *Cardiovascular Res* 1980; 14:81-92.
4. Fincke R, Hochman JS, Lowe AM, Menon V, Slater JN, Webb JG, LeJemtel TH, Cotter G. Cardiac power is the strongest hemodynamic correlate of mortality in cardiogenic shock: a report from the SHOCK trial registry. *J Am Coll Cardiol* 2004; 44:340-348
5. Kjørstad KE, Korvald C, Myrmed T. Pressure-volume-based single beat estimations cannot predict left ventricular contractility in vivo. *Am J Physiol* 2002;282:H1739-H1750.
6. Saba PS, Roman MJ, Ganau A, Pini R, Jones EC, Pickering TG, Devereux RB. Relationship of effective arterial elastance to demographic and arterial characteristics in normotensive and hypertensive adults. *J Hypertension* 1995; 13:971-977.
7. Sunagawa K, Maughan WL, Sagawa K. Optimal arterial resistance for the maximal stroke work studied in the isolated canine left ventricle. *Circ Res* 1985; 56:586-595.
8. Suga H. Ventricular energetics. *Physiological Reviews* 1990;70:247-277.
9. ten Velden GH, Elzinga G, Westerhof N. Left ventricular energetics. Heat loss and temperature distribution of canine myocardium. *Circ Res* 1982;50:63-73.
10. Toorop GP, Van den Horn GJ, Elzinga G, Westerhof N. Matching between feline left ventricle and arterial load: optimal external power or efficiency. *Am J Physiol* 1988;254:H279-285.



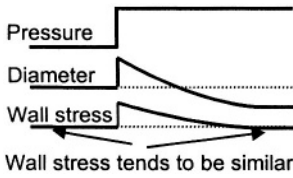
## Description

The relations between arterial pressure and flow in the coronary bed are under the influence of the humoral-nervous systems, and under local control, i.e. autoregulation. There is also the mechanical effect of the contracting cardiac muscle on coronary flow. Several other mutual interactions of smaller magnitude between the coronary vasculature and the cardiac muscle exist, which will be discussed below. The quantitative contribution of humoral and nervous control will not be discussed here. For a comprehensive description of coronary hemodynamics see [9,17].

### *Autoregulation of coronary flow*

In the beating heart and in the physiological pressure range (40 - 140 mmHg) the relation between mean coronary flow and mean perfusion pressure shows a rather constant mean coronary flow (Figure in box). With increased and decreased cardiac metabolism the plateau of the curve increases and decreases, respectively. The fact that the plateau of the autoregulation curve depends on cardiac metabolism suggests that metabolic

autoregulation is a primary effect that mainly plays a role in the smallest arterioles, which are in close contact with the cardiac muscle. A single mediator, originally thought to be adenosine, is too simple a theory for metabolic autoregulation. Several mediators play a role, usually in combination, and depending on the conditions. Metabolites such as adenosine, carbon dioxide, and pH, and ions, and oxygen may play a role. Mathematical modeling [5] and the proven relation between coronary vascular resistance and tissue and venous oxygen tension [21] suggest an important role of oxygen.



The myogenic autoregulation results from an intrinsic property of (smooth) muscle, which tries to maintain muscle tension constant. An increase in pressure initially increases the diameter and the wall stress. The subsequent vasoconstriction decreases vessel radius and increases wall thickness thereby reducing the wall stress (See Chapter 9). The myogenic response appears the strongest in the medium sized arterioles.

**THE MYOGENIC RESPONSE.**  
An increase in pressure increases vessel diameter and wall tension. Subsequent smooth muscle contraction reduces the diameter, and restores wall stress.

Endothelium mediated vasoactivity results from the fact that perfusion flow determines shear stress on the endothelial cells, which liberate vasodilators such as NO and prostaglandins. The main effect is in the larger, vessels, rather than in

the resistance vessels [10]. Especially during strong vasodilation and thus large flow, increased diameters keep the pressure drop over the conduit system minimal.

When perfusion pressure changes the myogenic response and endothelium mediated regulation will be activated first, and metabolic regulation may follow. For a change in cardiac metabolism, the metabolic regulation will be initiated first and the other two will follow.

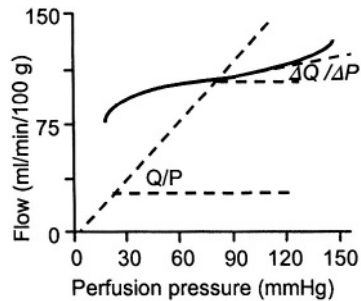
*Autoregulation gain*

Autoregulation gain,  $G$ , is a measure of the strength of autoregulation, and can be calculated as:

$$G = 1 - (\Delta Q / \Delta P) / (Q / P)$$

$$= 1 - (\Delta Q / Q) / (\Delta P / P)$$

with  $\Delta Q / \Delta P$  the slope of the mean pressure-mean flow relation and  $Q / P$  the slope of the line through the point of determination and the origin of the graph, the inverse of resistance. It can be seen that for perfect autoregulation the gain equals 1 and for no autoregulation, assuming the pressure-flow relation would go through the origin, the gain equals zero. Since the pressure-flow relation does, in general, not go through the origin, it has been suggested to use the slope of the instantaneous pressure-flow relation instead



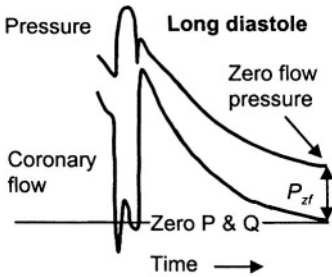
**AUTOREGULATION GAIN** is defined as one minus the ratio of the local slope ( $\Delta Q / \Delta P$ ) and the line through the origin ( $Q / P$ ), i.e.,  $1/R$ . Gain depends on perfusion pressure.

of  $Q/P$ . Autoregulation gain can be plotted as a function of pressure to obtain the range of regulation.

### Maximal vasodilation

Maximal vasodilation obtained pharmacologically (e.g., adenosine) may result in a stronger vasodilation than can be obtained physiologically by lowering blood pressure (see left figure in the box).

### Instantaneous pressure-flow relations



THE INSTANTANEOUS pressure-flow relation can be determined from long diastoles. It gives the 'state' of the bed, without the mechanical effect of the cardiac muscle. Adapted from [2], used by permission.

The coronary pressure-flow relations are under the influence of the vasomotor tone of the smooth muscle and the effect of the cardiac contraction on the vasculature. To get insight into the vasculature alone, the effect of cardiac contraction is to be minimized. This means that pressure-flow relations should be obtained in diastole.

Bellamy [2] studied pressure-flow relations in long diastoles obtained by vagal stimulation. Since the smooth muscle is slow, it is assumed that over a single long diastole, of about 1-2 seconds, vascular tone does not change. Thus the instantaneous pressure-flow relation describes the coronary vascular tree independently of the cardiac muscle contraction and for a constant vasomotor tone.

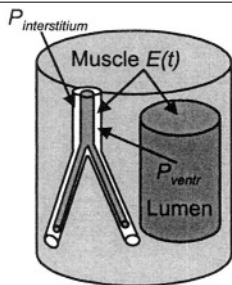
The instantaneous pressure-flow relations (see figure in the box) show an intercept,  $P_{zf}$ , with the pressure axis, the so-called zero-flow pressure. The zero-flow pressure and the inverse slope (i.e., resistance) increase with vasomotor tone. Several explanations have been given for the intercept pressure, none of which is generally accepted. Since the intercept pressure also is present with crystalloid perfusion, it is not the effect of plugging by blood cells [20]. Surface tension [14] has been proposed as a mechanism as well, but the changes in intercept with tone are hard to explain with this theory.

The zero-flow pressure may be an apparent intercept, which is related to the plateau of the pressure-volume relation of the arterioles [15] and thus results from a large compliance. Increased vasomotor tone increases the level of the plateau of the pressure-volume relation and this could explain the increase in the, apparent, intercept.

### Cardiac contraction and coronary flow

Coronary arterial inflow is impeded and venous outflow is augmented during cardiac contraction. When the coronary bed is vasodilated and cardiac muscle contractility is high, arterial flow may even reverse in early systole (see right figure in the box [7]).

The contracting cardiac muscle exerts its effect on the vasculature in three ways. The increasing stiffness of the muscle in systole (see  $E(t)$ , Chapter 13) has a similar effect on the interstitial volume and the blood vessels as it has on the lumen of the ventricle. This pumping action causes the vascular

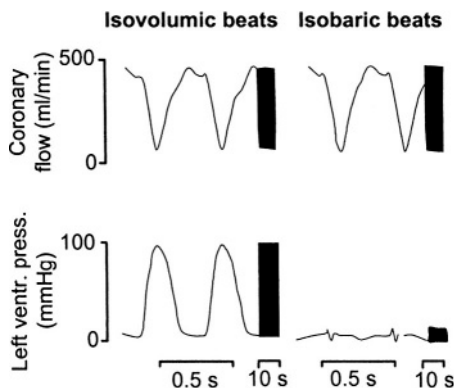


**CARDIAC CONTRACTION** implies increased stiffness of the muscle. For ventricular lumen and interstitium this increase in elastance results in a pumping action increasing pressure. Ventricular pressure is also transmitted to interstitium, giving an intramyocardial pressure. The result is decreased vascular volume and increased resistance.

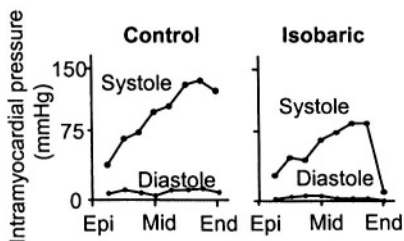
diameters and thus also vascular volume to decrease. Support for this mechanism is shown in the figure below, right. This direct effect of the varying elastance,  $E(t)$ , is similar for isovolumic and isobaric contractions, i.e., contractions without pressure generation in the ventricular lumen. The ventricular load affects ventricular pressure and ventricular outflow, but when the aortic and coronary sinus pressure are unaffected, a similar pumping effect on coronary flow during both isovolumic and isobaric contractions is found [11].

The other effect is that of the pressure in the left ventricle, which, incidentally, also arises from the varying elastic properties of the cardiac muscle (Chapter 13). This pressure generates a so-called intramyocardial or interstitial pressure, which acts on the outer surface of the blood vessels. The intramyocardial pressure is assumed to be equal to ventricular pressure at the subendocardium and negligible at the subepicardium [6]. However, there is some doubt regarding these assumptions, since

intramyocardial pressure is still considerable even when ventricular luminal pressure is negligible as in isobaric beats (figure below, left). Intramyocardial pressure decreases transmural pressure and thus vascular diameters and vascular volume. Finally muscle shortening affects the vasculature since by shortening the muscles increase in diameter. The increase in muscle diameter takes place at the expense of the vessels, thereby decreasing their diameters [25]. These two



**CORONARY FLOW DURING ISOVOLUMIC BEATS, left, and isobaric contractions, right, of the isolated blood perfused cat heart. From [11], used by permission.**



**INTRAMYOCARDIAL PRESSURES MEASURED** in the beating heart using the servo-null technique. The intramyocardial pressure is high in isobaric beats where ventricular luminal pressure is negligible. Adapted from [13], used by permission.

effects, muscle elastance changes and muscle thickening, play complementary roles, since for isovolumic beats left ventricular pressure is high and so is intramyocardial pressure but muscle thickening is small because the muscles do not shorten. For isobaric beats muscles shorten and thus thicken and this effect is larger than the pressure related effect. These two mechanisms also explain why cardiac contraction affects the subendocardial layers most and may

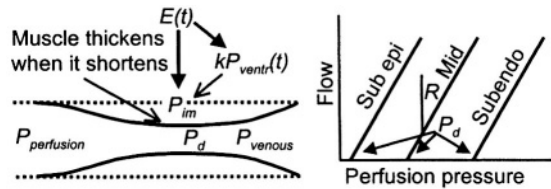
suggest the reason why the subendocardial layers are more prone to ischemia than subepicardial layers. All these effects act directly on the vessels and are not coupled via vascular compliance as has been suggested earlier. This implies that in the steady state of contraction, i.e., systolic arrest, diameters are decreased and resistance is increased. Mean flow is indeed decreased in systolic arrest [16].

Since normal contraction is dynamic, the rate of change of vascular volume results in a blood flow. The blood is therefore pumped, in a similar way to the ventricular pump, but since valves are absent, the blood is pumped to the arterial and to the venous side. The inflow of blood, at the arterial side, is thus decreased and the outflow, at the venous side, is increased.

Detailed calculations have shown that the varying stiffness of the cardiac muscle, the thickening of the shortening muscle, and the increased intramyocardial pressure resulting from left ventricular pressure during contraction all contribute to decreased vessel size and therefore the increased resistance and intramyocardial pumping. The contribution of these effects depends on the layer, mode of contraction and the contractility [22].

The summary is given in the figure. The pressure-flow relations show an intercept that depends on the layer, on contractility and left ventricular pressure.

When it is assumed that coronary perfusion only takes place in diastole we can approximate the coronary fractional perfusion time, i.e. relative to the heart period  $T$ , as  $T_d/T = 1 - T_s/T$ , with  $T_d$  and  $T_s$  the duration of diastole and systole, respectively. Thus with a heart rate of 60 bpm, and time of systole being 0.35 s the coronary fractional perfusion time is  $1 - 0.35/1 = 0.65$  s/s. When heart rate is increased to 120 bpm and ejection time decreased to 0.3 s the coronary fractional perfusion time is  $1 - 0.3/0.5 = 0.4$  s/s, thereby decreasing coronary perfusion.



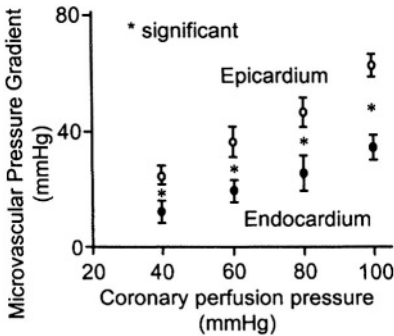
THE VASCULAR WATERFALL AND INTRAMYOCARDIAL PUMP result from cardiac muscle contraction and consists of a 'Starling resistor', which acts as a pressure regulator, including a resistance. This 'regulated' pressure,  $P_d$ , equals intramyocardial pressure,  $P_{im}$ , and gives the zero flow pressure intercept. The  $P_{im}$  depends on the layer in the wall. Muscle contraction results in stiffer environment and in ventricular pressure, both leading to  $P_{im}$ . When the muscle shortens it thickens at the expense of the vasculature. The waterfall states [6] that flow is proportional to perfusion pressure minus waterfall pressure,  $P_d$ , rather than perfusion pressure minus venous pressure. The variations in vascular diameters result in pumping [18], used by permission.

*Microvascular aspects*

Intramyocardial pressure has been measured for many years with different techniques [24]. A recent method is the measurement with the servo-null technique, using micropipettes (diameter in the micron range) so as to cause minimal damage [13]. The results of these measurements are shown in the figure on the previous page. Thus intramyocardial pressure is not simply proportional to ventricular pressure. For the interstitial space the varying elastance hypothesis was applied to explain why intramyocardial pressure is present and similar in isobaric and isovolumic beats [24].

*Both arteriolar and venular diameters decrease in systole.* The decrease in arteriolar and venular diameter between diastole and systole in subendocardial layers are about 12% and 25%, respectively [26]. Thus venules are not being compressed completely as would be expected when intramyocardial pressure is close to ventricular pressure. A theoretical explanation has been given, and it is also shown that partial venous collapse protects arterioles from large changes in diameter [23].

*Bridging.* When an epicardial vessel is located in the cardiac wall the vessel is greatly affected by cardiac contraction.



*THE NET PERFUSION PRESSURE, expressed as microvascular pressure gradient, is significantly smaller in the subendocardium than in the subepicardium.* Adapted from [4], used by permission.

but varies ('twinkling'). However, in areas where flow is large it remains large and where small it remains small. Large and small flows are not found at similar locations between animals. A partial explanation is based on the fractal rules of coronary geometry [1], but a complete explanation has not yet been given. Another explanation may be that cardiac myocytes are quite different in length and cross-section and larger cells require more oxygen.

*The Gregg effect.* Myocardial perfusion, in the absence of substrate and metabolite limitation, affects cardiac muscle contractility. It appears that increased perfusion opens Stretch Activated Channels, SAC's, thereby affecting both the Calcium handling and the contractile apparatus of the myocytes [12].

*Vascular emptying in systole augments cardiac muscle contraction.* During muscle shortening muscle diameter increases at the cost of the vascular volume. If the vascular volume cannot change, pressure is built up in the muscle cells and this intracellular pressure counteracts the force generated by the contractile apparatus so that the net force is smaller [25].

*Both endocardial and vascular endothelium modulate cardiac muscle contraction.* Removal or damaging of the endothelium results in a lower and shortened force generation [3]. In general NO modulates cardiac performance such that it is matched to oxygen consumption and perfusion.

*Coronary flow cools the heart.* Cardiac efficiency is about 20-25% (Chapter 17), implying that about 75% of the oxygen consumed is converted into heat. This heat is transported by diffusion to mediastinum and ventricular lumen as well as by convection by the coronary flow. At the

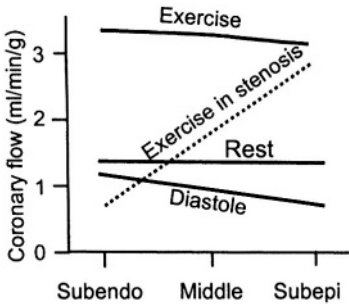
*Perfusion pressure in layers..* Microvascular perfusion pressure, expressed as arteriolar minus venular pressure is considerably lower in subendocardial layers than in subepicardial layers [4]. This is caused by the pressure drop over the transmural arteries and transmural veins and may, in part, explain why the subendocardium is more vulnerable to ischemia than the subepicardial layers.

*Coronary flow heterogeneity.* Local flows are different between locations. It varies from less than 50% to more than twice the mean flow. This variation is larger when the sample volume is smaller. Flow in small areas is not constant in time,

normal level of coronary flow, i.e., ~90 ml/min/100g, about 70% of the heat is transported by flow. For lower flow the transport by diffusion increases, and at a flow of 45 ml/min/100g convection and diffusion contribute about equally to cardiac cooling [19].

**Physiological and clinical relevance**

*Coronary flow in layers*



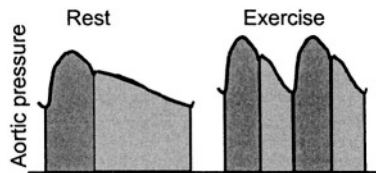
**BLOOD FLOW DISTRIBUTION** in cardiac layers. In diastole flow is about 20% larger in subendocardial than in subepicardial layers. At rest mean flow is equally distributed over the different layers. During exercise flow in the subendocardium tends to be slightly smaller than in the subepicardium. During exercise in the presence of a mild stenosis, coronary subendocardial flow will fall short.

Coronary heart disease is a major problem in the western world and understanding of the factors that determine the pathology of coronary function is therefore of utmost clinical importance.

The coronary flow has to be matched to cardiac metabolism and should thus vary with activity and exercise. In the healthy organism coronary flow is matched to demand. Autoregulation assures that during variations in pressure flow is maintained and that with increased metabolism flow is increased. When a stenosis is present the pressure distal to the stenosis may be too low for adequate perfusion and this is first experienced in exercise, when flow should increase. The explanation that cardiac ischemia is earlier apparent in subendocardial layers than in subepicardial layers is the partly the result of cardiac contraction and partly the result of the pressure drop over the transmural vessels..

*Supply-demand*

Although the anatomy is such that coronary vascular resistance in diastole is the smallest in the subendocardial layers, contraction still reduces flow so much in this layer that perfusion only takes place during diastole. Thus the perfusion pressure and the duration of diastole are the main determinants of flow when the vasculature is dilated to its physiological maximum. This has led to the supply - demand ratio (see Chapter 16). The area under the systolic part of aortic, or left ventricular pressure curve is an index of oxygen consumption, see the Tension Time Index (Chapter 16). The area under the diastolic pressure curve is a measure of supply. The supply-demand ratio appears an acceptable indication of subendocardial ischemia [8]. In exercise the supply-demand ratio is strongly decreased.



**THE SYSTOLIC AND DIASTOLIC PRESSURE-TIME AREAS.** Their ratio is considered to be a measure of the myocardial, subendocardial, supply-demand ratio. During exercise the diastolic area decreases and the systolic area may even increase.

The area under the diastolic pressure curve is a measure of supply. The supply-demand ratio appears an acceptable indication of subendocardial ischemia [8]. In exercise the supply-demand ratio is strongly decreased.

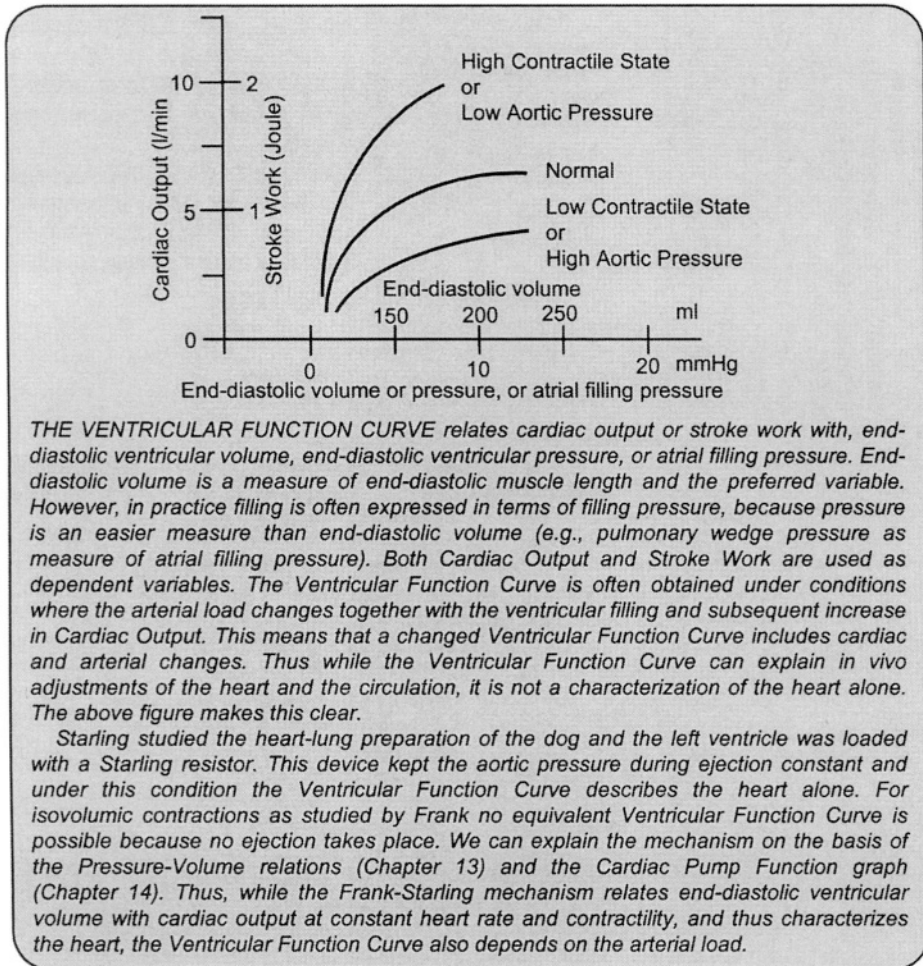
*Coronary Stenosis*

The effect of a coronary stenosis, in terms of perfusion, is quantified by coronary flow reserve, by relative flow reserve and by fractional flow reserve. The hemodynamic of the stenosis is discussed Chapter 5.

**References**

1. Bassingthwaite JB, King RB, Roger SA. Fractal nature of regional myocardial blood flow heterogeneity. *Circ Res* 1989;65:578-590.
2. Bellamy RF. Diastolic coronary artery pressure-flow relations in the dog. *Circ Res* 1978;43:92-101.
3. Brutsaert DL. Cardiac endothelial-myocardial signaling: Its role in cardiac growth, contractile performance, and rhythmicity. *Physiol Reviews* 2003;83:59-115.
4. Chilian WM. Microvascular pressures and resistances in the left ventricular subepicardium and subendocardium. *Circ Res* 1991;69:561-570.
5. Dankelman J, Spaan JAE, van der Ploeg CPB, Vergroesen I. Dynamic response of the coronary circulation to a rapid change in perfusion in the anaesthetised goat. *J Physiol (Lond)* 1989;419:703-715.
6. Downey JM, Kirk ES. Inhibition of coronary blood flow by a vascular waterfall mechanism. *Circ Res* 1975;36:753-760
7. Gregg DE, Green HD. Registration and interpretation of normal phasic inflow into the left coronary artery by an improved differential manometric method. *Am J Physiol* 1940;130:114-125.
8. Hoffman JIE, Buckberg JD. Myocardial supply:demand ratio - a critical review. *Am J Cardiol* 1978;41 :327-332.?
9. Hoffman JIE, Spaan JAE. Pressure-flow relations in the coronary circulation. *Physiol Rev* 1990;70:331-390.
10. Kuo L, Davis MJ, Chilian WM. Longitudinal gradients for endothelium-dependent and -independent vascular responses in the coronary microcirculation. *Circulation* 1995;92:518-525.
11. Krams R, van Haelst, ACTA, Sipkema P, Westerhof N. Can coronary systolic-diastolic flow differences be predicted by left ventricular pressure of by time-varying intramyocardial elastance? *Basic Res Cardiol* 1989;84:149-159.
12. Lamberts RR, van Rijen MH, Sipkema P, Franssen P, Sys SU, Westerhof N. Increased coronary perfusion augments cardiac contractility in the rat through stretch-activated ion channels. *Am J Physiol* 2002;282:H1334-H1340.
13. Mihailescu LS, Abel FL. Intramyocardial pressure gradients in working and nonworking isolated cat hearts. *Am J Physiol* 1994;266:H1233-H1241.
14. Sherman IA. Interfacial tension effects in the microvasculature. *Microvasc Res* 1981;22:296-307.
15. Sipkema P, Westerhof. N. Mechanics of a thin walled collapsible microtube. *Ann Biomed Eng* 1989;17(3):203-17.
16. Sipkema P, Takkenberg JJM, Zeeuwe PEM, Westerhof N. Left coronary pressure-flow relations of the beating and arrested rabbit heart at different ventricular volumes. *Cardiovasc Res* 1998;40:88-95.
17. Spaan JAE. *Coronary Blood Flow*. 1991, Dordrecht, Kluwer Acad Pres.

18. Spaan JAE, Breuls NPW, Laird JD. Diastolic-systolic coronary flow differences are caused by intramyocardial pump action in the anesthetized dog. *Circ Res* 1981;49:584-593.
19. Ten Velden GHM, Westerhof N, Elzinga G. Left ventricular energetics: heat loss and temperature distribution in the canine myocardium. *Circ Res* 1982; 50:63-73.
20. Van Dijk LC, Krams R, Sipkema P, Westerhof N. Changes in coronary pressure-flow relation after transition from blood to Tyrode. *Am J Physiol* 1988;255: H476-H482.
21. Vergroesen I, Noble MIM, Wieringa PA, Spaan JAE. Quantification of O<sub>2</sub> consumption and arterial pressure as independent determinants of coronary flow. *Am J Physiol* 1987;252:H545-H553.
22. Vis MA, Bovendeerd PH, Sipkema P, Westerhof N. Effect of ventricular contraction, pressure, and wall stretch on vessels at different locations in the wall. *Am J Physiol* 1997;272:H2963-H2975.
23. Vis MA, Sipkema P, Westerhof N. Compression of intramyocardial arterioles during cardiac contraction is attenuated by accompanying venules. *Am J Physiol* 1997;273:H1002-H1011.
24. Westerhof N. Physiological Hypothesis. Intramyocardial pressure. *Basic Res Cardiol* 1990;85:105-119.
25. Willemsen MJJM, Duncker DJ, Krams R, Dijkman M, Lamberts RR, Sipkema P, Westerhof N. Decrease in coronary vascular volume in systole augments cardiac contraction. *Am J Physiol* 2001;281:H731-H737.
26. Yada T, Hiramatsu O, Kimura A, Goto M, Ogasawara Y, Tsujioka K, Yamamori S, Ohno K, Hosaka H, Kajiyama F. In vivo observation of subendocardial microvessels in the beating porcine heart using a needle-probe videomicroscope with a CCD camera. *Circ Res* 1993;72:939-946.

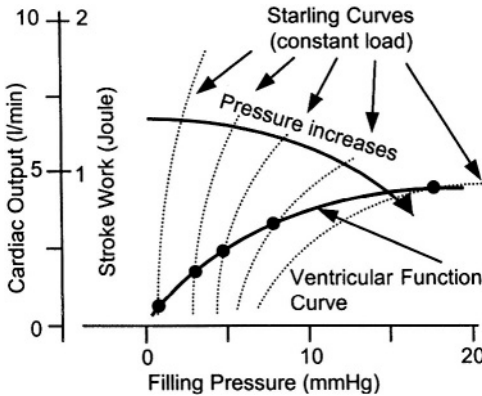


*THE VENTRICULAR FUNCTION CURVE relates cardiac output or stroke work with, end-diastolic ventricular volume, end-diastolic ventricular pressure, or atrial filling pressure. End-diastolic volume is a measure of end-diastolic muscle length and the preferred variable. However, in practice filling is often expressed in terms of filling pressure, because pressure is an easier measure than end-diastolic volume (e.g., pulmonary wedge pressure as measure of atrial filling pressure). Both Cardiac Output and Stroke Work are used as dependent variables. The Ventricular Function Curve is often obtained under conditions where the arterial load changes together with the ventricular filling and subsequent increase in Cardiac Output. This means that a changed Ventricular Function Curve includes cardiac and arterial changes. Thus while the Ventricular Function Curve can explain in vivo adjustments of the heart and the circulation, it is not a characterization of the heart alone. The above figure makes this clear.*

*Starling studied the heart-lung preparation of the dog and the left ventricle was loaded with a Starling resistor. This device kept the aortic pressure during ejection constant and under this condition the Ventricular Function Curve describes the heart alone. For isovolumic contractions as studied by Frank no equivalent Ventricular Function Curve is possible because no ejection takes place. We can explain the mechanism on the basis of the Pressure-Volume relations (Chapter 13) and the Cardiac Pump Function graph (Chapter 14). Thus, while the Frank-Starling mechanism relates end-diastolic ventricular volume with cardiac output at constant heart rate and contractility, and thus characterizes the heart, the Ventricular Function Curve also depends on the arterial load.*

## Description

In the intact organism the Ventricular Function Curve is usually presented as the relation between Stroke Volume (or Cardiac Output or stroke work) and ventricular filling. If we make a graph between filling volume and Cardiac Output, we can derive the Ventricular Function Curve from the pressure-volume relation as follows. If the aortic pressure and thus ventricular pressure in systole is kept constant (Starling experiment), Cardiac Output is proportional to end-diastolic volume. In the intact organism, however, the pressure increases with increasing Cardiac Output, and this increase in pressure depends on the neural and humoral regulatory mechanisms. If changes are performed so rapidly that regulation cannot set in, we follow a family of curves: for larger filling Cardiac Output increases but the higher pressure counteracts this increase in part (see figure on next page). Thus an increase in filling volume results in a smaller increase in Cardiac Output than



THE RELATION BETWEEN LEFT VENTRICULAR filling pressure and cardiac output depends on the pressure in systole, or simpler, aortic pressure. The family of curves, dotted lines, can be derived from Starling's experiments at constant aortic pressure. When the actual arterial load is present increased filling results in increased output and increased pressure, i.e., a lower Starling curve.

under the assumption of a constant arterial pressure, as in Starlings' experiment. We thus see that the Ventricular Function Curve depends on the heart in combination with the arterial load, and therefore characterizes ventriculo-arterial coupling and not the heart alone. The relation between diastolic filling and Cardiac Output is therefore more difficult to interpret than the original experiments by Frank and Starling.

Before the cardiac Echo technique became available, ventricular filling pressure or diastolic ventricular pressure was easier to determine than end-diastolic volume and the Ventricular Function Graph was therefore often presented in the form of filling pressure and Cardiac Output. The graph is, in general, more linear when volume is used as independent variable than when filling pressure is used, because of the nonlinear diastolic pressure-volume relation. When circumferential strain is determined together with myocardial stroke work (Chapter 14), the so-called Preload Recrutable Stroke Work can be calculated and plotted as a function of end-diastolic strain and an almost perfectly linear relationship is found [3].

Before the cardiac Echo technique became available, ventricular filling pressure or diastolic ventricular pressure was easier to determine than end-diastolic volume and the Ventricular Function Graph

*Global left ventricular contractile function compared between patients*

Indices of contractile function or contractility are dominated by the contribution of left ventricular (LV) cavity volume because arterial pressures are usually similar between patients. When end-systolic volume (ESV) and end-diastolic volume (EDV) are increased, while Stroke Volume, SV, is not changed, Ejection Fraction (EF) is decreased because  $EF = SV/EDV$ . MUGA, Multiple Gated Acquisitions, is the best method of assessment, at least in theory, because the radioactive counts from the LV cavity, when the blood is labeled, are proportional to volume. Other methods such as echocardiography (Echo) and magnetic resonance imaging (MRI) depend on assumptions about geometry. There is nothing to be gained in this assessment from invasive measurements.

*Invasive assessment of global ventricular function in the patient*

The maximum rate of rise of left ventricular pressure,  $dP_{LV}/dt_{max}$ , can be determined by measuring left ventricular pressure (LVP) with a catheter-tip manometer and passing the signal through an electronic differentiator. The signal has a prominent positive maximum, an index of global LV contractile function and contractility. There is also a prominent negative maximum,  $dP_{LV}/dt_{min}$ , which is a load dependent variable, and cannot be used as a measure of ventricular relaxation.

To be a measure of muscle function  $dP_{LV}/dt$  should be related to wall stress,  $\sigma$ . This can be done using LaPlace's law (Chapter 9).

$$\sigma = P_{LV} g_f$$

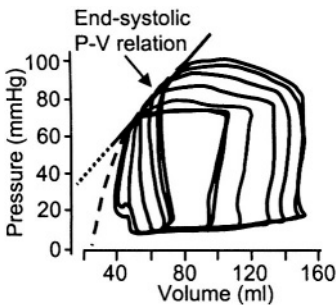
with  $g_f$  a geometry factor accounting for the (local) radius of curvature and myocardial wall thickness. By the chain rule, differentiating with respect to time, we obtain:

$$d\sigma/dt = g_f \cdot dP_{LV}/dt + P_{LV} \cdot dg_f/dt$$

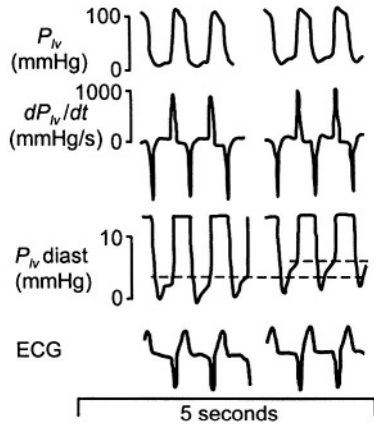
This shows that it is important to determine  $dP_{LV}/dt_{max}$  during isovolumic conditions so that  $g_f$  may be assumed constant, i.e.,  $dg_f/dt = 0$ , and

$$dP_{LV}/dt = (1/g_f) \cdot d\sigma/dt$$

With changes in filling the geometric factor  $g_f$  will change. At low volumes, such as during cardiac surgery with open chest, a change in  $dP_{LV}/dt_{max}$ , may result both from changes in muscle function and filling. In the closed chest, and in the catheter laboratory the geometric factor does, in general, not change so that  $dP_{LV}/dt_{max}$  gives useful information on global muscle function. At very large ventricular



END-SYSTOLIC PRESSURE-VOLUME RELATION as a measure of global ventricular function. Several pressure-volume loops, preferably obtained with changes in cardiac filling, are required to determine this relation. Approximations by assuming a straight relation, with slope  $E_{max}$ , stippled line, or measuring a single loop and assuming linearity and zero  $V_d$ , may lead to unacceptable errors.



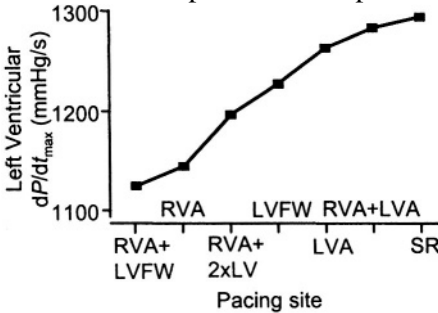
TIME DERIVATIVE OF LEFT VENTRICULAR PRESSURE,  $dP_N/dt$ , as a measure of global function. Increased filling, resulting in an increase in end-diastolic pressure (dashed lines) does not affect  $dP_N/dt$  but this index is sensitive to inotropic interventions. Adapted from [2], used by permission.

volumes an increase in the factor  $g_f$  may even result in a decrease in  $dP_{LV}/dt_{max}$ . Thus  $dP_{LV}/dt_{max}$  can be used only as a convenient volume independent index for changes in cardiac contractility in the catheter laboratory. In the figure above the record on the left was obtained with the patient in head-up tilt and the record on the right with the patient in head-down tilt. It can be seen that the left ventricular end-diastolic pressure is higher in the right hand record due to the increase in ventricular volume, but  $dP_{LV}/dt_{max}$  is unchanged [2].

*Merits and drawbacks of  $dP_{LV}/dt_{max}$  ESPVR and  $E_{max}$  as assessments of global contractility*

The theoretical gold standard for assessment of cardiac contractility is the End-Systolic Pressure-Volume Relation (ESPVR, figure on the left), but in practice this ESPVR is usually only obtainable invasively, as during cardiac surgery. Volume changes are required and they can be obtained by, partial, occlusion and release of the vena cavae. An increase in

contractility corresponds to an upward and leftward movement of the ESPVR. The slope of the relation,  $E_{max}$ , is only an acceptable index of contractility if the relation is straight. For a curved relation the slope depends on the chosen pressure. The straight-line extrapolation often suggests a negative, physically impossible, and thus virtual, intercept with the volume axis. Thus in open thorax experiments, where volume and pressure can be



$LVdP/dt_{max}$  DEPENDS ON PACING SITE. During ventricular pacing from various sites  $LVdP/dt_{max}$  is compared with its value during sinus rhythm (SR). RVA = Right Ventricular Apex; LVFW = Left Ventricular Free Wall; LVA = Left Ventricular Apex; 2xLV = LV free wall and apex. Redrawn from [4], used by permission.

measured, the ESPVR should be reported because it gives much more accurate information than the  $E_{max}$ .

The  $dP_{LV} / dt_{max}$  is unsuitable for comparing the contractility of patients because it is also an index of the synchronicity of contraction. This figure shows, as an example, that during conduction defects, e.g., bundle branch block or inappropriate pacing sites,  $dP_{LV} / dt_{max}$  is different. In general, the  $dP_{LV} / dt_{max}$  is highest during sinus rhythm (extreme right hand point). The End-Systolic Pressure-Volume Relation, ESPVR, has the same shortcoming. In other words, the two quantities do not quantify muscle contractility but overall pump function.

*Non-invasive assessment of global ventricular function in the patient*

By definition, non-invasive assessment rules out methods such as catheter-tip manometry and conductance catheter volume measurement. One approach that gained some popularity is calculating  $E_{max}$  by dividing peak aortic pressure, as an index of end-systolic left ventricular pressure, by end-systolic volume, obtained by Echo or MRI. In addition to the assumption of linearity of the ESPVR, the intercept volume is assumed to be negligible. These non-invasive approaches are subject to errors.

The assessment of contractility may be complicated by the nonlinearity, i.e., the pressure dependence of the ESPVR. Of course, if during an intervention mean arterial pressure does not change the nonlinearity of the ESPVR does not play a role and does not affect the results. If arterial pressure changes it is recommended that the changes in mean arterial pressure are accounted for. If there are no changes in mean pressure, it may be because the intervention does not affect the periphery, or that mean arterial pressure has been clamped by the baroreflex [1]. In either case end-systolic volume can be used as an inverse index of contractility. If the intervention of interest causes an increase in mean arterial pressure, a control run should be compared in which the mean arterial pressure changes are reproduced with a pure vasoconstrictor. The end-systolic volume can then be compared at similar mean arterial pressures between the two runs to deduce whether the unknown intervention included an inotropic response. If the intervention of interest causes a decrease in mean arterial pressure, a control run should be compared in which the mean arterial pressure changes are reproduced with a pure vasodilator. The end-systolic volume can then be

compared at similar mean arterial pressures between the two runs to deduce whether the unknown intervention included an inotropic response.

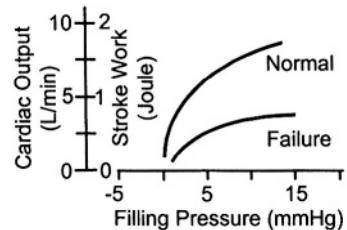
### *Assessment of change in regional left ventricular function*

Global contractile function can be affected both by contractility and by regional dysfunction, e.g. myocardial infarction. In the latter case, regional contractile function is of clinical importance, but cannot be studied in absolute terms as is the case with global function indices such as the ESPVR and  $dP_{LV}/dt_{max}$ . The pragmatic approach therefore is to study local wall movement to see whether it is impaired or, in some cases such as hypertrophic cardiomyopathy, enhanced. Dysfunctional myocardium may respond to a positive inotropic intervention, e.g. post-extra-systolic potentiation or dobutamine infusion. This indicates that the tissue is viable and may improve with reperfusion. This approach is followed in Stress-Echo and Stress-MRI investigations.

### Physiological and clinical relevance

The Ventricular Function Curve is very regularly used to demonstrate the effects of therapy on Cardiac Output.

An example is given in this figure where the Ventricular Function Curve is shown in control and heart failure. Again, one should be aware of the fact that the graphs do not reflect the differences in the heart alone but also contain what is changed in the arterial load.



*VENTRICULAR FUNCTION curves under normal conditions, and in heart failure. The characterization pertains to ventriculo-arterial interaction and not to the heart alone.*

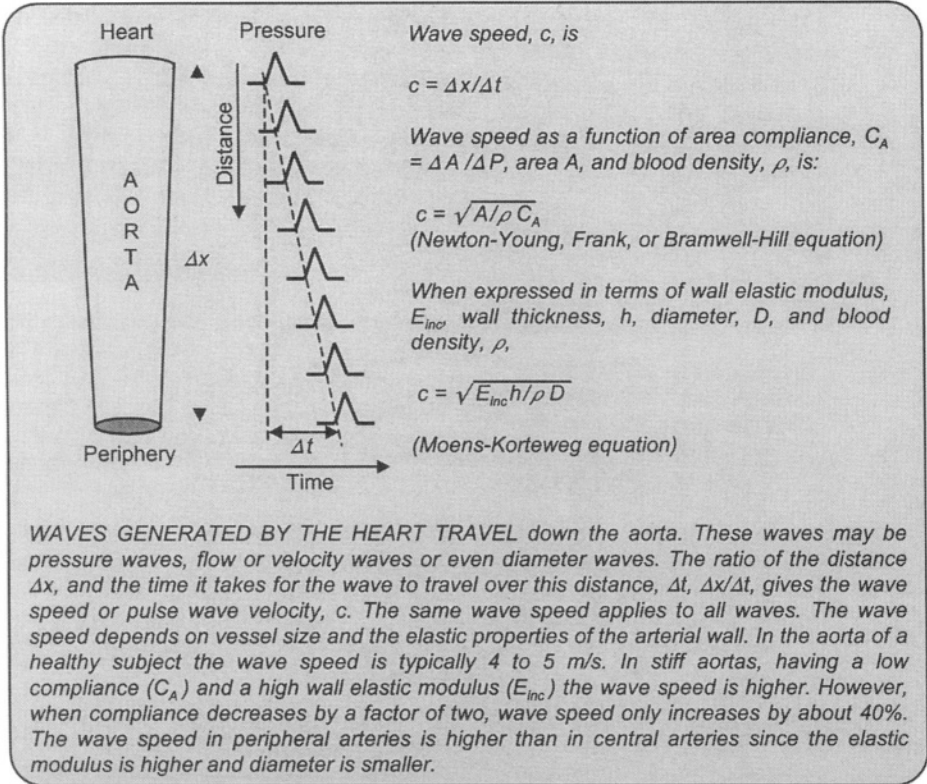
### References

1. Brooks CIO, White PA, Staples M, Oldershaw PJ, Redington AN, Collins PD, Noble MIM. Myocardial contractility is not constant during spontaneous atrial fibrillation in patients. *Circulation* 1998;98:1762-1768.
2. Drake-Holland AJ, Mills CJ, Noble MIM, Pugh S. The response to changes in filling and contractility of various indices of human left ventricular mechanical performance. *J Physiol (Lond)* 1990;422:29-39.
3. Glower DD, Spratt JA, Snow ND, Kabas JS, Davis JW, Olson CO, Tyson GS, Sabiston DC Jr, Rankin JS. Linearity of the Frank-Starling relationship in the intact heart: the concept of preload recruitable stroke work. *Circulation* 1984; 71:994-1009.
4. Prinzen, F.W, and Peschar, M. Relation between the pacing induced sequence of activation and left ventricular pump function in animals. *Journal of Pacing and Clinical Electrophysiology* 2002;25:484-498.

Part C  
Arterial Hemodynamics

# Chapter 20

# WAVE TRAVEL AND VELOCITY



## Description

The heart generates pressure and flow waves. Because of the elasticity of the aorta and the major conduit arteries, the pressure and flow waves are not transmitted instantaneously to the periphery, but they propagate through the arterial tree with a certain speed, which we call wave speed or pulse wave velocity ( $c$ ). In analogy to waves created by the drop of a stone on the surface of a lake, wave travel is characterized by the finite time it takes for the disturbance (wave) to cover a certain distance. The distance traveled by the wave over the time delay gives the wave speed, as schematically shown in the figure in the box. Also, in analogy with the stone dropped in the lake, the wave transmission takes place even in the absence of blood flow and is not related to the velocity of the blood. When a stone is dropped in a river, the waves superimpose on the water flow, and the wave fronts traveling downstream go faster than the wave fronts that move upstream. In other words, the velocity of the blood adds to the wave speed. However, since blood flow velocity is much smaller than wave velocity this effect is usually neglected.

*Wave speed depends on vessel compliance*

The wave speed can be related to the elasticity of the wall material via the Moens-Korteweg equation:

$$c = \sqrt{\frac{h \cdot E_{inc}}{2 \cdot r \cdot \rho}} = \sqrt{\frac{h \cdot E_{inc}}{D \cdot \rho}}$$

where  $E_{inc}$  is the incremental elastic modulus,  $\rho$  the blood density,  $h$  the wall thickness and  $r$ ,  $D$  the lumen radius and diameter. This equation is derived for non-viscous fluid but it is a good approximation for conduit arteries filled with blood. From the Moens-Korteweg equation, Frank (1920, [3]) and Bramwell and Hill (1929, [2]) derived another expression relating wave speed to compliance:

$$c = \sqrt{\frac{A}{\rho \cdot C_A}} = \sqrt{\frac{V \cdot \Delta P}{\rho \cdot \Delta V}}$$

with  $A$  the lumen area,  $C_A = \Delta A / \Delta P$  the area compliance, and  $\rho$  is blood density. Newton and Young derived this equation first and therefore it is also often called the Newton-Young equation.

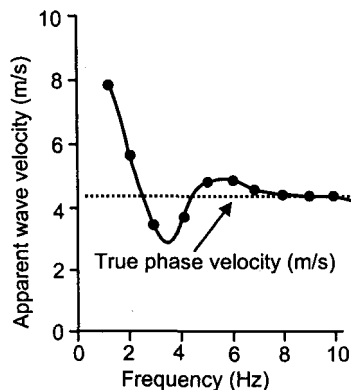
*Phase velocity and apparent phase velocity*

The phase velocity is essentially the wave speed determined by the properties of the vessel wall and blood density as presented above, i.e., the effects of reflections (Chapter 21) are not included. When two arterial pressures are measured these waves include the effect of reflections and with reflections present the formulas become more complex. When Fourier analysis is performed on two waves measured a distance  $\Delta x$  apart, the wave speed for each harmonic can be obtained by using the phase lag  $\Delta \varphi$  between the two harmonics. The apparent wave velocity,  $c_{app}$ , is then calculated for each harmonic as

$$c_{app,i} = \frac{2\pi \cdot \Delta x}{T_i \cdot \Delta \varphi_i} = \frac{2\pi \cdot f_i \cdot \Delta x}{\Delta \varphi_i}$$

with  $T_i$  the period, and  $f_i$  the frequency of the  $i^{\text{th}}$  harmonic. If the frequency is given in Hz,  $\Delta x$  in cm, and  $\Delta \varphi$  in radians,  $c_{app}$  will be in cm/s. The apparent wave velocity includes the effect of reflections and is therefore not a good measure of vessel compliance. The figure on the left shows the apparent wave velocity as a function of frequency. For high frequencies the apparent wave velocity approaches the true phase velocity because for high frequencies reflections become negligible (Chapter 23).

When the wave speed is determined from

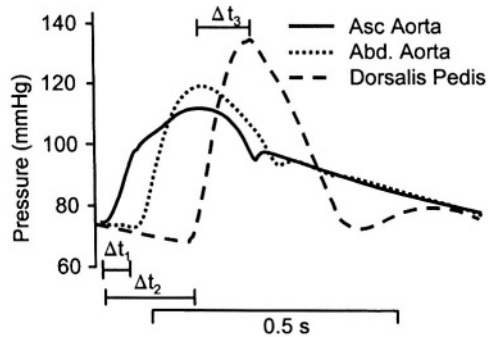


THE APPARENT WAVE VELOCITY is close to the phase velocity for high frequencies.

the foot of the wave the value is close to the apparent wave velocity at high frequencies and thus close to the phase velocity, so that we can obtain, from the foot-to-foot pulse wave velocity, information on vessel compliance.

### Methods to obtain wave speed

- *Time delay or foot-to-foot method.* This is the most direct method. Wave speed is estimated from the time it takes for the foot of the pressure, diameter, or blood velocity wave, to travel between two sites a known distance apart. The so calculated foot-to-foot wave velocity is close to the phase velocity and can be used to derive vessel compliance. The figure on the left shows

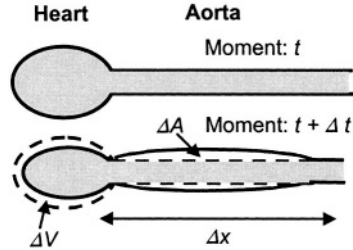


PRESSURE WAVES at different locations of the human arterial tree. Adapted from [6], used by permission.

realistic time delays for pressure waves recorded in the human aorta and the lower limbs [6]. For instance, the delay of the foot of the wave between ascending and thoracic aorta is  $\Delta t_1 = 0.056$  s, and the distance is  $\Delta x_1 = 0.25$  m. Thus, the resulting aortic wave speed,  $c$ , equals  $0.25/0.056$  m/s or  $c = 4.5$  m/s. The average wave speed from the aorta to the lower limb is  $\Delta x_2/\Delta t_2 = 1.25$  m/ $0.175$  s or  $c = 7.1$  m/s. Peripheral arteries are smaller, have relatively larger wall thickness, and are stiffer (higher  $E_{inc}$ ). Therefore, by virtue of the Moens-Korteweg equation, they have a higher wave speed. Note that the estimated aorta-to-dorsalis pedis wave speed is an average wave speed for the entire arterial pathway traveled by the wave (aorta, iliac, femoral, popliteal). The foot-to-foot method has been used in the above example to obtain the average wave speed between the ascending aorta and dorsalis pedis, with the foot-to-foot time delay being estimated as  $\Delta t_2 = 0.175$  s. If one had used the time delay based on peak systolic pressure ( $\Delta t_3 = 0.102$  s, in the figure), the estimated wave speed would have been  $c = 1.25$  m/ $0.102$  s =  $12.3$  m/s. This speed is much higher than the foot-to-foot method estimate of  $c = 7.1$  m/s. The overestimation is attributed partly to the fact that the artery is stiffer at higher distending pressures but is also partly attributed to wave reflections at peak systole. It is therefore generally accepted that the time delay should be calculated from the foot or the up-slope of the wave rather than the systolic part.

- *Wave speed derived from pressure and diameter measurements.* The Newton-Young equation permits the direct calculation of wave speed based on lumen cross-sectional area ( $A = \pi D^2/4$ ) and area compliance  $C_A$ . Simultaneous measurements of lumen diameter and pressure can be obtained using ultrasound and photoplethysmography or tonometry, respectively. Calculation of area gives the cross-sectional area-pressure relation. Based on compliance and area and using Newton-Young equation, wave speed can be derived as a function of pressure.

- Wave speed derived from flow and area measurements.* This method, see figure, is not often used, mainly because noninvasive flow and area measurements were not available in the past. MRI and ultrasonic technologies make it possible today to perform these noninvasive measurements. Imagine that the heart ejects into the aorta a certain volume  $\Delta V$  over a period  $\Delta t$ . The ejected volume will be ‘accommodated’ in the aorta by means of an increase in the aortic cross-sectional area  $\Delta A$  over a certain length  $\Delta x$ . The wave speed is the speed with which the perturbation in area,  $\Delta A$ , has traveled in the aorta, which is  $\Delta x / \Delta t$ . The volume ejected in the aorta is  $\Delta V = \Delta A \cdot \Delta x$  or  $\Delta x = \Delta V / \Delta A$ . Dividing by  $\Delta t$ , we obtain:



AREA AND FLOW changes as related to the wave speed.

$$c = \frac{\Delta x}{\Delta t} = \frac{\Delta V}{\Delta t \cdot \Delta A}$$

or since  $\Delta V / \Delta t$  is equal to the volume flow  $\Delta Q$

$$c = \frac{\Delta Q}{\Delta A}$$

From this relation we see that when ejection takes place in a stiff artery where the change in area,  $\Delta A$ , will be small, the wave speed will be high.

**Physiological and clinical relevance**

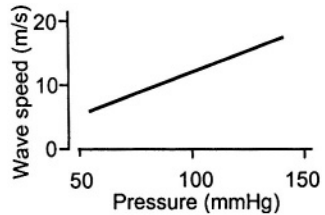
The above equations show that from wave speed wall elasticity ( $E_{inc}$ ) and area compliance  $C_A$  can be derived if the artery’s geometry (diameter and wall thickness) is known, thus, giving a good estimation of large vessel elasticity.

*Time delay or foot-to-foot method*

The wave speed between carotid artery and iliac or femoral artery can be measured noninvasively and is accepted as representative for aortic wave velocity. The wave speed allows estimation of aortic elasticity, and this noninvasive method is often used in hypertension research. The estimation of aortic length should account for the carotid length where the signal is measured. With aging the aorta becomes tortuous which results in an underestimation of length and thus also an underestimation in wave speed.

*Wave speed depends on pressure*

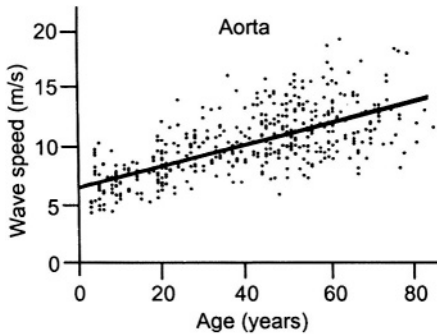
Based on compliance and area and using Newton-Young equation, wave speed can be derived as a function of pressure as shown here. Clearly wave speed is a strong function of pressure, due to the nonlinear elastic properties of the arterial wall.



WAVE SPEED as a function of pressure derived from diameter and pressure measured non-invasively in the human brachial artery.

*Wave speed depends on age*

With age, wave speed increases as shown in this figure where data were measured in normal human subjects, in the absence of atherosclerosis. The increase in wave speed by about a factor two between the ages 15 and 80 years implies a decrease in compliance by a factor four. The increase in aortic stiffness with age is primarily attributed to a progressive thinning, fraying and fracture of elastic laminae, likely due to repetitive cyclic stress of the pulsing pressure.

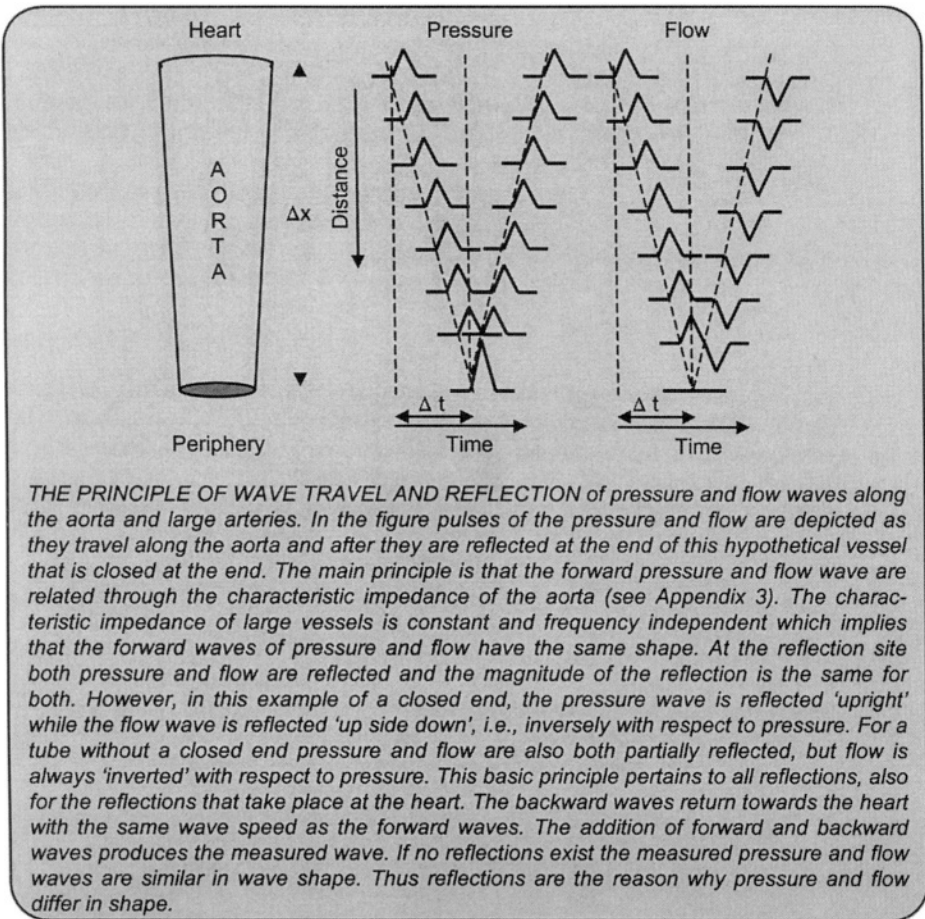


*PULSE WAVE VELOCITY of the aorta as a function of age in individuals with low prevalence of atherosclerosis in Beijing. From [1], used by permission.*

Although all wall constituents are subjected to the same pulse pressure and thus to the same cyclic stretch, it is mainly the elastin that cannot be re-synthesized sufficiently rapidly [4]. The net result is gradual replacement of elastin with collagen. The stiffer aorta implies reduced Windkessel function and higher pulse pressure (Chapter 24). The higher pulse pressure, in turn, may cause extra wear of the vessel wall resulting in more breakdown of elastin. It has been shown that pulse pressure is a better indicator than systolic blood pressure [5].

## References

1. Avolio AP, Chen S-G, Wang R-P, Zhang C-L, Li M-F, O'Rourke, MF. Effects of aging on changing arterial compliance and left ventricular load in a northern Chinese urban community. *Circulation* 1983;68:50-58.
2. Bramwell JC, Hill AV. The velocity of the pulse wave in man. *Proc Roy Soc Lond[Biol]* 1922;93:298-306.
3. Frank O. Die Elastizität der Blutgefäße. *Z Biol* 1920;71:255-272.
4. Martyn CN, Greenwald SE. Impaired synthesis of elastin in walls of aorta and large conduit arteries during early development as an initiating event in pathogenesis of systemic hypertension. *Lancet* 1997;350:953-955.
5. Mitchell GF, Moya LA, Braunwald E, Rouleau JL, Bernstein V, Geltman EM, Flaker GC, Pfeffer MA. Sphygmomanometrically determined pulse pressure is a powerful independent predictor of recurrent events after myocardial infarction in patients with impaired left ventricular function. *Circulation* 1997;96:4254-4260.
6. Remington JW, Wood EH. Formation of peripheral pulse contour in man. *J Appl Physiol* 1956;9:433-442.

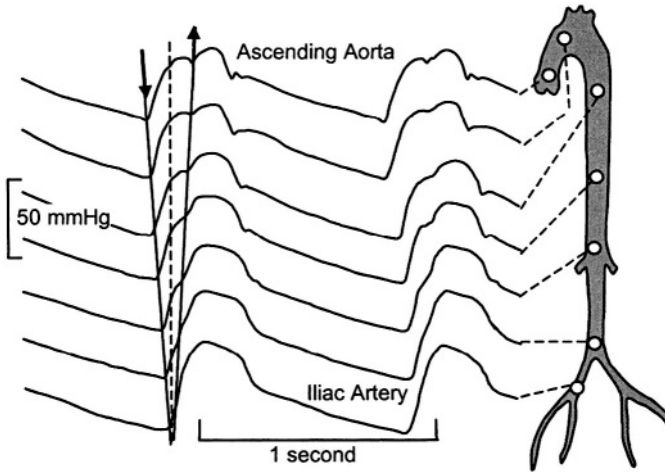


**Description**

Wave reflection takes place at all bifurcations and discontinuities of the vasculature. However, it turns out that the major reflections occur at the arterioles, i.e., in the periphery where many bifurcations are present over short distances. This leads to diffuse reflection. In addition, especially in the human, there appears to be a distinct reflection site in the distal abdominal aorta. An example of the distinct reflection is shown in this figure. The moment the reflected waves return at the heart depends on the length of the system and the wave speed. Since with age the wave speed increases, the reflections will return earlier in older subjects. The example is that of an older, healthy, person [1].

The amount of reflection is given by the reflection coefficient, which is defined for sinusoidal waves, as the ratio of the backward and forward waves and consists of a modulus or magnitude, and phase angle. Calculation of the reflection coefficient requires Fourier analysis because the coefficient is different for each harmonic (Appendix 1). The modulus of the reflection

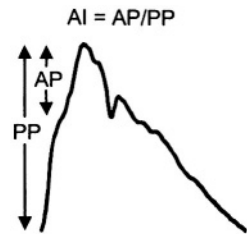
coefficient is the same for pressure and flow but the phase angle of pressure



*SIMULTANEOUSLY MEASURED PRESSURES IN THE HUMAN AORTA. The foot of the wave arrives later in the periphery and the reflected wave (inclination point) returns to the heart. The points are connected to show the later arrival at the heart compared to the distal aorta. The ECG is plotted at top and bottom to emphasize the time delays. Adapted from [1], used by permission.*

and flow differ by 180 degrees ('up side down'). Calculation of the reflection coefficient therefore requires Fourier analysis of the forward and backward (Chapters 21 & 22) pressure waves, as in the impedance calculations. In approximation, the ratio of the amplitudes of backward and forward waves can be used as a measure of the magnitude of reflection, usually in the form of the Reflection Index (see Chapter 22). The magnitude of the reflected wave with respect to the forward wave is related to the magnitude of the oscillation of the modulus of the input impedance (see Chapter 23).

The amount of reflection has also been related to the Augmentation Index, AI. The Augmentation Index became very popular, in part because it can be determined noninvasively and calibration of the signal is not required so that, for instance, applanation tonometry can be used. However, the Augmentation Index depends not only on the magnitude of the reflected wave but also on the time of return.

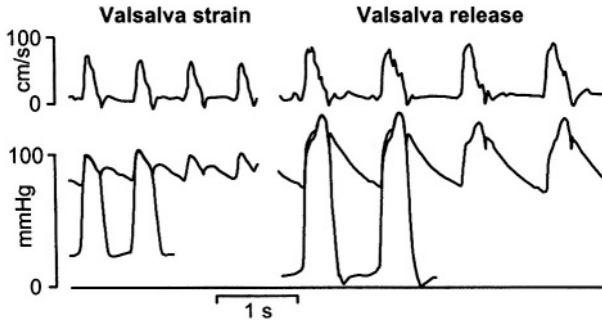


*THE AUGMENTATION INDEX (AI) is the augmented pressure (AP) divided by pulse pressure (PP). Calibration of blood pressure is not required.*

### Physiological and clinical relevance

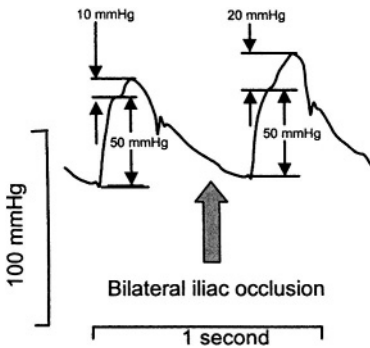
The amount of diffuse reflection depends on the vasoactive state of the peripheral vascular bed. With increased vasoconstriction the so-called diffuse reflections increase as well and pressure and flow become less alike in shape. For examples see below, and also Chapters 22 and 14. Inversely, during vasodilation pressure and flow in the aorta become more alike: a pressure

wave with an early peak, akin to the flow wave shape, is found in patients with a severely dilated state. With the Valsalva maneuver the transmural



DURING THE VALSALVA strain pressure and flow in systole become alike because diffuse reflections decrease in amplitude and wave speed decreases so that reflections return in diastole. After the release reflections return in systole. Adapted from [2], used by permission.

pressure in thoracic and abdominal aorta decreases [2]. This results in a more compliant aorta and a lower wave speed. The diffuse reflections decrease in magnitude and the reflected wave from the distinct reflection site arrives later in diastole. The overall result is that reflections that return in systole are negligible leading to a very similar shape of aortic pressure and flow in systole.



DISTINCT REFLECTION in the ascending aortic pressure is increased by mechanical compression of both iliac arteries. Adapted from [1], used by permission.

An experiment where the distinct reflection is increased is shown in the figure above. When both iliac arteries are manually occluded, the distinct reflection coefficient increases and the backward wave is increased resulting in a large Augmentation Index.

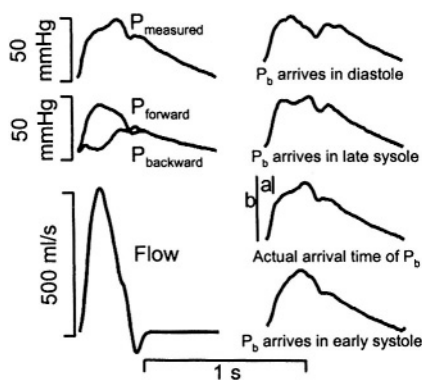
In hypertension, wave speed is increased. Resistance and thus diffuse reflections are also increased. This results in a large reflected wave in systole, adding to the forward wave resulting a large Augmentation Index, and in higher systolic pressure.

With increased reflection, and thus a higher Augmentation Index, the so-called supply-demand ratio of the cardiac muscle is negatively affected (see Chapter 16).

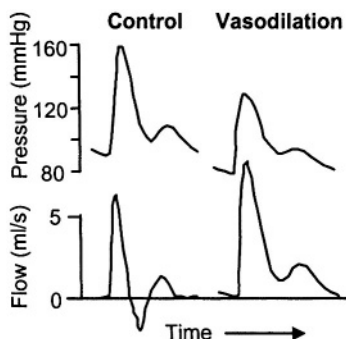
Not only the magnitude of the reflected wave but also the time of return is of importance. The moment the reflected wave returns in the ascending aorta depends on the wave speed and the distance between the reflection site and the heart. Thus the Augmentation Index does not only depend on the magnitude of reflection but it is affected by the moment the reflected waves return (see figure on next page). Therefore estimation of the magnitude of the reflections cannot be done solely based on the Augmentation Index.

Reflection in the periphery causes a backward flow wave that may be seen as a reversal of the measured flow wave, figure below right. This negative part of the flow wave is greatly reduced in vasodilation, when the reflection is smaller and thus the backward flow wave is smaller. Also, mean flow is larger, and the measured flow wave does not exhibit a reversal.

The distance between heart and the major reflection site has been called the effective length of the arterial system. However, the derivation of the effective length from the travel times of forward and backward waves is subject to errors because at the reflection site the reflected wave may be shifted in phase. This phase shift introduces time delay. From measurements of the time of arrival of the reflected wave in the proximal aorta it is not possible to distinguish between times resulting from travel per se and the phase shift [5]. Pythoud et al. have suggested a possible solution [4]. See also the Chapter 23.



THE AUGMENTATION INDEX, *a/b*, depends on the magnitude of reflection and time of return of the reflections. The pressure wave is separated into its forward and backward components (left). The backward wave is then shifted in time and the summated wave is calculated. It may be seen that the augmentation index strongly depends on the time of return of the reflected wave (right).



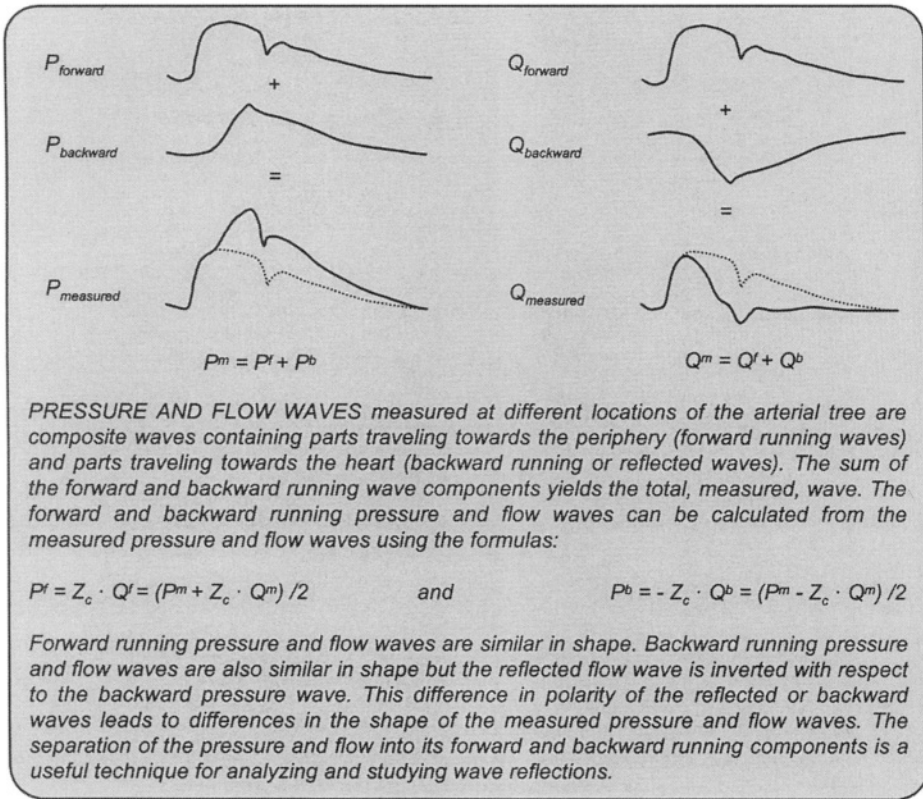
NEGATIVE BLOOD FLOW in part of the cardiac cycle results from inertia and reflections. With vasodilation the reflections decrease and flow reversal disappears (femoral artery). Adapted from [3], used by permission.

## References

1. Murgo JP, Westerhof N, Giolma JP, Altobelli SA. Aortic input impedance in normal man: relationship to pressure wave forms. *Circulation* 1980;62:101-116.
2. Murgo JP, Westerhof N, Giolma JP, Altobelli SA. Manipulation of ascending aortic pressure and flow wave reflections with the Valsalva maneuver: relationship to input impedance. *Circulation* 1981;63:122-132.
3. O'Rourke MF, Taylor MG. Vascular impedance of the femoral bed. *Circ Res* 1966;18:126-139.
4. Pythoud F, Stergiopoulos N, Westerhof N, Meister J-J. Method for determining distribution of reflection sites in the arterial system. *Am J Physiol* 1996;271: H1807-13.
5. Sipkema P, Westerhof N. Effective length of the arterial system. *Ann Biomed Engng* 1975;3:296-307.

## Chapter 22

## WAVEFORM ANALYSIS



### Description

At any location in the arterial tree, the measured pressure and flow waves are the sum of waves traveling from the heart towards the periphery (forward running waves) and waves traveling from peripheral arteries towards the heart (backward running waves). The backward running waves are often called reflected waves, simply because they arise from reflections of the forward running waves at arterial reflection sites.

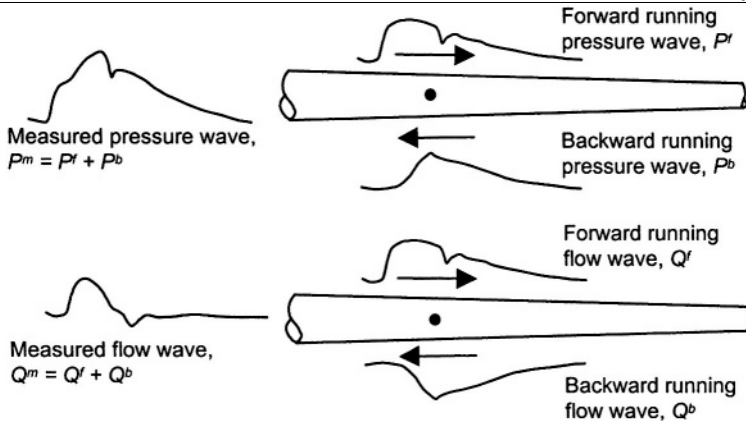
*Separation of waves into their forward and backward running components*

Consider the schematic diagram given on the next page. As mentioned above, at any arterial location the measured pressure and flow waves (shown on the left) are the sum of their forward and backward running components. So, we may write

$$P^m = P^f + P^b$$

and

$$Q^m = Q^f + Q^b$$



*PRINCIPLE OF THE SEPARATION of pressure and flow waves into their forward and backward running components.*

The forward running flow wave and the forward running pressure wave, are related through the relation,  $P^f = Z_c \cdot Q^f$ , with  $Z_c$  the local characteristic impedance of the vessel (for the definition of  $Z_c$  see Appendix 3). The reflected flow and the reflected pressure wave are also related by the characteristic impedance,  $P^b = -Z_c \cdot Q^b$ . The minus sign results from the fact that flow, compared with pressure, is reflected 'up side down' (Chapter 21). Substituting  $Q^f$  and  $Q^b$  into the above equations we obtain:

$$P^f = Z_c \cdot Q^f = (P^m + Z_c \cdot Q^m)/2$$

and

$$P^b = -Z_c \cdot Q^b = (P^m - Z_c \cdot Q^m)/2$$

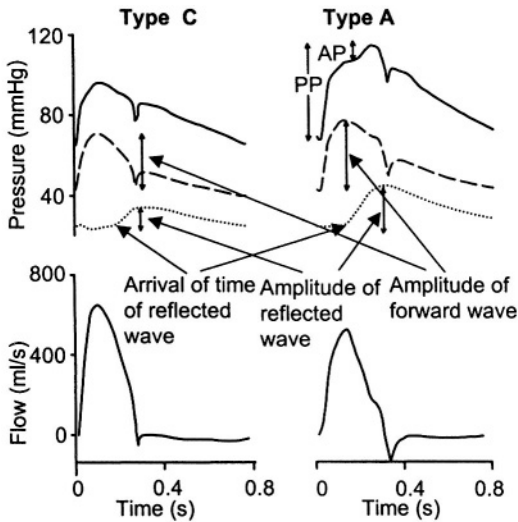
The above formulas are simple to use when the characteristic impedance,  $Z_c$ , is a real number, which means that we neglect the blood viscosity and the viscoelasticity of the wall. This is often a good approximation, especially when referring to conduit arteries, in which case we may calculate  $Z_c$  as:

$$Z_c = \rho \cdot c/A$$

with  $\rho$  blood density,  $c$  the local pulse wave velocity and  $A$  the luminal cross-sectional area. If, however, wall friction and viscoelasticity cannot be neglected, as in smaller vessels, then the same analysis holds and same equations apply, with the exception that the characteristic impedance  $Z_c$  is a complex number. In this case the analysis should be done in the frequency domain. This implies Fourier analysis (Appendix 1) of the measured pressure and flow waves, application of the above relations for each harmonic and inverse Fourier to reconstruct the time functions of the waves.

Another approach to the analysis of pressure and flow in a given arterial location is to look at very small portions of the traveling wave ( $dP$  or  $dQ$ ). This is called wave intensity analysis [1]. The application of 'wavelets' to separate the pressure and flows into their forward and backward running components leads to identical results when compared to the method expressed by the equations given above.

### Physiological and clinical relevance



ANALYSIS OF AORTIC PRESSURE WAVES (fully drawn) into their forward (dashed lines) and reflected, or backward, waves (dotted lines). The Type C beat pertains to a young adult and the Type A beat to an old subject.

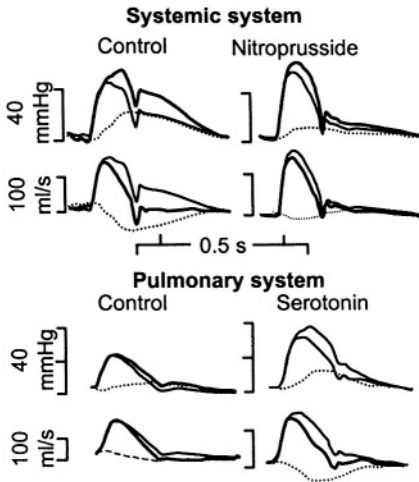
The analysis of arterial pressure and flow waves into their forward and backward running components can be used to quantify the role of wave reflections in certain physiological and pathological situations. The figure shows the aortic pressure and flow waves measured in young healthy adult, type C beat, and an older subject, type A beat [3]. The figure also shows the forward and backward running pressure components as dashed and dotted lines, respectively. For the type C beat we observe that the amplitude of the reflected wave is rather small and in the order of 12 mmHg. Further, the rise in the reflected wave takes place relatively late in systole. The net effect is that the addition of the reflected wave onto the forward wave does not lead to a significant increase in late systolic pressure. In contrast, in the old subject, we observe considerably higher amplitude of the reflected wave, which also arrives early in systole. Here the addition of the reflected wave to the forward wave leads to a very pronounced late systolic peak, resulting in a considerable increase in systolic pressure. The late systolic peak in the Type A beat results from wave reflection (Chapter 21) and has been related to the Augmentation Index, AI, defined as the ratio  $AP/PP$ . The limitation of the AI has been discussed in Chapter 21. The wave separation technique presented here is a better way for the quantification of reflection, and account for the timing, amplitude, and shape of the reflected waves.

#### Practical determination of characteristic impedance

In practice, the characteristic impedance of large vessels can be determined in two ways. The first is by averaging of the modulus of the input impedance between the 4th and tenth harmonic (Chapter 23). The second method is by taking the slopes of the aortic pressure and flow waves during the early part of the ejection phase,  $\Delta P$  and  $\Delta Q$ , and calculating their ratio:  $Z_c = (\Delta P/\Delta t)/(\Delta Q/\Delta t)$  [2]. Both methods rely on the fact that characteristic impedance is a pressure flow relation in the absence of reflections. Reflections are small in early systole and at high frequencies (see Chapter 23).

The analysis of arterial pressure and flow waves into their forward and backward running components can be used to quantify the role of wave reflections in certain physiological and pathological situations. The figure shows the aortic pressure and flow waves measured in young healthy adult, type C beat, and an older subject, type A beat [3]. The figure also shows the forward and backward running pressure components as dashed and dotted lines, respectively. For the type C beat we observe that the amplitude of the reflected wave is rather small and in the order of 12 mmHg. Further, the rise in the reflected wave takes place relatively late in

Reflections depend on the vascular bed and on its vasoactive state.



PRESSURE AND FLOW in aorta and common pulmonary artery are broken down in their forward and backward components. Thick lines, thin lines, and dashed lines give measured waves, forward waves, and backward waves, respectively. With vasodilation and vasoconstriction backward waves are reduced and increased, respectively. Adapted from [4], used by permission.

Wave reflections in the pulmonary circulation are less significant than in the systemic arterial tree [4]. Aortic pressure and flow and common pulmonary artery pressure and flow, are broken down in their forward and backward components. When the systemic bed is dilated, with nitroprusside, and the pulmonary arterial system is constricted, with serotonin, reflections decrease and increase, respectively. It should be noticed that when reflections are small in magnitude, the pressure and flow waves become similar in shape.

#### Reflection Index

The Reflection Index, RI, is the ratio of the amplitudes of the backward wave and the sum of the forward and backward waves:  $RI = P^b / (P^f + P^b)$ . Wave analysis, and thus the measurement of pressure and flow is required to obtain  $P^f$  and  $P^b$ . The RI gives a good measure of the amount of reflection.

#### Augmentation Index and shape of the waves

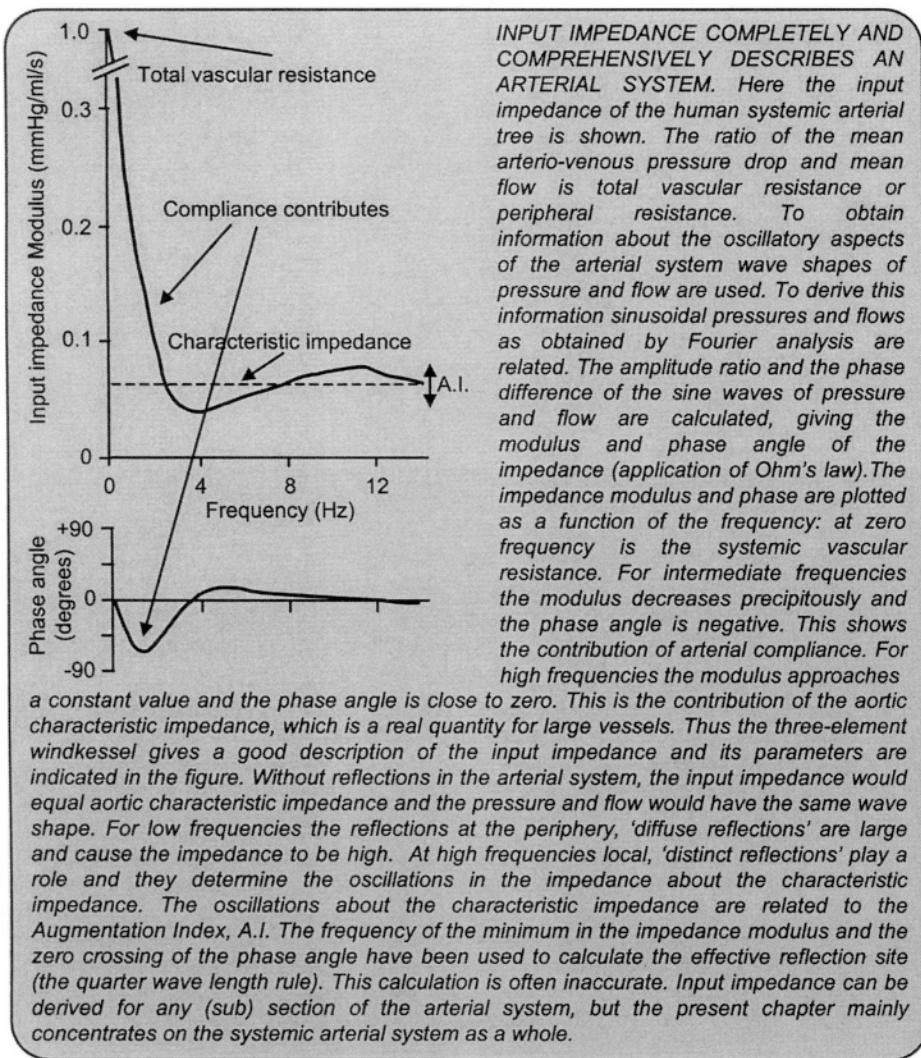
The Augmentation Index, AI, is derived from the measured pressure wave without the need for application of wave separation. However, while the Reflection Index, gives a good measure of the magnitude of (total) reflection, the Augmentation Index is determined by both the delay and the shapes of the forward and backward waves. In Chapter 21 it was shown that for the same magnitude and wave shape of the backward and forward waves the delay between them strongly determines Augmentation Index.

#### References

1. Jones CJ, Sugawara M, Kondoh Y, Uchida K, Parker KH. Compression and expansion wavefront travel in canine ascending aortic flow: wave intensity analysis. *Heart Vessels* 2002; 16:91-8.
2. Li JK. Time domain resolution of forward and reflected waves in the aorta. *IEEE Transact on Biomed Engng* 1986;33:783-785.
3. Murgo JP, Westerhof N, Giolma JP, Altobelli SA. Aortic input impedance in normal man: relationship to pressure wave forms. *Circulation* 1980;62:105-116.
4. Van den Bos GC, Westerhof N, Randall OS. Pulse-wave reflection: can it explain the differences between systemic and pulmonary pressure and flow waves? *Circ Res* 1982;51:479-485.

## Chapter 23

## ARTERIAL INPUT IMPEDANCE



### Description

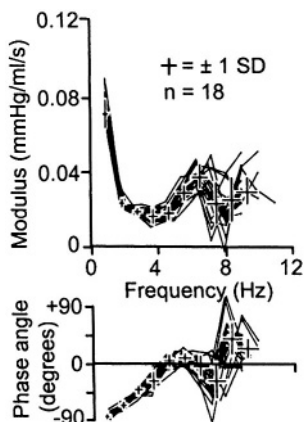
#### Definition of impedance

Impedance is the relation between the pressure difference and flow of a linear system, for sinusoidal or oscillatory signals. Impedance completely describes the system and it can be derived from pulsatile pressure difference and pulsatile flow and the application of Fourier Analysis. Inversely, when the impedance is known, a given flow allows for the calculation of pressure and vice versa. Systemic arterial and pulmonary arterial input impedance are a comprehensive description of the systemic and pulmonary arterial tree. Input

impedances of organ systems may be derived as well. The longitudinal, transverse and characteristic impedance are discussed in Appendix 3.

### *Derivation of input impedance*

In the calculations of input impedance we use both the mean values and the pulsatile part of the pressure and flow. We apply Fourier analysis of the aortic pressure and flow because the calculations are based on sinusoidal signals. The details and limitations of Fourier analysis are discussed in Appendix 1. To derive impedance Ohm's law is applied. For each pair of sine waves of pressure and flow we calculate the ratio of the amplitudes and the phase angle difference between them. To apply Ohm's law, i.e., to calculate impedance and vascular resistance, the system must be in the steady state, time-invariant, and linear. This means that the arterial system may not vary in time, e.g., vasomotor tone should be constant, that the relation between pressure and flow is a straight line, e.g., if a sine wave of pressure is applied a sine wave of flow should result. For a time-varying system the calculation of impedance does not lead to interpretable results. The coronary circulation, where resistance and elasticity vary over the heartbeat, the calculation of impedance from pressure and flow using Fourier analysis is not sensible. For a nonlinear system the calculation of impedance also does not lead to interpretable results. An example is the calculation of 'impedance' from ventricular pressure and aortic flow, where the aortic valves make the system nonlinear. The arterial system is not perfectly linear but the variations of pressure and flow over the heartbeat are sufficiently small so that linearity is approximated and the derived impedance is a meaningful description. It has been shown that some of the scatter of the input impedance data results from nonlinearity [7]



*SCATTER IN THE INPUT IMPEDANCE is caused, in part, by noise on the pressure and flow signals especially affecting the small amplitudes high harmonics. Non-linearity of the arterial system also contributes to the scatter. From [1], used by permission.*

These limitations in the calculations of input impedance also hold for the calculation of peripheral resistance. Mean aortic pressure divided by mean aortic flow only gives information on peripheral resistance if, over the period of determination, the peripheral resistance does not vary. Also, mean left ventricular pressure over mean aortic flow does not lead to a sensible result because the system includes the valves and is not linear.

Fourier analysis and subsequent calculation of the input impedance only gives information at frequencies that are multiples of the heart rate, i.e., harmonics. By pacing the heart at different rates, the frequency resolution can be increased.

Because the information contained in the signals for high frequencies is small, the higher harmonics (Appendix 1) are subject to noise, so that the impedance at high frequencies often scatters considerably. This limitation can be partly circumvented by analyzing more than one heartbeat and averaging the results. This can be done by using, for instance, an entire

respiratory cycle (steady state of oscillation) or by analyzing a series of beats individually followed by averaging [1].

In the systemic circulation venous pressure may be neglected (Chapter 6), so that the use and Fourier analysis of aortic pressure and flow gives a sufficiently accurate approximation of the input impedance. However, in the analysis of the pulmonary circulation venous pressure cannot be neglected.

In Appendix 2 the basic hemodynamic elements are discussed. For a resistor it holds that the sine waves of pressure and flow are in phase, i.e., the phase angle is zero. For compliance the flow is advanced with respect to pressure. This is seen as  $-90$  degrees in the impedance phase angle. For inertance flow is delayed, and shows as  $+90$  degrees for the impedance phase. The modulus of the impedance decreases with frequency,  $1/\omega C$  for compliance, and increases with frequency,  $\omega L$ , for the inertance, respectively. In Appendix 3 it is shown that in the case of the characteristic impedance of a large artery, like the aorta, the mass effects and compliance effects interact in such a way that sinusoidal pressure and flow waves are in phase, and their ratio is constant. Thus the impedance phase angle is zero and the modulus is constant and independent of frequency. This means that the amplitude ratio of pressure and flow is the same for all frequencies and the phase angle is zero. Thus for large vessels the characteristic impedance is similar to a resistance and is often called characteristic resistance, and modeled as a resistor. However, characteristic impedance is non-existent at zero Herz and no energy is lost in it. Thus when modeling characteristic impedance with a resistor these limitations must be kept in mind.

### *Explanation of input impedance*

*The Windkessel.* The qualitative description of the impedance given in the box refers to the Windkessel model. The original two-element Windkessel, proposed by Frank, consists of peripheral resistance,  $R_p$ , and total arterial compliance,  $C$ . From the information on input impedance, which became available in the 1960s, the idea of aortic characteristic impedance,  $Z_c$ , appeared [10]. However, we should keep in mind that when the characteristic impedance is modeled with a resistor the mean pressure over mean flow will be  $R_p + R_c$ , while it should be  $R_p$  only. Although this error is not large for the systemic circulation where  $R_c$  is about 7% of  $R_p$ , it leads to errors when, for instance the three-element Windkessel is used to estimate total arterial compliance. To correct for these shortcomings, a fourth element, the total arterial inertance (see Chapter 24) was introduced [6].

*Wave transmission.* From wave transmission we can explain the impedance as follows. For a reflectionless system the input impedance equals aortic characteristic impedance and, inversely, the difference between input impedance and characteristic impedance results from reflections. For low frequencies the reflections from bifurcating arteries and other discontinuities mainly from the periphery, where bifurcations occur over short distances, return to the proximal aorta resulting in an impedance that strongly differs from aortic characteristic impedance. For high frequencies, where wavelengths are less than the length of the arterial system, the waves return out of phase, and cancel each other out so that the arterial system appears reflectionless. Also damping is stronger for the high frequencies. For high frequencies input impedance is, therefore, close to the characteristic impedance and its phase angle is close to zero. The (small) oscillations of the

impedance modulus around the characteristic impedance, and the oscillations in phase angle, result from reflections relatively close to the heart. It has been suggested that in the human these reflections may occur at the aortic bifurcation or at the level of the renal arteries. This is considered a distinct reflection site. The ratio of backward and forward running wave amplitudes is related to the magnitude of the oscillations in the impedance modulus [1].

### *Effective length of the arterial system*

The effective length of the arterial system is used as a conceptual description to determine at what distance from the ascending aorta the major reflections arise. In this concept it is assumed that the arterial system behaves like a single tube, the aorta, with a single resistance, the peripheral resistance at its distal end. To derive the effective length it is assumed that the arterial system can be modeled by a single tube, the aorta, loaded with a resistance, peripheral resistance. Since the aortic characteristic impedance is a real number (no phase angle), the reflection coefficient is real as well. Let us consider a sinusoidal pressure and flow, with a wavelength 4 times the length of the aorta. When the forward pressure wave travels a quarter wave length to reach the end of the tube, and again one quarter wave length to return at the heart, the forward and reflected waves of pressure are 180 degrees out of phase and thus cancel. Thus the measured pressure wave is negligible. For the flow waves the same holds, but the flow waves are reflected 180 degrees out of phase (Chapter 21). Thus the forward and reflected flow waves are 360 degrees out of phase: 180 degrees results from the reflection and the other 180 degrees results from traveling half a wavelength. This means that forward and backward flow waves are in phase and the measured flow about twice the forward or backward wave. Thus for a frequency where this model system is a quarter of a wavelength long, pressure is negligible, and flow is large, and the modulus of the input impedance is small and the phase angle is zero. This is called the quarter wavelength principle.

Quantitatively we describe this phenomenon as follows. The wave speed,  $c$ , equals wavelength,  $\lambda$ , times frequency,  $f$ , thus,  $c = \lambda \cdot f$ . When the length of the tube is a quarter wave length,  $l = \lambda/4$ , and the minimum of the impedance is found at frequency  $f = c/\lambda = c/4 \cdot l$  or  $l = c/4 \cdot f$ . With a wave speed in the aorta of 6 m/s and the frequency of the minimum in the impedance modulus or zero crossing of the phase at 4 Hz, the effective length equals ~38 cm. However, the assumption of a single tube, loaded with the peripheral resistance as model of the systemic arterial tree, is too simple and often unrealistic. When the reflection coefficient is not real, i.e., when the phase of the pressure and flow waves are changed at the reflection site, the calculation may even lead to an effective length longer than the arterial system [4]. When the impedance modulus minimum and zero crossing of the phase angle are not at the same frequency, the assumption that the arterial system can be modeled with a single tube and a peripheral resistance is violated.

### *Impulse response*

Conceptually, it is rather awkward that while pressure and flow are functions of time, the input impedance is expressed as a function of frequency. There exists a characterization of the arterial system in the time domain. This characterization is the so-called impulse response function, which is the pressure that results from an impulse of flow, i.e., a short lasting flow, short

with respect to all travel and characteristic times of the arterial system, typically about 1-5 ms of duration. Because the impulse has a height with dimension ml/s and the duration is in seconds, the area under the impulse is ml. The pressure response resulting from this impulse is normalized with respect to the volume of the impulse and the units of the impulse response are therefore mmHg/ml. The calculation of the impulse response function from measured pressure and flow is complicated but straightforward [5]. When the measured flow is broken up in a number of short impulses, the proper addition of the impulse responses leads to the pressure as a function of time.

The input impedance and impulse response function are a 'Fourier pair'. Fourier analysis of the impulse response function leads to the input impedance and inverse transformation of input impedance leads to the impulse response function [5].

If the impulse response is short in duration with respect to the time constant of variation of the time varying system, it may be used to obtain a characterization of that system as a function of time. For example, if the duration of the impulse is a few milliseconds, and the system under study varies with a typical time of a few hundred milliseconds, the system can be characterized by the impulse response. In this way input impedance of the coronary arterial system was derived in systole and diastole [8].

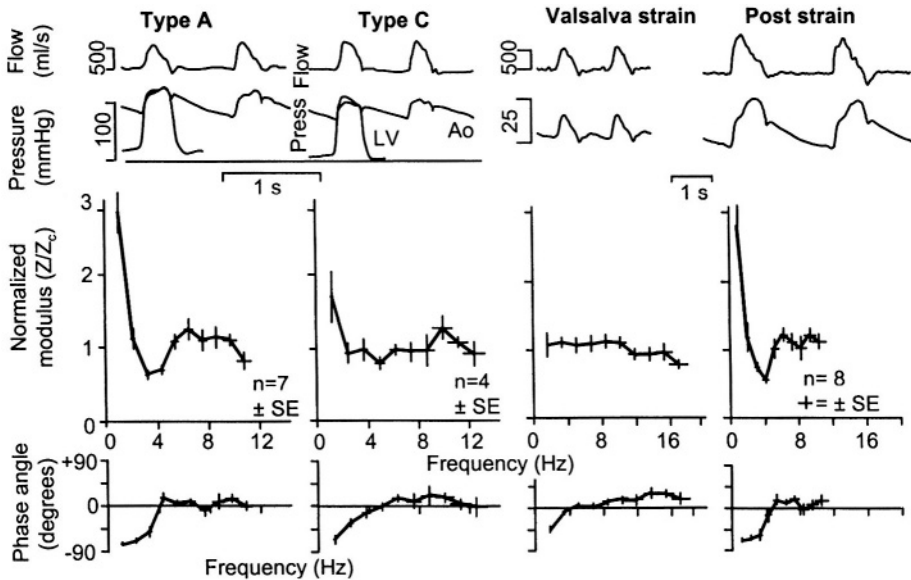
### **Physiological and clinical relevance**

As discussed above, derivation of input impedance requires sophisticated analysis of pressure and flow waves. Thus, routine clinical applications are seldom carried out. However, impedances calculated in the human and mammals have led to a much better understanding of arterial function. For instance, the three-element Windkessel as an extension of the two-element Windkessel of Frank could only be proposed after input impedance data became available. It has also been shown that the input impedance of different mammals, when normalized, is similar [9]. This explains, in part, why aortic pressures and flows are so similar in shape in all mammals (Chapter 30).

The arterial system can be described in terms of Windkessel models and distributed models. The main arterial parameters describing input impedance are peripheral resistance, total arterial compliance and aortic characteristic impedance. Recently the total arterial inertance has been suggested as the fourth element of the Windkessel [6]. It is often easier and more accurate to determine the windkessel parameters to describe the arterial system. With the modern computing techniques the calculation of the three or four parameters of the Windkessel model can be performed rapidly and gives directly interpretable results. For instance, a change in total arterial compliance can thus be obtained directly, while the impedance calculations can be avoided.

In terms of distributed models the pressure and flow waves can be better analyzed in terms of forward and backward running waves than in terms of impedance (Chapter 22). The amplitude ratio of the backward and forward waves appears to relate with the oscillations of the modulus of the impedance around the characteristic impedance. The time of arrival of the backward wave gives a better estimate of the effective length of the arterial system than the minimum in the impedance modulus or zero crossing of the phase angle.

The following examples show that, although the pressure and flow waves result from the interaction of the heart and arterial load, major features of the pressure wave shape arise from the arterial system and can therefore be related to aspects of the input impedance.



**TYPES OF BEATS RELATE TO INPUT IMPEDANCE.** In older subjects, Type A, with high pulse wave velocity, reflections return in systole and augment the pressure wave. The impedance oscillates about the characteristic impedance. In young subjects, Type C, reflections are smaller and return in diastole. The impedance oscillates less. Adapted from [1], used by permission.

**VALSALVA STRAIN** increases thoracic and abdominal pressures. The lower transmural pressure increases arterial compliance and lowers pulse wave velocity. Reflections diminish and return later, in diastole. An almost reflectionless situation appears where pressure and flow resemble each other and input impedance equals aortic characteristic impedance. In the release phase the reverse is true, reflections return in systole and are large. Adapted from [2], used by permission.

### *The characteristic pressure wave shapes in old and young subjects*

In older subjects, where arterial compliance is decreased and pulse wave velocity is increased (Chapter 20), the reflected waves return earlier in the cardiac cycle and thus arrive back in the ascending aorta during systole. The reflected waves add to the forward pressure wave resulting in a secondary increase in systolic pressure, a Type A wave (Chapter 22). The secondary increase in pressure relative to pulse pressure is called the Augmentation Index, AI. The AI is clearly seen in a so-called Type A beat. As a result of the strong reflection the input impedance oscillates around the characteristic impedance. In young subjects with small reflections that return in diastole due to the low pulse wave velocity, the pressure shows an early maximum,

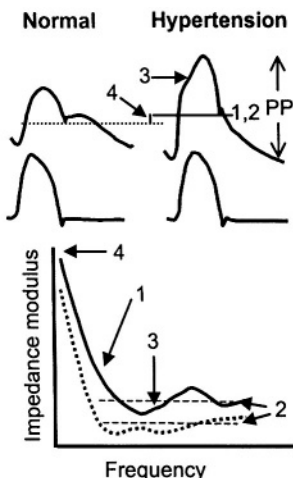
with negligible or negative augmentation, and the impedance oscillates only little.

*Changes in reflection*

In the figure on the right we see that during the Valsalva maneuver aortic pressure resembles aortic flow in wave shape [2]. During the Valsalva maneuver intra-thoracic and intra-abdominal pressures increase. The transmural pressure of the aorta decreases and the compliance increases leading to a decreased pulse wave velocity. As a result reflections return slower and arrive late in the cardiac cycle, in diastole. Reflections are probably also decreased in magnitude. The result is an almost reflectionless arterial system. Pressure and flow become similar in shape and the input impedance is close to the characteristic impedance of the aorta (Figure on previous page). After the release of the Valsalva maneuver, cardiac filling and transmural pressure are increased, Cardiac Output and pulse wave velocity are increased as well and reflections return in systole, and a large augmentation in the pressure is seen.

*Hypertension*

In the figure below we see the relation between systolic hypertension and the changes in the arterial system presented in the form of input impedance. With increasing age systolic pressure increases and diastolic pressure even decreases what. The main age-related change in the arterial system is decrease of arterial compliance. The decrease in compliance can be seen in the impedance graph: the modulus decreases less rapidly with increasing frequency (1) and the characteristic impedance is increased (2). The pulse wave velocity is also increased and therefore the waves reflected at the level of the lower abdominal aorta return earlier at the heart and augment the pressure wave in the ascending aorta. The result is larger oscillations of the impedance around the characteristic impedance and a larger pulse pressure (3). Peripheral resistance also increases somewhat and the result is a small increase in mean pressure (4).

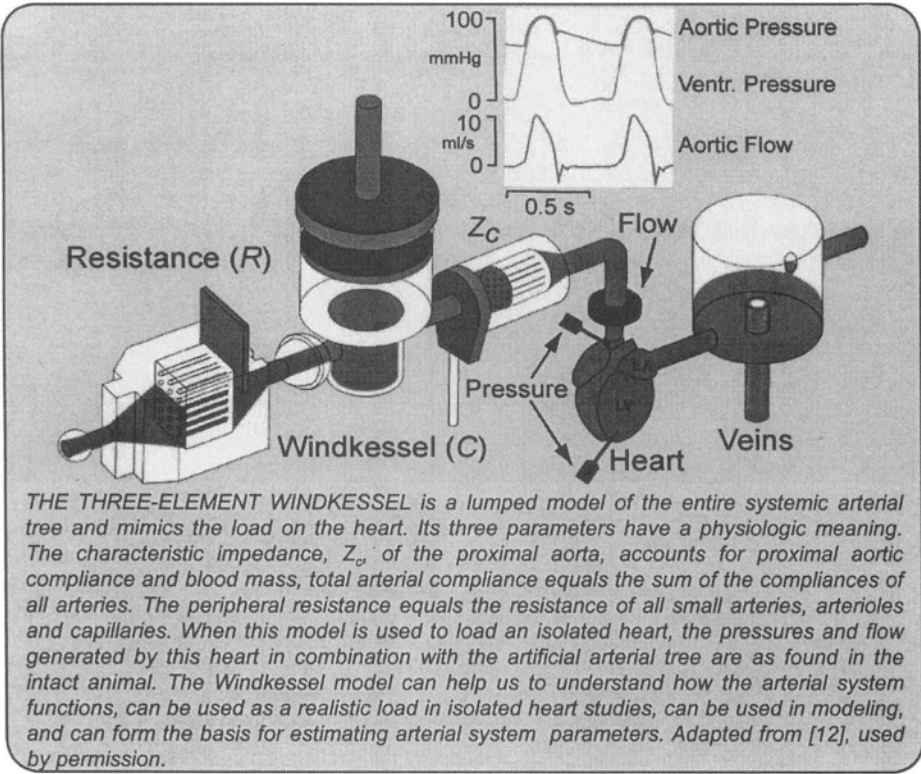


IN HYPERTENSION peripheral resistance and thus mean pressure is increased (4). Compliance is decreased resulting in a less rapid decrease in impedance, with frequency, 1, and a higher characteristic impedance, 2. Pulse pressure, PP, increases (1,2). Wave speed is increased, the impedance oscillates more around the characteristic impedance (3), and the wave is augmented (3). Adapted from [3], used by permission.

**References**

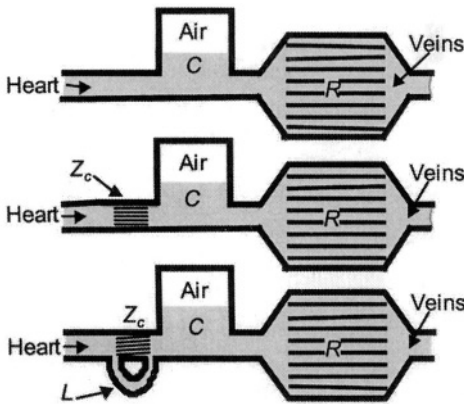
1. Murgo JP, Westerhof N, Giolma JP, Altobelli SA. Aortic input impedance in normal man: relationship to pressure wave forms. *Circulation* 1980;62:105-116.

2. Murgo JP, Westerhof N, Giolma JP, Altobelli SA. Manipulation of ascending aortic pressure and flow reflections with the Valsalva maneuver: relationship to input impedance. *Circulation* 1981;63:122-132.
3. O'Rourke MF. Pulsatile arterial haemodynamics in hypertension. *Australian and New Zealand J of Medicine* 1976;6 (suppl 2):40-48.
4. Sipkema P, Westerhof N. Effective length of the arterial system. *Ann Biomed Engng* 1975;3:296-307.
5. Sipkema P, Westerhof N, Randall OS. The arterial system characterized in the time domain. *Cardiovasc Res* 1980; 14:270-279.
6. Stergiopoulos N, Westerhof BE, Westerhof N. Total arterial inertance as the fourth element of the windkessel model. *Am J Physiol* 1999;276:H81-H88.
7. Stergiopoulos N, Meister J-J, Westerhof N. Scatter in the input impedance spectrum may result from the elastic nonlinearity of the arterial wall. *Am J Physiol* 1995;269:H1490-H1495.
8. Van Huis GA, Sipkema P, Westerhof N. Coronary input impedance during the cardiac cycle as obtained by impulse response method. *Am J Physiol* 1987;253: H317-H324.
9. Westerhof N, Elzinga G. Normalized input impedance and arterial decay time over heart period are independent of animal size. *Am J Physiol* 1991;261:R126-R133.
10. Westerhof N, Elzinga G, Sipkema P. An artificial system for pumping hearts. *J Appl Physiol* 1971 ;31:776-781.



**Description**

Three Windkessel models are given in the figure. Otto Frank, 1899, popularized the original two-element Windkessel. He reasoned that the decay



THE THREE WINDKESSELS. The two-element Windkessel (Frank) contains total peripheral resistance, mainly located in the arterioles ( $R$ ), and the total arterial compliance ( $C$ ), accounting for elasticity of all arteries, with the major contribution of the large conduit vessels. The three-element Windkessel contains the aortic characteristic impedance, accounting for the combined effects of compliance and inertance of the very proximal aorta, and forming a link with transmission line models. The four-element Windkessel contains total arterial inertance, playing a role at the very low frequencies. It also solves the problem that characteristic impedance, although having the dimension of a resistor, is not a real resistor and therefore mean pressure over mean flow equals  $Z_c + R$  in the three-element Windkessel.

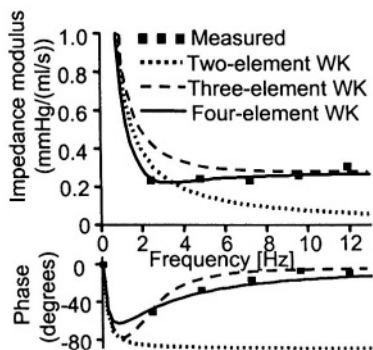
of diastolic pressure in the ascending aorta, when flow is zero, can be described by an exponential curve. The time constant,  $\tau$ , i.e., the time for pressure to decrease to 37% of the starting pressure, is given by the product of peripheral resistance,  $R$ , and the total arterial compliance,  $C$ ,  $\tau = RC$ . The larger the resistance the slower the blood, stored in the compliant conduit vessels, leaves the system and the longer the time constant will be. Also, the larger the compliance the more blood is stored, and the longer the time constant will be. Frank's objective was to derive Cardiac Output from aortic pressure. By measuring the pulse wave velocity over the aorta (carotid to femoral) together with, averaged, cross-sectional area, and using the Moens-Korteweg equation (Chapter 20) area compliance,  $C_A$ , can be estimated. When aortic length is also known volume compliance,  $C$ , is derived. Using  $\tau$  and  $C$ , the peripheral resistance can be calculated from  $R = \tau/C$ . From mean pressure and resistance, using Ohm's law, mean flow is then found. The assumption that all compliance is located in the aorta, thus neglecting the compliance of the smaller conduit vessels, introduces a small error. Only after pulsatile flows could be measured, and the arterial input impedance could be determined (Chapter 23), the shortcomings of the two-element Windkessel became clear.

The three-element Windkessel is based on Frank's two-element Windkessel with the addition of the characteristic impedance [12]. Input impedance shows, at high frequencies, a constant impedance modulus and a phase angle of about zero degrees (Chapter 23). This is not in line with the impedance of the two-element Windkessel that exhibits a continuously decreasing modulus and a phase angle that approaches minus 90 degrees for high frequencies. From a wave transmission and reflection standpoint, it can be reasoned that for high frequencies reflections in the proximal aorta cancel out and for a reflectionless aorta the input impedance equals its characteristic impedance (Chapter 22). Or, in other words, for high frequencies the input impedance equals the characteristic impedance of the proximal aorta. Aortic characteristic impedance is a real number, i.e., its modulus is constant with a value  $Z_c = \sqrt{\rho \cdot \Delta P / (\Delta A \cdot A)}$  and its phase angle is zero (Appendix 3). This behavior is also characteristic of a resistance. Therefore, a resistor has often been used to mimic the characteristic impedance of the proximal aorta. The introduction of the characteristic impedance or characteristic resistance as the third element of the Windkessel can be seen as bridging the lumped models and the transmission line models. However, the characteristic impedance is only present for oscillatory pressure and flow (Chapter 23).

The approximation of characteristic impedance by a resistor leads to errors in the low frequency range. When, for instance, total arterial compliance is determined from aortic pressure and flow by parameter estimation of the three elements of the Windkessel, the compliance is consistently overestimated. The reason is that the decrease of the impedance modulus and the negative phase angles at low frequencies are mainly determined by compliance.

The fourth element of the Windkessel was introduced to circumvent the inconsistency resulting from modeling the characteristic impedance by a resistance [8]. The four-element Windkessel is also shown in the figure on the previous page. It has been established that the inertance term equals total inertance of the arterial system. Using this four-element Windkessel model, total arterial compliance is estimated accurately from pressure and flow.

In summary, the characteristic impedance introduces transmission concepts into the Windkessel model and provides for a correct behavior of the model at high frequencies. The total arterial inertance improves the very low frequency behavior of the Windkessel.



THE INPUT IMPEDANCES of the two-element, three-element and four-element Windkessel models. The squares give the measured input impedance. The two-element Wind-kessel clearly falls short, especially in the high frequency range. The three-element Windkessel is also less accurate at very low frequencies. This is the result of the representation of the characteristic impedance by a resistance. The four-element Windkessel solves this problem. The  $R$ ,  $C$ , and  $L$  represent total arterial resistance, compliance and inertance. Adapted from [8], used by permission

When flow is zero, as in diastole, the decrease of aortic pressure, is characterized by the decay time, which equals  $RC$  for all three Windkessel models, if the analysis is started with some delay after valve closure (about 10% of the heart period).

These lumped models only mimic the behavior of the entire arterial system at its entrance. The input impedances of the Windkessels are given in the figure above. The integrated description of the entire arterial system means that pressures within these models have little meaning. The measurement of pressure distal of the characteristic impedance, for instance, does not represent the pressure in the more distal vascular system.

#### *Other lumped models*

Other lumped models are partly Windkessel models with more elements and partly tube models. More elements in the Windkessel may evolve to transmission line models, but often the parameters lose their physiologic meaning. Tube models consist of single tubes, loaded with a resistor or with a Windkessel model. Two tube models may consist of two tubes in parallel or in series (Chapter 25). Wave transmission, not existing in the Windkessel models, is present in the tube models, which gives them certain advantages.

### **Physiological and clinical relevance**

Windkessel models find their use as load for the isolated ejecting heart. The Windkessel parameters may be changed and cardiac pump function studied [1]. The figure on the next page shows an example of changes in peripheral resistance and total arterial compliance while cardiac contractility, heart rate and cardiac filling are maintained constant.

Another use of the Windkessel models is the estimation of arterial parameters. Several methods have been proposed to derive total arterial compliance [9]. These methods are:

- *The decay time method* described above.

- *The Stroke volume over Pulse Pressure method.* This method is rather old but has been reintroduced recently [2]. This ratio was shown to overestimate compliance [5] and should only be used for comparison.
- *The area method,* where the area under the diastolic aortic pressure divided by the pressure difference between start and endpoint is set equal to decay time.

$$RC = \int_{t_1}^{t_2} \frac{P}{P_1 - P_2} dt$$

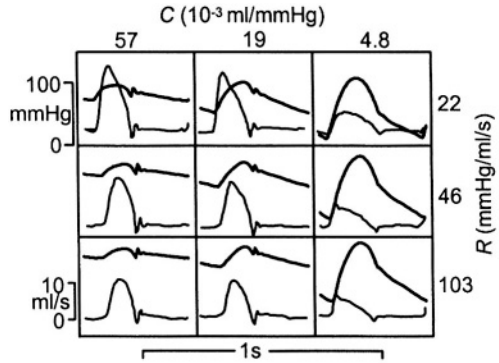
Knowing the RC time and calculating  $R$  by the ratio of mean pressure and mean flow the compliance can be derived [3,4].

- *The two-area method* is based on the following equation:

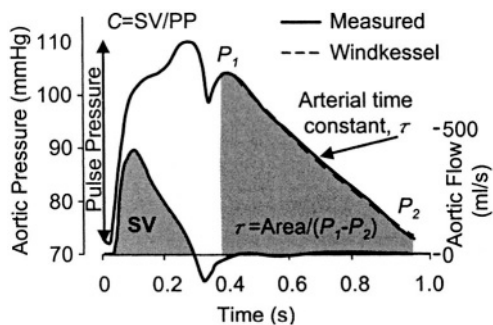
$$\int_{t_1}^{t_2} Q dt = C \cdot (P_2 - P_1) + \frac{1}{R} \int_{t_1}^{t_2} P dt$$

The equation is applied to two periods of the cardiac cycle; the period of onset of systole to peak systole and the period from peak systole to the end of diastole. Thus two equations with two unknowns,  $R$  and  $C$ , are obtained [7].

- *The pulse pressure method* is based on fitting the systolic and diastolic pressures predicted by the two-element Windkessel with measured aortic flow as input, to the measured values of systolic and diastolic pressure. Although the two-element Windkessel does not produce correct wave shapes the low frequency impedance is very close to the actual impedance and systolic and diastolic pressure are mainly determined by low frequencies [10].



AORTIC PRESSURE AND FLOW resulting from an isolated cat heart pumping into a three-element windkessel. The effect of changes in peripheral resistance (increasing downwards) and arterial compliance (decreasing to the right) are shown. The control condition (cat, left top panel). The advantage of the use of such a model is that all venous and cardiac parameters can be kept constant while varying one; here resistance or compliance. Adapted from [1] used by permission.



TOTAL ARTERIAL COMPLIANCE DETERMINATION.

- Stroke volume divided by Pulse Pressure.
- The decay time,  $\tau$ , of diastolic aortic pressure,  $\tau = RC$ . With  $R = P_{mean}/Q_{mean}$ ,  $C$  can be derived.
- Area method. The area under the diastolic aortic pressure divided by the pressure difference is used as a measure of the decay time.

- *The parameter estimation method* fits the three-element or four-element Windkessel using pressure

and flow as a function of time. When aortic flow is fed into the Windkessel the pressure is predicted. This pressure can be compared to the measured pressure. By minimization of the summed Root Mean Square Errors, RMSE, of the difference between measured and predicted pressures the best Windkessel parameters are obtained. In this way all the Windkessel parameters can be derived including a good estimate of characteristic impedance. Using the three-element Windkessel compliance is overestimated [5], but this is not the case using the four-element Windkessel [8]. Also pressure may be used and optimization of flow is then performed [9].

- *The input impedance method* fits the input impedance of the three-element or four-element Windkessel model to the measured input impedance, in a way similar to method 5.
- *The transient method* can be applied when pressure and flow are not in the steady state. Peripheral resistance can then not be calculated from mean pressure and mean flow, because aortic flow is not equal to peripheral flow. Using the three-element Windkessel with flow as input, pressure may be calculated while storage of blood in the large conduit arteries is accounted for. By curve fitting of the Windkessel parameters to obtain minimal difference between measured and predicted pressure the Windkessel parameters can be estimated accurately [11].
- *The wave velocity method.* Another method, not based on the Windkessel but on transmission of waves is mentioned here too. Using the Moens-Korteweg equation wave speed (in practice the foot-to-foot wave velocity,  $c_{ff}$ ) can be related to compliance  $c_{ff} = \sqrt{V\Delta P/\Delta V\rho}$  (see Chapter 20). When the wave speed between carotid and iliac arteries is measured, length  $l$ , and average cross-sectional area of the aorta is also determined,  $V$  can be calculated and total aortic compliance is obtained. Since the ascending aorta and other arteries are not included, total aortic compliance is lower than total arterial compliance.

It should be emphasized that all Windkessel-based methods are based on accurate pressure measurement in the proximal aorta. Methods 1 - 3 only require measurement of Cardiac Output, while methods 3 - 8 require ascending aortic flow wave shape. Method 9 requires two accurate pressure measurements.

Finally the three- or four-element Windkessel models can be used in lumped models of the whole cardiovascular system in combination with lumped cardiac models (See [6] as an example).

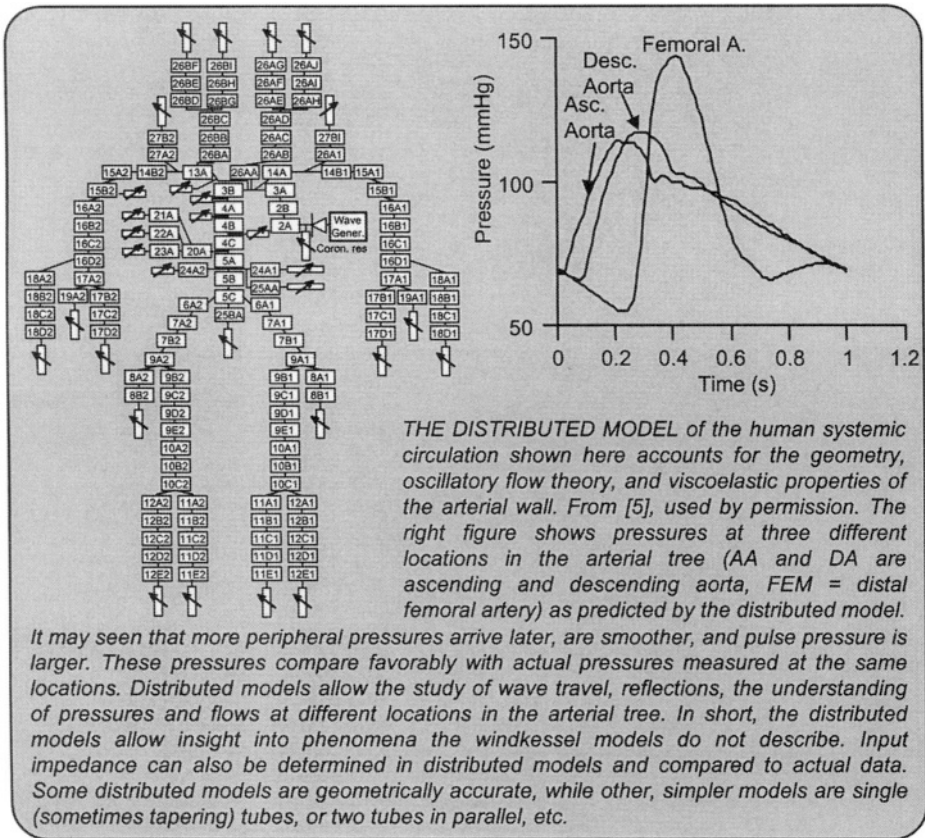
## References

1. Elzinga G, Westerhof N. Pressure and flow generated by the left ventricle against different impedances. *Circ Res* 1973;32:178-186.
2. Chemla, D., J. L. Hébert, C. Coirault, K. Zamani, I. Suard, P. Colin, and Y. Lecarpentier. Total arterial compliance estimated by stroke volume-to-aortic pulse pressure ratio in humans. *Am J Physiol* 1998;274:H500-H505.
3. Liu Z, Brin KP, Yin FCP. Estimation of total arterial compliance: and improved method and evaluation of current methods. *Am J Physiol* 1986;251 :H588-H600.

4. Randall OS, Esler MD, Calfee RV, Bulloch GF, Maisel AS, Culp B. Arterial compliance in hypertension. *New Zealand J Medicine* 1976;6:49-59.
5. Segers P, Brimiouille S, Stergiopulos N, Westerhof N, Naeije R, Maggiorini M, Verdonck P. Pulmonary arterial compliance in dogs and pigs: the three-element windkessel model revisited. *Am J Physiol* 1999;277:H725- H731.
6. Segers P, Stergiopulos N, Westerhof N. Quantification of the contribution of cardiac and arterial remodeling in hypertension. *Hypertension* 2000;36:760-765.
7. Self DA, Ewert RD, Swope RP, Latham RD. Beat-to-beat estimation of peripheral resistance and arterial compliance during +Gz centrifugation. *Aviation Space Environ Med* 1994;65:396-403.
8. Stergiopulos N, Westerhof BE, Westerhof N. Total arterial inertance as the fourth element of the windkessel model. *Am J Physiol* 1999;276:H81-H 88.
9. Stergiopulos N, Meister J-J, Westerhof N. Evaluation of methods for estimating total arterial compliance. *Am J Physiol* 1995;268:H1540-H1548.
10. Stergiopulos N, Meister J-J, Westerhof N. Simple and accurate way for estimating total and segmental arterial compliance: the pulse pressure method. *Ann Biomed Eng* 1994;22:392-397.
11. Toorop GP, Westerhof N, Elzinga G. Beat-to beat estimation of peripheral resistance and arterial compliance during pressure transients. *Am J Physiol* 1987;252:H1275-H1283.
12. Westerhof N, Elzinga G, Sipkema P. An artificial system for pumping hearts. *J Appl Physiol* 1971;31:776-781.

# Chapter 25

# DISTRIBUTED MODELS



## Description

The Windkessel models give an overall, lumped description of the arterial tree. Thus Windkessel models do not permit the study how pressure and flow waves propagate in the arterial tree. Modeling wave propagation requires the use of distributed models, such as the one shown in the box figure. The basic idea of distributed models is to break up the arterial tree into small segments, whose geometry and mechanical properties are known. The wave transmission characteristics of each arterial segment can be described using Womersley’s oscillatory flow theory (Chapter 8) or electrical transmission line theory (Appendix 3).

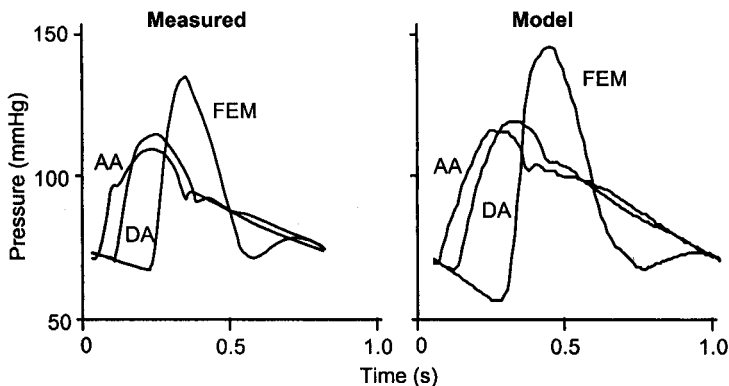
Distributed models of the arterial tree can also be constructed based on the one-dimensional (simplified) form of the blood flow equations describing the conservation of mass and momentum:

$$\partial Q / \partial x + \partial A / \partial t = 0$$

$$\partial Q / \partial t + \partial(Q^2 / A) / \partial x = -(1 / \rho) \cdot A \cdot \partial P / \partial x - 2\pi r \cdot \tau / \rho$$

where  $A$  is the vessel cross-sectional area and  $\tau$  is wall shear stress, usually estimated using Poiseuille's law. The two equations above have 3 variables: pressure  $P$ , flow  $Q$ , and area  $A$ . Therefore a constitutive law relating cross-sectional area,  $A$ , to pressure,  $P$ , is needed to form a system of 3 equations with 3 unknowns, which can be easily solved using different numerical techniques (i.e., finite differences, or method of characteristics).

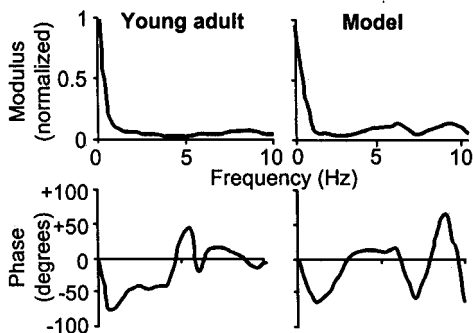
Distributed models have been extensively used to study different aspects



*CENTRAL AND PERIPHERAL PRESSURE WAVES of a distributed model, compared with actual pressure waves measured in similar locations in the human. AA = Ascending Aorta, DA = Descending Aorta, and FEM = Femoral Artery.*

of pressure and flow propagation, such as the effects of viscoelasticity, the effects of different forms of arterial disease on pressure and flow waves, wave reflections, the relation of peripheral to central pressure waves, etc. [3,4,5]. Distributed models predict pressure and flow waves that are fairly accurate and compare well to actual waves measured in the human. This can be seen in the figure, where measured arterial pressure waves in the human are compared to predicted pressure waves of a standard distributed model. Beyond an apparently good qualitative agreement, well known aspects of pressure wave propagation in arteries, such as the systolic pressure amplification, the smoothing of the pulse and the appearance of a secondary reflection in the diastolic part of a pressure wave in a peripheral artery are well predicted.

Global aspects of the distributed models, such as the aortic impedance, (figure at right) also compare favorably to reality. The figure shows the modulus and phase of the input impedance derived from a distributed human systemic arterial model as well as the input impedance measured in a



*INPUT IMPEDANCE of a distributed model (left), compared with the input impedance measured in a young healthy adult (right). The impedance modulus is normalized to the peripheral resistance to facilitate the comparison.*

young healthy adult. The figure also shows that the distributed model predicts all the typical features of the arterial input impedance. The rapid drop in modulus for the first few harmonics, the relatively flat modulus in the medium frequency range, and the correspondence between the point of minimum in impedance modulus and the zero-crossing of the phase angle.

### *Single tube and T-tube models*

Windkessel models and distributed models of the arterial tree represent the two extremes of available models of the arterial tree: the former are simple, contain 3 - 5 global parameters and therefore are easy to use but lack all aspects of wave travel. The latter offer a fairly complete representation of the arterial tree in terms of hemodynamics but require a large number of parameters namely geometry and elasticity of all arterial segments, and therefore are rather cumbersome in their use. Given the above limitations, several researchers have proposed models that are relatively simple but allow for the phenomena of wave travel and reflections. The simplest are the single tube and the asymmetric T-tube models. The single tube models are, as the name suggests, the combination of a tube representing mainly the aorta connected to a peripheral resistor or Windkessel as a model of the peripheral beds. The simplicity of the model is also its main handicap in the sense that all distal reflections come from a single point. A slightly more realistic model is a single tube with geometric tapering as model of the aorta. Asymmetric T-tube models, on the other hand, appear to yield a better description of the arterial tree in terms of input impedance and wave reflections. The asymmetric T-tube model consists of two parallel tubes, a short and small one representing the arterial tree of the upper extremities (head and arms) and a larger size tube accounting the thoracic and abdominal aorta and their branches including the legs [1,2]. The two tubes terminate either with a resistance or a Windkessel as model of the corresponding terminal bed.

### **Physiological and clinical relevance**

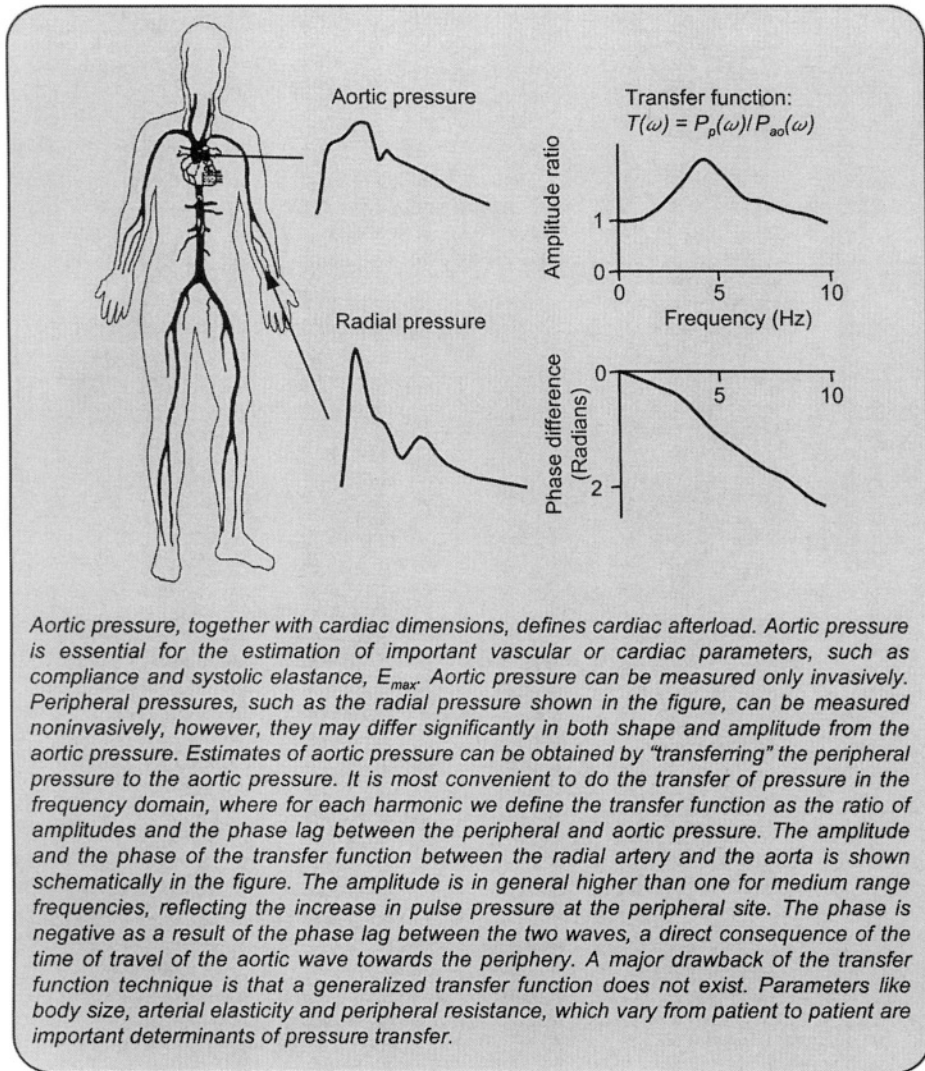
Distributed models have been used mostly for research as analytical tools because they are realistic for simulating a variety of physiological and pathological situations. Although, in principle, distributed models can be used to derive useful parameters of the arterial tree based on *in vivo* measurements, clinical use is difficult because of the large number of parameters required to construct a 'per patient' model.

In arterial modeling research the choice of model should depend on the degree of detail required and the focus desired. To understand the effect of total arterial compliance on integrated quantities such as aortic pressure and Cardiac Output, the Windkessel models suffice. To model detailed effects, such a local flows and pressures and their transmission, one needs to use distributed models.

### **References**

1. Campbell KB, Burattini R, Bell DL, Kirkpatrick RD, Knowlen GG. Time-domain formulation of asymmetric T-tube model of the arterial system. *Am J Physiol* 1990;258:H1761-H1774.

2. O'Rourke MF, Pressure and flow waves in systemic arteries and the anatomical design of the arterial system. *JAppl Physiol* 1967;23:139-149.
3. O'Rourke MF, Avolio AP. Pulsatile flow and pressure in human systemic arteries: studies in man and in a multi-branched model of the human systemic arterial tree. *Circ Res* 1980;46:363-372.
4. Stergiopoulos N, Young DF, Rogge TR. Computer simulation of arterial flow with applications to arterial and aortic stenosis. *J Biomech* 1992;25:1477-1488.
5. Westerhof N, Bosman F, De Vries CJ, Noordergraaf A. Analog studies of the human systemic arterial tree. *J Biomech* 1969;2:121-143.



### Description

Peripheral pressures can be measured noninvasively by different techniques. For example, finger pressure can be reliably measured by photoplethysmography, and radial artery and carotid artery pressure waveforms can be obtained with applanation tonometry. Both techniques are commercially available. Most clinicians use peripheral pressures and typically brachial pressure obtained with the classical sphygmomanometer. Brachial pressure is then used as a substitute for aortic pressure, or, even more so, as a global arterial pressure indicator. However, peripheral and central aortic pressures are not the same. The pressure waveform and the systolic and diastolic pressures can be substantially different between locations (see figure in the

box). In general, systolic pressure increases as we move from central to peripheral pressures, a phenomenon called ‘systolic peaking’, which is attributed to wave reflections at the peripheral vascular beds. Diastolic pressure tends to be slightly lower in peripheral vessels than in central arteries.

#### *Definition of Transfer function*

One way to obtain aortic pressure from a noninvasively measured peripheral pressure wave is to apply the so-called pressure transfer function. In essence, we define a transfer function,  $T$ , which is the ratio of the peripheral pressure wave,  $P_p$ , to the aortic pressure wave,  $P_{ao}$ . The two pressures can only be related to each other in the frequency domain (see Appendix 1). So for each harmonic, we define the amplitude of the transfer function as the ratio of amplitudes of the peripheral and aortic pressure wave and the phase of the transfer function as the difference in the phase between the peripheral and aortic pressure (See Appendix 1). This is mathematically expressed very simply as [2,3,4]:

$$T(\omega) = P_p(\omega)/P_{ao}(\omega)$$

The amplitude and the phase of the transfer function between the radial artery and the aorta is shown schematically in the figure in the box. The zero-frequency value of the transfer function is the ratio of mean peripheral arterial pressure to mean aortic pressure. Because of the small drop in mean pressure between the aorta and the peripheral artery, this ratio is slightly lower than 1. The amplitude of the transfer function is, in general, higher than one for medium range frequencies, reflecting the increase in pulse pressure at the peripheral site. For high frequencies the transfer function decreases to negligible values because high frequencies are damped while traveling. The phase is negative, as a result of the phase lag between the two waves, a direct consequence of the time it takes for the aortic wave to travel towards the periphery.

Several techniques are commercially available to obtain central from peripheral pressures, see [1 and 2]. These methods therefore should be used with utmost care.

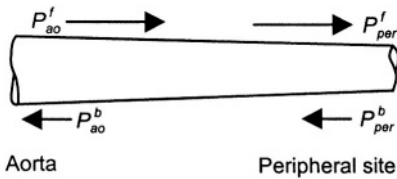
#### *Calibration of noninvasively determined pressure wave shapes*

Applanation tonometry and echotracking of wall motion are ways to obtain peripheral pressure wave shapes noninvasively, but calibration is not available. Sphygmomanometrically obtained, and thus calibrated values of systolic,  $P_{syst,br}$  and diastolic,  $P_{diast,br}$  pressure in the brachial artery, can help in the calibration [7]. A good estimate of calibrated carotid systolic pressure is to assume that mean pressure and diastolic pressure are not different between brachial to carotid artery:  $P_{diast,br} = P_{diast,car}$ , and  $P_{mean,br} = P_{mean,car}$ . Systolic pressure can then be derived assuming that mean pressure in the carotid artery,  $P_{mean,car}$ , equals  $P_{mean,car} = (P_{syst,car} + P_{diast,car})/2$  and in the brachial artery  $P_{mean,br} = (P_{syst,br} + 2P_{diast,br})/3$ . Rearrangement leads to:

$$P_{syst,car} = 2/3 P_{syst,br} + 1/3 P_{diast,br}$$

*Physical basis and simple mathematical model for Transfer Function*

A simple approach, which helps to understand the physical basis of the transfer function, is to consider the entire arterial pathway from the aorta to the peripheral site as a single tube. The aortic pressure wave,  $P_{ao}$ , consists of its forward running component,  $P_{ao}^f$ , and its backward running component or reflected wave,  $P_{ao}^b$ . At the peripheral site the forward and backward running wave components are  $P_p^f$  and  $P_p^b$ , respectively.



As a first approximation, we may assume that the forward wave at the peripheral site is identical to the forward wave at the aorta with the exception of a time delay between the two waves. This time delay is equal to the time it takes for the forward wave to travel from the aorta to the peripheral site, i.e.,  $\Delta t = l/c$ ,  $l$  being the distance and  $c$  the wave speed. In the frequency domain the time delay is expressed as a phase lag, which is equal to  $\omega\Delta t$ , and we may write

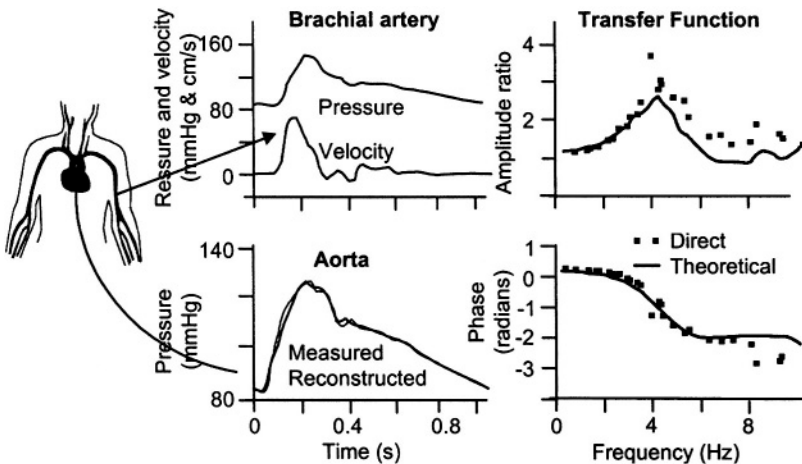
*THE FORWARD AND BACKWARD WAVES travel from heart to periphery and back.*

$$P_p^f = P_{ao}^f \cdot e^{i\omega\Delta t}$$

Following a similar reasoning, the reflected wave at the peripheral site is equal to the reflected wave in the aorta. However, because the reflected wave travels in the opposite direction, the aortic wave now lags the peripheral wave by the same time delay  $\Delta t$ . The transfer function,  $T$ , can thus be written as:

$$T(\omega) = P_p(\omega)/P_{ao}(\omega) = [P_p^f(\omega) + P_p^b(\omega)]/[P_{ao}^f(\omega) + P_{ao}^b(\omega)]$$

and thus:



*AORTA PRESSURE CAN BE DERIVED FROM BRACHIAL PRESSURE AND VELOCITY OR FLOW WAVES and the travel time of the waves between these two sites. The brachial pressure and flow (or velocity) can be used to calculate forward and reflected pressures. When the backward pressure is advanced and the forward pressure is delayed in time, subsequent addition results in aortic pressure. The theoretical transfer function is close to the measured data. Adapted from [6], used by permission.*

$$T(\omega) = [P_{ao}^f(\omega)e^{i\omega\Delta t} + P_{ao}^b(\omega)e^{-i\omega\Delta t}] / [P_{ao}^f(\omega) + P_{ao}^b(\omega)]$$

Dividing by  $P_{ao}^f$  and taking into account that  $P_{ao}^b/P_{ao}^f$  is equal to the reflection coefficient,  $\Gamma$ , we obtain the following final expression for the transfer function  $T$ :

$$T(\omega) = [e^{i\omega\Delta t} + \Gamma(\omega)e^{-i\omega\Delta t}] / [1 + \Gamma(\omega)]$$

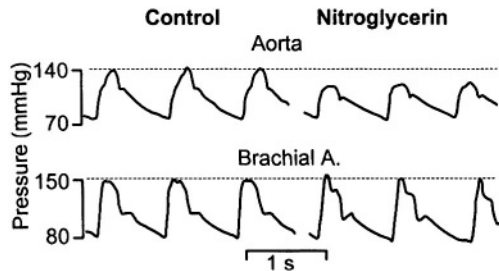
This single tube model suggests that the transfer function depends primarily on the reflection coefficient at the distal site and on the time of travel of the waves between the two sites. The model, of course, it is an oversimplification of reality, because it does not take into account the effects of wave damping, and nonlinear elasticity. The model applies to a single uniform vessel and thus cannot be applied when significant reflection sites exist between the aorta and the peripheral site, e.g., major bifurcations. The model gives, however, reasonable predictions of the transfer function between the aorta and the brachial artery, as shown in the figure on the previous page [6].

### Physiological and clinical relevance

This figure shows aortic pressure and brachial pressure measured in an individual under control conditions as well as after administration of nitroglycerin [5]. This figure shows that the transfer of pressure depends on the state of the vascular tree.

Under control conditions, systolic brachial pressure is approximately 150 mmHg, overestimating aortic pressure by 10 mmHg. Under nitroglycerin, systolic pressure in aorta drops significantly. Notice the disappearance of the late systolic reflected wave, apparently due to reduced reflections resulting from vasodilatory effects of nitroglycerin. Brachial systolic pressure, however, remains practically unchanged, now overestimating aortic pressure by more than 30 mmHg. This example demonstrates that peripheral pressure waves are not a reliable substitute for aortic pressure and their relation may vary depending on different physiological parameters, such as arterial vasomotor tone. Therefore, peripheral waves cannot give an accurate estimation of the load on the heart.

A major drawback of the transfer function technique is that a generalized function does not exist. Parameters like body size, arterial elasticity and peripheral resistance, which vary from patient to patient, are important determinants of pressure transfer. One may try to adjust the transfer function based on gender, body size, age, etc., but such an adjustment, which is based on statistical analysis of large population studies may not be precise [3]. One approach would be to use the simple model of pressure transfer presented above and try to derive a transfer function on a 'per patient' basis.

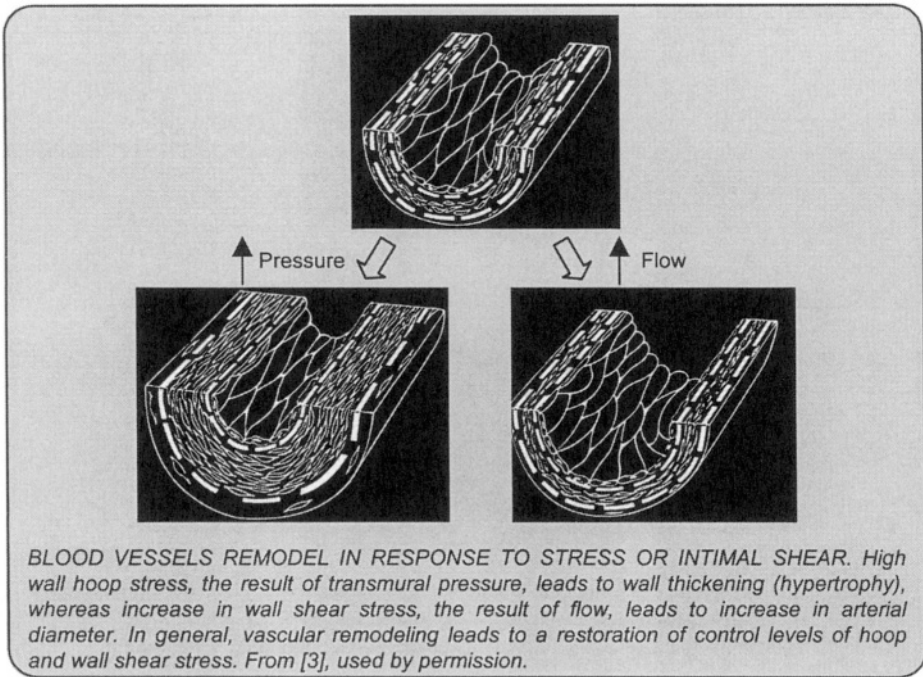


*SIMULTANEOUS recordings of aortic and brachial pressure waves under control conditions and after administration of nitroglycerin. During vasodilation systolic blood pressure in the brachial artery is not affected while systolic aortic pressure is lowered. Adapted from [5], used by permission.*

From a clinical standpoint it is the aortic pressure and not peripheral pressure that is of primary importance in a number of aspects. Aortic pressure is the main determinant of cardiac afterload, and it drives coronary perfusion. The aortic pressure waveform can be used to derive reliably arterial compliance based on a variety of methods (Chapter 24). During ejection, aortic pressure can be taken as a surrogate of left ventricular pressure and, together with noninvasive measurements of left ventricular volume, can be used to estimate cardiac parameters such as End-Systolic elastance (Chapters 13 and 18).

## References

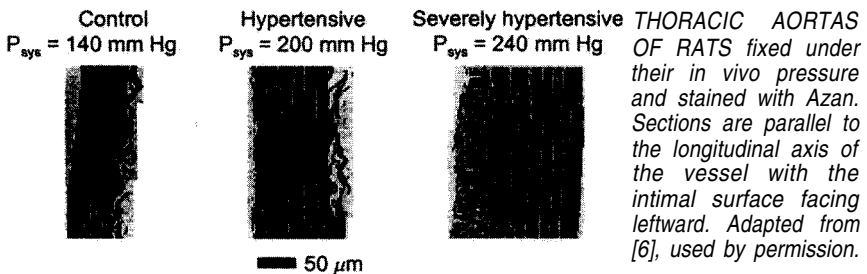
1. Adji A, O'Rourke MF. Determination of central aortic systolic and pulse pressure from the radial artery pressure waveform. *Blood Press Monit.* 2004 9:115-121.
2. Chen CH, Nevo E, Fetics B, Pak PH, Yin FCP, Maughan WL, Kass DA. Estimation of central aortic pressure waveform by mathematical transformation of radial tonometry pressure. Validation of a generalized transfer function. *Circulation* 1997;95:1827-1836.
3. Hope SA, Tay DB, Meredith IT, Cameron JD. Comparison of generalized and gender-specific transfer functions for the derivation of aortic waveforms. *Am J Physiol* 2002;283:H1150-H1156.
4. Karamanoglu M, O'Rourke MF, Avolio AP, Kelly RP. An analysis of the relationship between central aortic and peripheral upper limb pressure waves in man. *Eur Heart J* 1993;14:160-167.
5. Kelly RP, Gibbs HH, O'Rourke MF, Daley JE, Mang K, Morgan JJ, Avolio AP. Nitroglycerin has more favourable effects on left ventricular afterload than apparent from measurement of pressure in a peripheral artery. *Europ Heart J* 1990;11:138-144.
6. Stergiopulos N, Westerhof BE, Westerhof N. Physical basis of pressure transfer from periphery to aorta: a model based study. *Am J Physiol* 1998;274:H1386-H1392.
7. Van Bortel LM, Balkestein EJ, van der Heijden-Spek JJ, Vanmolkot FH, Staessen JA, Kragten JA, Vredeveld JW, Safar ME, Struijker Boudier HA, Hoeks AP. Non-invasive assessment of local arterial pulse pressure: comparison of applanation tonometry and echo-tracking. *J Hypertens* 2001;19:1037-1044.



**Description**

One of the fundamental characteristics of the living tissues is their ability to respond to changes in their mechanical environment by growth and remodeling. Growth and remodeling are processes which allow the living tissue to maintain an optimal environment under physiological development as well as under various pathologic conditions. The arterial wall responds to changes in transmural pressure and flow in terms of geometrical adaptation (e.g., hypertrophy), structural adaptation (e.g., change in scleroprotein content, stiffening) and functional adaptation (e.g., changes in endothelial function or vascular smooth muscle tone).

Although often referred to the macroscopic quantities of pressure and flow, vascular remodeling is better associated with their resulting wall hoop stress ( $\sigma$ ) and wall shear stress ( $\tau$ ). We recall that wall hoop stress and wall shear stress are related to transmural pressure through the law of Laplace,



$\sigma = P \cdot r / h$ , and flow through the law of Poiseuille,  $\tau = 4\eta \cdot Q / \pi r^3$ , respectively.

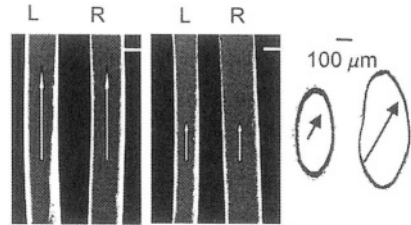
### *Vascular adaptation to changes in pressure*

Experimental studies have shown that an increase in pressure leads to a thickening of the arterial wall (hypertrophy). In general, the wall thickens, thereby lowering wall hoop stress down to control (normotensive) levels, thus counterbalancing the increase in pressure. An example of such adaptation is shown in the figure on the previous page.

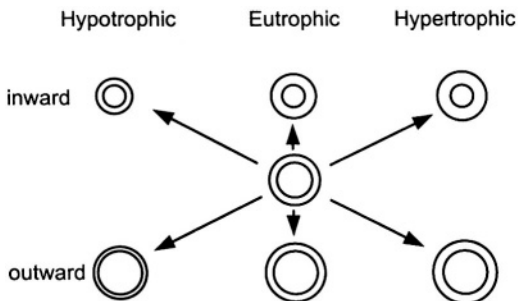
### *Vascular adaptation to changes in flow*

Acute changes in blood flow lead to adjustments in vessel caliber, via endothelium-dependent vasodilation or vasoconstriction. Chronic changes in flow lead to remodeling. Long-term, flow-induced remodeling is due to reorganization of cellular and extracellular wall components. The adaptive response to changes in blood flow has been studied in various animals and it was found that the vessel inner diameter adapts to preserve the level of wall shear at the intimal surface. Kamiya and Togawa [2] belong to the first who demonstrated that the adaptive response to an increase in flow leads to normalization in wall shear stress. They constructed an arteriovenous shunt between the carotid artery and jugular vein of a dog, which led to a significant increase in blood flow in the ipsilateral carotid and a decrease in blood flow in the contralateral one. Six to eight months after the operation, carotid diameter increased in the segment with high flow and decreased in the segment with low flow. The diameter change preserved wall shear stress within 15% of the pre-operation levels, despite the severe increase or decrease in flow.

Similar findings were reported by Langille and O'Donnel [4] on the rabbit



SCANNING ELECTRON MICROGRAPH of methacrylate casts of left and right rabbit carotids under control (left) and 2 weeks after left carotid flow was surgically reduced (middle). Histological cross sections of carotid arteries 2 weeks after left carotid flow was reduced (right). Reduction in flow leads to reduction in left carotid diameter (right) and normalization of intimal wall shear to control levels. Adapted from [4], used by permission.



CLASSIFICATION of different types of arterial remodeling. Adapted from [7], used by permission.

carotid, were a reduction in flow led to a reduction in internal diameter and restoration of wall stress (see figure above). Remodeling in response to increased flow appears to be associated with cell hyperplasia, structural changes in internal elastic lamina and adventitia as well as with the contractile properties of the artery. The endothelium and nitric oxide synthesis are the main mediators for the vessel

adaptation to flow. For example, inhibition of nitric oxide synthesis totally abolishes the capacity of the pig carotid artery to remodel and maintain control levels of wall shear in the presence of an arterio-venous shunt [8].

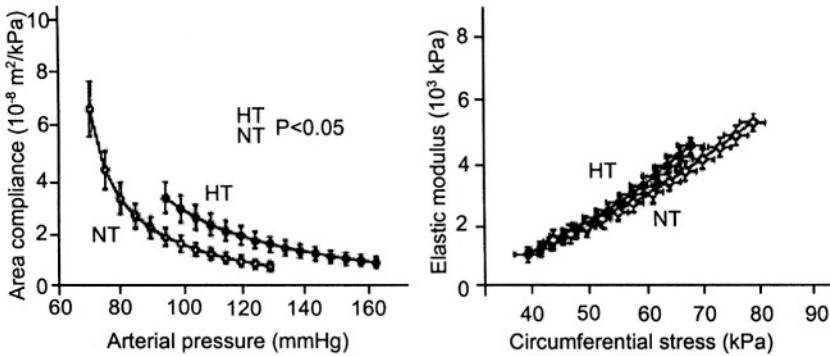
### Physiological and clinical relevance

#### *Arterial remodeling in hypertension*

In presence of essential hypertension, vascular resistance increases due to alterations in resistance vessel architecture, decrease in lumen diameter and increase in media thickness/lumen diameter ratio. This corresponds to a inward eutrophic remodeling, as schematically shown in the figure. The type of remodeling in resistance vessels depends on the type of hypertension and treatment. Human renal hypertension leads to inward hypertrophic remodeling. During anti-hypertensive treatment the situation is often reversed and outward eutrophic remodeling and hypertrophic remodeling is observed.

#### *Arterial remodeling in hypertension: large arteries*

Remodeling due to hypertension is known to increase wall thickness and restore wall hoop stress. In terms of compliance and elastic properties, arterial remodeling tends to be vessel specific. Aortic and carotid artery compliance are reduced in hypertension. Radial artery compliance and incremental elastic modulus, however, seem to be preserved in hypertensive patients [5]. It is important here to acknowledge the nonlinear nature of the compliance and elastic modulus curves. Compliance is expressed as a function of pressure (structural property) and elastic modulus as a function of strain (material property). We observe that at their corresponding operating pressure, normotensive and hypertensive radial arteries exhibit the same compliance, which is indicative of some kind of structural remodeling

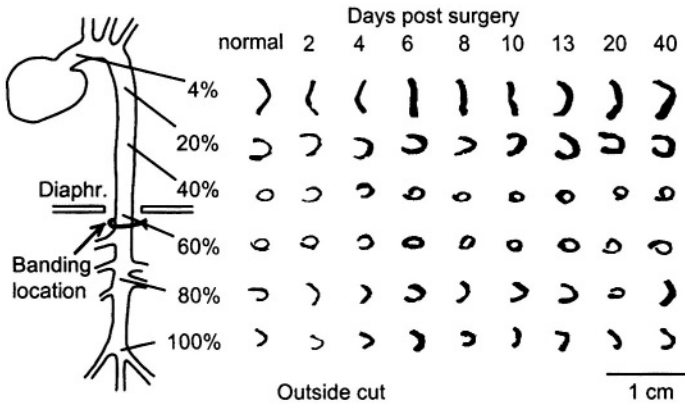


*RADIAL ARTERY area compliance (left) and elastic modulus (right) measured in vivo in a group of normotensive (NT, n = 22) and hypertensive subjects (HT, n = 25). When compared at their corresponding mean operating pressures (NT: 90 mmHg; HT: 121 mmHg) compliance was similar despite significant concentric hypertrophy. In normotensive subjects wall thickness is 0.28 mm compared to 0.40 mm in hypertensive patients. Internal diameter is the same and equal to 2.50 mm in both groups. The incremental elastic modulus-stress curve was essentially the same in normotensives and hypertensives, suggesting similar tissue properties in the two groups. Adapted from [5], used by permission.*

aiming to maintain normotensive compliance levels. Further, the incremental modulus-strain curve is identical in normotensive and hypertensive patients, which means that the intrinsic elastic properties of the wall material remained the same. This example demonstrates nicely the capacity of the radial artery to remodel in hypertension in a manner that normalizes wall stress by thickening, maintains control compliance levels despite exposure to higher pressure and preserves the intrinsic elastic properties of the arterial tissue.

*Residual stress in relation to growth and remodeling*

In Chapter 10 it was mentioned that both cardiac tissue and vascular tissue are not at a zero stress state when all loads are removed [1]. It was also postulated that residual stresses help maintain a uniform stress distribution across the wall. When, for different physiological or pathological reasons, the biomechanical environment to which the wall is subjected to is altered, mechanical stresses within the arterial wall will also be altered and their distribution will not be uniform. A remodeling process will likely take place



PHOTOGRAPHS OF AORTIC RINGS cut open radially to reveal their zero stress state (ZSS). The first column shows the ZSS in normal rats. The other columns show the change in ZSS after hypertension was induced by banding of the aorta above the coeliac trunc. Adapted from [1], used by permission.

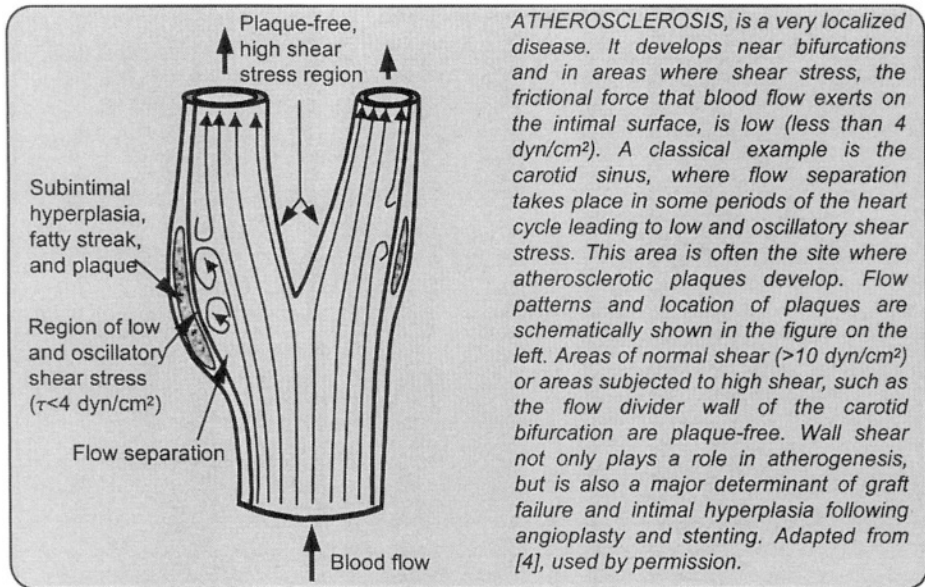
in order to restore stresses and strain to control levels.

Remodeling leads to changes in geometry and structure, with addition or resorption of mass. Consequently, the zero stress state will change. Changes in the zero stress state, or, equivalently, changes in the opening angle allow for the monitoring of arterial wall remodeling. The figure shows changes in wall thickness and opening angle in various positions along the aorta of rats, which received a very tight banding of the thoracic aorta just below the diaphragm. For the aorta above the banding site, which was exposed to higher pressure we observe a progressive thickening of the aortic wall during the entire post-surgery period. The aorta thickens its wall in order to compensate for the increase in pressure and thus restore stress to control levels. The opening angle, however, shows a non-monotonic evolution. Initially, the opening angle increases, which is indicative of higher growth in the internal wall layers. Later, as the wall thickens and stress levels are restored, the opening angle returns to control levels as well. The initial higher

growth in the internal wall layers is reflected by the increase in opening angle. This demonstrates that remodeling is dependent on the local stress distribution and also that wall remodeling affects the residual stress distribution within the arterial wall.

## References

1. Fung YC and Liu SQ. Change of residual strains in arteries due to hypertrophy caused by aortic constriction. *Circ Res* 1989;65:1340-1349.
2. Kamiya A and Togawa T. Adaptive regulation of wall shear stress to flow change in canine carotid artery. *Am J Physiol* 1980;239:14-29.
3. Langille LB. Blood flow-induced remodeling of the artery wall. In: *Flow-dependent regulation of vascular function*. 1995, edited by Bevan JA, Kaley G and Rubanyi GM. New York, Oxford University Press, 1995.
4. Langille BL and O'Donnell F. Reductions in arterial diameter produced by chronic decreases in blood flow are endothelium-dependent. *Science* 1986; 231:405-407.
5. Laurent S, Girerd X, Mourad J-J, Lacolley P, Beck L, Boutouyrie P, Mignot J-P, and Safar M. Elastic modulus of the radial artery wall material is not increased in patients with essential hypertension. *Arteriosclerosis and Thrombosis* 1994; 14:1223-1231.
6. Matsumoto T and Hayashi K. Stress and strain in hypertensive and normotensive rat aorta considering residual strain. *J Biomech Eng* 1996;118:62-73.
7. Mulvany MJ. Vascular remodelling of resistance vessels: can we define this? *Cardiovasc Res* 1999;41:9-13.
8. Tronc F, Wassef M, Esposito B, Henrion D, Glagov S, Tedgui A. Role of NO in flow-induced remodeling of the rabbit common carotid artery. *Arterioscler Thromb Vasc Biol* 1996;16:1256-1262.



### Description

Hemodynamic forces do not only regulate blood vessel geometry and structure, i.e., remodeling, but they can be considered also a main factors influencing the development of different forms of vascular disease, such as atherosclerosis, and aneurysms. Of particular importance is the role of shear stress, the minute force resulting from the friction that the flowing blood exerts on the luminal surface, on the localization and development of atherosclerosis.

Atherosclerosis is associated with genetic predisposition and systemic factors such as hypertension, hyperlipidemia, smoking, etc. However, the localized nature of the disease, which occurs principally in areas of disturbed flow such as near bifurcations and curvatures, cannot be explained by systemic factors, which apply equally throughout the vasculature. It is recognized today that atherosclerosis develops in areas where shear stress is low, typically less than 4 dyn/cm<sup>2</sup>, or 0.4 Pa, and changes direction during the cardiac cycle. An example is the wall of the carotid sinus, where local shear is low and flow separates during the decelerating phase of the heart cycle, leading to flow separation and thus flow reversal and change in shear stress direction (figure in the box). Other areas where low shear stress localizes with atherosclerosis are the coronaries, the infrarenal aorta and the femoral artery.

#### *Shear stress and endothelial function*

Apart from its non-thrombogenic protective role, the endothelial layer constitutes the mechano-sensing element, which senses the local flow conditions and produces autocrine and paracrine factors for the functional regulation of the arterial wall. Studies of endothelial cells *in vitro* and *in vivo*

have revealed the deleterious effect of low and oscillatory shear stress on endothelial function. Under physiological shear ( $\sigma > 10 \text{ dyn/cm}^2$ ) endothelial cells align in the direction of flow whereas they do not when exposed to low shear ( $\sigma < 4 \text{ dyn/cm}^2$ ). Low and oscillatory shear stress leads to inhibition of NO-synthase, greater endothelial cell cycling and increase in apoptosis. Low and oscillatory shear also contribute to local endothelial dysfunction, which may lead to enhanced monocyte adhesion, increased platelet activation, increased vasoconstriction, increased smooth muscle cell proliferation, and increased oxidant activity, thus constituting a likely model for atherogenesis. High shear stress induces an atheroprotective endothelial phenotype, increases NO production, and decreases the expression of vasoconstrictors, inflammatory response mediators, adhesion molecules and oxidants. Detailed discussion on the relation between shear stress and endothelial function can be found in the review articles by Davies et al. [1] and Malek et al.[4].

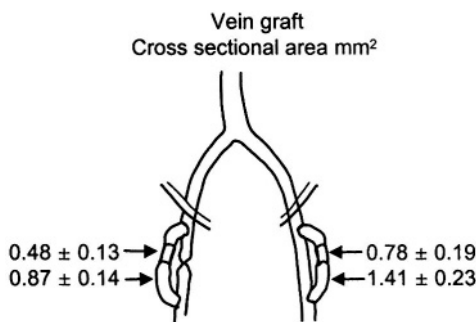
## Physiological and Clinical relevance

### *Assessing risk for atherosclerosis*

Ultrasound measurements in the carotid artery of healthy young adults aged 28-38 years revealed a significant inverse relation between the measured intima-media thickness and local shear stress. This suggests that there is a prognostic value in the assessment of local wall shear levels using non-invasive techniques, such as ultrasound Doppler or MRI.

Since the velocity profiles near a bifurcation depend strongly on the geometry, it has been suggested that there exist 'geometrical risk' factors for atherosclerosis. Certain branching geometries, i.e., high curvatures and large angles, would predispose to atherosclerosis, because they would lead more easily to flow separation and low shear stress regions.

### *Shear stress and intima hyperplasia in vein grafts*



*INTIMAL HYPERPLASIA in vein grafts. Adapted from [2], used by permission.*

Intima hyperplasia in vein grafts is also sensitive to wall shear. Dobrin et al. [2] examined the effect of all mechanical factors, pressure, extension, and shear stress, on intima hyperplasia and medial thickening in autogenous vein grafts in dogs. Autologous vein grafts were used to bypass a segment of the femoral artery. The femoral artery on one side was ligated, so that all femoral blood flow passed through the graft. The femoral artery at the opposite side was left patent, which permitted only part of the flow to pass through the vein graft. A stiff cuff was placed over the middle section of the vein grafts impeding radial expansion. Cross-sectional areas are given in the figure. The results show that intima hyperplasia is greater on both sides, in the distended, low shear, regions, than in the regions constrained by the cuffs, thus at high shear. Furthermore, intima hyperplasia was globally lower on the

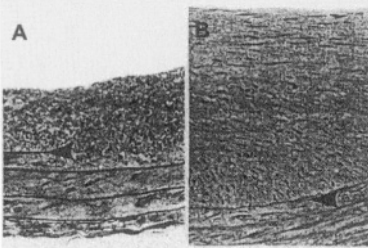
side with high flow, obtained by femoral artery ligation, as compared to the side where femoral artery was left patent, i.e., low flow.

### *Shear stress and intima hyperplasia in bypass grafts*

High shear stress inhibits neointima formation in artificial ePTFE grafts. Animal experiments have shown that exposure of implanted grafts to higher shear, by means of distal arteriovenous fistulas, leads to a decrease in the thickness of the already existing neointima hyperplasia.

Low and oscillatory wall shear stress patterns may also be responsible for the failure of bypass grafts. In the vicinity of an end-to-side anastomosis, blood flow is greatly disturbed. This is mainly due to the abrupt change in geometry. For vascular grafts, intima hyperplasia develops preferentially at the 'toe' and the 'heel' of the anastomosis. These are exactly the locations where flow separation, low wall shear stress and large gradients of wall shear stress take place.

### *Intima hyperplasia following angioplasty and stenting*



**HISTOLOGICAL SECTIONS** of the rat carotid subjected to high flow (A) and low flow (B) indicating the degree of intimal hyperplasia 2 weeks after balloon injury. Adapted from [3], used by permission.

Restenosis is an undesirable occlusive response to stent implantation after balloon angioplasty. In contrast to balloon angioplasty, where acute or subacute recoil represents the major mechanism of restenosis, stent restenosis is exclusively attributed to neointima proliferation, a tissue reaction often termed intima hyperplasia (IH). Morphological studies have demonstrated that neointima is caused by early smooth muscle cell ingrowth, which is then gradually replaced by extracellular matrix.

There is a good deal of scientific evidence that intima hyperplasia is sensitive to flow. Kohler and Jawien [3] studied the effects of flow on intima hyperplasia after balloon injury of the rat common carotid. Flow was increased, by ~35%, by ligation of the opposite common carotid artery or decreased, also by ~35%, by ligation of the ipsilateral internal carotid. Two weeks after the intervention, intima thickness, indicated by the distance between the artery lumen and arrow, was significantly higher in the low-flow group (figure B) as compared with the high flow group (figure A).

There appears also to be strong clinical evidence for the relation between post interventional flow and patency of balloon angioplasty. If local flow, thus wall shear stress, after balloon angioplasty is high, the artery is expected to remain patent. This observation, common to many physicians practicing balloon angioplasty, is substantiated by recent studies reporting increased long-term patency after angioplasty in lower extremity arteries when flows are high. Direct clinical proof of the inverse relationship between wall shear stress and intima thickness was given by Wentzel et al. [5].

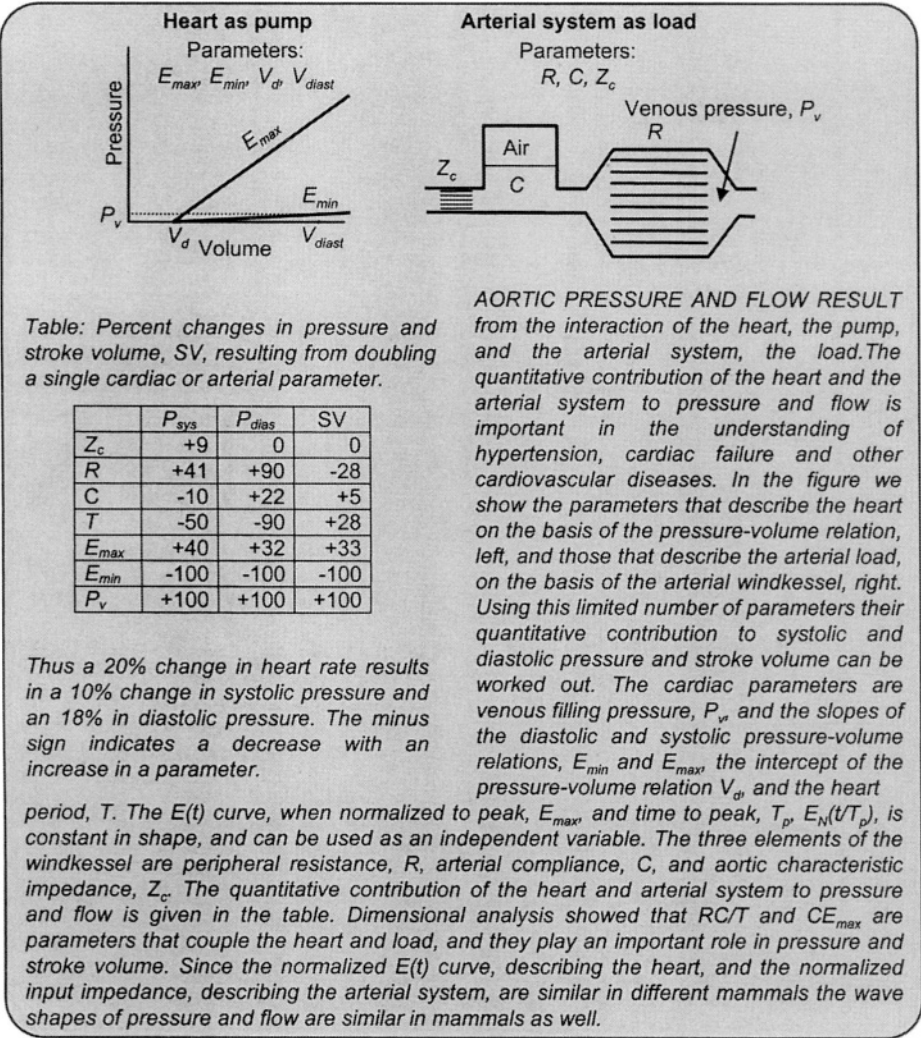
The restenosis problem following stent placement has been drastically reduced with the use of drug-eluting stents. Drug-eluting stents with the capability to deliver anti-inflammatory or anti-proliferative drugs directly to the adjacent arterial tissue, inhibit neointima hyperplasia and restenosis.

---

**References**

1. Davies PF, Barbee KA, Lal R, Robotewskyj A, and Griem ML. Hemodynamics and atherogenesis. Endothelial surface dynamics in flow signal transduction. *Ann N Y Acad Sci* 1995;748:86-102; discussion 102-103.
2. Dobrin, P B., Littooy FN, Endean ED. Mechanical factors predisposing to intimal hyperplasia and medial thickening in autogenous vein grafts. *Surgery* 1989;105:393-400.
3. Kohler T, Jawien A. Flow affects development of intimal hyperplasia after arterial injury in rats. *Arteriosclerosis and Thrombosis* 1992;12:963-971.
4. Malek AM, Alper SL, and Izumo S. Hemodynamic shear stress and its role in atherosclerosis. *JAMA* 1999;282:2035-2042.
5. Wentzel JJ, Krams R, Schuurbiens JC, Oomen JA, Kloet J, Van der Giessen WJ, Serruys PW, and Slager CJ. Relationship between neointimal thickness and shear stress after Wallstent implantation in human coronary arteries. *Circulation* 2001;103:1740-1745.

Part D  
Integration



**Description**

Blood pressure and Cardiac Output result from the interaction of the heart and arterial load. The contribution of the heart is obvious, because without its pumping action pressure and flow would not exist. However, the quantitative contribution of the heart and arterial load to pressure and flow under different physiological conditions and during various diseased states has not been sufficiently recognized. To quantitatively analyze the cardiac and arterial contributions to systolic and diastolic pressure and Stroke Volume, we make use of the simplified descriptions of the cardiac pump and the arterial load. The heart is described by the varying elastance model (Chapter 13), and the arterial system is described by the three-element Windkessel model (Chapter

24). Using these models the contribution of each parameter to pressure and flow can be quantified.

### *Dimensional analysis*

Dimensional analysis, or the concept of similitude, is a powerful method to systematically derive relations of a system and offers two major advantages [3]. First, it reduces the number of variables, and second, it groups the cardiac and arterial parameters in dimensionless terms, which are automatically scaled to heart rate and body size. This will be a particularly important issue when we discuss comparative physiology (Chapter 30). The parameters that describe the heart as a pump, including venous filling pressure, and the arterial system as the load are given in the box. The total number of parameters is 8: 5 for the heart and 3 for the arterial system.

The dependent variables systolic and diastolic pressure ( $P_s$  and  $P_d$ ) and Stroke Volume,  $SV$ , can be written as a function of these eight cardiac and arterial parameters. Dimensional analysis implies that when the variables and the parameters are non-dimensionalized, the number of non-dimensional parameters can be reduced by three. Three is the number of reference dimensions (time, force and length), describing the variables [3]. Thus five non-dimensional parameters remain. An intelligent choice is the following [6]:

$$P_s/P_v = \Phi_1 (Z_c/R, RC/T, CE_{min}, E_{max}/E_{min}, E_{min}V_d/P_v)$$

$$P_d/P_v = \Phi_2 (Z_c/R, RC/T, CE_{min}, E_{max}/E_{min}, E_{min}V_d/P_v)$$

$$SV \cdot E_{min}/P_v = \Phi_3 (Z_c/R, RC/T, CE_{min}, E_{max}/E_{min}, E_{min}V_d/P_v)$$

The symbols are explained in the box. The next step is to find the dependence of the non-dimensional variables on the non-dimensional parameters. It turns out experimentally that the parameter  $E_{min} \cdot V_d/P_v$  does not contribute to  $P_s/P_v$  and  $P_d/P_v$ ; that  $Z_c/R$  does not determine  $P_d/P_v$  and  $SV/V_d$ ; while  $E_{max}/E_{min}$  does not determine  $SV \cdot E_{min}/P_v$ . The contribution of  $Z_c/R$  to  $P_s/P_v$  turns out to be small [6] and is neglected. The relations then can be simplified to:

$$P_s/P_v \approx \Phi_1 (RC/T, CE_{min}, E_{max}/E_{min})$$

$$P_d/P_v \approx \Phi_2 (RC/T, CE_{min}, E_{max}/E_{min})$$

$$SV \cdot E_{min}/P_v \approx \Phi_3 (RC/T, CE_{min}, E_{min} \cdot V_d/P_v)$$

In all non-dimensional variables we see that the parameters  $RC/T$ , and  $C \cdot E_{min}$  appear. We call them ventriculo-arterial coupling parameters. This emphasizes the fact that the interaction of pump and load determines pressure and flow.

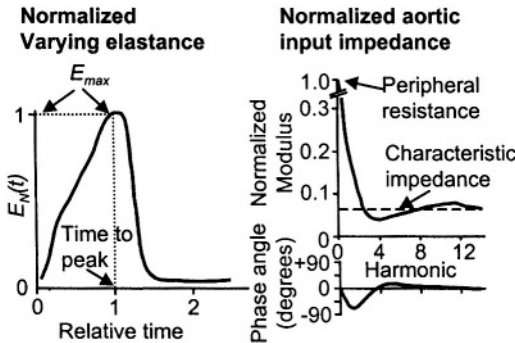
The Frank-Starling mechanism also emerges clearly from the above equations. Leaving all parameters the same, the pressures are simply proportional to venous pressure,  $P_v$ ,  $SV$  is also related to filling pressure, but in a more complex way.

The pressures also are dependent on  $E_{max}/E_{min}$  a measure of contractility of the heart. The Stroke Volume is also described by the rather complex term

$E_{min} \cdot V_d / P_v$ , which is related to diastolic ventricular filling and can be written as  $V_d / (V_{diast} - V_d)$ , with  $V_{diast}$  end-diastolic ventricular volume.

On the basis of the results obtained with the dimensional analysis we can perform a sensitivity analysis of pressure and Stroke Volume to individual parameters. The results are given in the table in the box.

We note that the normalized parameters  $RC/T$ ,  $CE_{min}$ ,  $E_{max}/E_{min}$  do not depend on body size, so that for similar venous pressures, aortic systolic and diastolic pressures will be similar in all mammals (see Chapter 30). Stroke Volume does depend on body size. The wave shapes of aortic pressure and flow result from the shape of the  $E(t)$  curve describing the pump and the input impedance describing the arterial load. Both, when normalized, are body size independent [5,7], explaining why aortic pressure and flow look alike in all mammals (Chapter 30).



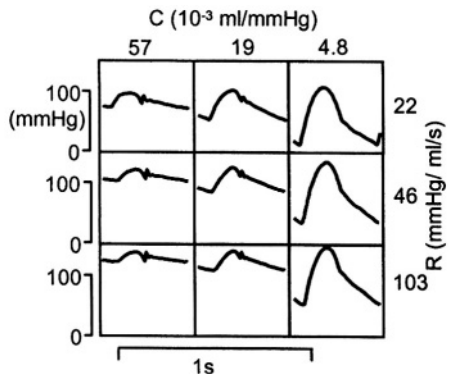
The normalized elastance curve and the normalized input impedance curve are similar, resulting in similar wave shapes of aortic pressure and flow.

**Physiological and clinical relevance**

The analysis shows in quantitative terms the contribution of cardiac and arterial parameters to blood pressure and Stroke Volume. It may be seen from the table in the box that resistance has a much stronger effect on systolic blood pressure than compliance has. However, changes in compliance are often considerably larger than resistance changes. For instance, between the ages of 20 and 70 years compliance may decrease by a factor of 3, thus increasing systolic blood pressure by 15%, while the age related resistance increase is about 10% resulting in a systolic pressure increase of slightly over 4%.

On the basis of the dimensionless parameters shown above it may be suggested to use  $E_{max} / E_{min}$  as a measure of contractility, because this ratio is size independent. The  $E_{max}$  alone is, of course depending on the ventricular volume.

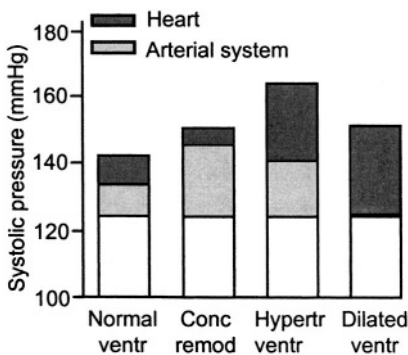
The theoretical results can be compared with biological data. Experimental data [1] obtained from the isolated heart loaded with a



AORTIC PRESSURE resulting from an isolated cat heart pumping into a three-element windkessel. The effect of changes in peripheral resistance and total arterial compliance are shown. Note that systolic pressure is little affected by decreasing compliance. Adapted from [1], used by permission.

Windkessel model indeed show that compliance changes alone have a small effect on systolic blood pressure and a larger effect on diastolic blood pressure. When compliance is decreased *in vivo* other parameters also change and systolic pressure increases and diastolic pressure decreases [2]. The main difference between the *ex vivo* and *in vivo* results is the adaptation of the heart during the decrease in compliance. The *ex vivo* heart, including filling, was unchanged while *in vivo* the heart adapts and Cardiac Output diminishes less than in the *ex vivo* situation. Thus, the changed cardiac function *in vivo* has an effect on blood pressure.

In the literature it is well established that hypertension results in ventricular hypertrophy and therefore a higher  $E_{max}$ . However, it is often not realized that hypertrophy causes changes in the properties of the cardiac pump such a increased wall thickness and that these changes may, in turn,



*CARDIAC AND ARTERIAL CONTRIBUTIONS TO SYSTOLIC pressure increase in four groups of hypertensive patients. Several stages in cardiac changes are depicted, 1. Normal ventricle; 2. Concentric remodeling; 3. Hypertrophied ventricle; and 4. Dilated left ventricle. Cardiac and arterial parameters derived from [5]. The white bar gives the systolic pressure of the normal cardiovascular system. In concentric remodeling most of the pressure increase results from the change in the arterial system. When the ventricle is dilated in hypertension most of the pressure increase is caused by the heart. Adapted from [4], used by permission.*

contribute to a further increase in blood pressure.

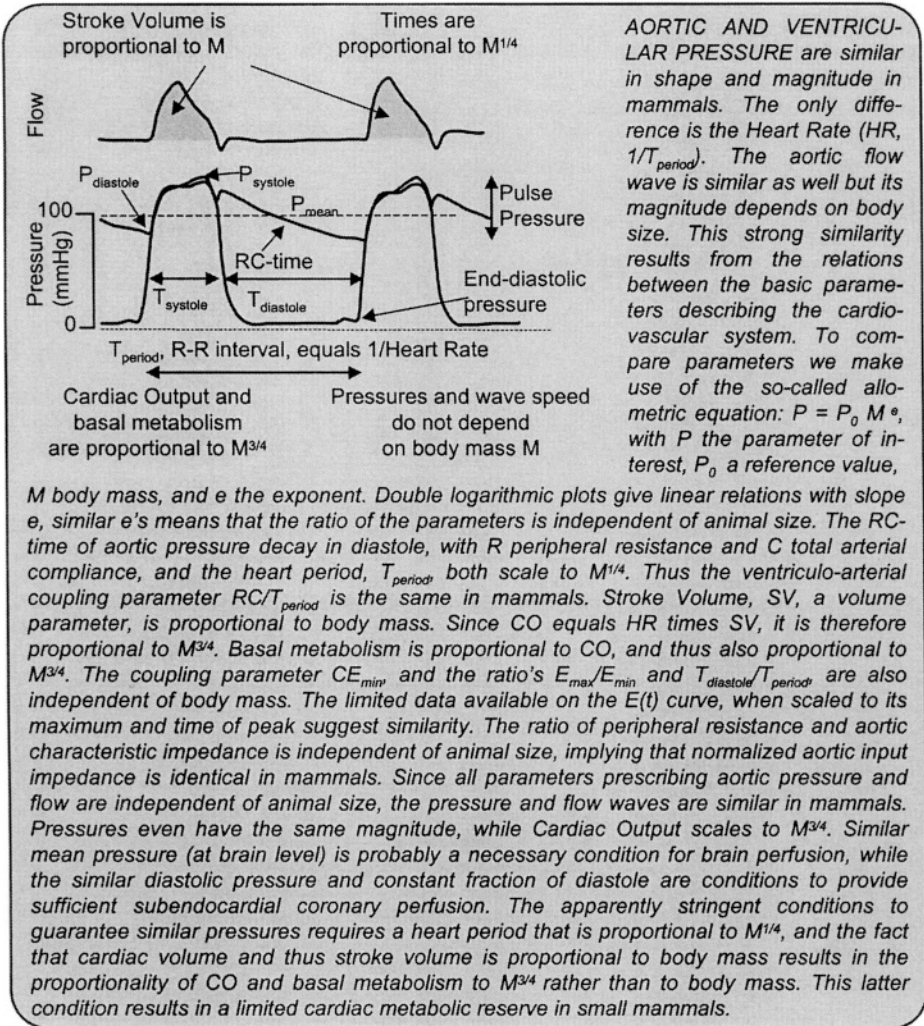
#### *Contribution of arterial system and heart in systolic hypertension*

Using the models as given in the figures in the box, the contributions of the heart and arterial system in four groups of hypertensive patients were calculated [4]. It may be seen that in concentric remodeling the increase in systolic blood pressure is mainly the result of the altered arterial system, while in eccentric hypertrophy the contribution to the increased systolic pressure is mainly the result of changed cardiac properties. This example therefore shows that both heart and arterial system need to be considered in hypertension research.

#### **References**

1. Elzinga G, Westerhof N. Pressure and flow generated by the left ventricle against different impedances. *Circ Res* 1973;32:178-186.
2. Randall OS, van den Bos GC, Westerhof N. Systemic compliance: does it play a role in the genesis of essential hypertension? *Cardiovasc Res* 1984; 18: 455-462.
3. Munson BR, Young DF, Okiishi TH. *Fundamentals of fluid mechanics*. 1994, New York, John Wiley & Sons.
4. Segers P, Stergiopoulos N, Westerhof N. Quantification of the contribution of cardiac and arterial remodeling to hypertension. *Hypertension* 2000;36:760-765.

5. Senzaki H, Chen C-H, Kass DA. Single-beat estimation of end-systolic pressure-volume relation in humans: a new method with the potential for noninvasive application. *Circulation* 1996;94:2497-2506.
6. Stergiopoulos N, Meister J-J, Westerhof N. Determinants of Stroke Volume and systolic and diastolic aortic pressure. *Am J Physiol* 1996;270:H2050-H2059.
7. Westerhof N, Elzinga G. Normalized input impedance and arterial decay time over heart period are independent of animal size. *Am J Physiol* 1991;261:R126-R133.



**Description**

Comparative physiology is based on the allometric equation:

$$PA = PA_0 \cdot M^e$$

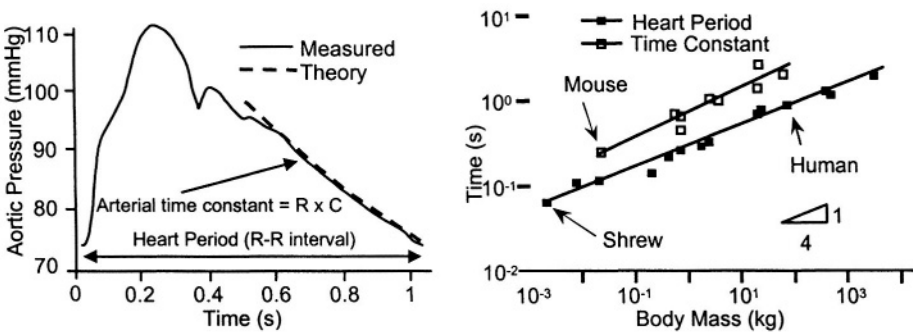
with  $PA$  the parameter of interest,  $PA_0$  a reference value,  $M$  body mass, and  $e$  the exponent. When the logarithm of both sides is taken the equation can be rewritten as:

$$\log PA = \log PA_0 + e \log M$$

This equation states that, when a parameter  $PA$  is plotted against body mass  $M$ , in a double logarithmic plot, a straight line with slope  $e$  is obtained. If two parameters have the same slope (same  $e$ ), the ratio of the parameters

does not depend on body mass, i.e., the ratio is independent of the size (mass) of the animal.

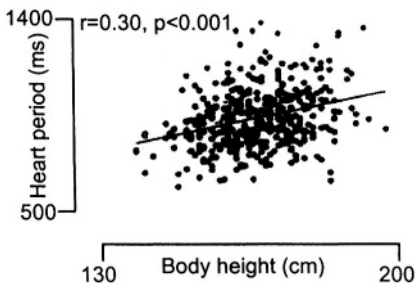
The coupling parameter  $RC/T$  (see Chapter 29) is an example of the study of comparative physiology, where it is shown that the characteristic time of the arterial system, RC-time, and the characteristic time of the heart, the heart period,  $T$ , have the same exponent implying that their ratio is independent of body mass [12]. The similar pulse pressure found in mammals can be understood on the basis of this mass-independence as follows. Total arterial compliance,  $C$ , is proportional to Stroke Volume divided by pulse pressure,  $PP$  so that  $C \propto SV/PP$ . Mean pressure is equal to Resistance,  $R$ , times Cardiac Output:  $P_{mean} = R \cdot CO$ . The Cardiac Output equals Heart Rate times Stroke Volume, and Heart Rate =  $1/T$ . Therefore  $P_{mean}/PP \propto RC\text{-time}/T$ . This implies that, with similar mean pressure, the pulse pressure, and therefore also the systolic and the diastolic pressures are the same in mammals. The



AORTIC PRESSURE (left) AND A LOG-LOG PLOT OF HEART PERIOD AND RC-TIME (right). The aortic pressure shows an exponential decay in diastole, characterized by the arterial parameter RC-time, i.e., peripheral resistance,  $R$ , times total arterial compliance,  $C$ . The heart period is a cardiac parameter. Both times show an increase with body mass with an exponent of  $1/4$ . This implies that the ratio of the two, the ventriculo-arterial coupling parameter  $RC/T_{period}$  is the same in mammals. Adapted from [12], used by permission.

ratio of Pulse Pressure and mean pressure,  $PP/P_{mean}$ , is called the fractional pulse pressure.

The finding that the heart period increases with body mass predicts, even in a single species that heart period increases also with body length. This was indeed shown to be the case in man.

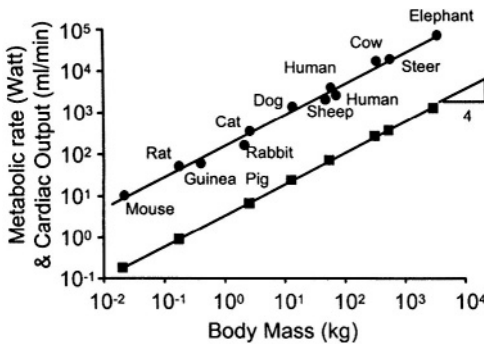


HEART PERIOD RELATES TO BODY HEIGHT in humans. Body height is a measure of body mass. Adapted from [10], used by permission.

In general, volumes are proportional to body mass, i.e.,  $M^{+1}$  and so are cardiac volume and Stroke Volume [5]. With  $CO = HR \cdot SV$ , it follows that  $CO$  is proportional to  $M^{3/4}$ . This is indeed what is found and is shown in the first figure on the next page.

Other comparative data are scarce but if we assume similar material properties, and with volumes proportional to body mass [1, 5], it follows that the slope of the diastolic and systolic pressure-volume relations, are proportional to  $M^{-1}$ , and also that

total arterial compliance,  $C$ , is proportional to body mass. Thus, the coupling



**CARDIAC OUTPUT AND BASAL METABOLISM** are proportional and increase with body mass to the power  $3/4$ . Data on metabolic rate from [8] and data on CO from [1], used by permission.

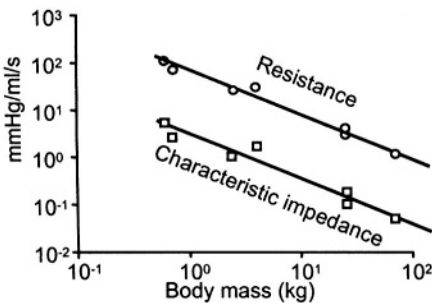
parameters  $CE_{min}$  and  $CE_{max}$ , are independent of body mass (see Chapter 29). The ratio of  $E_{max}$  and  $E_{min}$  equals systolic over diastolic pressure for isovolumic beats and this ratio is similar in mammals, thus  $E_{max}/E_{min}$  is size independent. In the data published on the  $E(t)$  curve, those of man and dog are not dissimilar in shape, when normalized with respect to time of peak and peak value [9]. Quantitative data on a whole range of mammals is not available yet.

(figure below left). This implies that this ratio is similar in mammals. Therefore the aortic input impedance is similar when scaled with respect to the characteristic impedance or peripheral resistance and plotted as a function of harmonic, i.e., as multiples of the heart rate (Appendix 31). When a three-element Windkessel is assumed as acceptable model of the systemic arterial tree (Chapter 24), the input impedance can be written as:

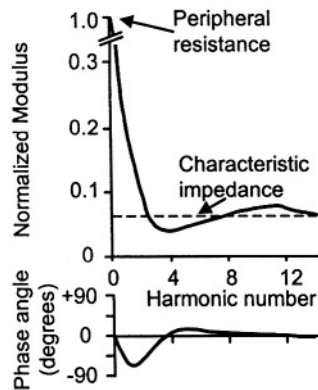
When we plot the characteristic impedance and peripheral resistance as a function of body mass we find parallel lines again

$$Z_{in} / Z_c = \frac{1 + R/Z_c + 2 \cdot \omega \cdot n \cdot RC / T}{1 + 2j \cdot \omega \cdot n \cdot RC / T}$$

where  $n$  the harmonic number. With  $RC/T$  and  $R/Z_c$  independent of animal size, the normalized arterial input impedance is the same as shown in the figure below right [12]. Thus, the aortic pressure and flow wave shapes are related in a similar way in all mammals. This in turn implies that with similar pressure wave shapes, the flow waves are similar too.

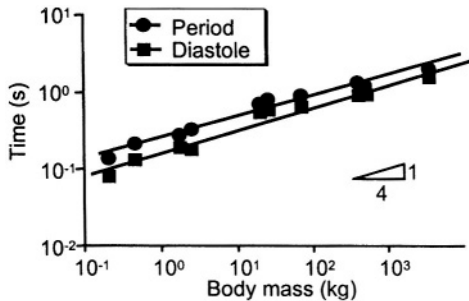


**THE RATIO OF PERIPHERAL RESISTANCE** and aortic characteristic impedance is independent of animal size. Adapted from [12], used by permission.



**NORMALIZED INPUT IMPEDANCE** is similar in mammals. This implies that the harmonics of pressure and flow are treated similarly and thus their wave shapes are the same.

The non-dimensional ventriculo-arterial coupling parameters,  $CE_{max}$  and  $RC/T$  (Decay time of diastolic aortic pressure over heart period, Chapter 29) are independent of animal size. Together with the above the final result is that in all mammals pressure waves are similar in shape and magnitude and flow waves are also similar in shape, but the magnitude relates to body mass to the power  $3/4$ . It was also shown that the size of the heart results in optimal external power production [4].



HEART PERIOD AND DURATION OF DIASTOLE are plotted as a function of body mass. The parallel lines imply that diastole is a fixed fraction of the heart period. Adapted from [12], used by permission

It has also been suggested that shear stress would be similar in mammals too (Chapters 27 and 28). Shear stress is proportional to  $Q/r^3$ , and since  $CO$  scales to  $M^{3/4}$ , and  $r$  to  $M^{1/3}$ , shear stress scales to  $M^{3/4}/M = M^{-1/4}$ . Shear stress is probably not very tightly controlled (Chapters 27 & 28) and certainly is not the same in different vessels.

The allometric relations of heart period and duration of diastole are given here. The relations are again parallel, which means that in mammals diastole is a constant fraction of the heart period. Subendocardial perfusion mainly takes place in diastole, and thus depends on diastolic pressure duration of diastole. With these two quantities similar, the coronary fractional perfusion time (Chapter 18) is similar in mammals as well, so that coronary perfusion conditions are also similar.

### Basal whole body and cardiac metabolism

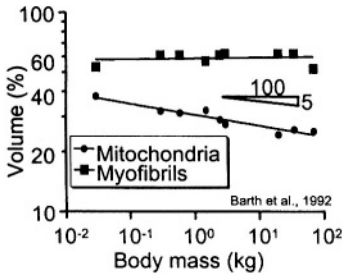
Basal whole body metabolism and Cardiac Output are both proportional to body mass as  $M^{3/4}$  (figure on the previous page). Why  $CO$  is proportional to  $M^{3/4}$  was explained above. Apparently metabolism is related to  $CO$ , but other suggestions have been given [11]. Basal metabolism and  $CO$  may be closely related because oxygen carrying capacity of the blood is similar in mammals.

In summary, the rigorous control of blood pressure appears to demand that heart rate is coupled to the  $RC$ -time of the arterial system. This, in combination with a  $SV$  that is proportional to body mass, results in the  $3/4$  power law of  $CO$  and whole body metabolism.

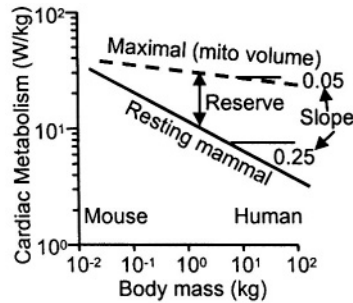
### Cardiac metabolism

It is well known that cardiac metabolism per gram heart tissue is higher in small than in large animals. The oxygen consumption is proportional to the Pressure Volume Area,  $PVA$ , times Heart Rate,  $HR$ , or approximately  $[P_{systolic} \cdot SV \cdot HR + \frac{1}{2} P_{systolic} \cdot (V_{end-systolic} - V_d)] \cdot HR$  (see Chapter 15), and, since volumes scale to  $M^1$ ,  $VO_2$  relates to body mass to the power  $3/4$  as well. This  $3/4$  law of total heart metabolism implies that when cardiac metabolism is expressed per gram tissue it decreases with increased body mass to the power  $1/4$ , i.e.,  $M^{-1/4}$ . Mitochondrial relative volume, as a measure of maximal energy

expenditure per unit mass, decreases with body mass as  $M^{-0.05}$  [2]. In other words, the difference between maximal metabolism and resting metabolism, i.e. the metabolic reserve, decreases in smaller mammals.



THE FRACTIONAL VOLUMES of myofibrils and mitochondria in cardiac muscle cells as a function of body mass. Mitochondrial volume is a measure of maximal energy production and use. Data from [2].



MAXIMAL AND RESTING energy expenditure per gram both decrease with animal size. Since the slopes are different the energy reserve for small mammals is small.

*Pulse wave velocity and reflections*

Experimental data show that pulse wave velocity is independent of animal size. This can be seen from basic vascular data where the Young modulus of elasticity,  $E$ , and wall thickness over radius,  $h/r$ , are species independent and, as a consequence wave speed (Moens-Korteweg equation),

$$c = \sqrt{\frac{h \cdot E}{2 \cdot r \cdot \rho}}$$

is independent of body size as well.

The return of the reflected waves at the heart equals traveled length over wave speed. Length of the arteries is proportional to  $M^{1/3}$ , so that the return time of reflections is also proportional to  $M^{1/3}$ . The heart period is proportional to  $M^{1/4}$ . This small difference in power makes reflections return in the about the same part of the cardiac cycle in most mammals.

**Physiological and clinical relevance**

Comparative physiology of the cardiovascular system shows that the heart and arterial system act to produce similar magnitude and wave shape of pressures and similar wave shapes of flow in mammals. This strongly suggests that pressure magnitude and wave shape are important. It has indeed been shown that high pressure, e.g., hypertension, is a strong indicator of cardiovascular pathology. Recent epidemiological data point to the strong relation between pulse pressure and cardiovascular morbidity and mortality [3,7]. The magnitude of pulse pressure, together with the about  $2.5 \cdot 10^9$  pulsations in a lifetime, may play a role in fatigue and fracture of the arterial wall. Martyn and Greenwald [6] argue that the synthesis of elastin is slow and that damage takes years to repair. The decrease in elastin may be the

reason that with age aortic diameter increases and the wall becomes stiffer, because vessel elasticity becomes gradually more determined by the collagen, which gradually replaces elastin.

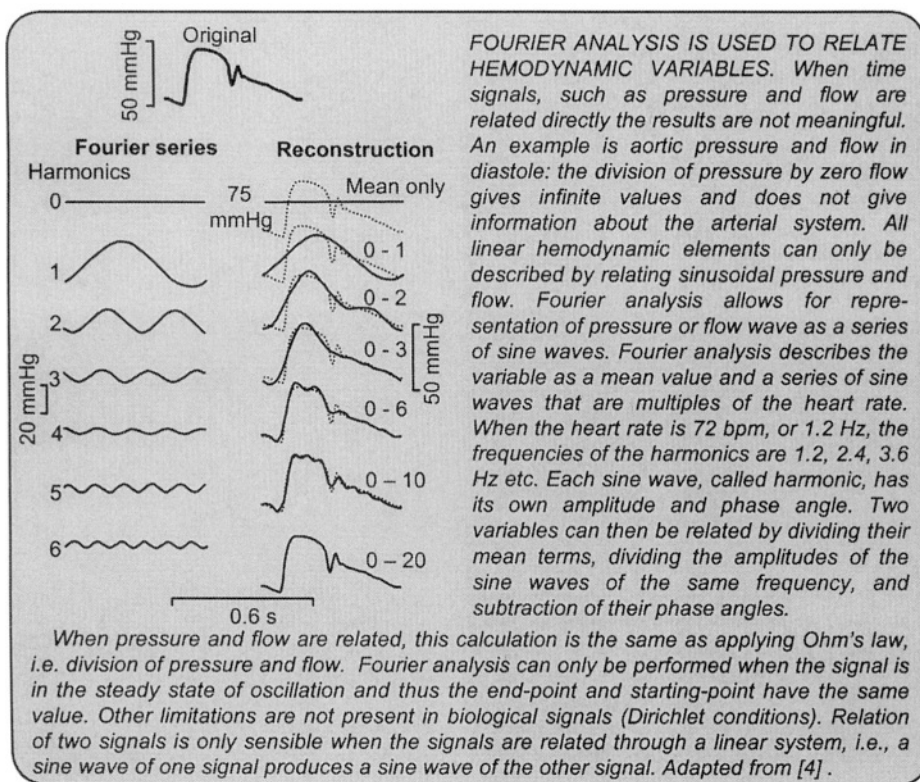
It has been argued that all mammals have the same number of heartbeats over their life span. Thus small animals with high heart rates live shorter than large animals. Vascular damage may be an argument. However, metabolism per gram decreases with increasing body mass. The lower metabolism per gram in larger mammals may imply a lower production of oxygen radicals and less cellular damage.

## References

1. Altman PL, Dittmer DE (eds). *Biological handbook*. 1971, Bethesda, Fed Am Soc Exptl Biol, pps 278, 320, 336-341.
2. Barth E, Stämmler G, Speiser B, Schaper J. Ultrastructural quantification of mitochondria and myofilaments in cardiac muscle from 10 different animal species including man. *J Mol Cell Cardiol* 1992;24:669-681.
3. Benetos A, Safar M, Rudnichi A, Smulyan H, Richard JL, Ducimetieere P, Guize L. Pulse pressure: a predictor of long-term cardiovascular mortality in a French male population. *Hypertension* 1997;30:1410-1415.
4. Elzinga G, Westerhof N. Matching between ventricle and arterial load. *Circ Res* 1991;68:1495-1500.
5. Holt JP, Rhode EA, Kines H. Ventricular volumes and body weight in mammals. *Am J Physiol* 1968;215:704-714
6. Martyn CN, Greenwald SE. Impaired synthesis of elastin in walls of aorta and large conduit arteries during early development as an initiating event in pathogenesis of systemic hypertension. *Lancet* 1997;3502:953-5.
7. Mitchell GF, Moye LA, Braunwald E, Rouleau JL, Bernstein V, Geltman EM, Flaker GC, Pfeffer MA. Sphygmomanometrically determined pulse pressure is a powerful independent predictor of recurrent events after myocardial infarction in patients with impaired left ventricular function. *Circulation* 1997;96:4254-60.
8. Schmidt-Nielsen K. *Scaling. Why is animal size so important?* 1984, London New York, Cambridge Univ Press, pp 57.
9. Senzaki H, Chen C-H, Kass DA. Single beat estimation of end-systolic pressure-volume relation in humans: a new method with the potential for noninvasive application. *Circulation* 1996;94:2497-2506.
10. Smulyan H, Marchais SJ, Pannier B, Guerin AP, Safar ME, London GM. Influence of body height on pulsatile hemodynamic data. *J Am Coll Cardiol* 1998;31:1103-1109.
11. West GB, Woodruff WH, Brown JH. Allometric scaling of metabolic rate from molecules and mitochondria to cells and mammals. *PNAS* 2002;99:2473-2478.
12. Westerhof N, Elzinga G. Normalized input impedance and arterial decay time over heart period are independent of animal size. *Am J Physiol* 1991;261:R126-R133.

# Part E Appendices

## Appendix 1 TIMES & SINES: FOURIER ANALYSIS



### Description

Fourier analysis breaks a periodic signal up in a series of sine waves. The sine waves of two hemodynamic variables (e.g., pressure and flow) can then be used to derive an input-output relation, such as an input impedance (Chapter 23) or transfer function (Chapter 26). The technique to perform Fourier analysis is now readily available and therefore easy to perform. It is not a curve fitting technique but a straightforward calculation. The analysis results in a mean term and series of sine waves. The mean term is often called the zeroth harmonic. The sine waves have frequencies that are multiples of the basic frequency, e.g., heart rate, and are called harmonics. The first harmonic equals the frequency of the heart rate, the second harmonic is twice the heart rate, etc.

In the left part of the figure in the box the individual harmonics are given each having an amplitude and phase angle. The phase angle is best seen from the starting point of the sine wave. We see that the amplitudes of the harmonics are decreasing in amplitude. On the right hand side the reconstruction is presented. It is simply the addition of the sine waves at the same moments in time. Using 10 harmonics the signal is almost completely reconstructed, and with 20 harmonics the signal is completely reconstructed. This means that aortic pressure is described by approximately 15 harmonics. It turns out that the smoother the signal the fewer harmonics are required to

describe it. Ventricular pressure can be described by about 10 harmonics. Thus, in general, the information in hemodynamic signals such as pressure, flow and diameter contains information up to 15 harmonics, i.e., 15 times the heart rate.

This knowledge is important with respect to measurement techniques. To measure a sine wave well at least two points are required (the Nyquist criterion [1]). Thus sampling should be done with at least twice the highest frequency, i.e. the highest harmonic, in the signal. In hemodynamics this means that the sampling rate should be at least twice as high as the frequency of the highest harmonic, thus 30 times the heart rate. If dealing with human hemodynamics, with a heart rate of 60 bpm, the rate is 1 cycle per second (1 Hz) and sampling should be done with a rate higher than 30 samples per second. If we measure in the rat with a rate of 420 bpm, or 7 Hz, sampling rate should be at least 210 samples per second. Along the same lines one can reason that equipment used in hemodynamics should be sufficiently fast so that 15 times the heart rate can be accurately measured.

In practice we use a large safety factor of about 3 or 4, and therefore a sampling rate of 100 Hz is certainly sufficient for the human at rest. In exercise the sampling rate should be increased by the same factor as the increase in heart rate.

### *Limitations*

The following limitations apply to the use of Fourier analysis [4].

1. Fourier analysis may only be performed periodic signals. In practice this means that the signal value at the start and end of the period to be analyzed should be the same. In other words only single heart beats or multiples of full beats, where start values and end values of the signals are equal may be analyzed.
2. Fourier analysis can always be performed on signals in the steady state of oscillation. However, the calculation of the relation of two signals only leads to useful results when the system is linear, which means that sine wave input leads to sine wave output. The system should also be time invariant. Despite the nonlinear relations between pressure and diameter and pressure and flow etc., in many situations nonlinearity is not so strong that large errors result. However, the scatter in modulus and phase of the input impedance has been suggested to result from nonlinearity of the arterial system [3].
3. The amplitudes of the higher harmonics decrease in amplitude and are therefore more subject to noise than the lower harmonics. Thus the high frequency information should be considered with care.
4. Fourier analysis gives data at multiples of the heart rate only. Thus the frequency resolution is limited. Pacing of the heart at different rates, including high heart rates, improves the resolution of frequency and also high frequency information.

It is also advisable to analyze a number of beats (~10) in the steady state to reduce noise [2]. This can be done by analysis per beat, and averaging the derived harmonics of these beats. It is, in principle, equally accurate to analyze a series of beats. When the heart rate is 75 bpm, i.e., 1.25 Hz, and a series of 10 beats is analyzed, harmonics are obtained at multiples of 0.125 Hz. However, only the harmonics 1.25 Hz, 2.50 Hz, etc. contain accurate information.

### Physiological and clinical relevance

Fourier analysis and the subsequent calculation of the amplitude ratio and phase angle difference per harmonic of two hemodynamic signals give information about a linear and time invariant system. An example is input impedance (Chapter 23). An important other example is the calculation of the pressure transfer function (Chapter 26). When radial and aortic pressure are measured, the Fourier analysis of these two signals and subsequent calculation of their amplitude and phase relation leads to the transfer function, which describes the arterial system in between these two sites. Once the transfer function is known, radial pressure can be used to derive aortic pressure as long as the arterial system does not change.

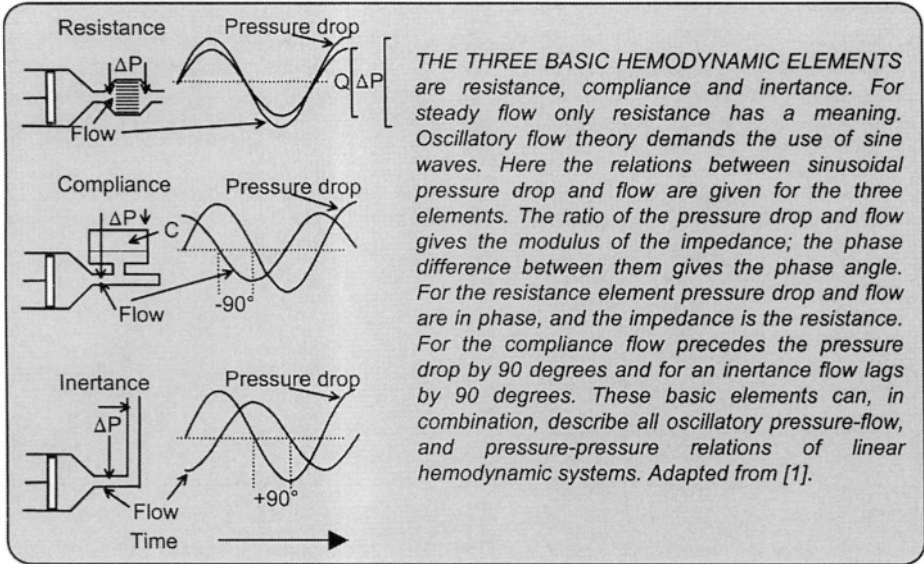
Nonlinearity of the system e.g., cardiac valves, the pressure-flow relation over a stenosis etc., does not allow calculations based on this linear approach. For instance, systemic vascular resistance and impedance can be calculated from aortic pressure minus venous pressure and aortic flow but not from ventricular pressure and flow.

The oscillatory flow theory is also based on sinusoidal relations between pressure drop over and flow through a segment of artery (Chapter 8).

### References

1. Hamming RW. *Digital filters*. 1977, Englewood Cliffs NJ, Prentice Hall.
2. Murgó JP, Westerhof N, Giolma JP, Altobelli SA. Aortic input impedance in normal man: relationship to pressure wave forms. *Circulation* 1980;62:105-116.
3. Stergiopoulos N, Meister J-J, Westerhof N. Scatter in the input impedance spectrum may result from the elastic nonlinearity of the arterial wall. *Am J Physiol* 1995;269:H1490-H1495.
4. Westerhof N, Sipkema P, Elzinga G, Murgó JP, Giolma JP. Arterial impedance. In: Hwang NHC, Gross DR, Patel DJ. *Quantitative cardiovascular studies*. 1979, Baltimore MD; University Park Press.

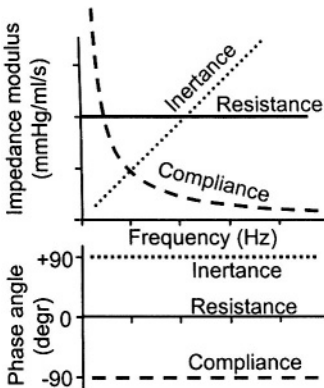
## Appendix 2 BASIC HEMODYNAMIC ELEMENTS



### Description

The impedance of the three basic hemodynamic elements is shown in the figure [1]. For the resistance, the pressure drop and flow are in phase and their amplitude ratio gives the value of the resistance. For the compliance, the sine wave of flow precedes the pressure drop, and they are 90 degrees out of phase, i.e., a quarter of the whole sine wave. The ratio of the amplitudes of the pressure drop and the flow decreases inversely with the frequency. Thus, for a flow with constant amplitude, the higher the frequency the lower the pressure is. This is formulated as follows: the modulus of the impedance,  $|Z(\omega)|$  equals  $1/\omega \cdot C$ , with  $C$  compliance and  $\omega$  the circular frequency,  $\omega = 2\pi \cdot f$ ,  $f$  being the frequency in Hz (cycles per second). Increasing frequency implies decreasing impedance modulus. The phase angle is  $-90$  degrees for all frequencies.

For the inertance the impedance modulus equals  $|Z(\omega)| = \omega \cdot L = 2\pi \cdot f \cdot L$ . Thus for a constant flow amplitude, the pressure amplitude increases with frequency. The phase angle is  $+90$  degrees for all frequencies.



*INPUT IMPEDANCE of the three basic hemodynamic elements as a function of frequency. The impedance modulus at zero Hz of inertia is negligible and of compliance is infinite.*

---

**Physiological and clinical relevance**

All linear and time invariant hemodynamic systems, for instance the entire systemic arterial tree, the pulmonary vascular system, or a pressure transfer function can be quantitatively described by a combination of these basic elements. Linear means that when the input (e.g., pressure) is a sine wave, the output (e.g., flow) should also be a sine wave.

*Limitations*

The arterial system is not linear. For instance, the pressure-volume relation of the arteries is not straight. Other aspects such as inlet length, curvature of vessels etc., result in nonlinear behavior. Nevertheless, in most practical aspects this non-linearity does not affect the results obtained by linear analyses much. Thus, systemic vascular resistance and aortic input impedance can be calculated and this information is meaningful. However, calculating the relation between mean and oscillatory ventricular pressure and aortic flow does not lead to useful results because of the strong nonlinearity of the aortic valves.

**References**

1. Westerhof N, Sipkema P, Elzinga G, Murgo JP, Giolma JP. Arterial impedance. *In: Hwang NHC, Gross DR, Patel DJ. Quantitative cardiovascular studies.* 1979, Baltimore MD; University Park Press.

# Appendix 3 VESSEL SEGMENT

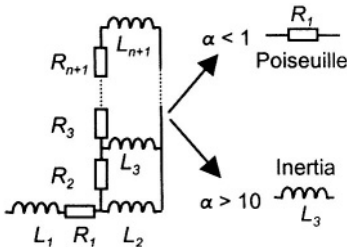
Hydraulic representation

Electrical representation

A SEGMENT OF BLOOD VESSEL is an important building block of arterial models. In principle, distributed models, single or two-tube models, and lumped models are based on these building blocks. The basic hemodynamic elements constituting the building block are inertia,  $L' = \rho/\pi r^2$ , resistance,  $R' = 8\eta/\pi r^4$ , and compliance,  $C' \approx 3\pi r^3/2Eh$ , the prime indicating that the values are given per unit of length. The inertia and resistance describe the relation between pressure drop ( $\Delta P$ ) and flow ( $Q$ ), and in combination they are called the longitudinal impedance,  $Z_l' = j\omega L' + R'$ . The compliance accounts for the change in diameter with transmural pressure ( $P_t$ ). The diameter change implies storage of blood and relates to the difference of flows into and out of the segment. The relation between the flow difference and transmural pressure is called transverse impedance,  $Z_t' = 1/j\omega C'$ . For large arteries resistance may be omitted, for very small vessels only resistance remains.

The basic elements also describe important arterial parameters: wave speed ( $c = \sqrt{Z_t'/L'}$ ) and characteristic impedance ( $Z_c = \sqrt{Z_l' Z_t'}$ ). For large (conduit) arteries, where the viscous effects can be neglected,  $c = 1/\sqrt{L' C'}$  and  $Z_c = \sqrt{L' / C'}$ . We see that a less compliant and/or smaller artery has a higher wave speed and characteristic impedance. The various expressions for wave speed can be derived from the above. Oscillatory flow theory gives a more accurate description of the longitudinal impedance. Accounting for the viscoelastic properties of the arterial wall gives a more accurate description of the transverse impedance.

## Description



*The longitudinal impedance*

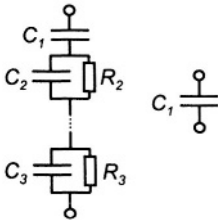
The relation between the pressure drop and flow of a uniform segment of blood vessel is given by Womersley's oscillatory flow theory and called longitudinal impedance [3]. The longitudinal impedance in electrical form is given in the figure on the next page [1]. For small arteries, i.e., for small values of Womersley's  $\alpha$ , the longitudinal impedance per unit length,  $Z_l'$ , equals  $8 \cdot \eta \cdot l / \pi r^4$ . It is thus an resistance described by Poiseuille's equation. For large values of  $\alpha$ , i.e. for large arteries, the longitudinal impedance per length reduces to an inductance only, and equals  $Z_l' = i \omega \cdot \rho / \pi r^2 = i \omega \cdot \rho / A$ .

THE LONGITUDINAL IMPEDANCE of a segment of artery in electrical terms. The ladder network results from oscillatory flow theory. For large arteries with large  $\alpha$  the inertial term is the only one of importance. Adapted from [1], used by permission.

*The transverse impedance*

The transmural pressure difference, i.e., the oscillatory pressure between lumen and external environment, is related to volume changes (see Chapter

**Viscoelastic Elastic**



THE TRANSVERSE IMPEDANCE of a segment of artery in electrical form. The dashpot-spring representation is shown in Chapter 10. The ladder network results from the complex elastic modulus. Adapted from [2], used by permission.

11). Volume changes can be related to flow, and therefore we can use the term transverse impedance. The transverse impedance for a viscoelastic wall material is shown in the figure on the next page.[2]. For large conduit arteries, where the wall is almost purely elastic, this can be simplified to a single compliance,  $C = \Delta V / \Delta P = (\Delta A / \Delta P) \cdot l$ . The compliance per unit length is then  $C' = \Delta A / \Delta P$ . The compliance element can be written in a different form using the Law of Laplace, to obtain stress from pressure, and accounting for cylindrical geometry to relate volume to radius. The expression for compliance then becomes  $C = 3\pi \cdot l \cdot r_i^2 \cdot (r_i + h)^2 / E \cdot h \cdot (2r_i + h)$ , or when  $h \ll r_i$ ,  $C \approx 3\pi \cdot r_i^3 \cdot l / 2E \cdot h$ . The transverse impedance per length is  $Z_t' = 1/i\omega \cdot C'$ . From the formulas given in the box we see that inertance is proportional to  $r_i^{-2}$ , and resistance to  $r_i^{-4}$ . This implies that resistance increases most strongly towards the periphery and this is why it is the overriding element there. Compliance decreases towards the periphery, with  $r_i^3$ , meaning that peripheral vessels contribute little to overall compliance.

In other words compliance is mainly located in the conduit arteries. We should remember that all three basic elements are determined not only by the material properties but also by the geometry.

*Wave speed and characteristic impedance*

Wave speed and characteristic impedance are two important blood vessel parameters characterizing its wave transmission and reflection properties. These two quantities can be derived from so-called wave transmission theory, in analogy to what happens in telegraph lines, or antenna cables, for the transmission of electromagnetic waves. We will here give a simpler approach in which we neglect the effect the viscous resistance thereby omitting the damping of waves while they travel. This approximation is permitted since wave travel and characteristic impedance are of interest only in the large conduit arteries, where the resistance effects are small.

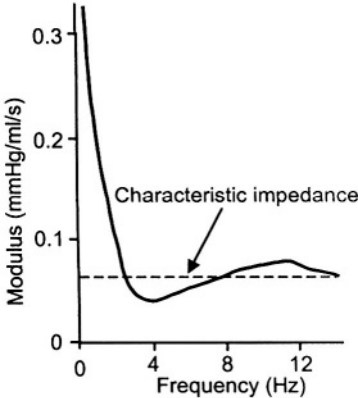
Wave speed is the velocity with which a disturbance travels through a blood vessel. It can be pressure, flow or wall movement. The wave speed  $c = \sqrt{Z_t' / Z_t} = 1 / L' C'$ . Rewriting this gives  $c = \sqrt{A \cdot \Delta P / \Delta A \cdot \rho} = \sqrt{V \Delta P / \Delta V \cdot \rho}$ . This formula of the wave speed was derived by Frank (1920), and later by Bramwell and Hill (1922). The wave speed according to Newton and Young is  $c = \sqrt{K / \rho}$  with  $K = A \Delta P / \Delta A = V \Delta P / \Delta V$ .

Using  $A = \pi r^2$  and thus  $\Delta A = 2\pi r \cdot \Delta r$ , we arrive at  $c = \sqrt{r \cdot \Delta P / 2 \Delta r \cdot \rho}$ . This form is useful in the estimation of wave speed from changes in radius and pressure. Inserting  $C' \approx 3\pi \cdot r_i^3 / 2E \cdot h$  and  $L' = \rho / \pi \cdot r^2$  leads to  $c = \sqrt{2E \cdot h / 3r \cdot \rho}$ . However, using  $\Delta P / \Delta r = h / r \cdot (\Delta \sigma / \Delta r)$  gives  $c = \sqrt{E \cdot h / 2r \cdot \rho}$ . The difference results from the way the formula is derived, and equals the factor 1 - Poisson ratio<sup>2</sup>, with the Poisson ratio being 0.5 for incompressible wall material, this equals 3/4, and 2/3 times 3/4 equals 1/2. The difference in the square root of 2/3 and 1/2 is about 15%.

The choice of formula depends on the information desired. If local compliance is to be derived, the Frank or Bramwell-Hill equation is

preferred. If the material constant is to be obtained the Moens-Korteweg equation is to be used.

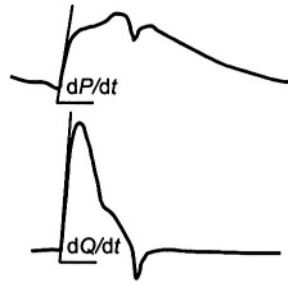
When the heart ejects it has to accelerate the blood into a compliant aorta. Thus what the heart encounters first during ejection is the combination of the effects of compliance and inertance. Inertance increases the load but



The characteristic impedance can be estimated from the input impedance modulus at high frequencies:  
 $Z_c = \text{averaged } |Z_{in}|$  for harmonics 4 - 10

compliance makes it easier to eject. The combined effect is given by the characteristic impedance  $Z_c = \sqrt{Z_i' \cdot Z_i'} = \sqrt{L'/C'}$ . The  $Z_c$  is called the characteristic impedance because it is characteristic for the vessel and it impedes the flow. Using the equations given above for the thin walled vessel we get:  $Z_c = \sqrt{(\rho/A)/(\Delta A/\Delta P)} = \sqrt{\Delta P/A\Delta A}$ . Since pressure and diameter are in phase the characteristic impedance of large vessels is a real, frequency independent parameter. If we take the proximal aorta as an example, the ventricle encounters, during the initial part of ejection, an impedance to flow that is the characteristic impedance of the proximal aorta. If the heart were loaded with the peripheral resistance directly the load would be much higher, because the characteristic impedance of the aorta is about 7% of

systemic peripheral resistance. If the aorta were infinitely long or if no reflections would return to the heart (Chapter 21), the characteristic impedance would be the load on the heart and the pressure and flow waves would have the same shape. Thus reflections cause the differences between the wave shape of pressure and flow. It also holds that early in ejection when no reflections are returning yet from the periphery, the pressure and flow are related through the characteristic impedance. This allows calculation of characteristic impedance from the ratio of the slopes of (aortic) pressure and flow (Chapter 22).



CHARACTERISTIC IMPEDANCE can be estimated from the initial phase of ejection, where reflections are minimal:  
 $Z_c = dP/dt/dQ/dt$ .

Since, for high frequencies, corresponding to short time scales, the arterial tree approaches a reflectionless system, the input impedance at high frequencies is close to the characteristic impedance of the vessel where the impedance is determined (Chapter 23). This allows for an estimation of characteristic impedance from the modulus of the input impedance at high frequencies (figure on the right). In practice the averaged impedance modulus between the fourth to tenth harmonic is used.

It can be seen that  $c/Z_c = A/\rho$ , and with  $\rho \sim 1$  in the cgs system, it holds that  $c/Z_c = A$ . Thus, if the input impedance is determined from velocity and pressure, characteristic impedance equals wave speed.

### Physiological and clinical relevance

From the above we see that with smaller radius, as found towards the periphery, the importance of resistance becomes greater than inertance and compliance and in the very small arterioles only the resistance remains, 'Resistance Vessels'. In large conduit blood vessels, as the human aorta, the resistance term becomes negligible and inertance and compliance accurately describe a segment of large, conduit, artery.

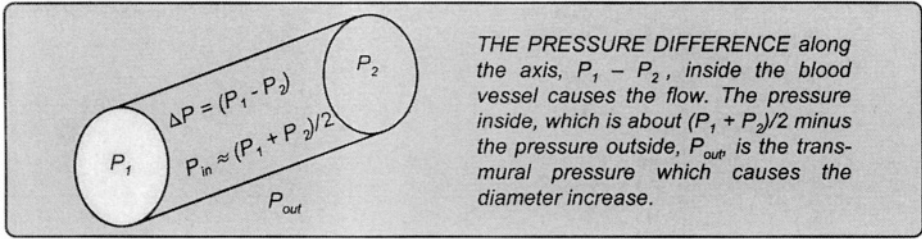
For large vessels where the wave speed is usually studied (aorta, carotid artery, and large leg and arm arteries) the resistive term is negligible so that damping of the waves is not taken into account. In these arteries there is a direct relation between the compliance and inertance with wave speed and characteristic impedance. When smaller vessels are studied the situation gets much more complex, the wave is not only transmitted but also damped.

Wave transmission is easily studied noninvasively (Chapter 20) and can give information about vessel compliance without the need to determine pressure. A decrease in aortic compliance with age by a factor of 3 increases the pulse wave velocity by about 70% ( $\sqrt{3}$ ), assuming constant radius. Decreased compliance also results in increased characteristic impedance. Both the decrease in compliance, and the increase in characteristic impedance lead to a higher pulse pressure.

### References

1. Jager GN, Westerhof N, Noordergraaf A. Oscillatory flow impedance in electrical analog of arterial system. *Circ Res* 1965;16:121-133.
2. Westerhof N, Noordergraaf A. Arterial viscoelasticity. A generalized model. *J Biomech* 1970;3:357-379.
3. Womersley JR. *The mathematical analysis of the arterial circulation in a state of oscillatory motion*. 1957, Wright Air Dev. Center, Tech Report WADC-TR-56-614.

## Appendix 4 BASIC ASPECTS



### Description

#### *Pressure and flow*

Pressure is the force applied per unit area. In hemodynamics we always think of pressure in terms of a pressure difference. The pressure difference along the axis, or pressure gradient, is the pressure that causes the flow of blood. The pressure difference between the inside and outside of a vessel or the heart, which is often called transmural pressure, causes the wall distension.

Flow ( $Q$ ) is given in ml/s or in liters/minute (Cardiac Output). Often the terms *volume flow* or *flow rate* are used and they are here considered synonymous to the term flow. The velocity, or flow velocity of blood,  $v$ , is given in cm/s. The volume flow, and the flow velocity averaged over the cross-sectional area of a vessel are related through the cross-sectional area,  $A$ ,  $v \cdot A = Q$ .

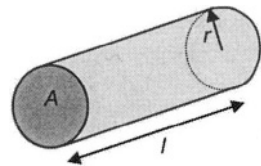
Pressure and flow result from the properties of the heart as a pump and the characteristics of the arterial system. However, the so generated pressure and flow, can be used to obtain the properties of the arterial system and the heart. For instance, aortic minus venous pressure divided by aortic flow gives total peripheral resistance. For other applications see Chapters 14 and 23.

#### *Pulsatile and oscillatory pressure and flow*

Pressure and flow vary during the cardiac cycle and are therefore called pulsatile pressure and flow. When pressure and flow are subjected to Fourier analysis and written as a series of sine waves (Appendix 1) we call them oscillatory pressure and flow. The zero term equals the mean value and the harmonics are the oscillatory terms. Womersley's oscillatory flow theory pertains to sinusoidal pressure-flow relations.

#### *Area*

In the figure the two areas of a blood vessel are shown. The area  $A = \pi r^2$ , the so-called cross-sectional area, is the area where the pressure acts to cause flow. The law of Poiseuille connects the pressure gradient to flow via this area to the second power, namely to  $r^4$ . The cross-sectional area of the human aorta is about  $6 \text{ cm}^2$  and of an arteriole it is about  $30 \text{ } \mu\text{m}^2$ . The total cross-sectional area of all capillaries



TWO AREAS are of importance: The cross-sectional area,  $A = \pi r^2$ , where the pressure acts to push blood forward, and the lateral area, which equals  $2\pi r l$ , and is used for exchange.

together is about  $5000 \text{ cm}^2$  or  $0.5 \text{ m}^2$ .

The lateral area or exchange area is the area involved in the exchange of oxygen, substrates and metabolites between tissue and blood. This area is calculated as:  $2\pi r \cdot l$ , with  $l$  length. The total exchange area of all capillaries together is about  $6000 \text{ m}^2$ .

#### *Wave speed differs from flow velocity*

Blood flow velocity is the speed with which the molecules and cells in the blood move from heart to periphery on the arterial side and back ('venous return') on the venous side. The, mean, velocity of blood in the aorta is about  $15 \text{ cm/s}$ , maximum velocity of blood in systole in the aorta is about  $100 \text{ cm/s}$ , and in the capillaries the average velocity is about  $0.5 \text{ mm/s}$ .

Wave speed or wave velocity is the velocity with which the pressure wave, the diameter variation and the flow wave travel. The wave speed pertains to pulsatile phenomena, and depends on vessel size and vessel elasticity (Chapter 20). The values of wave speed are between  $4$  and  $10 \text{ m/s}$ , thus much higher than the blood flow velocity.

#### *Volume, Flow and Circulation Time*

Volumes of compartments, flow and circulation time can be determined using an identifiable, nontoxic indicator that does not leave the compartment under study. Examples of indicators are dyes, radioactive tracers, or cold saline (thermodilution technique). For the last indicator a correction for disappearance from the circulation is made.

Blood volume can be determined by an intravenous injection of an amount,  $m_d$ , of a dye. The measurement of the concentration of the marker,  $[C]$ , in a blood sample, after complete mixing, allows for the calculation of the blood volume,  $V$ . When the concentration in the blood is  $[C] = m_d/V$  it follows that  $V = m_d/[C]$ . The injection may be performed in any blood vessel and the sample may be taken from any vessel as well.

Blood flow can be determined from a rapid injection of an indicator, amount  $m_d$ , and measurement of the concentration-time curve of the indicator in the blood. This is called the indicator dilution technique to determine mean flow. The flow is calculated as  $m_d/\text{area}$  under the time-concentration curve. In the indicator dilution technique, flow is determined at the location of injection, while the location of detection of the concentration-time curve is free. For instance, injection of a dye in the left atrium, guarantees good mixing, and allows for the estimation of Cardiac Output. The measurement of the concentration-time curve may take place in any artery and is thus rather free to choose.

In the indicator dilution technique cold saline is often used, and the method is then called the thermodilution technique. The most frequently used method is by flow guided catheter, injection of cold saline in the right atrium or right ventricle and measurement of the temperature in the pulmonary artery. The commercially available apparatuses correct for heat loss.

Circulation time is obtained by rapidly injecting an indicator at one location,  $x_1$ , and measurement of the arrival time at another location,  $x_2$ . Circulation time alone is of limited use but in combination with flow it allows estimation of the vascular volume between the two points. The volume of vascular bed between  $x_1$  and  $x_2$  equals the circulation time between

$x_1$  and  $x_2$  times volume flow. The circulation time of the entire circulation is about 1 minute.

*The Navier-Stokes equations*

The Navier-Stokes equations form the basis of all fluid dynamics, including hemodynamics, and can be found in textbooks on fluid mechanics (Appendix 5). They are the equations of motion of the fluid due to the forces acting on it such as pressure and gravity, and the equations include the effect of fluid density and viscosity. It is a group of three sub-equations, each for one of the three spatial dimensions.

The exact mathematical solution of these general equations is not possible because of their nonlinear character, so that large computers are required to solve them for each situation. The software to solve the equations is available. One of the terms representing this method is Computational Flow Dynamics.

Under simplifying assumptions the Navier-Stokes equations can be solved. Poiseuille's law, Pulsatile Flow Theory and Bernoulli's equation, etc., are examples of a straightforward derivation.

## Appendix 5 BOOKS FOR REFERENCE

- Bevan JA, Kaley G, Rubanyi GM. *Flow-dependent regulation of vascular function*. 1995, New York, Oxford University Press.
- Braunwald E (Ed). *Heart Disease*, 2001, Philadelphia & Sydney, WB Saunders, sixth edn.
- Burton AC. *Physiology and Biophysics of the Circulation*. 1972, Chicago, Year Book Medical Publ., 2nd edn.
- Caro CG, Pedley TJ, Schroter RC, Seed WA. *The mechanics of the circulation*. 1978, Oxford & New York, Oxford Univ Press.
- Chien KR (Ed). *Molecular basis of cardiovascular disease*. Philadelphia & London, Saunders, 1999.
- Cowen SC, Humphrey JD. *Cardiovascular soft tissue mechanics*. 2002, Dordrecht & Boston, Kluwer Acad Publ.
- Crawford MH, DiMarco JP, Paulus WJ. *Cardiology*. 2004, Edinburgh & London, Mosby.
- Drzewiecki GM, Li J. K-J. *Analysis and assessment of cardiovascular function*. 1999, New York & Heidelberg, Springer Verlag.
- Fozzard HA, Haber E, Jennings RB, Katz AM, Morgan HE. *The Heart and Cardiovascular System: Scientific Foundations*. 1991, New York; Raven Press, 2<sup>nd</sup> edn.
- Fung, YC. Biomechanics. *Mechanical Properties of Living Tissues*. 1981, New York & Heidelberg, Springer-Verlag.
- Fung, YC. Biodynamics. *Circulation*. 1984, New York & Heidelberg, Springer-Verlag.
- Fung, YC. *Biomechanics*. 1990, New York & Heidelberg, Springer-Verlag.
- Fung, YC, Perrone N, Anliker M. *Biomechanics*. 1972, Englewood Cliffs, Prentice-Hall.
- Glantz SA. *Mathematics for biomedical applications*. 1979, Berkeley, Univ California Press.
- Guyton AC, Hall JE. *Textbook of medical physiology*, 2000, Philadelphia & Sydney, WB Saunders, tenth edn.
- Hwang NHC, Normann NA. *Cardiovascular flow dynamics and measurements*. 1977, Baltimore MD; University Park Press.
- Hwang NHC, Gross DR, Patel DJ. *Quantitative cardiovascular studies*. 1979, Baltimore MD; University Park Press.
- Jaffrin MY, Caro CG. *Biological Flows*. 1995, New York, Plenum Press.
- Milnor WR. *Hemodynamics*. 1989, Baltimore & London; Williams & Wilkins, 2<sup>nd</sup> edn.
- Munson BR, Young DF, Okiishi TH. *Fundamentals of fluid mechanics*. 1994, New York, John Wiley & Sons, 2<sup>nd</sup> edn.
- Nichols WW, O'Rourke MF. *McDonald's blood flow in arteries*. 1998, London, Edward Arnold, 4<sup>th</sup> edn.
- Noble MIM. *The cardiac cycle*. 1979, Oxford & London, Blackwell Scientific Publications.

- Noordergraaf A. *Hemodynamics*. 1969, In Bio-engineering, H.P. Schwan Ed. New York, McGraw-Hill.
- O'Rourke MF. *Arterial function in health and disease*. 1982, Edinburgh & London, Churchill Livingstone.
- O'Rourke MF, Kelly RP, Avolio AP. *The arterial pulse*. 1992, Philadelphia PA, Lea & Febiger.
- Ottesen JT, Olufsen MS, Larsen JK. *Applied mathematical models in human physiology*. 2004, Philadelphia PA, Society Industrial and Applied Mathematics (SIAM).
- Sagawa K, Maughan L, Suga H, Sunagawa K. *Cardiac contraction and the pressure-volume relationship*. 1988, New York & Oxford, Oxford University press.
- Schmidt-Nielsen L. *Scaling*. 1984, New York, Cambridge Univ Press.
- Spaan JAE. *Coronary blood flow*. 1991, Dordrecht & Boston. Kluwer Acad Publishers.
- Strackee J, Westerhof N. *The physics of heart and circulation*. 1992, Bristol & Philadelphia, Inst of Physics Publishing.
- Talbot SA, Gessner U. *Systems physiology*. 1973, New York & London, John Wiley.
- Weibel ER. *Symmorphosis*. 2000, Cambridge, Harvard Univ Press; 2000
- Westerhof N, Gross DR. *Vascular dynamics*. 1989, New York & London, Plenum Press.
- Yin FCP. *Ventricular/vascular coupling*. 1986, New York & Heidelberg, Springer Verlag.

## Appendix 6 SYMBOLS

$a$	acceleration ( $\text{m/s}^2$ )
$A$	Area ( $\text{cm}^2$ )
$A^*$	Amplitude
AI	Augmentation Index (dimensionless)
$b$	constant
bpm	Heart Rate (beats per minute)
$c$	Pulse Wave Velocity or wave speed ( $\text{m/s}$ )
$c_{ff}$	Foot-to-foot wave velocity ( $\text{m/s}$ )
$c_{app}$	apparent wave velocity
$C$	Compliance $\Delta V/\Delta P$ ( $\text{ml/mmHg}$ )
$C_A$	Area Compliance ( $\text{cm}^2/\text{mmHg}$ )
$C_D$	Diameter Compliance ( $\text{cm/mmHg}$ )
CO	Cardiac Output ( $1/\text{min}$ )
$d$	derivative
$\partial$	partial derivative
$d, D$	Diameter ( $\text{cm}$ )
$D$	Distensibility ( $\Delta V/V\Delta P$ , $1/\text{Bulk Modulus}$ )
$E$	Elastance ( $\text{mmHg/ml}$ )
$E_{es}$	End-Systolic Elastance or Maximal Elastance ( $\text{mmHg/ml}$ )
$E_{inc}$	Incremental modulus of elasticity ( $\text{mmHg/ml}$ )
$E_m$	Murray energy term
$E_{max}$	Maximal or End-Systolic Elastance, slope of the ESPVR ( $\text{mmHg/ml}$ )
$E_{min}$	Diastolic Elastance ( $\text{mmHg/ml}$ )
$E_p$	Peterson modulus ( $r_0\Delta P/\Delta r_0$ , $\text{mmHg}$ )
EF	Ejection Fraction (%)
ESPVR	End-Systolic Pressure-Volume Relation
$E(t)$	Time Varying Elastance
$f$	Frequency ( $\text{Hz}$ , $1/\text{s}$ )
$F$	Force ( $\text{N}$ )
FFR	Fractional Flow Reserve
FMD	Flow mediated Dilation
$g$	gravity ( $\text{m/s}^2$ )
$g_f$	geometry factor
$G$	Gain (dimensionless)
$G$	Conductance ( $1/R$ , $\text{ml/mmHg s}$ )
$h$	(wall) thickness
HR	Heart Rate (beats per minute, bpm)
Ht	Hematocrit
$i$	$\sqrt{-1}$
$J_0, J_1$	Bessel functions, order 0, 1
$l$	length ( $\text{cm}$ )
$L$	Inertia ( $\text{mmHg/ml/s}^2$ )
$l_{inlet}$	inlet length ( $\text{cm}$ )
$m$	mass ( $\text{kg}$ )
$m_d$	amount of substance, e.g., dye ( $\text{g}$ or $\text{M}$ )
$M$	Body mass ( $\text{kg}$ )
$P$	Pressure ( $\text{mmHg}$ , $\text{kPa}$ )
$P_{es}$	End-Systolic Pressure ( $\text{mmHg}$ , $\text{kPa}$ )
$P^f$	Forward or incident Pressure wave
$P^m$	Measured Pressure Wave
$P^b$	Backward or reflected Pressure wave ( $\text{mmHg}$ , $\text{kPa}$ )
$P_s, P_d$	Systolic and Diastolic Blood Pressure ( $\text{mmHg}$ , $\text{kPa}$ )

$P_v$	Venous filling Pressure (mmHg, kPa)
$P_{mean}$	Mean Blood Pressure (mmHg, kPa)
$P_{O_2}$	Partial oxygen Pressure (mmHg)
$PP$	pulse pressure ( $P_s - P_d$ , mmHg, kPa)
PVA	Pressure Volume Area (mmHg ml)
$Q$	(Volume) Flow ml/s or l/min
$Q^f$	Forward Flow wave
$Q^b$	Backward Flow wave
$r$	radius
$r_i, r_o$	internal and external radius
$R$	Resistance (mmHg/ml/s)
$R_c$	Characteristic Resistance
Re	Reynolds number ( $2\rho \cdot v \cdot r/\eta$ , dimensionless)
RPP	Rate Pressure Product (mmHg s)
SV	Stroke Volume (ml)
$t$	time (s)
T	Transferfunction
$T$	Heart Period (s), Transfer function
TTI	Tension Time Index (mmHg s)
$T_{su}$	surface tension (N/m)
$v$	velocity (cm/s)
V	Volume (ml)
$V_d$	Intercept Volume (ml)
$V_{ed}$	End-Diastolic Volume (ml)
$V_{es}$	End-Systolic Volume (ml)
$V_{O_2}$	Oxygen Consumption (per beat)
W	Work, Energy (Joule)
WSS	Wall Shear Stress (kPa)
$x$	Location
$z$	Height difference
Z	(input) impedance (modulus in mmHg/ml/s; phase in degrees)
$Z_c$	characteristic impedance (modulus in mmHg/ml/s; phase in degrees)
ZSS	Zero Stress State
$\alpha$	Womersley's parameter ( $\alpha^2 = r^2\omega\rho/\eta$ , dimensionless)
$\epsilon$	strain $\Delta l/l$ (dimensionless)
$\epsilon_t$	tranverse strain (dimensionless)
$\phi$	phase angle (degrees or radians; $\pi$ radians =180 degrees)
$\gamma$	shear rate (1/s)
$\eta$	(absolute or dynamic) viscosity (cP or Pa.s)
$\lambda$	wave length (cm)
$\pi$	3.1415...
$\rho$	(blood) density ( $g/cm^3$ )
$\sigma$	stress and hoop stress ( $Pa = N/m^2$ )
$\tau$	shear stress (Pa) and decay time (s)
$\omega$	circular frequency ( $2\pi f$ )
$\Delta$	difference, 'gradient'
$\Gamma$	reflection coefficient (dimensionless)
$\theta$	angle (degrees)

## Appendix 7 UNITS AND CONVERSION FACTORS

	SI-system (kg m s)	cgs-system (g cm s)	medical units
Area Compliance, $C_A$	$1 \text{ m}^2/\text{Pa} = 1 \text{ m}^4/\text{N}$	$10^4 \text{ cm}^4/\text{dyn}$	$1.33 \cdot 10^6 \text{ cm}^2/\text{mmHg}$
Compliance, $C$	$1 \text{ m}^3/\text{Pa} = 1 \text{ m}^5/\text{N}$	$10^5 \text{ cm}^5/\text{dyn}$	$1.33 \cdot 10^8 \text{ ml}/\text{mmHg}$
Diameter Compl., $C_D$	$1 \text{ m}^4/\text{Pa} = 1 \text{ m}^3/\text{N}$	$10^3 \text{ cm}^4/\text{dyn}$	$1.33 \cdot 10^4 \text{ cm}/\text{mmHg}$
Density, $\rho$	$1 \text{ kg}/\text{m}^3$	$10^{-3} \text{ g}/\text{cm}^3$	
Elastance, $E$	$1 \text{ Pa}/\text{m}^3 = 1 \text{ N}/\text{m}^5$	$10^{-5} \text{ dyn}/\text{cm}^5$	$7.5 \cdot 10^{-9} \text{ mmHg}/\text{ml}$
Energy-work, $W$	<b>1 Joule</b> = $1 \text{ N} \cdot \text{m} = \text{Pa} \cdot \text{m}^3$	$10^7 \text{ erg (dyn} \cdot \text{cm)}$	$7.5 \text{ mmHg} \cdot \text{ml} = 0.239 \text{ cal}^*$
Flow, $Q$	$1 \text{ m}^3/\text{s}$	$10^6 \text{ cm}^3/\text{s} = 10^6 \text{ ml}/\text{s}$	( $1 \text{ l}/\text{min} = 16.66 \text{ ml}/\text{s}$ )
$dQ/dt$	$1 \text{ m}^3/\text{s}^2$	$10^6 \text{ ml}/\text{s}^2$	
Force, $F$	$1 \text{ N} = 1 \text{ kg} \cdot \text{m}/\text{s}^2$	$10^5 \text{ dyn} = 1 \text{ g} \cdot \text{cm}/\text{s}^2 \sim 10^2 \text{ g (wt)}$	
Frequency, $f$	$\text{Hz} = \text{s}^{-1}$	$\text{Hz} = \text{s}^{-1}$	$\text{min}^{-1}$ (60 bpm = 1 Hz)
Frequency circular, $\omega$	$2\pi f \text{ Hz}$		
Inertance, $L$	$1 \text{ Pa} \cdot \text{s}^2/\text{m}^3 = \text{N} \cdot \text{s}^2/\text{m}^5$	$10^{-5} \text{ dyn} \cdot \text{s}^2/\text{cm}^5$	$7.5 \cdot 10^{-9} \text{ mmHg} \cdot \text{s}^2/\text{ml}$ with 360 degrees = $2\pi$ radians
Phase angle, degrees			
Power, $W$	$1 \text{ Watt} = 1 \text{ J}/\text{s}$	$10^7 \text{ erg}/\text{s}$	$7.5 \text{ mmHg} \cdot \text{ml}/\text{s}$
Pressure, $P$ & Stress, $\sigma$	<b>1 Pa</b> = $1 \text{ N}/\text{m}^2$	$10 \text{ dyn}/\text{cm}^2 = 1.36 \text{ gwt}/\text{cm}^2$	$7.5 \cdot 10^{-3} \text{ mmHg}$
$dP/dt$	$1 \text{ Pa}/\text{s}$	$10 \text{ dyn}/\text{cm}^2/\text{s}$	$7.5 \cdot 10^{-3} \text{ mmHg}/\text{s}$
Resistance, $R$	$1 \text{ Pa} \cdot \text{s}/\text{m}^3 = \text{N} \cdot \text{s}/\text{m}^5$	$10^{-5} \text{ dyn} \cdot \text{s}/\text{cm}^5$	$7.5 \cdot 10^{-9} \text{ mmHg} \cdot \text{s}/\text{ml}$
Shear rate, $\gamma$	$\text{s}^{-1}$	$\text{s}^{-1}$	$\text{s}^{-1}$
Shear stress, $\tau$	<b>1 Pa</b> = $1 \text{ N}/\text{m}^2$	$10 \text{ dyn}/\text{cm}^2 = 1.36 \text{ g}/\text{cm}^2$	$7.5 \cdot 10^{-3} \text{ mmHg}$
Velocity (wave-)	$\text{m}/\text{s}$	$\text{m}/\text{s}$	$\text{m}/\text{s}$
Viscosity, $\eta$	<b>1 Pa</b> ·s = $1 \text{ N} \cdot \text{s}/\text{m}^2$	$10 \text{ dyn} \cdot \text{s}/\text{cm}^2 = 10 \text{ Poise}$	
Decay time ( $R \cdot C$ )	$\text{s}$	$\text{s}$	$\text{s}$
$L \cdot C^{**}$	$\text{s}^2$	$\text{s}^2$	$\text{s}^2$
<b>1 ml O<sub>2</sub>***</b>	$\sim 20 \text{ J}$	$20 \cdot 10^7 \text{ erg (dyn} \cdot \text{cm)}$	$150 \text{ mmHg} \cdot \text{ml} = 4.8 \text{ cal}^*$
<b>1 ml O<sub>2</sub>/min***</b>	$\sim 0.33 \text{ Watt}$	$0.33 \cdot 10^7 \text{ erg}/\text{s}$	$2.5 \text{ mmHg} \cdot \text{ml}/\text{s}$

\*  $1 \text{ Cal} = 10^3 \text{ cal}$

\*\* when L and C are expressed per length:  $1/\sqrt{L \cdot C'} = \text{m}/\text{s}$  (velocity).

\*\*\*for fatty acids and glucose metabolism; not for protein metabolism

$$1 \text{ kPa} = 7.5 \text{ mmHg} = 10 \text{ cm H}_2\text{O} = \text{mN}/\text{mm}^2$$

*Contractile efficiency* is the inverse of the slope of the relation between Pressure Volume Area and oxygen consumption per beat.

*Economy of contraction* is defined as oxygen consumption used for isovolumic contractions.

*Efficiency* is the ratio of external, or produced mechanical power, and input power or oxygen consumption per time.

Strain, Reynolds number, and Womersley's parameter, do not have a dimension, but one needs to work in a single system.

# Index

## A

- Adhesion
  - molecule, 144
- Adventitia, 138
- Afterload, 55;61;135
- Aging, 45; 46; 102
- Allometry, 155; 158
  - body mass, 59; 78; 155; 156; 157; 158; 160
  - characteristic time, 156
  - heart period, 156; 159
- Anastomosis, 16; 145
- Anemia, 6
- Aneurysm, 143
- Angina pectoris, 19
- Angioplasty, 145
- Aorta
  - aging, 102
  - aortic valve, 64; 114
  - characteristic impedance, 119; 122; 171
  - compliance, 102; 107; 122; 171
  - elasticity, 99; 103; 107; 171
  - flow, 8; 114; 151; 165; 174
  - human, 16; 172; 173
  - opening angle, 140
  - pressure, 23; 26; 30; 46; 59; 60; 64; 66; 69; 70; 73; 91; 94; 111; 112; 114; 115; 119; 122; 125; 131; 132; 134; 135; 151; 157; 165
  - reflectipn, 122; 133; 134
  - resistance, 22; 23
  - section, 8; 13; 44; 122; 171
  - transfer, 133
  - wall, 140
  - wave speed, 102; 116; 119; 172
- Apoptosis, 144
- Applanation tonometry, 106; 131; 132
- Area
  - compliance, 42; 45; 100; 101; 102; 122
  - cross-sectional area, 7; 9; 12; 19; 24; 25; 26; 32; 35; 42; 101; 102; 110; 128; 173
  - exchange area, 174
  - lateral area, 174
- Arterial model
  - distributed, 117; 127; 128; 129
  - lumped, 58; 122; 123; 125
  - single tube, 116; 123; 129; 133; 134
  - transmission line, 122; 123
  - T-tube, 129
  - tube, 123
  - two-tube, 123
- Arterial wall, 10; 17; 30; 32; 38; 102; 137; 138; 140; 143
  - elasticity, 36; 102
  - Fracture, 159
  - friction, 110
  - mass, 140
  - shear, 5; 128; 137; 138; 145
  - stress, 31; 33; 138; 140
  - tension, 31
  - thickness, 31; 33; 45; 46; 82; 100; 139; 140; 159
  - tracking, 42; 132
- Arteriole, 22; 23; 25; 82; 83; 86; 105; 172; 173
  - Pressure-Volume Relation, 83
  - resistance, 22; 24
- Arteriovenous shunt, 138
- Artery
  - compliance, 45; 46; 64; 115; 118; 119; 135; 156
  - conduit artery, 23; 24; 30; 39; 82; 99; 122; 170
  - diameter, 86
  - disease, 128
  - effective length, 108; 116; 117
  - flow, 16; 83
  - large, 5; 23
  - load, 59; 68; 69; 75; 92; 95; 118; 149; 151
  - pressure, 24; 92; 94; 111; 131; 132
  - pressure and flow wave, 111
  - pressure-diameter relation, 39; 43; 45
  - pressure-volume relation, 45; 46; 168
  - segment, 30; 127; 165
  - stenosis, 17; 18
  - system, 8; 13; 30; 114; 116; 117; 118; 119; 123; 149; 150; 152; 156; 158; 159; 168; 173
  - systemic arterial tree, 112; 116
  - tree, 21; 30; 99; 109; 127; 129; 171
  - wall. *See* Arterial wall
- Atherogenesis, 144
- Atherosclerosis, 10; 103; 143; 144
  - atheromatous plaque, 17
  - bifurcation, 143; 144
  - curvature, 143; 144
  - endothelial function, 16; 143; 144
  - flow reversal, 143
  - flow separation, 143; 144; 145
  - hyperlipidemia, 143
  - smoking, 143

- Augmentation, 67; 119  
 Augmentation Index, 106; 107; 111;  
 112; 118
- Autocrine, 143
- Autoregulation, 24; 81; 87  
 curve, 81  
 gain, 82; 83  
 metabolic, 82  
 myogenic, 24; 82  
 range, 83
- ## B
- Balloon injury, 145
- Bernoulli, 11; 12; 13; 17; 19
- Beta-block, 67
- Bifurcation, 10; 13; 105; 115; 134; 143;  
 144
- Blood  
 density, 4; 11; 15; 16; 25; 26; 29; 100;  
 110  
 Fahraeus-Lindqvist effect, 5  
 flow, 5; 6; 9; 11; 13; 18; 25; 30; 85;  
 127; 138; 144  
 mass, 25; 29  
 velocity, 24; 173; 174  
 velocity gradient, 8; 10  
 velocity profile, 3; 7; 8; 10; 29; 30; 144  
 viscosity. *See* Viscosity
- Bridging, 86
- Bundle branch block, 94
- ## C
- Calcium, 52; 54  
 handling, 54  
 intracellular, 52
- Caloric equivalent, 75
- Capillary, 9; 13; 22; 24; 173; 174  
 pressure, 24
- Cardiac  
 efficiency, 78; 79  
 filling, 13  
 function, 24; 60; 152  
 ischemia, 19; 24; 61; 67; 73; 85; 86; 87  
 metabolism, 74; 78; 81; 87; 158  
 muscle, 33; 42; 51; 52; 53; 54; 55; 65;  
 73; 81; 83; 84; 85  
 output, 16; 23; 24; 30; 54; 60; 61; 65;  
 66; 67; 69; 71; 78; 91; 92; 95; 119;  
 122; 125; 129; 149; 152; 156; 158;  
 173; 174  
 pump function, 13; 54; 58; 59; 63; 64;  
 65; 66; 67; 68; 75; 77; 79; 94; 123
- Cardiovascular morbidity, 159
- Casson, 5
- Cell culture, 54
- Characteristic impedance, 25; 110; 111;  
 115; 116; 117; 118; 119; 122; 123;  
 157; 170; 171; 172
- Circulation  
 systemic, 23; 70; 115
- Circulation time, 174
- Coanda effect, 12
- Coarctation, 17; 18; 19
- Collagen, 36; 103; 160
- Comparative physiology, 150; 155; 156
- Compliance, 25; 41; 42; 43; 44; 45; 46;  
 83; 100; 101; 103; 115; 119; 122; 129;  
 139; 151; 152; 167; 170; 172  
 addition, 44  
 area compliance, 42; 45; 100; 101;  
 102; 122  
 diameter compliance, 42; 45  
 total arterial compliance, 45; 115; 117;  
 122; 123; 157  
 vessel, 100; 101; 172
- Compliance determination  
 area method, 124  
 decay time method, 123  
 input impedance method, 125  
 parameter estimation method, 124  
 pulse pressure method, 124  
 stroke volume over pulse pressure  
 method, 124  
 transient method, 125  
 two-area method, 124  
 wave velocity method, 125
- Conductance, 22; 94
- Conduction defect, 94
- Contraction, 52; 54; 60; 61; 65; 66; 83;  
 84; 85; 86; 87  
 contractile function, 92; 95  
 contractility, 52; 53; 55; 57; 59; 61; 62;  
 64; 65; 66; 67; 68; 75; 83; 85; 86;  
 92; 93; 94; 95; 150  
 contracting heart, 32; 57  
 dP/dt, 92; 93; 94; 95  
 economy, 79  
 efficiency, 79  
 endothelium, 86  
 index of contractility, 93; 94  
 inotropic response, 52; 55; 94; 95  
 isobaric, 73; 84  
 isovolumic, 66; 72; 75; 79  
 protein, 33  
 synchronicity, 94  
 unloaded contraction, 73

- Coronary  
 Fractional perfusion time, 85; 158  
 Coronary circulation, 114  
 autoregulation, 81; 82; 83  
 cardiac metabolism, 74; 81; 87; 158  
 cardiac muscle, 81; 83  
 endothelium, 86  
 exercise, 87  
 flow, 76; 77; 81; 83; 84; 86; 87  
 flow reserve, 19; 88  
 fractal rule, 86  
 Gregg effect, 86  
 heterogeneity, 86  
 instantaneous pressure-flow relation, 82; 83  
 intracellular pressure, 86  
 maximal vasodilation, 19  
 metabolic autoregulation, 82  
 myogenic autoregulation, 24; 82  
 stenosis, 88  
 supply-demand, 87  
 transmural vessel, 87  
 'twinkling', 86  
 vascular emptying, 86  
 vascular resistance, 82; 87  
 vasculature, 81  
 Coupling  
 ventriculo-arterial coupling, 150; 156; 157; 158  
 Coupling parameter, 79; 156; 157

## D

- Determination  
 characteristic impedance, 111; 125  
 compliance, 42  
 ejection fraction, 79  
 elastance, 42  
 flow reserve, 19  
 impedance, 113; 114  
 isometric force, 54  
 maximal elastance, 59  
 pressure-volume relation, 41; 57; 58; 59; 61; 79; 93  
 pump function graph, 68  
 reflection site, 116  
 viscosity, 5; 9  
 wave speed, 101; 102  
 Young modulus, 39  
 Diastole, 32; 39; 41; 42; 45; 54; 60; 61; 69; 83; 86; 87; 117; 119; 158  
 diastolic pressure-time index, 73  
 duration, 73; 87  
 elastance, 45

- filling, 26; 39; 41; 45; 59; 60; 61; 65; 66; 68; 75; 79; 91; 92; 93; 150; 151; 152  
 long diastole, 83  
 preload, 55  
 pressure, 73; 87; 119; 122; 131; 149; 150; 151; 152; 156; 157  
 pressure, end-diastolic, 93  
 volume, end-diastolic, 91; 92  
 Dimensional analysis, 151  
 Dimensionless, 150  
 Distensibility, 42; 45  
 area distensibility, 42  
 bulk modulus, 42; 43  
 diameter distensibility, 42  
 Dobutamine, 95  
 Doppler, 10; 30; 144

## E

- Edema, 13; 45  
 Effective arterial elastance, 78  
 Effective length, 108; 116; 117  
 Efficiency, 76  
 cardiac, 78; 79  
 contractile, 79  
 Murray's law, 9; 10; 30  
 Einstein, 4  
 Ejection  
 fraction, 79; 92  
 phase, 26; 32; 59; 111  
 Elastance, 41; 42; 44; 45; 58; 78  
 addition, 44  
 diastolic, 45  
 end-systolic, 59; 79; 135  
 intercept volume, 57; 61; 62; 79; 94  
 load independence, 58  
 maximal, 57; 58; 59; 61; 62; 72; 93; 94; 150; 151; 152; 157  
 minimal, 150; 151; 157  
 slope of end-systolic pressure-volume relation, 57; 61  
 time-varying, 58; 60; 61; 84; 85; 149  
 varying stiffness, 85  
 Elastic lamina, 103  
 Elastic modulus, 32; 36; 37; 39; 43; 45; 100; 139  
 complex modulus, 37  
 incremental modulus, 35; 140  
 pressure-strain modulus, 42; 43  
 Young modulus, 32; 35; 36; 39; 42; 45; 159  
 Elasticity, 35; 36; 42; 43; 45; 100; 102; 114; 159; 160; 174

conduit artery, 39; 99; 122; 170  
 dashpot, 37  
 spring, 37; 38  
 stress-strain relation, 36  
 volume, 42; 45  
 wall, 36; 102  
 Elastin, 36; 103; 159  
 Endothelium, 82; 138  
   autocrine, 143  
   barrier function, 10  
   cell, 10; 82; 143  
   damage, 10  
   function, 16; 137; 143; 144  
   mechanosensing, 143  
   NO-synthase, 144  
   paracrine, 143  
 Energy, 9; 11; 37; 52; 55; 69; 70; 73; 159  
   conservation, 13  
   kinetic, 11; 13  
   maximal, 158  
   mechanical, 15  
   minimal energy cost, 9  
   potential, 11  
   Pressure Volume Area, 72; 74; 79  
   Rate Pressure Product, 72; 74  
   Tension Time Index, 72; 73; 74; 87  
 Essential hypertension, 139  
*ex vivo*, 152  
 Excitation-contraction coupling, 73

## F

Fahraeus-Lindqvist effect, 5  
 Fistula, 24  
 Flow  
   deceleration, 16; 26; 143  
   disturbed, 143  
   flow mediated dilation, 10  
   laminar, 7; 15; 16; 18  
   negative, 26  
   oscillatory, 10; 29; 30; 127; 165; 169;  
     173  
   oscillatory flow theory, 10; 29; 30;  
     127; 165; 169; 173  
   pulsatile, 16; 17  
   reserve, 19  
   reserve, fractional, 20; 179  
   reversal, 26; 143  
   separation, 143; 144; 145  
   steady, 7; 16; 18; 29  
   velocity, 13  
   wave, 30; 67; 99; 106; 107; 108; 109;  
     110; 111; 112; 115; 116; 117; 118;  
     125; 127; 128; 157; 158; 171; 174

Force  
   force-length relation, 53  
   force-velocity relation, 53  
   isometric, 52; 53  
 Fourier analysis, 64; 106; 110; 114; 115;  
   117; 163; 164; 165; 173  
   amplitude, 29; 37; 114; 163; 164; 165  
   Fourier pair, 117  
   frequency domain, 110  
   harmonic, 30; 100; 105; 110; 157; 163;  
     164; 165; 171; 173  
   highest harmonic, 164  
   linear, 114; 164; 165  
   nonlinear, 64; 114  
   phase angle, 114; 163; 165  
   reconstruction, 163  
   sampling, 164  
   series of sine waves, 30; 163; 173  
   sinusoidal signal, 114  
   steady state, 114; 115; 164  
   time-invariant, 165  
   time-varying, 114; 117  
 Fracture, 103  
 Frank, 57; 60; 66; 92; 100; 115; 117; 121;  
   122; 170  
 Frank-Starling mechanism, 52; 60; 66;  
   150  
 Fung, 43

## G

Geometric tapering, 129  
 glyocalix, 22  
 Gorlin, 11  
 Graft  
   bypass, 144; 145  
 gravity, 11; 175; 179  
 Gregg effect, 86

## H

Hagen-Poiseuille, 7  
 Hayashi, 43  
 Heart  
   Frank-Starling mechanism, 52; 60; 66;  
     150  
   period, 69; 156; 159  
   rate, 60; 64; 65; 66; 68; 70; 71; 73; 74;  
     75; 79; 114; 150; 157; 158; 160;  
     163; 164  
   Heart failure, 55; 67; 95  
     acute, 55  
   Heat, 76; 86; 174  
     convection, 76; 86

diffusion, 76; 86  
 Hemodialysis, 16  
 Hemodynamic elements  
   basic, 115; 167  
   compliance, 25; 41; 42; 43; 44; 45; 46;  
     83; 100; 115; 119; 122; 139; 151;  
     152; 167; 170; 172  
   inertance, 25; 26; 29; 30; 115; 122;  
     167; 169; 170; 172  
   resistance, 5; 8; 10; 15; 21; 22; 23; 24;  
     25; 26; 29; 30; 69; 115; 122; 139;  
     151; 157; 167; 169; 170; 172  
 Herschel-Bulkley, 5  
 Hill equation, 53  
 Hooke, 31; 35  
 Hyperlipidemia, 143  
 Hypertension, 33; 39; 46; 67; 102; 107;  
   139; 143; 152; 159  
 Hypertrophy, 45; 46; 152  
   concentric, 33; 45; 61; 67; 74  
   eccentric, 61; 62  
   hypertrophic cardiomyopathy, 95  
   vascular. *See* Remodeling, vascular

## I

Impedance, 69; 70; 106; 114; 115; 116;  
 117; 119; 157; 165; 167; 170; 171; 172  
   characteristic, 25; 110; 111; 115; 116;  
     117; 118; 119; 122; 123; 157; 170;  
     171; 172  
   input, 30; 70; 111; 114; 115; 116; 117;  
     118; 119; 122; 125; 128; 129; 151;  
     157; 163; 165; 171  
   longitudinal, 30; 169  
   minimum modulus, 129  
   modulus, 70; 105; 106; 111; 115; 116;  
     117; 119; 122; 128; 167; 171  
   nonlinear, 114  
   normalized, 157  
   phase angle, 105; 114; 115; 116; 122;  
     129; 165; 167  
   real part, 70  
   scatter, 114  
   transverse, 170  
   zero crossing of the phase angle, 116;  
     117  
 Impulse response, 116; 117  
*in vitro*, 143  
*in vivo*, 5; 10; 30; 37; 41; 42; 46; 54; 77;  
   129; 143; 152  
 Indicator, 159; 174  
 Indicator dilution technique, 174  
   thermodilution, 174

Inertance, 25; 26; 29; 30; 115; 122; 167;  
 169; 170; 172  
   addition, 26  
   total arterial, 115; 117; 122; 123  
 Inlet length, 5; 8; 168  
 Inotropic drug, 55  
 Internal elastic lamina, 138  
 Intima, 16; 144; 145  
 Intramyocardial pump  
   isobaric contraction, 73; 84  
   isovolumic contraction, 66; 79  
   pumping action, 83  
   varying elastance, 58; 60; 61; 84; 85  
 Ischemia, 19; 24; 61; 67; 73; 85; 86  
   cardiac, 87  
 Isobaric contraction, 73; 84  
 Isovolumic contraction, 66; 72; 75; 79

## J

Jet, 12

## L

LaGrange, 35  
 Lamé, 31  
 Langendorff, 79  
 Langewouters, 43  
 LaPlace, 31; 32; 33; 39; 45; 53; 77; 93  
 Lumen diameter, 100; 101; 139

## M

Magnetic resonance  
   imaging. *See* MRI  
   spectroscopy, 77; 78  
 Mass  
   arterial wall, 140  
   body, 59; 78; 155; 156; 157; 158; 160  
   effective, 25  
   heart, 59  
   ventricular wall, 74  
 Material property, 25; 35; 43; 45; 139;  
   156; 170  
 Metabolic autoregulation, 82  
 Metabolism, 70; 74; 75; 79; 81; 82; 87;  
   158; 160  
   free fatty acid, 75  
   glucose, 75; 77  
 Method of characteristics, 128  
 Model. *See* Arterial model  
 Moens-Korteweg equation, 100; 101; 122;  
   125; 159; 171  
 Monocyte, 144

Morbidity, 46; 103  
 Mortality, 46; 103; 159  
 MRI, 9; 10; 42; 59; 79; 92; 94; 95; 102; 144  
 Murray's law, 9; 10; 30  
   minimal energy cost, 9  
 Muscle, 32; 36; 39; 54; 55; 61  
   afterload, 55; 61  
   cardiac, 33; 42; 51; 52; 53; 54; 55; 65; 73; 81; 83; 84; 85  
   contractile apparatus, 33; 51; 61; 86  
   cross-bridge, 52  
   excitation-contraction, 73  
   fiber stress, 32  
   force-length relation, 53  
   force-velocity relation, 53  
   isometric force, 52; 53  
   myocyte, 54  
   myosin, 52; 53  
   papillary, 54  
   sarcomere, 51; 52; 53; 54; 55; 61  
   shortening, 84; 85; 86  
   skinned, 54  
   smooth, 24; 36; 83; 137; 144; 145  
   strip, 54  
   thickening, 84; 85  
   trabecula, 54  
   tropomyosin, 52  
   troponin, 52  
   velocity of shortening, 53  
 Myocardial infarction, 55; 95  
 Myocardium, 95  
   subendocardium, 84; 86  
   subepicardium, 84  
 Myogenic autoregulation, 24; 82

## N

Navier-Stokes, 7; 13; 29; 175  
 Newton, 3; 7; 8; 11; 25; 29; 100; 170  
 Nitroglycerin, 134  
 Noise, 114; 164  
 Noninvasive, 9; 42; 45; 79; 102; 131; 132; 135; 172  
   calibration, 132  
 Non-invasive, 59; 94; 144  
 Nyquist, 164

## O

Ohm's law, 8; 21; 22; 114; 122  
 Opening angle, 38; 140  
 Oscillatory flow theory, 10; 29; 30; 127; 165; 169; 173

Oxidant, 144  
 Oxygen, 5; 6; 33; 71; 174  
   caloric equivalent, 75  
   consumption, 70; 71; 72; 73; 74; 75; 76; 77; 78; 79; 86; 87  
   radical, 160  
   supply, 6; 33; 73  
   tension, 6; 82  
   transport, 5  
 Oxygen consumption  
   Pressure Volume Area, 72; 74; 79; 158  
   Rate Pressure Product, 72; 74  
   supply-demand, 87  
   Tension Time Index, 72; 73; 74; 87

## P

Pacing, 94; 114  
 Paracrine, 143  
 Parameter estimation, 122; 124  
 Pericardium, 44  
 Photoplethysmography, 101; 131  
 Plasma skimming, 5; 10  
 Platelet activation, 144  
 Poiseuille, 5; 7; 8; 9; 10; 15; 17; 18; 21; 22; 23; 24; 29; 30; 128; 138; 169; 173  
 Poisson, 35; 170  
 Polycythemia, 6  
 Position  
   standing, 13  
   supine, 13; 23  
 Positron Emission Tomography, 77  
 Power, 65; 69; 70; 75; 77; 78; 79; 159; 173  
   average, 69  
   input, 75  
   maximum, 77  
   mean, 69; 70  
   oscillatory, 70  
   pulsatile, 70  
 Preload, 55  
 Pressure  
   aortic. *See under* Aorta  
   applanation tonometry, 106; 131; 132  
   arterial. *See under* Artery  
   brachial, 132  
   capillary, 24  
   carotid, 132  
   diastolic, 73; 87; 119; 122; 131; 132; 149; 150; 151; 152; 156; 157  
   difference, 7; 9; 23; 26; 173  
   dP/dt, 92; 93; 94; 95

drop, 5; 7; 8; 11; 12; 15; 18; 19; 21;  
22; 23; 29; 30; 82; 86; 87; 165; 167;  
169  
dynamic, 11  
end-diastolic, 93  
finger, 131  
gradient, 9; 12; 13; 15; 19; 21; 29; 173  
hydrostatic, 11; 13  
interstitial, 84  
intramyocardial, 84; 85; 86  
isovolumic ventricular, 65  
late systolic, 111  
mean arterial, 23; 24; 94  
oscillatory, 18; 25; 30; 173  
perfusion, 9; 81; 82; 86; 87  
peripheral, 59; 131; 132; 134  
pressure area relation, 43  
pressure diameter relation, 43  
pressure flow relation, 29; 30; 63; 82;  
85; 87; 165; 173  
Pressure Volume Area, 72; 74; 79; 158  
pressure wire, 12  
pulmonary artery, 23; 112  
pulsatile, 29; 173  
pulse, 45; 46; 103; 118; 119; 132; 156;  
172  
pulse, morbidity, 46; 103  
pulse, mortality, 46; 103; 159  
reservoir, 24  
servo-null technique, 85  
source, 24; 64; 66; 67  
systolic, 132  
systolic, 150; 152  
systolic amplification, 128  
transfer function, 132; 134; 165  
transmural, 13; 31; 38; 44; 84; 119;  
137; 169; 173  
type A beat, 111  
type C beat, 111  
venous. *See under* Vein  
ventricular. *See under* Ventricle  
ventricular filling, 64; 92  
wave, 30; 67; 99; 101; 106; 107; 109;  
110; 111; 112; 115; 116; 117; 118;  
119; 127; 128; 131; 133; 135; 157;  
158; 171; 174  
zero-flow. *See* Zero-flow pressure  
Pressure volume relation, 39; 41; 46  
curvature, 42  
slope, 59  
Pressure-volume relation  
veins, 46  
Pressure-Volume Relation, 57  
diastolic, 58; 59; 61; 92

end-systolic pressure, 65; 78  
end-systolic pressure-volume relation,  
57; 59; 61; 62; 72; 78; 93; 94  
loop, 58; 59; 62; 69  
Pressure Volume Area, 72; 74; 79; 158  
slope, 57; 61  
Prostaglandin, 82  
Pulmonary, 23; 45; 61; 70; 174  
circulation, 23; 70; 112; 115  
Pulse pressure, 45; 46; 103; 118; 119;  
132; 156; 172  
fractional, 156  
morbidity, 46; 103  
mortality, 46; 103; 159  
Pump function, 13; 54; 58; 59; 63; 64; 67;  
94; 123  
dP/dt, 92; 93; 94; 95  
flow source, 64; 66; 67  
Function Curve, 91; 95  
mean ventricular pressure, 65  
pressure source, 24; 64; 66; 67  
pressure-volume loop, 59; 62; 69  
pressure-volume relation, 53; 57; 59;  
60; 61; 62; 65; 91  
pump function graph, 54; 63; 64; 65;  
66; 67; 68; 75; 77; 79  
ventricular pressure, 59; 64; 91; 92; 94

## Q

Quarter wave length rule, 116

## R

Reflection, 10; 26; 67; 73; 105; 106; 107;  
108; 112; 115; 118; 119; 122; 129;  
159; 171  
backward flow, 67; 108; 110; 116  
backward pressure, 67; 110  
backward wave, 67; 105; 106; 107;  
108; 109; 111; 112; 116; 117; 118;  
133; 134; 159  
bifurcation, 10; 13; 105; 115; 134; 143;  
144  
coefficient, 105; 107; 116; 134  
diffuse, 105; 106; 107  
distinct, 105; 107; 116  
forward flow, 67  
forward pressure, 67; 118  
forward wave, 106; 107; 109; 111;  
116; 117; 133  
index of, 106; 112  
phase angle, 105  
phase lag, 132; 133

reflectionless, 115; 119; 122; 171  
 site, 107; 108; 109; 116; 134  
 wave, 30; 101; 111; 128; 129; 132  
 Reflection Index, 106; 112  
 Remodeling, vascular, 10; 137  
   eutrophic, 139  
   extracellular matrix, 145  
   functional adaptation, 137; 140  
   geometrical risk, 144  
   hoop stress, 137; 138; 139  
   hyperplasia, 16; 138; 144; 145  
   hypertrophy, 33; 137; 138; 139  
   intima, 16; 144; 145  
   large artery, 33; 139; 172  
   neointima, 145  
   opening angle, 140  
   outward eutrophic, 139  
   restenosis, 145  
   structural adaptation, 137  
   wall shear stress, 10; 137; 138; 145  
 Remodeling, ventricular. *See* Hypertrophy  
 Resistance, 5; 8; 10; 15; 21; 22; 23; 24;  
   25; 26; 29; 30; 69; 107; 114; 115; 122;  
   139; 151; 157; 167; 169; 170; 172  
   addition, 21  
   arteriolar, 22; 24  
   arteriole, single, 22  
   characteristic, 115; 122  
   peripheral, 19; 22; 23; 24; 64; 78; 114;  
     115; 116; 117; 119; 122; 123; 157;  
     171; 173  
   peripheral resistance unit, 23  
   vascular, 22; 23; 66; 114; 139; 165  
   venous, 22  
 Respiratory cycle, 115  
 Reynolds number, 8; 15; 16

## S

Sarnoff, 71; 72  
 Scatter, 114  
 Scintigraphy, 78  
 Sensitivity analysis, 151  
 Shear, 3; 4; 5; 8; 9; 10; 30; 137; 138; 143;  
   144; 145; 158  
   force, 3; 10  
   oscillatory, 144  
   rate, 3; 4; 5; 8; 10  
   stress, 3; 4; 8; 9; 10; 30; 82; 137; 138;  
     143; 144; 145; 158  
   wall, 5; 8; 9; 10; 128; 137; 138; 139;  
     144; 145  
 Similitude, 150  
 Sine wave, 30; 114; 115; 163; 164

Sinus rhythm, 94  
 Sinusoidal signal, 29; 114  
 Smoking, 143  
 Sphygmomanometry, 79; 131; 132  
 Starling, 24; 60; 66; 91  
   equilibrium, 24  
   resistor, 60  
 Steady state, 85; 114; 115; 125; 164  
 Stenosis, 11; 12; 16; 17; 18; 19; 87; 88;  
   165  
   compliant, 19  
   distal pressure loss, 18  
   effective area, 12  
   flow velocity, 12  
   post-stenotic dilatation, 16  
 Stent, 145  
 Strain, 35; 36; 37; 38; 39; 45; 92; 139;  
   140  
   longitudinal, 35  
   transverse, 35  
 Stress, 3; 5; 8; 9; 10; 31; 32; 33; 35; 36;  
   37; 38; 39; 45; 77; 93; 103; 137; 140;  
   143; 144; 145  
   circumferential, 31; 38  
   fiber, 32  
   hoop, 10; 31; 137; 138; 139  
   LaGrangian, 35  
   local, 32; 141  
   opening angle, 38; 140  
   relaxation, 37  
   residual, 38; 140; 141  
   yield, 4  
   zero stress state, 38; 140  
 Stretch activated channel, 86  
 Stroke  
   volume, 54; 60; 61; 65; 78; 91; 92;  
     149; 150; 151; 156; 158  
   work, 69; 91; 92  
 Subendocardium, 73; 76; 84; 86; 87  
   ischemia, 87  
 Subepicardium, 53; 76; 84; 86; 87  
 Suga, 73  
 Supply-demand ratio, 73; 87; 107  
 Surface tension, 31  
 Systemic  
   arterial tree, 112; 116  
   circulation, 23; 70; 115  
 Systole, 13; 26; 32; 39; 42; 45; 54; 55; 60;  
   61; 73; 83; 86; 91; 101; 111; 117; 119  
   arrest, 85  
   end-systolic pressure-volume relation,  
     57; 59; 61; 62; 72; 78; 93; 94  
   end-systolic volume, 92; 94  
   hypertension, 119; 152

late systolic peak, 111  
 late systolic pressure, 111  
 peaking, 132  
 pressure, 45; 61; 73; 101; 107; 119;  
 132; 134; 150; 151; 152; 156  
 pressure amplification, 128

## T

Temperature, 54; 76; 174  
 Tension, 31; 38; 53; 54  
 surface, 31; 83  
 Tension Time Index, 72; 73; 74; 87  
 Time  
 characteristic, 117; 156  
 circulation, 174  
 decay, 123  
 domain, 116  
 invariant, 114; 164; 165  
 Tension Time Index, 72; 73; 74; 87  
 varying system, 58; 114; 117  
 Tonometry, 101; 132  
 Transfer function, 131; 132; 133; 134;  
 163; 165  
 Transmural  
 artery, 86  
 pressure, 13; 31; 38; 44; 84; 119; 137;  
 169; 173  
 vein, 86  
 Turbulence, 15; 16; 17

## U

Ultrasound, 9; 10; 30; 42; 59; 92; 94; 95;  
 101; 144

## V

Valsalva maneuver, 107; 119  
 Valves  
 aortic valve, 64; 114  
 Varying elastance, 58; 60; 61; 84; 85; 149  
 Vascular  
 hypertrophy. *See* Remodeling, vascular  
 remodeling. *See* Remodeling, vascular  
 resistance, 22; 23; 66; 114; 139; 165  
 smooth muscle, 24; 36; 83; 137; 144;  
 145  
 Vasoconstriction, 82; 106; 138; 144  
 Vasodilation, 20; 82; 83; 94; 106; 108;  
 138  
 Vasomotor tone, 10; 83; 114; 134  
 Vein, 24; 174  
 collapse, 86

diameter, 86  
 pooling, 13  
 pressure, 13; 23; 24; 61; 115; 150; 151;  
 165; 173  
 resistance, 22

## Veins

pressure-volume relation, 46

## Vena contracta, 12

## Ventricle

end-diastolic volume, 151  
 load, 84  
 lumen, 32; 61; 77; 83; 84  
 pressure, 26; 27; 32; 53; 59; 60; 64; 69;  
 70; 72; 84; 85; 86; 91; 92; 94; 114;  
 135; 165  
 relaxation, 92  
 ventriculo-arterial coupling, 70; 78; 92;  
 150; 156; 157; 158  
 volume, 53; 59; 65; 72; 77; 93; 135;  
 151  
 wall. *See* Ventricular wall

## Ventricular wall

mass, 74  
 pressure, 44  
 stress, 32; 74; 77  
 thickness, 74  
 volume, 32

## Vessel segment, 25; 30

## Viscoelasticity, 37; 110; 128

creep, 37  
 hysteresis, 37  
 Maxwell model, 37  
 stress relaxation, 37

## Viscometer, 5; 9

## Viscosity

anemia, 6  
 anomalous, 4  
 dynamic, 3  
 Einstein, 4  
 Fahraeus-Lindqvist, 5  
 hematocrit, 4  
 kinematic, 4  
 non-Newtonian, 4  
 plasma skimming, 5; 10  
 polycythemia, 6  
 unit, 3  
 viscometer, 9

## Vortices, 15

## W

## Wall

arterial. *See* Arterial wall  
 ventricular. *See* Ventricular wall

## Wave

- damping, 115; 134; 170; 172
  - flow, 99; 107; 108; 110; 116; 125; 128; 158; 174
  - length, 116
  - measured flow, 108
  - measured pressure, 112; 116
  - propagation, 127; 128; 129
  - separation, 111; 112
  - travel, 30; 99; 116; 129; 133; 170
- Wave velocity, 25; 100; 101; 102; 103; 105; 107; 116; 118; 119; 133; 159; 170; 171; 172; 174
- apparent, 100; 101
  - apparent phase velocity, 100
  - Bramwell-Hill, 170
  - foot-to-foot pulse wave velocity, 101
  - Frank, 100; 170
  - Moens-Korteweg, 100; 101; 122; 125; 159; 171
  - Newton-Young, 100; 101; 102; 170
  - phase velocity, 100; 101
  - pulse wave velocity, 99; 110; 118; 119; 122; 159; 172
- Wave velocity and flow velocity, 174

- Whole body metabolism, 158
- Windkessel, 30; 39; 103; 115; 117; 121; 122; 123; 129; 149; 152
- four-element, 115; 122; 124; 125
- three-element, 115; 117; 122; 124; 125; 149; 157
- two-element, 115; 117; 121; 122; 124
- Womersley, 10; 29; 30; 127; 169; 173
- Work, 69; 70; 79
- external, 69; 78
- stroke, 69; 91; 92
- Working point, 39; 41; 75; 77

**Y**

- Young, 100
- Young modulus, 32; 35; 36; 39; 42; 45; 159

**Z**

- Zero stress state, 38; 140
- Zero-flow pressure, 83; 85